UNIVERSITY OF SOUTHAMPTON

Synthesis and Coordination Chemistry of Telluroether Ligands

by

Simon David Orchard

A Thesis Submitted for the
Degree of Doctor of Philosophy

Department of Chemistry

September 2000

UNIVERSITY OF SOUTHAMPTON

ABSTRACT

FACULTY OF SCIENCE

CHEMISTRY

Doctor of Philosophy

Synthesis and Coordination Chemistry of Telluroether Ligands

by Simon David Orchard

A range of bi- and tridentate telluroether complexes are described, along with the syntheses of new acyclic and cyclic ligands containing telluroether functions. These species have been characterised by analysis, IR and multinuclear NMR (^{1}H, $^{13}C\{^{1}H\}$, $^{31}P\{^{1}H\}$, ^{55}Mn, $^{77}Se\{^{1}H\}$, $^{125}Te\{^{1}H\}$) spectroscopy (where applicable) and mass spectrometry, along with the X-ray crystal structures of several examples.

The syntheses of the ditelluroether complexes $[Mn(CO)_3(L\text{-}L)X]$ {X = Cl, Br or I; L-L = $MeTe(CH_2)_3TeMe$, $PhTe(CH_2)_3TePh$ and o-$C_6H_4(TeMe)_2$} and $[Re(CO)_3(L\text{-}L)X]$ (X = Cl or Br) are described, along with the crystal structures of $[M(CO)_3\{o\text{-}C_6H_4(TeMe)_2\}Cl]$ (M = Mn or Re). Detailed comparisons of the spectroscopic data for these and analogous thio- and selenoether species have revealed that the telluroether compounds show significantly enhanced σ-donation compared to the lighter chalcogens. The analogous tripodal complexes $[Mn(CO)_3(L^3)][CF_3SO_3]$ {L^3 = $MeC(CH_2EMe)_3$ (E = S, Se or Te) and $MeC(CH_2TePh)_3$}, have been prepared and structurally characterised. Increased σ-donation is again observed down group 16, with significantly enhanced donation by the $MeC(CH_2TeMe)_3$ ligand.

A range of homoleptic platinum group metal and group 11 metal complexes has been prepared with the group 16 tripodal ligands and a range of coordination modes observed. The species $[M(L^3)_2][PF_6]_2$ {M = Pd or Pt; L^3 = $MeC(CH_2EMe)_3$ (E = Se or Te) and $MeC(CH_2TePh)_3$} have been synthesised, with the crystal structure of $[Pt\{MeC(CH_2SeMe)_3\}_2][PF_6]_2$ revealing distorted square planar Se_4 coordination at Pt(II) with the remaining arm of each tripod uncoordinated. For the hexaseleno- and hexatelluroether complexes, $[Ru(L^3)_2][CF_3SO_3]_2$, both ligands adopt a facial arrangement, confirmed by the X-ray crystal structures of thio- and selenoether analogues. The group 11 metal complexes $[Cu(L^3)_2][PF_6]$, $[Ag\{MeC(CH_2TeR)_3\}_2][CF_3SO_3]$ (R = Me or Ph) and $[Ag\{MeC(CH_2SeMe)_3\}][CF_3SO_3]$ have also been synthesised. The structure of the Ag(I) selenoether species reveals a distorted trigonal planar geometry at the metal centre derived from one bidentate selenoether and one monodentate selenoether ligand. These units are then linked to adjacent Ag(I) ions to give a one dimensional linear chain cation.

The syntheses of the organometallic complexes $[M(cod)(L^3)][PF_6]$ and $[M(C_5Me_5)(L^3)][PF_6]_2$ {M = Rh or Ir; L^3 = $MeC(CH_2SeMe)_3$, $MeC(CH_2TeMe)_3$ and $MeC(CH_2TePh)_3$} are described along with the crystal structures of four of the M(I) species. Comparisons of the spectroscopic data for the M(I) complexes reveals superior σ-donation by the ligand $MeC(CH_2TeMe)_3$ compared with its selenoether analogue, with the M(III) complexes showing the reverse trend.

The complexes $[RuCl_2(PPh_3)(L^3)]$ and $[RuCl_2(dmso)(L^3)]$ {L^3 = $MeC(CH_2SeMe)_3$, $MeC(CH_2TeMe)_3$ and $MeC(CH_2TePh)_3$} have been prepared. Reaction of $[RuCl_2(dmso)\{MeC(CH_2ER)_3\}]$ (E = Se, R = Me; E = Te, R = Ph) with $Ag[CF_3SO_3]$ in refluxing MeCN has given the species $[Ru(NCMe)_3\{MeC(CH_2ER)_3\}]^{2+}$ with the lability of the acetonitrile ligands being established *via* the preparation of mixed-tripod complexes.

Improved syntheses for the ligands $MeC(CH_2EMe)_3$ (E = S or Se) are reported along with the synthesis for the new tripodal ligand $MeC(CH_2TePh)_3$. The compounds 2,3,6,7-tetrahydro-1*H*,5*H*-dicyclopenta[1,4][1'4']ditellurin, 1,2-di(2-bromo-1-cyclopentenyl)ditellurane and telluranthrene are also reported as part of an investigation into the chemistry of dilithium 1,2-cyclopenteneditellurolate. The syntheses of the macrocyclic ligands [11]aneS_2Te, [12]aneS_2Te and [14]aneS_3Te, along with their Ag(I) complexes, are discussed.

For My Mum and Andy

Contents Page

List of Tables

List of Figures

List of Schemes

Acknowledgements

Firstly, and most importantly, I would like to thank my supervisors Bill Levason and Gill Reid for all their support, encouragement and enthusiasm over the last three years. Bill must also be acknowledged for introducing me to the wonders of the AM360 NMR spectrometer and special thanks also go to Gill for helping me solve many of my crystallographic disorder problems and for always seeing the bright side of a result, whether planned or not.

I would also like to thank Mrs Joan Street for the huge amount of time she has spent in keeping the rather weary AM360 NMR machine up and running, when at times things looked very bleak. She has helped me out on numerous occasions in bringing the machine back to life and keeping it that way for as long as possible.

Thanks are also due to Mr Bhavesh Patel, and especially Dr. Tony Genge, for all their invaluable help in solving X-ray crystal structures. I would also like to thank Dr. John Langley and Miss Julie Hernimann for running my FAB mass spectra.

Huge thanks also are due to Dr. Vicki Tolhurst for being an amusing lab partner in 7025 and 2005, her constant singing was even occasionally enjoyable, as was her groovy dancing. She also had a great input into the 'tellurium' project, and was always on hand with good advice on generally everything.

I would also like to thank all the present and past members of the Chemistry Department and particularly the Inorganic Section. Special acknowledgements go to Julie Connolly and Nick Holmes for generally helping me out in the first few months of my Ph.D. and to Sarah Bowes and, of course, Sandra Turin for all those aerobic sessions.

Special thanks go to my Mum, Jo and Andy for their support over the years, undergraduate and postgraduate. I would also like to thank my friends outside of the world of chemistry for their advice whether I wanted it or not.

Finally, I would like to acknowledge the EPSRC for three years of financial support and the RSC for a conference bursary, enabling me to go to the ICCC34 in Edinburgh.

Abbreviations

Techniques

ES MS	Electrospray Mass Spectrum
FT	Fourier Transform
FAB	Fast Atom Bombardment
IR	Infra Red
NMR	Nuclear Magnetic Resonance
MS	Mass Spectrometry
UV	Ultra Violet
Vis	Visible
VT NMR	Variable Temperature Nuclear Magnetic Resonance

Solvents

dmf	N,N,-Dimethylformamide
dmso	Dimethyl sulfoxide
Et_2O	Diethyl ether
THF	Tetrahydrofuran

Miscellaneous

acac	Acetylacetonate
3-NOBA	3-Nitrobenzyl-alcohol
TMS	Tetramethylsilane
F_c/F_c^+	Ferrocene/Ferrocenium
Bu	Butyl
Et	Ethyl
Me	Methyl
Ph	Phenyl
R	Alkyl or aryl
δ	Chemical shift
ppm	parts per million
w	Weak
m	Medium
s	Strong
br	Broad
M	metal
cod	cycloocta-1,5-diene
Cp	cyclopentadiene
[9]aneS_3	1,4,7-trithiacyclononane
[10]aneS_3	1,4,7-trathiacyclodecane
[14]aneS_4	1,4,8,11-tetrathiacyclotetradecane
[8]aneSe_2	1,5-diselenacyclooctane
[16]aneSe_4	1,5,9,13-tetraselenacyclohexadecane
[12]aneTe_3	1,5,9-tritelluracyclododecane

Chapter 1

Introduction

1.1 Introduction

Tellurium was first observed in ores mined in the gold districts of Transylvania and was isolated in 1782, by the Austrian chemist F. J. Müller von Reichenstein, a few years after the discovery of oxygen. Müller named it *'metallum problematicum'* since it showed none of the expected properties of antimony with the name tellurium, meaning 'earth', being given to the element by another Austrian chemist, H. M. Klaproth, the discoverer of zirconium and uranium.[1]

Despite the first organic derivatives of tellurium being prepared by Wohler in 1840 [2] and the immense amount of literature associated with the organic and coordination chemistry of thioethers, both seleno- and telluroethers have received relatively little attention until comparatively recently. This is very well illustrated by a review article in 1965 [3] which cites less than 30 references to metal complexes with selenium and tellurium ligands, and a review in 1981 which is still dominated by thioethers.[4] This may be compared to a more recent article, in 1993, which is devoted purely to seleno- and telluroether ligand syntheses and complexation.[5]

This slow development was at least partly due to the scarcity of elemental tellurium from which all preparations began. However, more recently this apparent lack of interest in the heavier chalcogens may be attributed to a variety of causes including the widely held view that SeR_2 and TeR_2 are weak donors, except to soft metal centres, and that their chemistry is little different from their more familiar thioether analogues. Added to this, they are also toxic, extremely malodorous and were thought to be only of academic interest, lacking any applications. Indeed all compounds of selenium and tellurium should be treated as potentially toxic, since the elements are taken up by the kidneys, spleen and liver, and even in minute concentrations cause headaches, nausea, and irritation of the mucous membrane. Despite this, selenium has been found to play an essential role in the dietary systems of humans and may be involved in the protection against certain cancers. It should also be noted that no human fatalities have been attributed to either selenium or tellurium poisoning.

The interest in both selenium and tellurium chemistry has subsequently increased with the development of selenoether ligand chemistry in the previous 30 years, although the analogous tellurium chemistry is only now beginning to emerge as an area of significant growth. This recent appeal can be attributed to the fact that both selenium and tellurium may be observed by modern multinuclear FT NMR instrumentation, which provides an excellent spectroscopic probe to follow ligand synthesis reactions, metal complexation and subsequent

reaction chemistry. In contrast, sulfur possesses only an insensitive quadrupolar nucleus (Table 1.1).

In addition to their inherent interest, these systems have potential applications in important and diverse fields including metal ion recognition and detection,[6, 7] as carrier ligands for radionuclides used in medical imaging and therapy,[8] photography[9] and new conducting materials.[10] Research into the prospect of using thio- and selenoether ligands as catalysts has also yielded favourable results. The $PtCl_2(SePh_2)_2/SnCl_2$ system may be an example of other species which are catalytically active for the homogeneous hydrogenation of non-aromatic alkenes[11] and recently the catalytic application of $[Rh(PPh_3)_2([9]aneS_3)][PF_6]$ has been investigated.[12]

Table 1.1. NMR properties of sulfur, selenium and tellurium.

Isotope	Spin	Natural Abundance/ %	Relative Receptivity [a]
^{33}S	$^3/_2$	0.76	1.7×10^{-5}
^{77}Se	½	7.6	5.3×10^{-4}
^{125}Te	½	7.0	2.2×10^{-3}

[a] relative to the ^1H nucleus.

1.2 Synthesis of Organo-Tellurium Compounds

The lack of development in telluroether chemistry, compared to that of selenoethers, is in part due to the greater difficulty in handling tellurium ligands, which are significantly more air sensitive and malodorous than their corresponding selenium analogues. Further to this is the inherent weakness of the tellurium-carbon bond, which can result in elimination of the carbon backbone and subsequent telluride formation during ligand synthesis and metal complexation reactions. Due to these difficulties, the monodentate telluroether ligands constitute the major category of the limited number of tellurium ligands now known.[13, 14]

However, the organic chemistry of tellurium has been increasingly investigated in recent years showing tellurium to have a rich chemistry differing significantly from the better-known lighter chalcogenides.[15] There are many methods associated with incorporating tellurium into organic molecules, although for the chemistry discussed in this thesis many are not suitable since tellurium is often oxidised to Te(IV). However, those that are potentially useful are outlined below.

- Insertion of tellurium into carbon-metal bonds (Equations 1 to 3).[16, 17, 18]

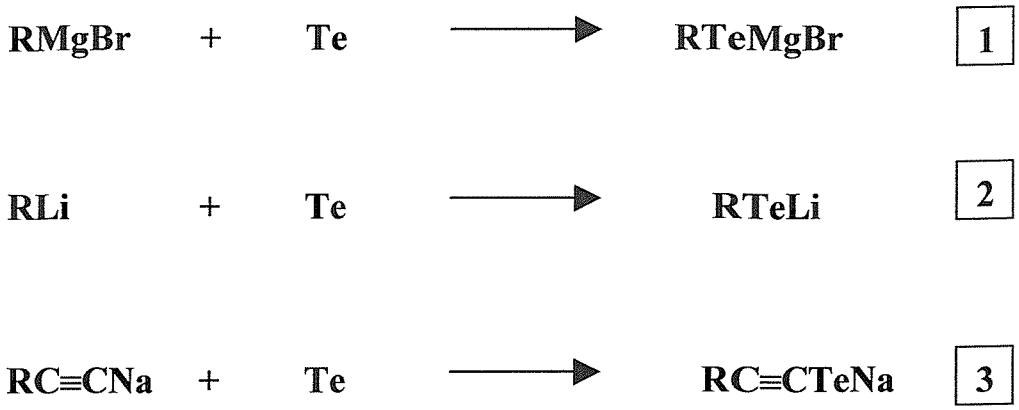

Treatment of these unstable intermediates with the appropriate reagent required for the synthesis of tellurides or ditellurides may then be carried out (Equations 4 and 5).

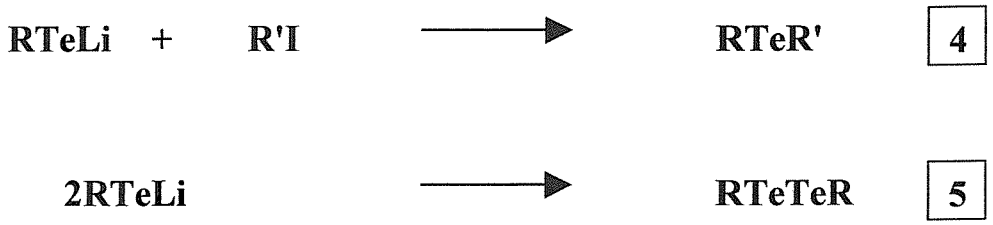

- Alkali metal tellurides. Organic halides will readily alkylate alkali metal tellurides. These telluride reagents have been prepared in an aqueous medium,[19] liquid ammonia,[20] and more recently in dmf.[21] Typical reactions are represented below (Equations 6 and 7).

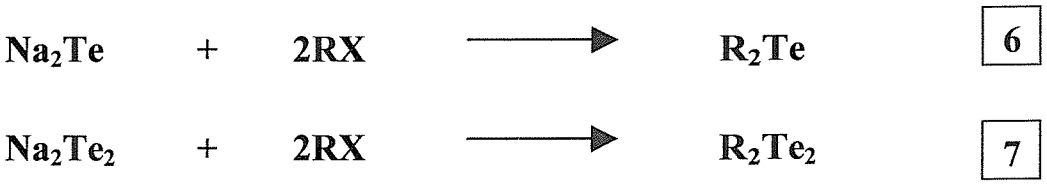

The ditelluroalkanes, $RTe(CH_2)_nTeR$, (R = Me, Ph, 4-$EtOC_6H_4$) have proved difficult to obtain and are only known for certain values of n (n = 1, 3, 6 and 10).[22] They were eventually synthesised by the addition of $X(CH_2)_nX$, (X = Br, I) to a frozen solution (-196 °C) of RTeLi in THF and subsequent thawing. Of particular interest is that for n = 2 the required ligand is not obtained, the reaction of RTeLi with XCH_2CH_2X instead leading to the formation of RTeTeR and elimination of CH_2CH_2. However C_2 bridged telluroethers may be obtained as

the *o*-phenylenebis(telluroether) ligands, *o*-$C_6H_4(TeR)_2$ (R = Ph, Me) which have been synthesised by an analogous route *via* the reaction of RTeLi with *o*-$C_6H_4Br_2$.[23] For $n = 4$ or 5, the corresponding heterocyclic ring is obtained (Equations 8 and 9).

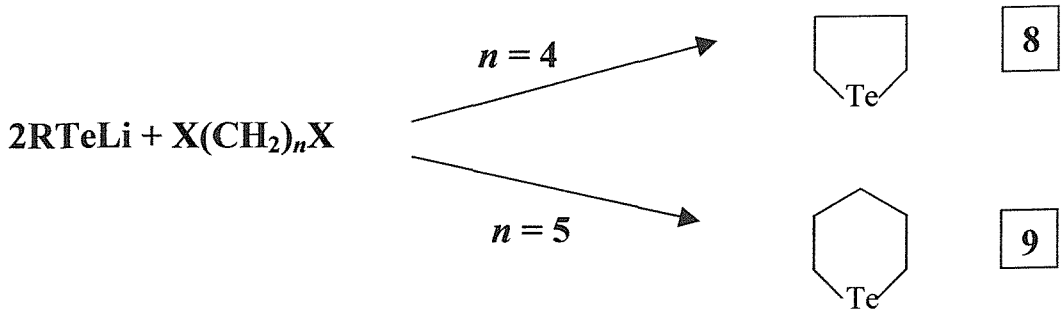

Very few examples of polytelluroether ligands have been prepared, however the ligands $MeC(CH_2TeMe)_3$ and $C(CH_2TeR)_4$ (R = Ph, 4-$EtOC_6H_4$).[22, 24] have been reported *via* the reaction of excess RTeLi with $MeC(CH_2Br)_3$ or $C(CH_2Br)_4$. A few hybrid polydentates containing one or (rarely) two tellurium donors in combination with nitrogen have been described,[25, 26] along with the first tellurium containing macrocyclic schiff base (Figure 1.1) prepared by the condensation of bis(2-formylphenyl)telluride with ethane-1,2-diamine.[27] Just one homoleptic macrocycle, 1,5,9-tritelluracyclododecane has been reported *via* a particularly ingenious synthetic procedure which is illustrated in Scheme 1.1.[28] The crystal structure of the chlorinated product is shown in Figure 1.2.

Figure 1.1. Structure of the macrocyclic schiff base.[27]

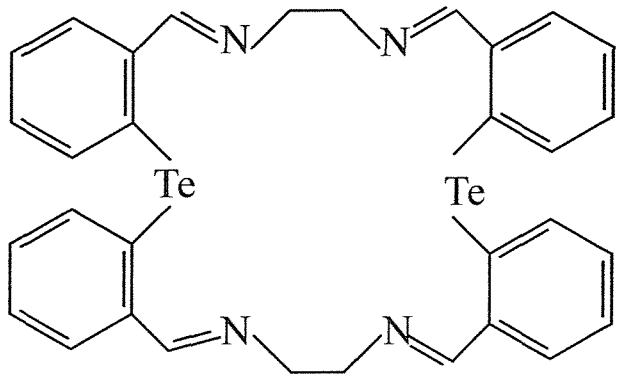

Scheme 1.1. Synthesis of 1,5,9-tritelluracyclododecane.

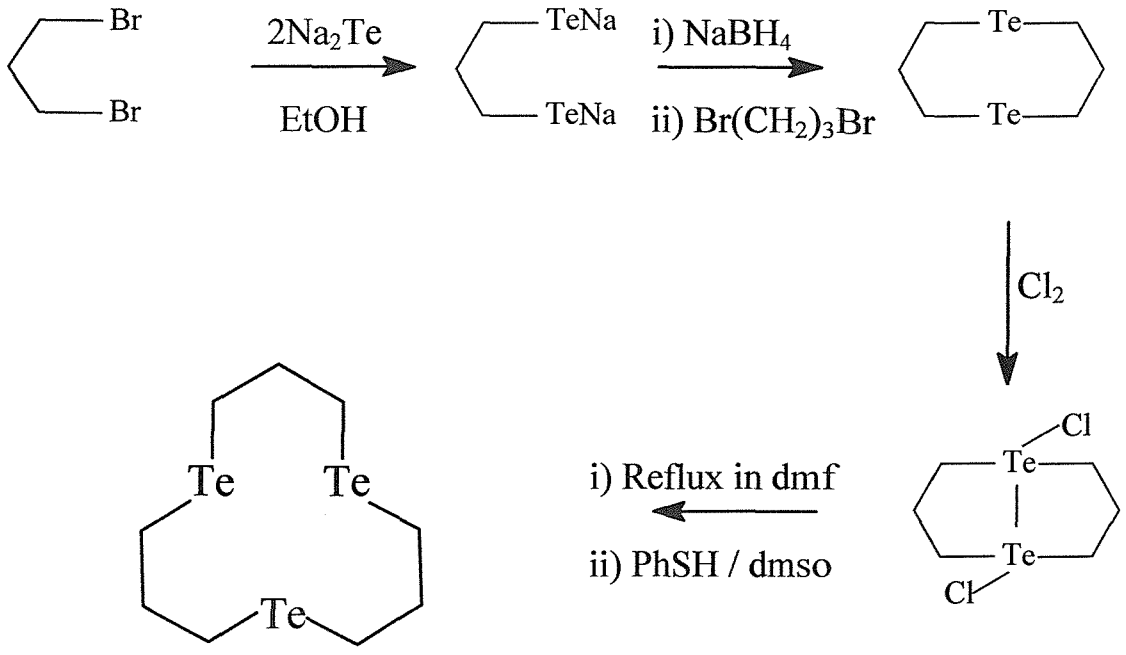

Figure 1.2. Single crystal X-ray structure of 1,1,5,5,9,9-hexachlorotritelluracyclododecane.[28]

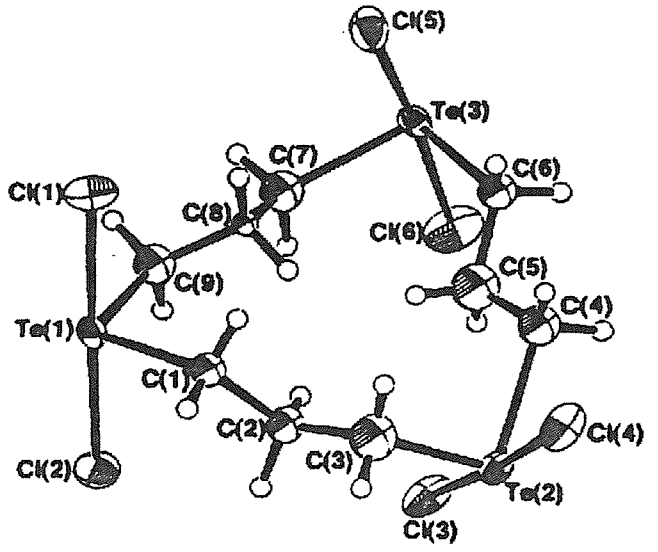

1.3 Metal-Ligand Bonding

1.31 The M-ER$_2$ Bond (E = S, Se or Te)

Although the bonding nature of tertiary phosphines to transition metal centres has been reviewed on a number of occasions,[29] the corresponding factors influencing the bonding of neutral group 16 donor ligands have attracted little attention with most of the work being concentrated on thioethers. Murray and Hartley in their 1981 review detailed the relevant data collected on the structures and bonding in thio-, seleno- and telluroether complexes, although the data dealing with the heavier donor ligands were restricted to just four X-ray crystal structures.[4] Since then, although many more complexes have now been structurally elucidated, the understanding of the M-Se or M-Te bond is still limited.[5]

In contrast to group 15 ligands, steric effects are relatively unimportant since the group 16 donor atom has just two R substituents. Conversely, the presence of the second lone pair is expected to be a complication since it may participate in either π-donation to the metal centre, or alternatively be a source of π-repulsion. Further, π-acceptance is also possible with the difficulties in establishing π-acceptor behaviour being similar to those for tertiary phosphine complexes.[29] Early work generally assumed the acceptor orbital to be the (S, Se, Te)*nd* orbitals, however this proposal is open to the same criticism encountered for group 15 ligands, i.e. that the *nd* orbital is too high in energy to contribute significantly to the bonding, thereby inferring that the acceptor orbitals must be mainly the E-C (E = S, Se, Te) σ^* combinations.

Schumann and co-workers have reported structural data and carried out extended Hückel molecular orbital calculations on the series of complexes $[CpFe(CO)_2EMe_2]^+$ (E = S, Se, Te).[30] These have shown that the inertness and stability of the Fe-E bonds lie in the order Te >> Se > S, and comparable calculations on group 15 analogues, and upon model Fe-EH_3 systems, where the second lone pair is protonated, have shown that π-bonding in the group 16 complexes is negligible. This increased σ-donation is consistent with the decreasing electronegativity of the group 16 donor atoms as the group is descended (Table 1.2) and generally applies for low oxidation state metal complexes, where the spatial extension of the metal *d* orbitals is greatest and thus overlap with the large Te σ-orbital is adequate.

Table 1.2. Electronegativity of S, Se and Te using the Pauling Scale.

Element	Electronegativity
S	2.58
Se	2.55
Te	2.10

In medium to high oxidation state complexes poorer orbital match both of the size and energy between the large, soft tellurium σ-orbital and the contracted, hard metal *d* orbitals results in telluroether complexes being much less stable than the corresponding thio- or selenoether complexes. The stability of Se > S remains, as expected, due to the reduced electronegativity and hence better donation by the selenium.[5]

1.32 The Stereochemistry of the M-E Bond (E = S, Se, Te)

Single crystal X-ray diffraction studies on group 16 complexes have shown the chalcogen atom to be in a pyramidal environment, with tetrahedral bond angles about sulfur, selenium or tellurium and the single remaining lone pair in an essentially pure sp^3 hybrid orbital (Figure 1.3).

Figure 1.3. Stereochemistry of a group 16 ligand upon coordination to a metal centre, where E = S, Se or Te.

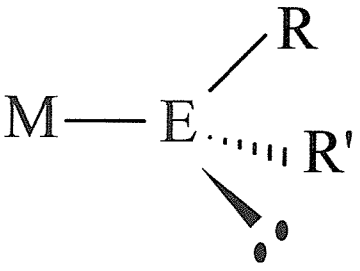

Therefore, a ligand with two different R groups on the chalcogen atom becomes chiral upon coordination to a metal centre and for a simple ligand, RER', two enantiomers are possible. For monodentate ligands, where rotation about the M-E bond is a low energy

process, these enantiomers are NMR indistinguishable under normal conditions. However, for chelating ligands where rotation about the M-E bond is not generally energetically feasible, the different invertomers may be observed providing that they are not interconverting rapidly *via* pyramidal inversion. The most common mechanism (Figure 1.4) involves the interchange of two energetically equivalent configurations *via* a planar transition state.

Figure 1.4. Intramolecular rearrangement *via* a planar intermediate.

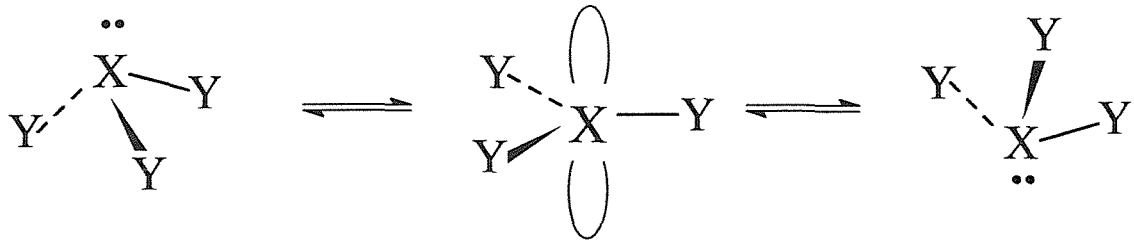

Only a reversal of configuration occurs with no actual chemical bonds being broken, and this is considered the most common mechanism for chalcogen complexes. Other alternative inversion mechanisms have been shown to exist including the dissociation and recombination of one (or more) of the three substituents on the central atom and bimolecular exchange. However, since both these mechanisms involve the cleavage of the metal-chalcogen bonds which are generally strong, neither of these mechanisms is thought to be of importance for this work.

Various studies have investigated pyramidal inversion in chalcogen transition metal complexes[31] and a review on NMR studies of pyramidal inversion is available.[32] Many factors have been shown to influence atomic inversion energies including:

- Nature of the inverting centre.[33, 34, 35, 36]
  - Generally inversion barriers are in the order Te > Se > S, although quantitative data for tellurium are almost completely absent from the literature.
- Nature of the metal centre.[37]
  - Coordination of a chalcogen lone pair of electrons to a transition metal dramatically lowers the chalcogen atom's barrier to pyramidal inversion. The presence of the metal can have two effects. The first will be to decrease the *s* character of the lone pair ground state in line with the electropositive nature of the metal, thereby allowing

easier access to the transition state. The second possible factor is the effect of $(p\text{-}d)\pi$ conjugation between the chalcogen and metal, again contributing to the stabilisation of the planar transition state.

- π-Conjugation effects in the ligands.[37]
  - There is a noticeable fall in inversion energy when the possibility of conjugation is introducted into the organic moiety of the ligand.
- Ligand ring strain effects.[34, 35, 36]
  - There is generally a lowering in the inversion energy from a five-membered chelate ring to a six-membered chelate ring, due to the lowered angle constraint for access to the transition state.
- Influence of *trans* ligands.[38]
  - The *trans* influence is essentially inductive in nature and is attributed to a weakening of the metal-chalcogen bond.

1.4 Telluroether Complexes

The first coordination complex with a tellurium containing ligand was reported by Fritzman in 1915, *cis*-$[Pt\{Te(CH_2Ph)_2\}_2Cl_2]$ [39] and although since then many monodentate telluroether complexes have been reported, characterisation has often been limited to just elemental analysis and a melting point. Consequently, only in the last 20 years has a reasonable body of spectroscopic data been collected, and this is still much more fragmented than that of other group 15 or 16 donor ligands.

Low oxidation state complexes have mostly involved substituted carbonyl complexes, for example photolysis of $[Et_4N][V(CO)_6]$ with $TePh_2$ in THF yields the brown complex $[Et_4N][V(CO)_5(TePh_2)]$.[40, 41] Other examples include niobium,[42] chromium,[43] molybdenum,[44] tungsten,[45] manganese,[46] rhenium,[47] iron[48] and cobalt[49] carbonyl species. Medium oxidation state complexes that have been prepared include $[CpCo(TeMe_2)_3]^{2+}$,[50] $[\{CuCl(TeEt_2)\}_n]$,[51] *mer*-$[RhL_3Cl_3]$ (where L = a number of heterocyclic telluroethers)[52] and a number of palladium(II) and platinum(II) complexes of the type $[ML_2X_2]$ (where X = halide, L = telluroether).[53] There are no recent reports of medium oxidation state complexes with the metals of groups 4 to 7.

The differences between telluroethers and their lighter homologues, discussed earlier, are illustrated by the fact that although monodentate selenoether complexes have been prepared

for Os(VI), Os(IV), Ir(IV) and Pt(IV), all attempts to prepare the analogous telluroether complexes have failed.[54, 55, 56, 57, 58]

Recently a variety of transition metal complexes including low-valent carbonyl derivatives of Mo(0) and Mn(I), platinum group metal halides and group 11 metal centres, have been reported with the ligand 1,3-dihydrobenzo[*c*]tellurophene, as a study into the bonding modes of tellurophene ligands. This showed that for these complexes, coordination of the tellurophene ligand was *via* the lone pair on the Te atom (Figure 1.5).[59] McWhinnie and co-workers have studied other examples of such heterocyclic organotellurium compounds. The reaction of dibenzotellurophene with triiron dodecacarbonyl resulted in the removal of tellurium from the aromatic system and the isolation of ferrole, $[C_{12}H_8Fe_2(CO)_6]$. This contrasts with the lack of reactivity of dibenzothiophene.[60] The use of $^{125}Te\{^1H\}$ NMR spectroscopy to determine the bonding modes of these systems has also been demonstrated,[61] along with a study into heterocyclic organotellurium compounds as precursors for new organometallic derivatives of rhodium.[62] Such systems are potentially useful as models for hydrodesulfurisation. The coordination and rearrangement of cyclic telluroethers on a rhodium-rhodium bond has also been reported as part of a more thorough study into thioethers.[63]

Figure 1.5. Single crystal X-ray structure of $[Mo(CO)_4\{1,3\text{-dihydrobenzo}[c]\text{tellurophene}\}_2]$.[59]

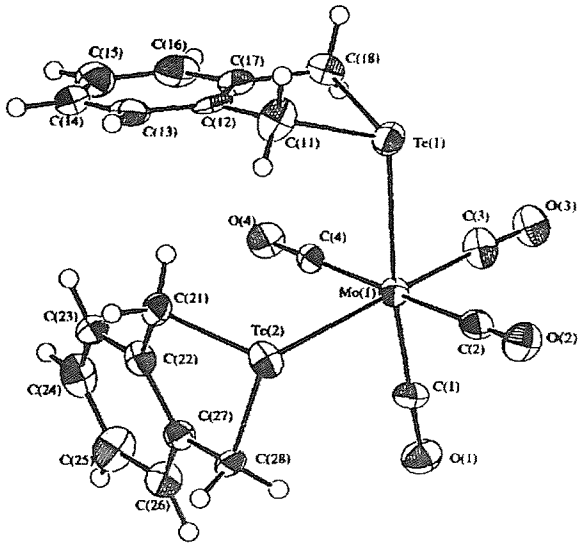

Although the ditelluroether ligands were only synthesised 10 years ago, thorough investigations into their coordination chemistry have been carried out.[22] Despite this, although $RTeCH_2TeR$, (R = Me, Ph) may be easily prepared, few complexes of these methylene backbone ligands have been reported. Indeed just the homoleptic copper(I) and silver(I) complexes $[M_n(MeTeCH_2TeMe)_{2n}][BF_4]_n$[64] and the group 10 polymeric complexes $[MLCl_2]_n$ (M = Pd, Pt; L = $MeTeCH_2TeMe$, $PhTeCH_2TePh$) have been synthesised and fully characterised by spectroscopic means.[65]

The largest number of ditellura- metal complexes in the literature involve the ligands $RTe(CH_2)_3TeR$ and *o*-$C_6H_4(TeR)_2$ (R = Me, Ph) with examples of complexes involving five-membered chelate rings containing the latter ligands. Interestingly although the red-brown cobalt(III) complexes $[Co\{o\text{-}C_6H_4(TeMe)_2\}_2X_2][BPh_4]$ (X = Br, I)[66] have been prepared, attempts to synthesise complexes of $MeTe(CH_2)_3TeMe$ with nickel(II) or cobalt(II) halides have been unsuccessful.[67] The reaction of *o*-$C_6H_4(TeMe)_2$ and $RTe(CH_2)_3TeR$ (R = Me, Ph) with iridium trichloride in ethanol gives the insoluble fawn complexes $[Ir(L\text{-}L)Cl_3]$ which are probably halide-bridged polymers and may be converted into $[N^nBu_4][Ir(L\text{-}L)Cl_4]$ *via* refluxing with N^nBu_4Cl in 2-methoxyethanol.[53, 68]

The greatest number of complexes of these ligands are with the Pd(II) and Pt(II) metal centres. The first examples prepared were the yellow or orange species $[M\{RTe(CH_2)_3TeR\}X_2]$ (R = Me, Ph; X = Cl, Br, I)[69] with the complexes of *o*-$C_6H_4(TeMe)_2$[53] and *o*-$C_6H_4(TePh)_2$[67] being subsequently synthesised. The X-ray crystal structure of *meso*-$[Pd\{PhTe(CH_2)_3TePh\}Br_2]$ is shown in Figure 1.6,[69] and was the first reported structure of a chelating ditelluroether ligand. Interestingly the homoleptic complexes $[M(L\text{-}L)_2]^{2+}$ (L-L = $RTe(CH_2)_3TeR$, *o*-$C_6H_4(TeR)_2$; R = Me, Ph) were not formed even when treated with an excess of ligand.[69] A study of $[Pd\{o\text{-}C_6H_4(TeMe)_2\}I_2]$ showed that heating this species for short periods in dmso resulted in monodemethylation, leading to the formation of the species $[\{Pd(o\text{-}C_6H_4(TeMe)Te)I\}_4]$.[70]

The coordination chemistry of bidentate telluroethers with large chelate rings (*p*-$EtOC_6H_4)Te(CH_2)_nTe(C_6H_4OEt\text{-}p)$ (*n* = 6, 7, 8, 9 and 10) with palladium(II) and platinum(II) halides has also been reported.[71]

Figure 1.6. Single crystal X-ray structure of *meso*-[Pd{PhTe(CH$_2$)$_3$TePh}Br$_2$].[69]

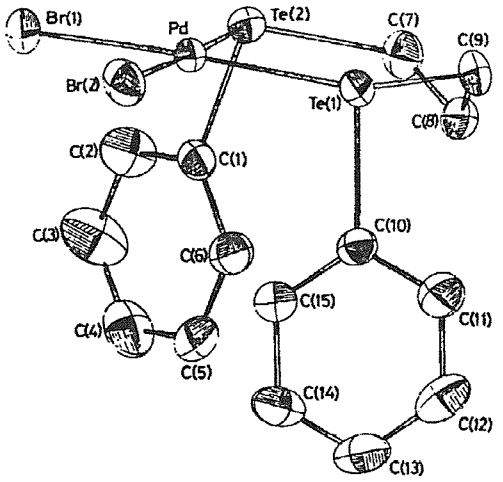

Interestingly, attempts to prepare the Pt(IV) halide complexes, [Pt(L-L)X$_4$] {L-L = MeTe(CH$_2$)$_3$TeMe, PhTe(CH$_2$)$_3$TePh or *o*-C$_6$H$_4$(TeMe)$_2$; X = Cl, Br, I} have failed, although three Pt(IV) complexes of the type [PtMe$_3$I(L-L)] have been synthesised *via* the reaction of [{PtMe$_3$I}$_4$] and the ligand in CHCl$_3$. These species have been studied *via* dynamic NMR spectroscopy as part of an investigation into pyramidal inversion processes.[36]

Recently homoleptic complexes have been reported with copper(I) and silver(I) metal centres of the type [Cu(L-L)$_2$][PF$_6$][72] and [Ag(L-L)$_2$][BF$_4$][73, 74] as well as the first telluroether adducts of tin(IV) halides, [Sn(L-L)X$_4$] {L-L = MeTe(CH$_2$)$_3$TeMe, PhTe(CH$_2$)$_3$TePh or *o*-C$_6$H$_4$(TeMe)$_2$; X = Cl or Br} (Figure 1.7).[75]

Figure 1.7. Single crystal X-ray structure of [SnBr$_4${*o*-C$_6$H$_4$(TeMe)$_2$}].[75]

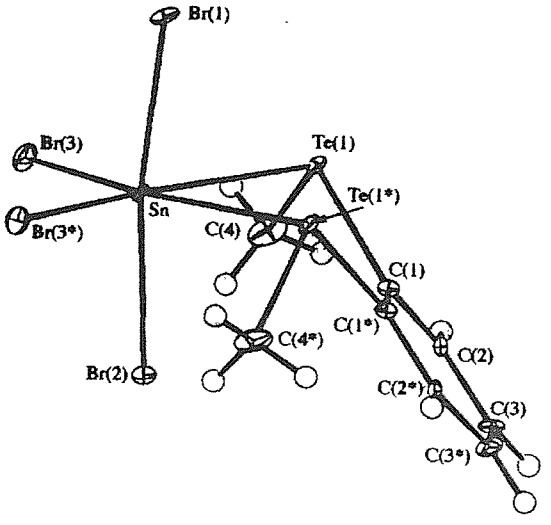

The lack of multidentate telluroether acyclic and cyclic ligands subsequently results in a scarcity of complexes with such ligands. Copper(I) diimine complexes with tellura-crowns have been reported as a spectrochemical and luminescence ion probe for soft metal ions.[76] The synthesis of the first cationic Pd(II) complex of a tellurium-containing polyaza macrocycle (Figure 1.8) has recently been communicated.[77] Previous to the work in this thesis, no complexes had been synthesised using the two multidentate ligands available, $MeC(CH_2TeMe)_3$ and $C(CH_2TePh)_4$.

Figure 1.8. Single crystal X-ray structure of Pd(II) complex with a tellurium-containing polyaza macrocycle.[77]

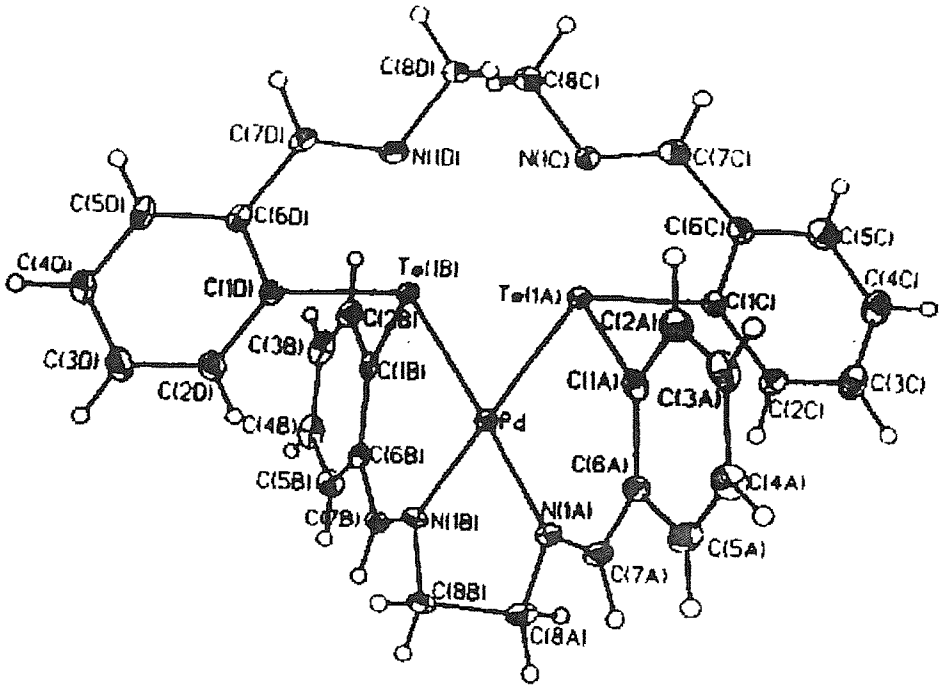

1.5 Complexes with the Tripodal Ligands $MeC(CH_2EMe)_3$ (E = S or Se)

The coordination chemistry of tridentate face capping donor ligands has been extensively developed over the last decades with such ligands as 1,4,7-trithiacyclononane, hydridotris(pyrazoly)borate and 1,4,7-triazacyclononane being at the forefront of these studies.[78] The ligand field properties of these systems have enabled them to find applications in bioinorganic[79] and organometallic chemistry[80] and in coordination compounds which possess novel magnetic properties.[81] While apparently similar in providing a *fac*-X_3 donor set, each imparts significantly different electronic and structural properties to metal complexes.

The chemistry associated with tripodal group 15 ligands, in particular triphos, $MeC(CH_2PPh_2)_3$, has received particular attention. These ligands offer the prospect of combining the catalytic properties associated with phosphine ligands with the stereochemical constraints and geometrical control tripodal ligands impart on the metal centre.[82] Such complexes with the platinum group metals have been studied by Bianchini and co-workers who have mimicked the hydrodesulfurisation process with the metals ruthenium[83] and iridium[84] along with the hydroformylation of alkenes using the species [(sulfos)Rh(cod)] (sulfos = $^-O_3S(C_6H_4)CH_2C(CH_2PPh_2)_3$) supported on a silica surface *via* hydrogen bonding.[85] The reaction of the rhodium alkyl and aryl complexes [(triphos)Rh(R)(η^2-C_2H_4)] (R = Me, Et or Ph) with white phosphorus in THF at room temperature to give the species [(triphos)Rh(η^1:η^2-P_4R)] has also recently been communicated. This reaction represents the first example of P-C bond formation from white phosphorus through the mediation of a transition metal complex and illustrates the novel reaction nature of such triphos complexes.[86]

The group 16 tripodal ligands, $MeC(CH_2EMe)_3$ (E = S, Se or Te), in contrast to triphos, have received little or no attention before this study. Most of the chemistry in the following Chapters will discuss the properties of the seleno- and telluroether ligands, however in order to gain some information of the background on such species the thioether ligand will also be considered here.

The first complexes prepared with the ligand $MeC(CH_2SMe)_3$ were the osmium(IV) and chromium(III) species [Os{$MeC(CH_2SMe)_3$}X_4] and [Cr{$MeC(CH_2SMe)_3$}X_3] (X = Cl or Br).[87, 88] Although the coordination chemistry of this ligand has not been studied in detail, many derivatives have been prepared, including the chiral ligand

$MeC(CH_2SEt)(CH_2S^iPr)(CH_2S^tBu)$, along with its molybdenum(0) tricarbonyl complex.[89] The phenyltris((*tert*-butylthio)methyl)borate ligand, $[PhB(CH_2S^tBu)_3]^-$ (PhTt), has also recently been studied by Riordan and co-workers, along with its complexes [(PhTt)Tl], [(PhTt)CoCl] and [(PhTt)NiCl].[90] These studies have included similar complexes with tetrakis((methylthio)methyl)borate.[91] Rabinovich has lately initiated an investigation into the properties of the ligand $MeSi(CH_2SMe)_3$, reporting the group 6 complexes $[M(CO)_3\{MeSi(CH_2SMe)_3\}]$ (M = Cr, Mo and W)[92] (Figure 1.9) and the one-dimensional copper(I) coordination polymer $[Cu_3\{MeSi(CH_2SMe)_3\}_2Br_3]_n$ (Figure 1.10).[93]

Figure 1.9. Single crystal X-ray structure of $[Cr(CO)_3\{MeSi(CH_2SMe)_3\}]$.[92]

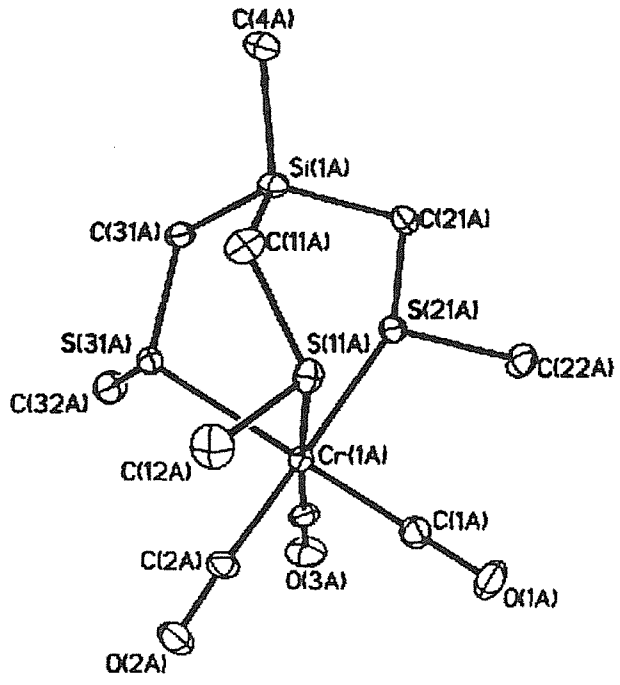

Figure 1.10. Single crystal X-ray structure of $[Cu_3\{MeSi(CH_2SMe)_3\}_2Br_3]$ showing two asymmetric units of the infinite chain structure.[93]

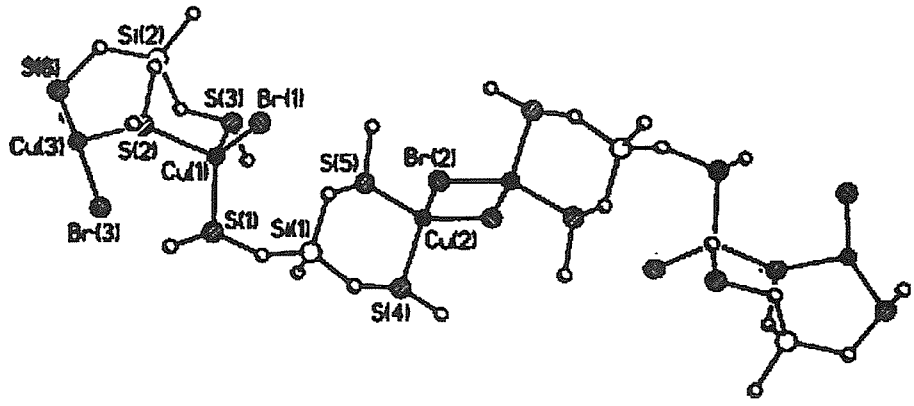

In contrast to the extensive chemistry associated with preparing thioether tripodal derivatives, just two selenoether tripods have been prepared $MeC(CH_2SeR)_3$ (R = Me or Ph).[94] One paper has been published reporting their coordination chemistry, discussing the species $[M\{MeC(CH_2SeMe)_3\}Cl_2]$ (M = Pd or Pt), $[M\{MeC(CH_2SeMe)_3\}Cl_3]$ (M = Rh, Ru or Ir) and $[Os\{MeC(CH_2SeMe)_3\}Cl_3]$.[95]

1.6 Characterisation Techniques

There are many methods available for the determination of the identity of chemical species and a range of spectroscopic techniques have been used in this thesis. Knowledge of well established techniques such as ^{1}H, $^{13}C\{^{1}H\}$ and $^{31}P\{^{1}H\}$ NMR, UV/Vis and IR spectroscopies, and elemental analysis is assumed and requires no further introduction.

1.61 NMR Spectroscopy

NMR spectroscopy has been used extensively to characterise and study the complexes discussed here. Although the use of ^{1}H and $^{13}C\{^{1}H\}$ NMR are well established procedures, manganese-55, selenium-77 and tellurium-125 NMR spectroscopy are not so well known, and so these techniques will be discussed.

1.611 Manganese-55 NMR Spectroscopy

A particular interest of this study was the possibility of recording the ^{55}Mn NMR spectra of the manganese(I) complexes reported (Chapters 2 and 3). Manganese-55 (100%, I = 5/2, Ξ = 24.840 MHz) possesses a moderately high quadrupole moment (Q = 0.55 x 10^{-28} m^2) and thus for complexes with less than O_h or T_d symmetry the considerable electric field gradient is expected to result in substantial broadening of the resonances.[96] However, manganese-55 is a highly sensitive nucleus with a relative receptivity (compared to ^{1}H) of 0.175 and so, the collection of spectra is easy. The total variation in manganese shielding covers a range of 3000 ppm.[97] Previous manganese-55 NMR studies have involved several classes of compound including $[Mn_2(CO)_{10}]$ and its derivatives,[98] $[Mn(CO)_5X]$ (X = Cl, Br, I)[99] and *fac*-$[Mn(CO)_3(MeCN)_3]^+$.[100]

1.612 Selenium-77 and Tellurium-125 NMR Spectroscopy

Although both selenium-77 and tellurium-125 nuclei are of moderate and good NMR receptivity respectively, rather more work has been done on the former due to the higher overall activity in selenium chemistry. The first reports of tellurium-125 NMR involved indirect study *via* coupling to protons in ^{1}H NMR spectroscopy,[101] but since then, almost all

involved direct study utilising Fourier Transform methods. Although tellurium-125 has a negative magnetogyric ratio (-8.498 x 10^7 rad T^{-1} s^{-1}),[102] proton-tellurium distances are usually so great that the Nuclear Overhauser Effect is normally negligible, and standard spin-1/2 methods may be used for both ^{77}Se and ^{125}Te nuclei in the majority of cases.

Several reference compounds have been used in selenium-77 and tellurium-125 NMR, although it is now generally accepted that Me_2Se and Me_2Te are the most suitable reference materials. It has, however, been found that the chemical shifts of Me_2Se and Me_2Te are relatively sensitive to solvent and concentration and thus all chemical shifts are reported relative to neat samples. In fact, variations of about 10 ppm for selenium-77 and 20 ppm for tellurium-125 can occur with solvent and temperature for any resonance.[103]

An important feature of selenium-77 and tellurium-125 NMR spectroscopy is that tellurium and selenium shielding run closely parallel in equivalent compounds, and thus a plot of $\delta(^{125}Te)$ against $\delta(^{77}Se)$ is linear with a gradient of *ca.* 1.8.[104] To some extent, the great sensitivity of $\delta(^{125}Te)$ to electronic changes may be attributed to the larger radial expansion term for tellurium in the paramagnetic nuclear shielding equation given below (where the Q terms denote the imbalance of charge in the valence shell, and ΔE is an effective excitation energy).

$$\sigma_p = -[(\langle r_{5p}^{-3} \rangle)/\Delta E] * \Sigma Q$$

A similar expression exists for Se involving the mean inverse cube of the radius of the 4p orbitals. However, the ratio $\langle r_{5p}^{-3} \rangle(Te)/\langle r_{4p}^{-3} \rangle(Se)$ = *ca.* 1.25, and so this would imply that a still unexplained factor must come from the difference in the ΔE terms.

O'Brien and co-workers have reviewed over 400 tellurium-125 chemical shift values and the overall chemical shift range is thought to exceed 4000 ppm, with the general observation that electron withdrawal from tellurium leads to decreased shielding and hence a more positive chemical shift.[105]

1.62 Mass Spectrometry

Mass spectrometry of tellurium containing compounds is complicated by the fact that tellurium has eight naturally occurring isotopes of reasonable abundance (Table 1.3).

Table 1.3. Relative abundance of tellurium isotopes.

Isotope	Abundance/%	Isotope	Abundance/%
120	0.09	125	6.99
122	2.46	126	18.71
123	0.87	128	31.79
124	4.61	130	34.48

This makes it easy to identify a tellurium-containing fragment by its characteristic isotope pattern (Figure 1.11), but fragments of similar *m/z* values may have overlapping peaks making complete analysis difficult. In order to simplify the work described here all calculated *m/z* values are based upon the most abundant isotope, tellurium-130.

The inherent weakness of the Te-C bond compared with C-O, C-S and C-Se analogues is often demonstrated in the fragmentation behaviours upon ionisation. A good review of the mass spectrometry of tellurium containing compounds is available.[106]

Figure 1.11. Characteristic isotope pattern for tellurium containing species.

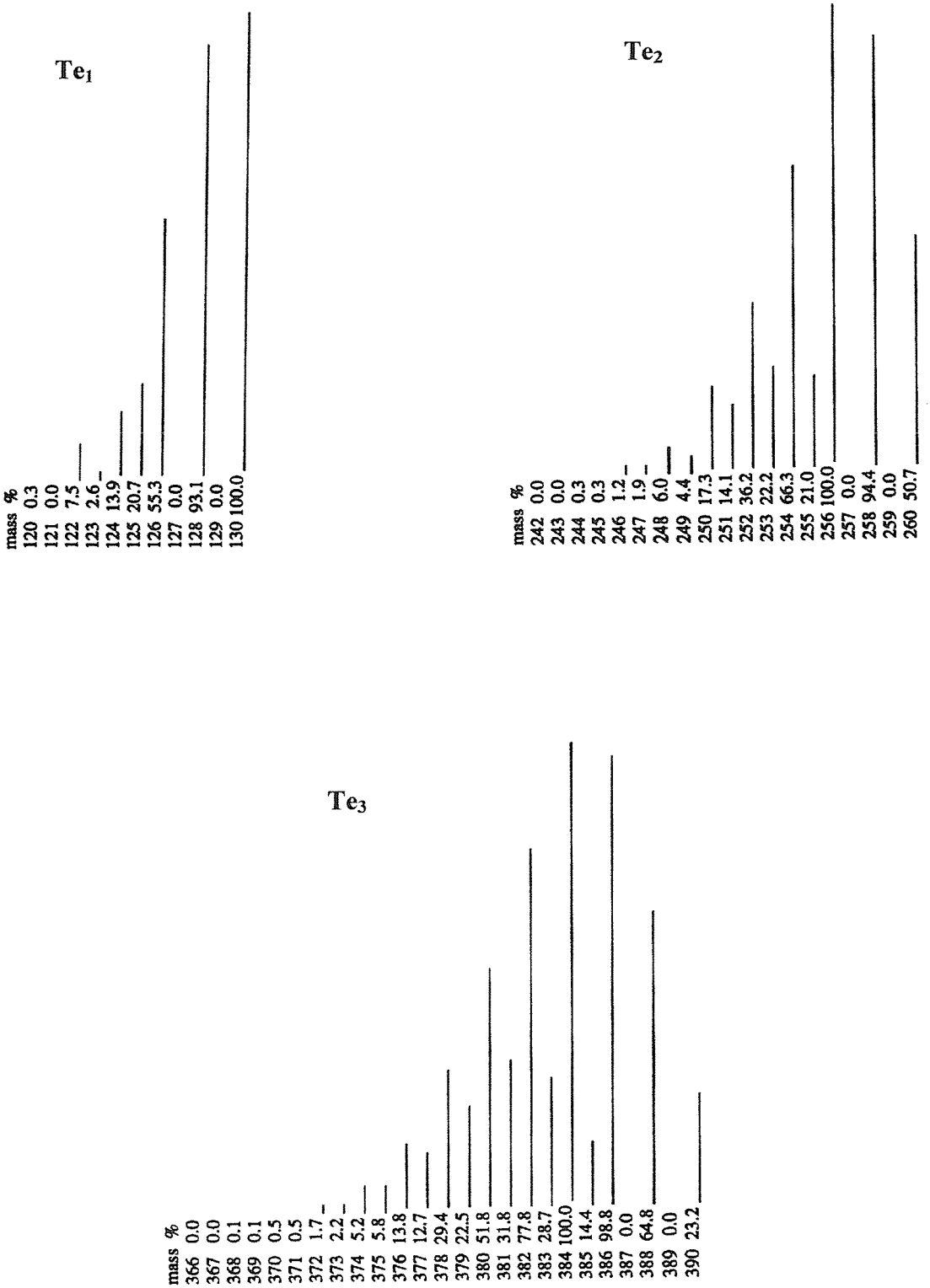

1.7 Aims of this Study

The research discussed in this thesis investigates the coordination chemistry of telluroether ligands by comparison with the analogous selenoether derivatives and may be divided conveniently into three sections.

The first section examines the bonding properties of low valent Mn(I) carbonyl species with bidentate telluroether ligands using a range of spectroscopic techniques (Chapter 2). Detailed comparisons of the spectroscopic data for these and analogous thio- and selenoether species have been made and are interpreted in terms of the relative coordination abilities of group 16 donor ligands.

The second section reports investigations into the properties of the tripodal group 16 ligands, in order to study the properties of these ligands and specifically multidentate telluroether ligands. Chapter 3 discusses the preparation of Mn(I) complexes, with Chapter 4 reporting the synthesis of a range of homoleptic platinum group and group 11 metal complexes, thereby probing the coordination modes of these ligands. Chapter 5 extends this work to low and medium oxidation state rhodium and iridium organometallic complexes, with Chapter 6 reporting some reaction chemistry of piano-stool Ru(II) species.

Finally, Chapter 7 discusses the preparation of the tripodal ligands, along with some chemistry associated with dilithium 1,2-cyclopenteneditelluride. The synthesis of new acyclic and cyclic mixed donor thio-telluroether ligands is then described, along with the coordination chemistry of the cyclic ligands with Ag(I).

1.8 References

[1] M. E. Weeks, *Discovery of the Elements,* 6th edn., Journal of Chemical Education, Easton, Pa., 1956: Selenium and Tellurium, pp. 303-319; Klaproth-Kitaibel letters on tellurium, pp. 320-37.

[2] F. Wohler, *Ann. Chem.,* 1840, **35**, 111.

[3] S. E. Livingstone, *Q. Rev. Chem. Soc.,* 1965, **19**, 386.

[4] S. G. Murray and F. R. Hartley, *Chem. Rev.*, 1981, **81**, 365.

[5] E. G. Hope and W. Levason, *Coord. Chem. Rev.,* 1993, **122**, 109.

[6] T. Yoshida, T. Adachi, T. Ueda, M. Kaminaka, N. Sasaki, T. Higuchi, T. Aoshima, I. Mega, Y. Mizobe and M. Hidai, *Angew. Chem. Int. Ed. Eng.,* 1989, **28**, 1040.

[7] L. F. Lindoy, *The Chemistry of Macrocyclic Ligand Complexes,* Cambridge University Press, Cambridge, 1989.

[8] S. W. Burchiel and B. A. Rhodes (eds.), *Radioimmunoimaging and Radioimmunotherapy,* Elsevier, Essex, U.K.

[9] H. J. Glysing, M. Lelental, M. G. Mason and L. J. Gerenser, *J. Photogr. Sci.,* 1982, **30**, 55.

[10] M. B. Dines and M. Marrocco, in *Extended Linear Chain Compounds*, J. S. Miller (ed.), Plenum, New York, 1982, Vol. 2.

[11] H. A. Tayim and J. C. Bailar, Jr., *J. Am. Chem. Soc.,* 1967, **89**, 4330.

[12] A. F. Hill and J. D. E. T. Wilton-Ely, *Organometallics*, 1997, **16**, 4517.

[13] H. J. Gysing, *Coord. Chem. Rev.,* 1982, **42**, 133.

[14] H. J. Gysing, in '*Proceedings of the Fourth International Conference on the Organic Chemistry of Selenium and Tellurium'*, F. J. Berry and W. R. McWhinnie (eds.), The University of Aston, Birmingham, 1983, pp. 32.

[15] S. Patai and Z. Rappoport (eds.), *The Chemistry of Organic Selenium and Tellurium Compounds,* Wiley, New York, 1986, Vols. 1 and 2.

[16] W. S. Haller and K. J. Irgolic, *J. Organomet. Chem.,* 1972, **38**, 97.

[17] N. Petragnani and M. de Moura Campos, *Chem. Ber.,* 1963, **96**, 249.

[18] Yu. A. Boiko, B. S. Kupin and A. A. Petrov, *Zh. Org. Khim.,* 1969, **5**, 1553.

[19] L. Tschugaeff and W. Chlopin, *Chem. Ber.,* 1914, **47**, 1269.

[20] L. Brandsma and H. E. Wijers, *Rec. Trav. Chim. Pays-Bas,* 1963, **82**, 68.

[21] B. Grushkin and M. N. Saltzman, U. S. Patent 3965 049. (*Chem. Abs.,* 1976, **85**, 124606.)

[22] E. G. Hope, T. Kemmitt and W. Levason, *Organometallics*, 1988, **7**, 78.

[23] T. Kemmitt and W. Levason, *Organometallics*, 1989, **8**, 1303.

[24] H. M. K. K. Pathirana, W. R. McWhinnie and F. J. Berry, *J. Organomet. Chem.*, 1986, **312**, 323.

[25] R. Kaur, H. B. Singh and R. J. Butcher, *Organometallics*, 1995, **14**, 4755.

[26] A. K. Singh, V. Srivastava and B. L. Khandelwal, *Polyhedron*, 1990, **9**, 851.

[27] S. C. Menon, H. B. Singh, R. P. Patel and S. K. Kulshreshtha, *J. Chem. Soc., Dalton Trans.*, 1996, 1203.

[28] Y. Takaguchi, E. Horn and N. Furukawa, *Organometallics*, 1996, **15**, 5112.

[29] W. Levason, in *The Chemistry of Organophosphorus Compounds*, F. R. Hartley (ed.), Wiley, New York, 1990, Vol. 1, Chap. 15 and references therein.

[30] H. Schumann, A. A. Arif, A. L. Rheingold, C. Janiak R. Hoffmann and N. Kuhn, *Inorg. Chem.*, 1991, **30**, 1618.

[31] E. W. Abel, S. K. Bhargava and K. G. Orrel, *Prog. Inorg. Chem.*, 1984, **32**, 1.

[32] K. G. Orrell, *Coord. Chem. Rev.*, 1989, **96**, 1.

[33] R. J. Cross, T. H. Green and R. Keat, *J. Chem. Soc., Dalton Trans.*, 1976, 1150.

[34] E. W. Abel, S. K. Bhargava, K. Kite, K. G. Orrell, V. Šik and B. L. Williams, *J. Chem. Soc., Dalton Trans.*, 1982, 583.

[35] E. W. Abel, A. R. Khan, K. Kite, K. G. Orrell and V. Šik, *J. Chem. Soc., Dalton Trans.*, 1980, 1175.

[36] E. W. Abel, K. G. Orel, S. P. Scanlan, D. Stephenson, T. Kemmitt and W. Levason, *J. Chem. Soc., Dalton Trans.*, 1991, 591.

[37] E. W. Abel, S. K. Bhargava, K. Kite, K. G. Orrell, V. Šik and B. L. Williams, *Polyhedron*, 1982, **1**, 289.

[38] P. C. Turley and P. Haake, *J. Am. Chem. Soc.*, 1967, **89**, 4617.

[39] E. Fritzman, *J. Russ. Phys. Chem. Soc.*, 1915, **47**, 588.

[40] K. Ihmels and D. Rehder, *Organometallics*, 1985, **4**, 1340.

[41] D. Rehder, K. Ihmels, D. Wenke and P. Oltmanns, *Inorg. Chim. Acta*, 1985, **100**, L13.

[42] J. W. Freeman and F. Basolo, *Organometallics*, 1991, **10**, 256.

[43] H. Hausmann, M. Hoefler, T. Kruck and H. W. Zimmermann, *Chem. Ber.*, 1981, **114**, 975.

[44] N. Kuhn, H. Schumann and E. Zauder, *J. Organomet. Chem.*, 1988, **354**, 161.

[45] H. Fischer and U. Gerbing, *J. Organomet. Chem.*, 1986, **299**, C7.

[46] G. Bremer, R. Boese, M. Keddo and T. Kruck, *Z. Naturforsch. Teil B*, 1986, **41**, 981.

[47] P. Jaiter and W. Winder, *Inorg. Chim. Acta,* 1987, **134**, 201.

[48] N. Kuhn and H. Schumann, *J. Organomet. Chem.,* 1984, **276**, 55.

[49] S. Rossi, J. Pursiainen and T. A. Pakkanen, *J. Organomet. Chem.,* 1990, **397**, 81.

[50] N. Kuhn, H. Schumann, M. Winter and E. Zauder, *Chem. Ber.,* 1988, **121**, 111.

[51] R. K. Chadha and J. E. Drake, *J. Organomet. Chem.,* 1985, **286**, 121.

[52] T. Kemmitt, W. Levason, R. D. Oldroyd and M. Webster, *Polyhedron,* 1992, **11**, 2165.

[53] T. Kemmitt and W. Levason, *Inorg. Chem.,* 1990, **29**, 731.

[54] D. J. Gulliver and W. Levason, *J. Chem. Soc., Dalton Trans.,* 1982, 1895.

[55] R. A. Cipriano, W. Levason, R. A. S. Mould. D. Pletcher and N. A. Powell, *J. Chem. Soc., Dalton Trans.,* 1988, 2677.

[56] R. A. Cipriano, W. Levason, D. Pletcher, N. A. Powell and M. Webster, *J. Chem. Soc., Dalton Trans.,* 1987, 1901.

[57] R. A. Cipriano, W. Levason, R. A. S. Mould, D. Pletcher and M. Webster, *J. Chem. Soc., Dalton Trans.,* 1990, 339.

[58] S. K. Harbron and W. Levason, *J. Chem. Soc., Dalton Trans.,* 1985, 205.

[59] W. Levason, G. Reid and V. -A. Tolhurst, *J. Chem. Soc., Dalton Trans.,* 1998, 3411.

[60] K. Singh, W. R. McWhinnie, H. L. Chen, M. Sun and T. A. Hamor, *J. Chem. Soc., Dalton Trans.,* 1996, 1545.

[61] K. Badyal, W. R. McWhinnie, J. Homer and M. C. Perry, *J. Organomet. Chem.,* 1998, **555**, 279.

[62] K. Badyal, W. R. McWhinnie, H. Li Chen and T. A. Hamor, *J. Chem. Soc., Dalton Trans.,* 1997, 1579.

[63] M. P. Devery, R. S. Dickson, B. W. Skelton and A. H. White, *Organometallics,* 1999, **18**, 5292.

[64] J. R. Black, N. R. Champness, W. Levason and G. Reid, *Inorg. Chem.,* 1996, **35**, 4432.

[65] A. F. Chiffey, J. Evans, W. Levason and M. Webster, *J. Chem. Soc., Dalton Trans.,* 1994, 2835.

[66] J. L. Brown, T. Kemmitt and W. Levason, *J. Chem. Soc., Dalton Trans.,* 1990, 1513.

[67] T. Kemmitt and W. Levason, unpublished results, 1987-1988.

[68] R. A. Cipriano, L. R. Hanton, W. Levason, D. Pletcher, N. A. Powell and M. Webster, *J. Chem. Soc., Dalton Trans.,* 1988, 2483.

[69] T. Kemmitt, W. Levason and M. Webster, *Inorg. Chem.,* 1989, **28**, 692.

[70] T. Kemmitt, W. Levason, M. D. Spicer and M. Webster, *Organometallics,* 1990, **9**, 1181.

[71] A. W. Downs, P. Granger, W. R. McWhinnie and H. M. K. K. Pathirana, *Inorg. Chim. Acta*, 1988, **143**, 161.

[72] J. R. Black and W. Levason, *J. Chem. Soc., Dalton Trans.,* 1994, 3225.

[73] J. R. Black, N. R. Champness, W. Levason and G. Reid, *J. Chem. Soc., Dalton Trans.,* 1995, 3439.

[74] J. R. Black, N. R. Champness, W. Levason and G. Reid, *Inorg. Chem.* 1996, **35**, 1820.

[75] A. R. J. Genge, W. Levason and G. Reid, *J. Chem. Soc., Dalton Trans.,* 1997, 4549.

[76] V. W. -W. Yam, Y. -L. Pui, W. -P, Li, K. K. -W. Lo and K. -K. Cheung, *J. Chem. Soc., Dalton Trans.,* 1998, 3615.

[77] S. C. Menon, A. Panda, H. B. Singh and R. J. Butcher, *J. Chem. Soc., Chem. Commun.,* 2000, 143.

[78] S. Trofimenko, *Chem. Rev.,* 1993, **93**, 943.

[79] F. Mani, *Coord. Chem. Rev.,* 1992, **120**, 325.

[80] P. J. Pérez, P. S. White, M. Brookhart and J. L. Templeton, *Inorg. Chem.,* 1994, **33**, 6050.

[81] R. Hotzelmann and K. Wieghardt, *Inorg. Chem.,* 1993, **32**, 114.

[82] H. A. Mayer and W. C. Kaska, *Chem. Rev.,* 1994, **94**, 1239.

[83] C. Bianchini, A. Meli, S. Moneti, W. Oberhauser, F. Vizza, V. Herrera, A. Fuentes and R. A. Sánchez-Delgado, *J. Am. Chem. Soc.,* 1999, **121**, 7071.

[84] C. Bianchini, A. Meli, M. Peruzzini, F. Vizza, S. Moneti, V. Herrera and R. A. Sánchez-Delgado, *J. Am. Chem. Soc.,* 1994, **116**, 4370.

[85] C. Bianchini, D. G. Burnaby, J. Evans, P. Frediani, A. Meli, W. Oberhauser, R. Psaro, L. Sordelli and F. Vizza, *J. Am. Chem. Soc.,* 1999, **121**, 5961.

[86] P. Barbaro, M. Peruzzini, J. A. Ramirez and F. Vizza, *Organometallics,* 1999, **18**, 4237.

[87] R. Ali, S. J. Higgins and W. Levason, *Inorg. Chim. Acta,* 1984, **84**, 65.

[88] L. R. Gray, A. L. Hale, W. Levason, F. P. McCullough and M. Webster, *J. Chem. Soc., Dalton Trans.,* 1984, 47.

[89] R. Soltek, G. Huttner, L. Zsolnai and A. Driess, *Inorg. Chim. Acta,* 1998, **269**, 143.

[90] P. J. Schebler, C. G. Riordan, I. A. Guzei and A. L. Rheingold, *Inorg. Chem.,* 1998, **37**, 4754.

[91] C. Ohrenberg, P. Ge, P. Schebler, C. G. Riordan, G. P. A. Yap and A. L. Rheingold, *Inorg. Chem.,* 1996, **35**, 749.

[92] E. D. Dobbin, C. D. Incarvito, K. -C. Lam, L. M. Liable-Sands, D. Rabinovich, A. L. Rheingold, H. W. Yim and L. M. Tran, *Inorg. Chem.,* 1999, **38**, 2211.

[93] T. E. Concolino, E. E. Pullen, L. M. Liable-Sands, D. Rabinovich, A. L. Rheingold, H. W. Yim and L. M. Tran, *Inorg. Chem.,* 1999, **38**, 6234.

[94] D. J. Gulliver, E. G. Hope, W. Levason, G. L. Marshall, S. G. Murray and D. M. Potter, *J. Chem. Soc., Perkin Trans. II,* 1984, 429.

[95] E. G. Hope, W. Levason, G. L. Marshall and S. G. Murray, *J. Chem. Soc., Dalton Trans.,* 1985, 2185.

[96] D. Rehder, in *Multinuclear NMR*, J. Mason (ed.), Plenum, New York, 1987, Chap. 19.

[97] R. Garth Kidd and R. J. Goodfellow, in *NMR and the Periodic Table*, R. K. Harris and B. E. Mann (eds.), Academic Press, London, 1978, Chap. 8.

[98] A. Kekeci and D. Rehder, *Z. Naturforsch., Teil B*, 1981, **36**, 20.

[99] F. Calderazzo, E. A. C. Lucken and D. F. Williams, *J. Chem. Soc. A*, 1967, 154.

[100] D. Rehder, H.-Ch. Bechtold, A. Kekeci, H. Schmidt and M. Z. Siewing, *Z. Naturforsch., Teil B*, 1982, **37**, 631.

[101] H. C. E. McFarlane and W. McFarlane, *J. Chem. Soc., Dalton Trans.,* 1973, 2416.

[102] G. H. Fuller, *J. Phys. Chem. Ref. Data 5*, 1976, 835.

[103] H. C. E. McFarlane and W. McFarlane, in *Multinuclear NMR,* J. Mason (ed.), Plenum, New York, 1987, ch. 15.

[104] N. P. Luthra and J. D. Odom, in *The Chemistry of Organic Selenium and Tellurium Compounds,* S. Patai and Z. Rappoport (eds.), Wiley, New York, 1986, Vol. 1, Chap. 6.

[105] D. H. O'Brien, K. J. Irgolic and C. -K. Huang, *Proc. Int. Conf. Org. Chem. Selenium, Tellurium, 4th*, 1983, 469.

[106] G. D. Sturgeon and M. L. Gross, in *The Chemistry of Organic Selenium and Tellurium Compounds*, S. Patai and Z. Rappoport (eds.), Wiley, New York, 1986, Vol. 1, pp. 243 - 286.

Chapter 2

Manganese(I) Ditelluroether Tricarbonyl Halide Complexes

2.1 Introduction

In comparison to the other transition metals, the organometallic chemistry of manganese does not have a particularly extensive history, essentially dating from 1949 with the first reference to $[Mn_2(CO)_{10}]$,[1] although this species was not fully characterised until 1954.[2] In contrast, the carbonyl complexes of the adjacent elements in the periodic table, $[Cr(CO)_6]$, $[Fe(CO)_5]$, $[Co_2(CO)_8]$ and $[Ni(CO)_4]$, were all reported in the late 18th and early 19th centuries.[3] However, since the discovery of $[Mn_2(CO)_{10}]$ the development of organo-manganese chemistry has kept in step with the rapid expansion of modern organometallic chemistry.

Manganese pentacarbonyl iodide was prepared in 1954 by the carbonylation of MnI_2 and was the first reported member of the series, $[Mn(CO)_5X]$ (X = Cl, Br or I),[2] with the other halide complexes being subsequently synthesised in 1959, *via* the cleavage of the metal-metal bond in $[Mn_2(CO)_{10}]$ by the respective halogen.[4] Since then, these compounds have served as important synthetic precursors in many studies on organo-manganese compounds. Interestingly, the preparation of $[Mn(CO)_5F]$ has yet to be achieved.

Substitution of the carbonyl groups in $[Mn(CO)_5X]$ by neutral ligands has been widely studied, with the complexes generally prepared either thermally or *via* UV photolysis, with mono-, bi- and tridentate arsine and particularly phosphine ligands receiving most attention.[3] Indeed various studies have been undertaken on phosphine complexes, including kinetics of formation,[5] X-ray structure determination[6] and electrochemical studies.[7] Recently a detailed study into a series of bidentate phosphine, arsine and stibine complexes has been reported within the Southampton research group, describing detailed spectroscopic data.[8] In comparison, group 16 ligands have been rather neglected. Thioethers are the most studied, with the bidentate species *fac*-$[Mn(CO)_3\{MeS(CH_2)_2SMe\}Br]$,[9] *fac*-$[Mn(CO)_3\{PhS(CH_2)_2SPh\}Br]$[10] and *fac*-$[Mn(CO)_3\{(MeSCH_2CH_2)_2S\}Br]$[9], together with various monodentate complexes, being reported in the literature.[3] Selenoethers have faired somewhat worse with just one bidentate complex *fac*-$[Mn(CO)_3\{MeSe(CH_2)_2SeMe\}Br]$,[11] and the monodentate species *fac*-$[Mn(CO)_3(SePh_2)_2X]$ (X = Cl, I)[12] and *fac*-$[Mn(CO)_3(SeMe_2)_2Br]$[13] being reported. However, recently a systematic study of thio-[14] and selenoether[15] bidentate complexes of the type *fac*-$[Mn(CO)_3(L\text{-}L)X]$ {X = Cl, Br or I; L-L = $RE(CH_2)_nER$ or *o*-$C_6H_4(EMe)_2$, E = S, Se; R = Me, Ph, n = 2; R = Me, n = 3} has been published by this research group. Detailed multinuclear (^1H, $^{13}C\{^1H\}$, $^{77}Se\{^1H\}$ (where appropriate) and ^{55}Mn) NMR data were discussed, and for several complexes, X-ray crystal

structure determinations were undertaken. The ^{55}Mn NMR spectroscopic studies showed that $\delta(^{55}Mn)$ for the diselenoether complexes is to low frequency of their thioether analogues by *ca.* 100 ppm, suggesting that there is more electron density associated with the Mn(I) centre in the selenoether species.

Various monodentate telluroether complexes with $[Mn(CO)_5X]$ have been prepared, with the complexes *fac*-$[Mn(CO)_3(TePh_2)_2X]$ (X = Cl, Br or I),[16] *fac*-$[Mn(CO)_3(TeMe_2)_2X]$ (X = Br,[13] I)[17] and *cis*-$[Mn(CO)_4(TeR_2)Br]$ (R = Me, Et)[18] being reported, albeit with limited spectroscopic data.

The organometallic chemistry of rhenium is less extensively explored than that of manganese, but has evolved dramatically since the mid-1980s. Dirhenium decacarbonyl was first prepared in 1941 and is still generally the most important starting material for much of the organometallic chemistry of rhenium.[19]

The carbonyl halide $[Re(CO)_5X]$ (X = Cl, Br or I) species have also proved to be convenient rhenium precursors. These reactions generally involve refluxing the ligand and carbonyl halide in an appropriate solvent, with this procedure being suitable for most ligand types. The vast majority of the complexes in the literature are with group 15 ligands and generally mono- to tris- substitution has been observed, with complexes such as *cis*-$[Re(CO)_4(PMe_2Ph)I]$[20] and *mer, cis*-$[Re(CO)_2(PMe_3)_3Br]$[21] being reported.

Complexes with monodentate group 16 ligands have also been synthesised, including $[Re(CO)_3(EMe_2)_2Br]$, $[Re(CO)_4(EMe_2)Br]$ (E = S, Se or Te)[13] and $[Re(CO)_4(TeMe_2)I]$.[17] Abel and co-workers have studied a large number of bidentate thio- and selenoether complexes of the type *fac*-$[Re(CO)_3(L\text{-}L)X]$ {X = Cl, Br or I; L-L = $MeE(CH_2)_nEMe$ (n = 2 or 3, E = S or Se) or MeECH=CHEMe (E = S or Se)}[22] and *fac*-$[Re(CO)_3(MeSZSeMe)X]$ {X = Cl, Br or I; Z = CH_2CH_2 or *o*-C_6H_4},[23] reporting detailed spectroscopic data along with a discussion of invertomer populations.

This Chapter discusses the synthesis, characterisation and spectroscopic properties of a series of ditelluroether complexes of Mn(I) and Re(I) carbonyl halides of the type *fac*-$[Mn(CO)_3(L\text{-}L)X]$ {X = Cl, Br or I; L-L = $MeTe(CH_2)_3TeMe$, $PhTe(CH_2)_3TePh$ or *o*-$C_6H_4(TeMe)_2$} and *fac*-$[Re(CO)_3(L\text{-}L)X]$ {X = Cl or Br; L-L = $MeTe(CH_2)_3TeMe$ or *o*-$C_6H_4(TeMe)_2$}.

These complexes have been characterised by analysis, IR and multinuclear NMR (^{1}H, $^{13}C\{^1H\}$, ^{55}Mn, $^{125}Te\{^1H\}$) spectroscopy as well as FAB mass spectrometry. X-ray

crystallographic studies have also been conducted on the complexes *fac*-[$Mn(CO)_3${*o*-$C_6H_4(TeMe)_2$}Cl] and *fac*-[$Re(CO)_3${*o*-$C_6H_4(TeMe)_2$}Cl].

Detailed comparisons of the spectroscopic data for these and analogous thio- and selenoether species have been made in order to probe the nature of the bonding between the metal and chalcogen donor. Specifically, comparison of the force constants of the C_s symmetry $M(CO)_3$ fragments and the relative magnitudes of $\delta(^{55}Mn)$ and the $\delta(^{125}Te)/\delta(^{77}Se)$ ratio of analogous compounds have been interpreted in terms of the relative coordinating abilities of the bidentate group 16 donor ligands.

2.2 Results and Discussion

The reaction of $[Mn(CO)_5X]$ (X = Cl, Br or I) with ditelluroether ligand, L-L, {L-L = $MeTe(CH_2)_3TeMe$, $PhTe(CH_2)_3TePh$ or *o*-$C_6H_4(TeMe)_2$} in 1:1 mol ratio in chloroform gave the species *fac*-$[Mn(CO)_3(L\text{-}L)X]$ in moderate yield. The corresponding rhenium complexes *fac*-$[Re(CO)_3(L\text{-}L)X]$ {X = Cl or Br; L-L = $MeTe(CH_2)_3TeMe$ or *o*-$C_6H_4(TeMe)_2$} have been prepared similarly from $[Re(CO)_5X]$. The reactions were monitored by solution IR spectroscopy in the carbonyl region and the reaction vessels were wrapped with aluminium foil to exclude light. The Mn(I) and Re(I) complexes with $MeTe(CH_2)_3TeMe$ or *o*-$C_6H_4(TeMe)_2$ are air stable as solids, but decompose slowly in solution. The manganese complexes of $PhTe(CH_2)_3TePh$, are also air stable as solids but decompose rapidly in solution thereby limiting the spectroscopic data that could be collected. The complexes $[Mn(CO)_3(Me_2E)_2Cl]$ (E = S, Se, Te) and *fac*-$[Re(CO)_3\{o\text{-}C_6H_4(EMe)_2\}Br]$ (E = S, Se) were made similarly for comparison. These compounds have been characterised using ^1H, $^{13}C\{^1H\}$, ^{55}Mn and $^{125}Te\{^1H\}$ NMR spectroscopy, FAB mass spectrometry, IR spectroscopy and elemental analysis.

The solution IR spectra of the isolated products were recorded in $CHCl_3$ since the complexes were poorly soluble in non-polar solvents. For all complexes, the spectra exhibited three ν(CO) bands (Table 2.8 and Figure 2.1). Although both the *fac-* and *mer-cis* isomers lead to three ν(CO) modes, the intensities and frequencies for the complexes reported here are consistent with other *fac* group 16 complexes, thereby leading to an assignment of C_s symmetry (2A' + A") consistent with a *fac* geometry.[14, 15] Solid state IR spectra (CsI discs) were also obtained and generally showed more than three ν(CO) modes, which may be attributed to intermolecular interactions, along with bands corresponding to the presence of the ditelluroether ligands.

For a given manganese ditelluroether, the highest frequency CO stretching vibration generally shifts to lower frequency upon changing X from Cl to Br to I, while the other two bands are virtually insensitive to changing halogen. Little change is observed in any of the three bands upon changing the ditelluroether ligand from *o*-$C_6H_4(TeMe)_2$ to $PhTe(CH_2)_3TePh$, nevertheless upon changing to $MeTe(CH_2)_3TeMe$ a lowering in frequency is observed for all three bands.

For the rhenium complexes, the A'(2) band is shifted to higher frequency, whereas the other two bands are observed at lower frequency compared to their manganese analogues. It

is also interesting to note that all three ν(CO) bands for the rhenium complexes are insensitive to changes in halogen, although upon changing ditelluroether from *o*-$C_6H_4(TeMe)_2$ to $MeTe(CH_2)_3TeMe$ a lowering in frequency of all three bands is again observed.

Figure 2.1. IR spectrum ($CHCl_3$) of the carbonyl stretching region for *fac*-[$Mn(CO)_3${*o*-$C_6H_4(TeMe)_2$}Cl].

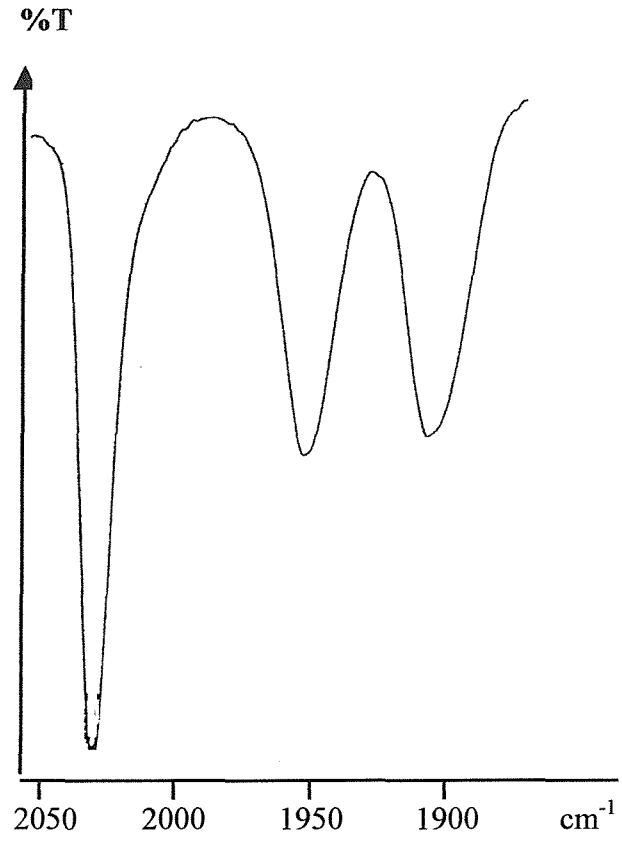

The FAB mass spectrum of each complex showed prominent $[M(CO)_3(L\text{-}L)X]^+$, $[M(L\text{-}L)X]^+$ and $[M(CO)_3(L\text{-}L)]^+$ ions with the correct isotopic distribution. However, as discussed in Section 1.62, fragments with similar *m/z* values can have overlapping peaks, hence making complete analysis difficult. This was found to be the case for the chloro-complexes where the clusters of peaks for $[M(CO)_2(L\text{-}L)Cl]^+$ and $[M(CO)_3(L\text{-}L)]^+$ were overlapping.

2.21 NMR Spectroscopy

As discussed in Chapter 1, coordination of the ditelluroether ligands to a metal centre leads to chirality at Te. For the complexes *fac*-$[M(CO)_3(L\text{-}L)X]$ four stereoisomers (invertomers) are possible; *meso-1, meso-2* and a DL pair (Figure 2.2). These invertomers may be easily identified by NMR spectroscopy providing that they are not interconverting *via* pyramidal inversion at the tellurium donor (the DL pair are NMR equivalent and due to the lack of a plane of symmetry each RTe- group affords a separate resonance).[24] ^{1}H, $^{13}C\{^{1}H\}$, ^{55}Mn (where applicable) and $^{125}Te\{^{1}H\}$ NMR spectra have been recorded for all the compounds isolated.

Figure 2.2. The possible invertomers for the complexes, *fac*-$[Mn(CO)_3\{MeTe(CH_2)_3TeMe\}X]$.

meso-2

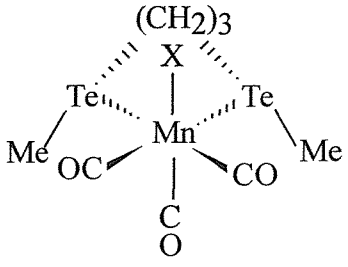

meso-1

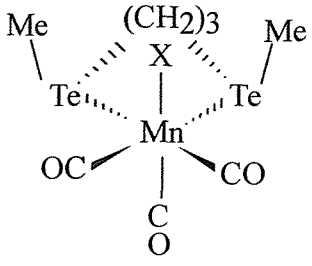

DL pair

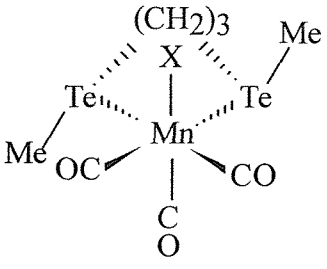

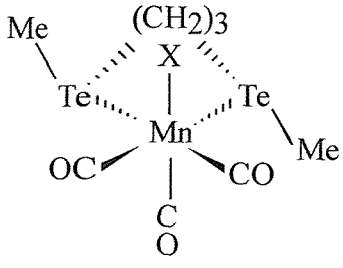

Previous work has shown that pyramidal inversion barriers increase in the order S < Se < Te and for these telluroether complexes, inversion has been found to be slow on the NMR time-scales appropriate to each of the observed nuclei, thereby enabling resonances for individual invertomers to be observed (Table 2.6 and Experimental Section).[24] The relative abundance of the invertomers is a subtle reflection of both steric and electronic factors and hence varies widely in different systems. When fewer resonances than expected are observed in a particular spectrum this may reflect either a low abundance of one form, or since chemical shift differences are often small, accidental coincidence of resonances. Detailed variable-temperature NMR studies were not undertaken since the ^{55}Mn quadrupolar broadening makes these systems unsuitable for quantitative measurements.[25]

fac-[Mn(CO)$_3${MeTe(CH$_2$)$_3$TeMe}X] (X = Cl, Br or I) complexes. The ^{1}H NMR spectrum of *fac*-[Mn(CO)$_3${MeTe(CH$_2$)$_3$TeMe}Cl] showed four δ(Me) resonances (2.12, 2.19, 2.22, 2.27 ppm) consistent with the presence of significant amounts of all invertomers: *meso-1* (1 resonance), *meso-2* (1 resonance), and DL (2 resonances). Similarly, four δ(Me) resonances were observed in the ^{13}C{^{1}H} NMR spectrum (-9.7, -10.5, -12.1, -12.6 ppm) and four signals in the ^{125}Te{^{1}H} spectrum (280, 234, 203, 185 ppm).

For all the complexes studied, the δ(CO) resonances in the ^{13}C{^{1}H} spectra were very broad, spanning several ppm. This may be explained by closer examination of the system. Two δ(CO) resonances are expected per isomer thereby leading to a total of six CO resonances over a fairly small chemical shift range. Further, the manganese-55 quadrupolar nucleus (Q = 0.55 x 10^{-28} m^2) is directly bonded to the CO groups and therefore influences these signals, resulting in overlapping broad resonances. This prevents useful comparison of the δ(CO) chemical shifts with those in complexes with other neutral ligands. Broad δ(CO) resonances were also observed in the thio-[14] and selenoether[15] analogues of these complexes, where it was found that cooling a sample of *fac*-[Mn(CO)$_3${MeS(CH$_2$)$_2$SMe}Br] to 220 K resulted in a noticeable sharpening of the CO resonances, although individual resonances were still not discernible.

The manganese(I) complexes reported here have C_s local symmetry and although the line widths for manganese-55 NMR spectra generally vary greatly with the electric field gradient at the nucleus, line widths for these complexes have been found to be moderate (≤ 3000 Hz). Therefore, the δ(^{55}Mn) resonances of individual invertomers were generally resolved (Table 2.6, Figure 2.3) and hence the ^{55}Mn NMR spectrum of *fac*-[Mn(CO)$_3${MeTe(CH$_2$)$_3$TeMe}Cl] showed the expected three resonances (-644, -594, -581 ppm) corresponding to the presence

of all invertomers. Similar ^{1}H, $^{13}C\{^{1}H\}$, $^{125}Te\{^{1}H\}$ and ^{55}Mn NMR data were obtained for the complexes *fac*-[$Mn(CO)_3${$MeTe(CH_2)_3TeMe$}X] (X = Br or I). The ^{55}Mn NMR spectrum of *fac*-[$Mn(CO)_3${$MeTe(CH_2)_3TeMe$}Br] is shown in Figure 2.3, although one of the invertomers was not present in significant quantity.

Figure 2.3. ^{55}Mn NMR spectrum (89.27 MHz, $CH_2Cl_2/CDCl_3$, 300 K) of *fac*-[$Mn(CO)_3${$MeTe(CH_2)_3TeMe$}Br] showing two of the three NMR distinguishable invertomers.

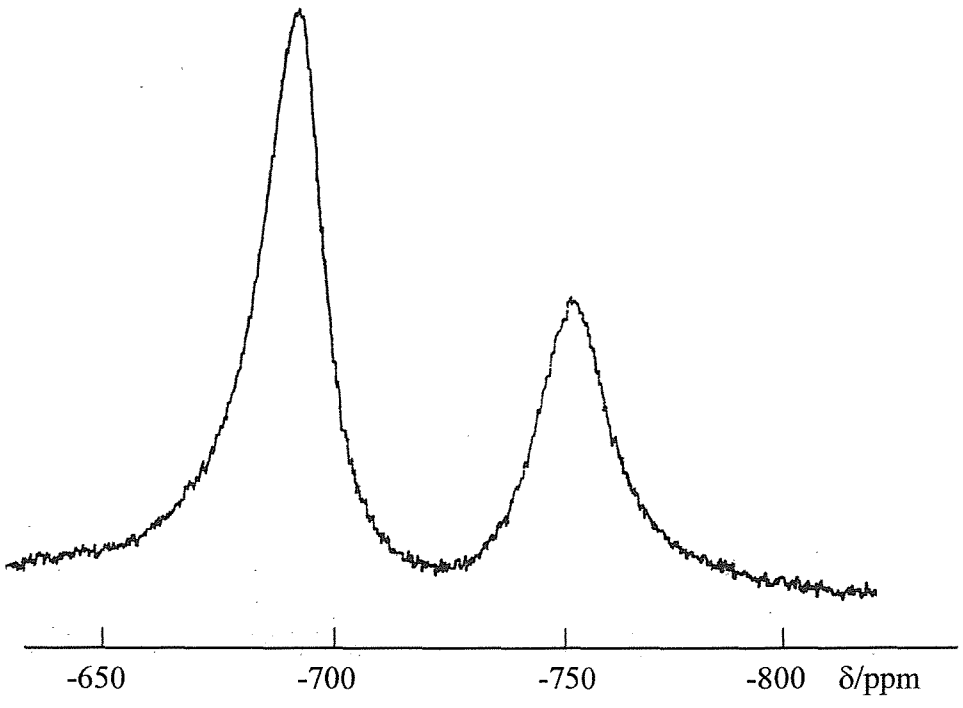

fac-[$Mn(CO)_3${o-$C_6H_4(TeMe)_2$}X] (X = Cl, Br or I) complexes. The NMR spectra for these complexes indicated that just two invertomers were present in substantial amounts. For example, the complex *fac*-[$Mn(CO)_3${o-$C_6H_4(TeMe)_2$}I], exhibited three δ(Me) resonances both in the ^{1}H NMR (2.17, 2.19, 2.67 ppm) and $^{13}C\{^{1}H\}$ NMR (2.4, 0.8, -1.2 ppm) spectra indicating that the DL and one *meso* form were present. Comparison with data on related systems suggests that the *meso-1* form, which often has destabilising X...Me interactions is likely to be the least populated invertomer therefore implying *meso-2* is present.[26] Interestingly, the $^{125}Te\{^{1}H\}$ NMR spectrum showed just two resonances (806, 786 ppm),

rather than the expected three, probably due to the coincidence of two resonances. The ^{55}Mn NMR spectrum, however, gave the expected two signals (-1146, -1050 ppm). Similar ^{1}H, ^{13}C{^{1}H}, ^{125}Te{^{1}H} and ^{55}Mn NMR data were obtained for the complexes *fac*-[Mn(CO)$_3${*o*-C$_6$H$_4$(TeMe)$_2$}X] (X = Cl, Br).

fac-[Mn(CO)$_3${PhTe(CH$_2$)$_3$TePh}X] (X = Cl or Br) complexes. These complexes were found to be extremely air and light sensitive when in solution and they decomposed rapidly, despite the solvent being thoroughly degassed with dinitrogen. Therefore, due to the long accumulation times required for both ^{125}Te{^{1}H} and ^{13}C{^{1}H} NMR, these spectra could not be obtained. Even the ^{1}H NMR spectra showed significant decomposition, with only broad resonances obtained, preventing identification of individual invertomers. However, for ^{55}Mn NMR spectra accumulation times were just a few minutes for moderately concentrated solutions and so ^{55}Mn NMR spectra were easily obtained. For the complex *fac*-[Mn(CO)$_3${PhTe(CH$_2$)$_3$TePh}Br] two signals were observed (-634, -568 ppm), with three resonances for the chloro- complex (-435, -500, -613 ppm). This is perhaps due to increased destabilising X...Ph interactions for the bromo- complex, due to the larger steric bulk of Br compared to Cl thereby disfavouring the *meso-1* invertomer. Despite the short acquisition times required, the reliability of these data must be questioned as to if these signals refer to the required complexes or to decomposition products. The solution IR of the NMR solutions was therefore taken directly after the spectra was observed, and showed the carbonyl region remaining unchanged to that of a fresh sample.

[Mn(CO)$_3$(EMe$_2$)$_2$Cl] (E = S, Se or Te) complexes. The [Mn(CO)$_3$(EMe$_2$)$_2$Cl] (E = S or Se) complexes may be readily identified as *fac* isomers by comparison of their IR and NMR spectra (Tables 2.6 and 2.8) with their bidentate ligand analogues. Their IR spectra showed three strong ν(CO) stretches similar in frequency to the analogous bidentate complexes with the NMR spectra illustrating one species present in solution. However the product of the reaction of TeMe$_2$ with [Mn(CO)$_5$Cl] exhibited two closely spaced δ(Me) resonances in both the ^{1}H and ^{13}C{^{1}H} NMR spectra of approximately equal intensity, and two δ(^{125}Te) resonances at 161 and 271 ppm. The ^{55}Mn NMR spectrum showed a moderately sharp peak at δ -637 ($w_{1/2}$ = 1600 Hz), but on longer accumulations a very broad feature at δ -920 ($w_{1/2}$ = 20 000 Hz) was observed. A second species however was not evident in the carbonyl region of the solution IR spectrum. This behaviour is very similar to that observed in the [Mn(CO)$_5$Cl]-SbPh$_3$ system,[27] and the second species may be identified as the *mer-trans*-

$[Mn(CO)_3(TeMe_2)_2Cl]$ isomer, which is consistent with the much broader ^{55}Mn resonance. In the stibine system, the two ν(CO) frequencies of the *mer-trans* isomer are very similar in energy to the two lower bands in the *fac* form, accounting for the difficulty in identifying the second form from the IR spectrum.[27]

fac-[Re(CO)$_3${MeTe(CH$_2$)$_3$TeMe}X] (X = Cl or Br) complexes. The ^1H NMR of *fac*-$[Re(CO)_3\{MeTe(CH_2)_3TeMe\}Br]$ showed three δ(Me) resonances (2.24, 2.30, 2.34 ppm) corresponding to the presence of the DL and one *meso* invertomers. However, the $^{125}Te\{^1H\}$ NMR spectrum showed four resonances (+78, +57, -4.5, -6.0 ppm) and the $^{13}C\{^1H\}$ NMR spectrum, four δ(Me) peaks (-10.4, -10.3, -9.2, -8.5 ppm), thereby indicating the presence of all invertomers. Therefore, it would seem likely that again two resonances are coinciding, in this case in the ^1H NMR spectrum. Similar NMR data were obtained for the chloro- complex, and the δ(Me) region of the $^{13}C\{^1H\}$ NMR spectrum is shown in Figure 2.4.

Figure 2.4. δ(Me) region of the $^{13}C\{^1H\}$ NMR Spectrum (90.1 MHz, $CH_2Cl_2/CDCl_3$, 300 K) of *fac*-$[Re(CO)_3\{MeTe(CH_2)_3TeMe\}Cl]$ showing the presence of *meso* and DL invertomers.

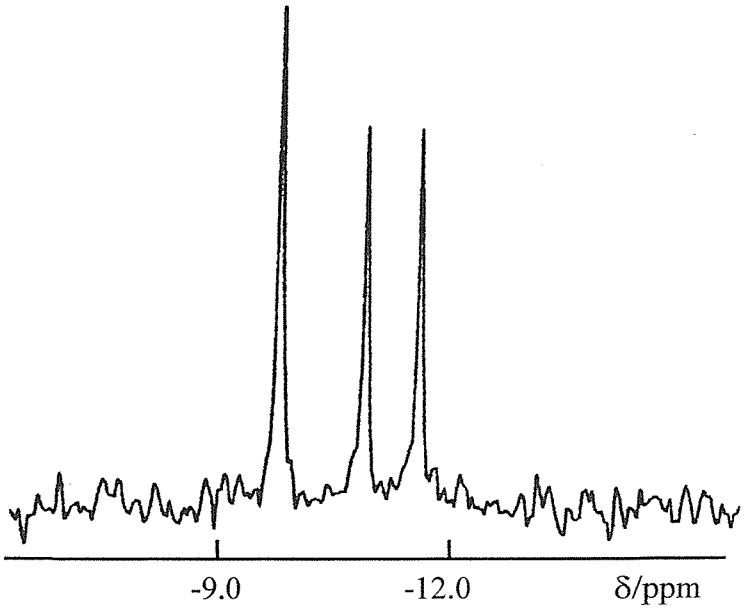

fac-[Re(CO)$_3${o-C$_6$H$_4$(TeMe)$_2$}X] (X = Cl or Br) complexes. The bromo- complex exhibited three resonances in the ^{125}Te{^{1}H} NMR spectrum (616, 607, 594 ppm) indicating the presence of the DL pair and *meso-2* invertomers, with three δ(Me) resonances in the ^{1}H NMR (2.32, 2.58, 2.40 ppm) and ^{13}C{^{1}H} NMR (-0.2, -1.2, -2.7 ppm) spectra being consistent with this. Interestingly, the chloro- complex showed four resonances in the ^{125}Te{^{1}H} NMR spectrum (629, 625, 612, 600 ppm) (Figure 2.5) and four δ(Me) signals in the ^{1}H NMR spectrum (2.35, 2.43, 2.50, 2.57 ppm) indicating the presence of all four invertomers. The ^{13}C{^{1}H} NMR spectrum, however, exhibited just two δ(Me) signal (-1.6, -4.7 ppm), evidently because the DL δ(Me) signals were too weak to be observed even after the data being collected overnight.

Figure 2.5. ^{125}Te{^{1}H} NMR spectrum (113.6 MHz, $CH_2Cl_2/CDCl_3$, 300 K) of *fac*-[Re(CO)$_3${*o*-C$_6$H$_4$(TeMe)$_2$}Cl].

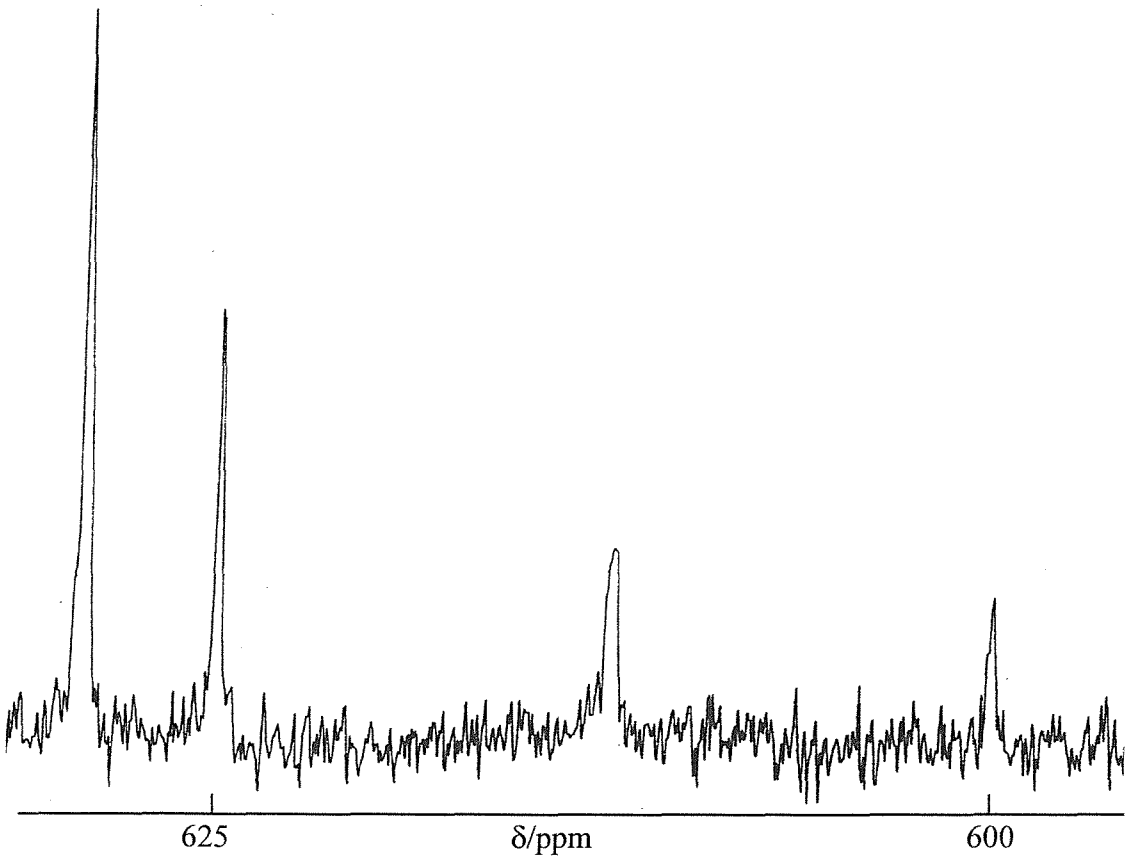

2.22 X-ray Crystallography

Prior to this study, there were no structurally characterised examples of ditelluroether complexes of metal carbonyls reported in the literature. Therefore, single crystal X-ray structure analyses have been carried out on *fac*-[$Mn(CO)_3\{o\text{-}C_6H_4(TeMe)_2\}Cl$] and *fac*-[$Re(CO)_3\{o\text{-}C_6H_4(TeMe)_2\}Cl$]. Crystals of the complexes were obtained from the vapour diffusion of light petroleum ether into a solution of the appropriate complex in $CHCl_3$. The compounds are isostructural, both showing (Figures 2.6 and 2.7, Tables 2.1 - 2.5) a distorted octahedral geometry at the metal centre, with a *fac* arrangement for the three CO ligands and the chelating ditelluroether adopting the *meso-2* arrangement, with both Me groups directed on the same side of the MTe_2C_2 plane. The Te-M-Te angles involved in the chelate rings are 87.60(4) and 85.42(3)° respectively. The Mn-X and Mn-C distances are very similar to those in analogous thio- and selenoether complexes [$Mn(CO)_3\{MeSCH_2CH_2SMe\}Cl$] (Mn-Cl = 2.3810(9), Mn-C = 1.796(3) - 1.823(3) Å),[14] and [$Mn(CO)_3\{MeSeCH_2CH_2SeMe\}Cl$] (Mn-Cl = 2.406(4), Mn-C = 1.79(2) - 1.80(2) Å)[15] whilst the Mn-E (E = S, Se, Te) bond lengths increase along the series as would be expected due to the increased radii of E.

Table 2.1. Crystallographic data collection and refinement parameters for *fac*-[Mn(CO)$_3${*o*-C$_6$H$_4$(TeMe)$_2$}Cl] and *fac*-[Re(CO)$_3${*o*-C$_6$H$_4$(TeMe)$_2$}Cl].

	fac-[Mn(CO)$_3${*o*-C$_6$H$_4$(TeMe)$_2$}Cl]	*fac*-[Re(CO)$_3${*o*-C$_6$H$_4$(TeMe)$_2$}Cl]
Formula	$C_{11}H_{10}ClMnO_3Te_2$	$C_{11}H_{10}ClReO_3Te_2$
Formula weight	535.79	667.06
Crystal System	Monoclinic	Monoclinic
Space group	$P2_1/n$	$P2_1/n$
a, Å	12.721(3)	12.728(6)
b, Å	8.340(6)	8.405(8)
c, Å	13.976(3)	14.095(6)
β/°	93.16(2)	93.24(4)
V, Å^3	1480(1)	1505(1)
Z	4	4
D_{calc}, g/cm^3	2.404	2.943
μ(Mo-K$_\alpha$), cm^{-1}	49.12	121.70
Unique obs. reflections	2798	2847
Obs. reflections with [$I_o > 2\sigma(I_o)$]	1755	1875
No. of parameters	163	163
R	0.029	0.031
R_w	0.029	0.026

$R = \Sigma (|F_{obs}|_i - |F_{calc}|_i) / \Sigma |F_{obs}|_i$, $R_w = \sqrt{[\Sigma w_i (|F_{obs}|_i - |F_{calc}|_i)^2 / \Sigma w_i |F_{obs}|_i^2]}$

Figure 2.6. X-ray crystal structure of *fac*-[Mn(CO)$_3${*o*-C$_6$H$_4$(TeMe)$_2$}Cl] with numbering scheme adopted. Ellipsoids are drawn at 40 % probability.

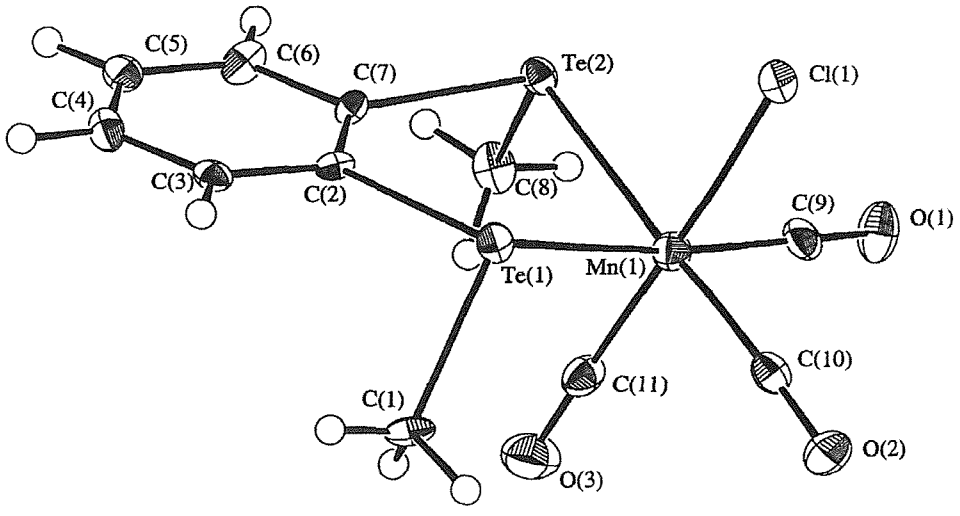

Table 2.2. Selected bond lengths for *fac*-[Mn(CO)$_3${*o*-C$_6$H$_4$(TeMe)$_2$}Cl].

Atom	Atom	Distance/Å	Atom	Atom	Distance/Å
Te(1)	Mn(1)	2.598(1)	Te(1)	C(1)	2.139(8)
Te(1)	C(2)	2.136(8)	Te(2)	Mn(1)	2.613(1)
Te(2)	C(7)	2.138(8)	Te(2)	C(8)	2.135(8)
Mn(1)	Cl(1)	2.411(2)	Mn(1)	C(9)	1.821(9)
Mn(1)	C(10)	1.819(9)	Mn(1)	C(11)	1.791(9)

Table 2.3. Selected bond angles for *fac*-[Mn(CO)$_3${*o*-C$_6$H$_4$(TeMe)$_2$}Cl].

Atom	Atom	Atom	Angle(°)	Atom	Atom	Atom	Angle(°)
Mn(1)	Te(1)	C(1)	106.5(3)	Mn(1)	Te(1)	C(2)	101.9(2)
C(1)	Te(1)	C(2)	92.8(3)	Mn(1)	Te(2)	C(7)	100.6(2)
Mn(1)	Te(2)	C(8)	102.8((2)	C(7)	Te(2)	C(8)	94.4(3)
Te(1)	Mn(1)	Te(2)	87.60(4)	Te(1)	Mn(1)	Cl(1)	83.23(6)
Te(1)	Mn(1)	C(9)	173.9(3)	Te(1)	Mn(1)	C(10)	93.0(3)
Te(1)	Mn(1)	C(11)	92.5(3)	Te(2)	Mn(1)	Cl(1)	87.82(7)
Te(2)	Mn(1)	C(9)	88.9(3)	Te(2)	Mn(1)	C(10)	179.2(3)
Te(2)	Mn(1)	C(11)	90.2(3)	Cl(1)	Mn(1)	C(9)	91.7(3)
Cl(1)	Mn(1)	C(10)	91.7(3)	Cl(1)	Mn(1)	C(11)	175.4(3)
C(9)	Mn(1)	C(10)	90.5(4)	C(9)	Mn(1)	C(11)	92.5(4)
C(10)	Mn(1)	C(11)	90.3(4)				

Figure 2.7. X-ray crystal structure of *fac*-[Re(CO)$_3${*o*-C$_6$H$_4$(TeMe)$_2$}Cl] with numbering scheme adopted. Ellipsoids are drawn at 40 % probability.

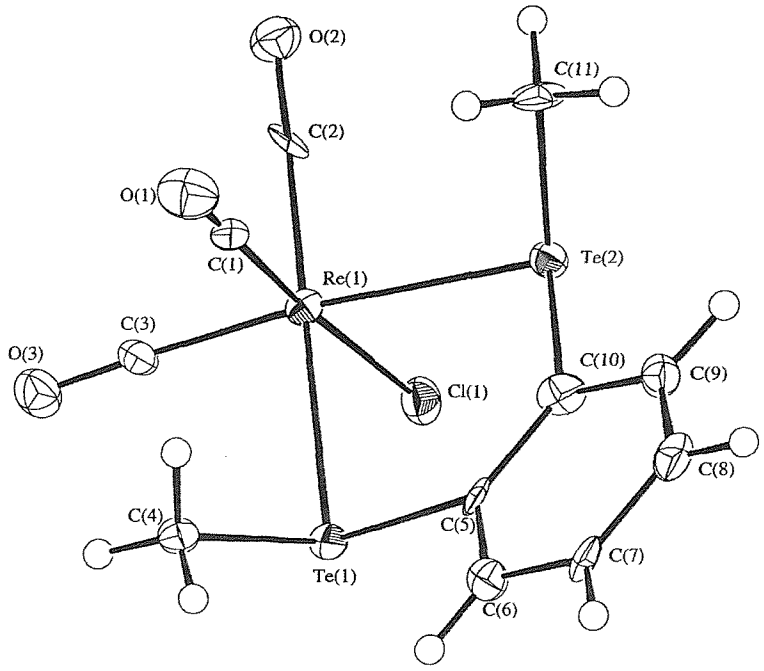

Table 2.4. Selected bond lengths for *fac*-[Re(CO)$_3${*o*-C$_6$H$_4$(TeMe)$_2$}Cl].

Atom	Atom	Distance/Å	Atom	Atom	Distance/Å
Re(1)	Te(1)	2.7416(9)	Re(1)	Te(2)	2.729(1)
Re(1)	Cl(1)	2.508(3)	Re(1)	C(1)	1.93(1)
Re(1)	C(2)	1.91(1)	Re(1)	C(3)	1.91(1)
Te(1)	C(4)	2.12(1)	Te(1)	C(5)	2.14(1)
Te(2)	C(10)	2.12(1)	Te(2)	C(11)	2.16(1)

Table 2.5. Selected bond angles for *fac*-[Re(CO)$_3${*o*-C$_6$H$_4$(TeMe)$_2$}Cl].

Atom	Atom	Atom	Angle(°)	Atom	Atom	Atom	Angle(°)
Te(1)	Re(1)	Te(2)	85.42(3)	Te(1)	Re(1)	Cl(1)	87.33(7)
Te(1)	Re(1)	C(1)	91.2(3)	Te(1)	Re(1)	C(2)	178.7(3)
Te(1)	Re(1)	C(3)	89.9(3)	Te(2)	Re(1)	Cl(1)	82.47(7)
Te(2)	Re(1)	C(1)	92.4(4)	Te(2)	Re(1)	C(2)	94.1(3)
Te(2)	Re(1)	C(3)	174.1(3)	Cl(1)	Re(1)	C(1)	174.8(4)
Cl(1)	Re(1)	C(2)	93.8(3)	C(1)	Re(1)	C(3)	91.3(5)
C(1)	Re(1)	C(2)	87.7(5)	Re(1)	Te(1)	C(4)	101.7(3)
C(2)	Re(1)	C(3)	90.7(5)	C(4)	Te(1)	C(5)	93.5(4)
Re(1)	Te(1)	C(5)	100.1(3)	Re(1)	Te(2)	C(11)	106.2(3)
Re(1)	Te(2)	C(10)	101.1(3)	C(10)	Te(2)	C(11)	93.6(5)

2.23 Some Comparisons

Recent work within the Southampton research group has investigated the spectroscopic and structural properties of dithio-[14] and diselenoether[15] analogues of the manganese complexes discussed here. In an attempt to identify the trends in bonding properties of L-L (L-L = dithio-, diseleno- or ditelluroether) in metal carbonyl complexes, a comparison of selected spectroscopic and structural data have been undertaken.

2.231 Crystallographic Comparisons

Comparisons of structural data on dithio-, diseleno- and ditelluroether complexes involving Cu^{I}, Ag^{I} and Sn^{IV} metal centres, have shown an increase in *d*(M-E) of *ca.* 0.1 Å from E = S to Se, and a further increase of *ca.* 0.15 Å from E = Se to Te.[28] For the *fac*-$[Mn(CO)_3(L\text{-}L)X]$ complexes the increase is again about 0.1 Å between *d*(Mn-S) and *d*(Mn-Se). However, the further increase to *d*(Mn-Te) is only *ca.* 0.13 Å. A similar difference in *d*(Re-Se/Te) exists between *fac*-$[Re(CO)_3\{MeSe(CH_2)_2SeMe\}I]$[26] and *fac*-$[Re(CO)_3\{o\text{-}C_6H_4(TeMe)_2\}Cl]$. However, some caution must be employed in interpreting such differences since the number of examples is small and also the data, in some cases, refer to different bidentate ligands and chelate ring sizes. It is, however, notable that in $[CpFe(CO)_2(EMe_2)]^+$ the Fe-Te bond length also appears shorter than expected, compared with the Fe-S/Se bond lengths.[29] With these cautions noted, the data support the view that the tellurium ligands form shorter and hence stronger bonds to metal carbonyls than would be expected from extrapolation of data on complexes with other metals.

2.232 Comparison of NMR Spectroscopic Data

Spectroscopic data, specifically the ^{55}Mn, $^{77}Se\{^1H\}$ and $^{125}Te\{^1H\}$ NMR data (Table 2.6), in the series of *fac*-$[Mn(CO)_3(L\text{-}L)X]$ complexes may also be compared. In order to simplify the comparisons, the chemical shifts for the different invertomers of each complex have been averaged. The manganese-55 chemical shifts for each set of halogen complexes are slightly more positive than those for the corresponding $[Mn(CO)_5X]$ species (X = Cl, δ -1005; Br, δ -1160; I, δ -1485).[30] Further, for each set of ditelluroether complexes upon changing X, $\delta(^{55}Mn)$ shifts approximately 150 ppm to low frequency according to the series

Cl > Br > I, consistent with the trend observed for the parent manganese(I) pentacarbonyl halides. However, the most interesting trend is observed as the group 16 donor atom is changed. Inspection of Figure 2.8 and Table 2.6 clearly shows that the ^{55}Mn NMR chemical shifts move progressively to lower frequency as the donor atom is changed S → Se → Te. This increased shielding of the manganese nucleus parallels the decrease in ν(CO) (see later) which is evidence, assuming π-back bonding to the chalcogen is negligible, that E → Mn σ-donation (E = S, Se, Te) increases in the same direction.[31]

Figure 2.8. Typical ^{55}Mn Chemical Shift ranges for *fac*-[Mn(CO)$_3$(L-L)X], {X = Cl, Br or I; L-L = RE(CH$_2$)$_n$ER (E = S, Se; R = Me, Ph, *n* = 2; R = Me, *n* = 3; E = Te; R = Me, Ph, n = 3) and *o*-C$_6$H$_4$(EMe)$_2$ (E = S, Se, Te)}.

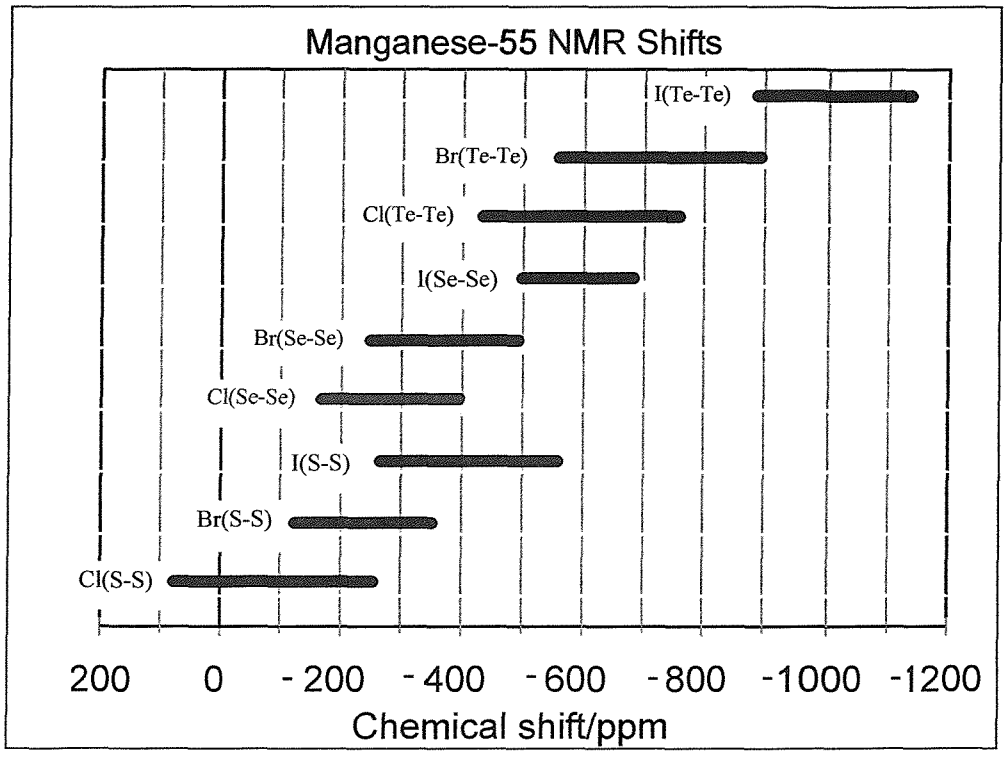

The coordination shifts (ΔR = $\delta_{complex}$ - $\delta_{free\ ligand}$) in the ^{125}Te{^{1}H} NMR spectra (Table 2.7) show the usual dependence upon chelate ring size, being small for the six membered rings in complexes of MeTe(CH$_2$)$_3$TeMe, and very large for the five membered rings formed by *o*-C$_6$H$_4$(TeMe)$_2$, giving further confirmation that the ditelluroethers are chelating in all of the complexes.[32, 33]

Table 2.6. Selected ^{55}Mn, $^{77}Se\{^1H\}$ and $^{125}Te\{^1H\}$ NMR Data.

Compound	$\delta^{55}Mn$[a]/ppm	$\delta^{125}Te\{^1H\}$[b]/ppm
fac-		
$[Mn(CO)_3\{o\text{-}C_6H_4(TeMe)_2\}Cl]$	-774 (3000), -717 (1500)	829, 824 (br)
$[Mn(CO)_3\{o\text{-}C_6H_4(TeMe)_2\}Br]$	-901 (2800), -827 (1660)	818, 817, 815
$[Mn(CO)_3\{o\text{-}C_6H_4(TeMe)_2\}I]$	-1146 (2800), -1050 (1200)	806, 786
$[Mn(CO)_3\{MeTe(CH_2)_3TeMe\}Cl]$	-644 (2000), -594(sh), -581 (1700)	280, 234, 203, 185
$[Mn(CO)_3\{MeTe(CH_2)_3TeMe\}Br]$	-753 (1855), -690 (1640)	260, 213, 180, 165
$[Mn(CO)_3\{MeTe(CH_2)_3TeMe\}I]$	-975 (1500), -916 (1500), -888(sh)	226, 225, 206, 135
$[Mn(CO)_3\{PhTe(CH_2)_3TePh\}Cl]$	-435 (1080), -500 (1000), -613 (1120)	Decomposes (see text)
$[Mn(CO)_3\{PhTe(CH_2)_3TePh\}Br]$	-634 (1200), -568 (1500)	Decomposes (see text)
$[Mn(CO)_3(SMe_2)_2Cl]$	-57 (800)	-
$[Mn(CO)_3(SeMe_2)_2Cl]$	-205 (2200)	66[c]
$[Mn(CO)_3(TeMe_2)_2Cl]$	-637 (1600), -920 (20000)[d]	161, 271[d]
$[Re(CO)_3\{o\text{-}C_6H_4(TeMe)_2\}Cl]$	-	629, 625, 612, 599.5
$[Re(CO)_3\{o\text{-}C_6H_4(TeMe)_2\}Br]$	-	616, 606.5, 593.5
$[Re(CO)_3\{MeTe(CH_2)_3TeMe\}Cl]$	-	101, 77, 20, 19.5
$[Re(CO)_3\{MeTe(CH_2)_3TeMe\}Br]$	-	78, 57, -4.5, -6
$[Re(CO)_3\{o\text{-}C_6H_4(SeMe)_2\}Br]$	-	305, 294, 289, 272[c]

[a] in $CH_2Cl_2/CDCl_3$ solution at 300 K, relative to external $KMnO_4$ in water, $w_{1/2}$ (Hz) in parenthesis. [b] in $CH_2Cl_2/CDCl_3$ solution at 300 K, relative to neat external $TeMe_2$. [c] $^{77}Se\{^1H\}$ NMR, in $CH_2Cl_2/CDCl_3$ solution at 300 K, relative to neat external $SeMe_2$. [d] resonance of *mer-trans* isomer.

For many comparable organo-selenium and -tellurium compounds the ^{77}Se and ^{125}Te chemical shifts show very consistent trends and often the $\delta(^{125}Te)/\delta(^{77}Se)$ ratio is 1.7-1.8 and the $^{1}J(Te\text{-}X)/^{1}J(Se\text{-}X)$ ratio *ca.* 2-3.[34] Such trends have been observed in Pd(II) and Pt(II) diseleno- and ditelluroether complexes.[33, 35] Since both Mn and Re are quadrupolar nuclei, no one-bond couplings were resolved, but the chemical shifts are listed in Table 2.6. To simplify the comparisons the average chemical shift for the different invertomers of each complex has been used and the results are given in Table 2.7. The $\delta(^{125}Te)/\delta(^{77}Se)$ ratio ranges from 2.1 to 2.9, and although clearly the spread of values suggest that individual figures should be treated with some caution, the overall trend is very clear. The ^{125}Te chemical shifts found for the coordinated telluroethers in the present carbonyl complexes are much more positive than expected, either by comparison with the ^{77}Se chemical shifts in the selenoether analogues, or by similar comparisons with the same ligands bound to medium oxidation state metal centres. Similar conclusions have been reached by Schumann and co-workers, from studies of the complexes $[CpFe(CO)_2(EMe_2)]^+$ (E = O, S, Se, Te).[36]

Table 2.7. Comparison of NMR data for the complexes *fac*-$[Mn(CO)_3(L\text{-}L)X]$.

Complex[a]	$\delta(^{77}Se)$[b]	$\Delta(^{77}Se)$[c]	$\delta(^{125}Te)$[b]	$\Delta(^{125}Te)$[c]	$\delta(^{125}Te)/\delta(^{77}Se)$
fac-					
$[Mn(CO)_3\{MeE(CH_2)_3EMe\}Cl]$	91	17	225.5	121.5	2.48
$[Mn(CO)_3\{MeE(CH_2)_3EMe\}Br]$	79	5	204.5	100.5	2.59
$[Mn(CO)_3\{MeE(CH_2)_3EMe\}I]$	67.5	-6.5	198	94	2.9
$[Mn(CO)_3\{o\text{-}C_6H_4(EMe)_2\}Cl]$	397	195	826.5	454.5	2.08
$[Mn(CO)_3\{o\text{-}C_6H_4(EMe)_2\}Br]$	387	185	817	445	2.11
$[Mn(CO)_3\{o\text{-}C_6H_4(EMe)_2\}I]$	386	184	796	424	2.06
$[Mn(CO)_3(EMe_2)_2Cl]$	66	66	161	161	2.44

[a] E = Se, Te. [b] averaged chemical shifts from Table 2.6 and reference 15 in ppm. [c] $\delta_{complex} - \delta_{free\ ligand}$ in ppm.

2.233 Trends in ν(CO)

The carbonyl stretching vibrations are listed in Table 2.8 along with literature data on isostructural dithio- and diselenoether complexes. The force constants were calculated using the usual secular equations[37] (shown below) and the co-ordinate system used is shown in Figure 2.9.

$$\begin{vmatrix} \mu k_1 - \lambda & \sqrt{2}k_i \\ \sqrt{2}k_i & \mu(k_2 + k_i) - \lambda \end{vmatrix} = 0$$

$$\lambda = \mu(k_2 - k_i)$$

(where μ is the reduced mass of the CO group, *viz.* (16.00 + 12.01)/(16.00 x 12.01) = 0.14583 and $\lambda = (5.8890 \times 10^{-2})\nu^2$ where ν is the frequency in cm^{-1})

Solution of these three equations was achieved *via* elimination of k_1 and k_2 to obtain a quadratic equation in k_i, solution of which gave a positive and negative value of k_i. The negative root was rejected, and the positive value for k_i used to calculate k_1 and k_2. For each complex, the three possible assignments of the three fundamental ν(CO) vibrations were investigated. The assignment eventually used, A'(2) > A" > A'(1), is the same as that used in similar complexes, and gave chemically sensible force constants ($k_i > 0$, $k_1 < k_2$),[37, 38] and resulted in internally consistent trends. Other assignments gave either complex force constants using A" > A'(2) > A'(1), or $k_2 < k_1$ using A'(1) > A'(2) > A".

Figure 2.9. Co-ordinate system used for *fac*-[M(CO)$_3$XY$_2$] complexes, where Y = S, Se or Te and X = Cl, Br or I.

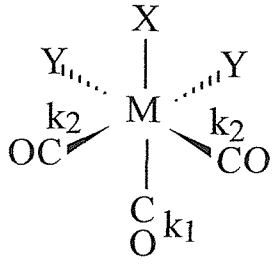

Table 2.8. [M(CO)$_3$(L-L)X] ν(CO) frequencies and derived force constants.

Complex	ν(CO)[a]/cm^{-1}			k_1	k_2	k_i
fac-	A'(2)	A"	A'(1)	in millidynes Å^{-1}		
[Mn(CO)$_3${*o*-C$_6$H$_4$(TeMe)$_2$}Cl]	2026(s)	1957(m)	1916(m)	15.07	15.90	0.4312
[Mn(CO)$_3${*o*-C$_6$H$_4$(TeMe)$_2$}Br]	2024(s)	1956(m)	1917(m)	15.09	15.87	0.4234
[Mn(CO)$_3${*o*-C$_6$H$_4$(TeMe)$_2$}I]	2020(s)	1954(m)	1918(m)	15.10	15.83	0.4086
[Mn(CO)$_3${MeTe(CH$_2$)$_3$TeMe}Cl]	2021(s)	1949(m)	1906(m)	14.93	15.79	0.4487
[Mn(CO)$_3${MeTe(CH$_2$)$_3$TeMe}Br]	2019(s)	1949(m)	1907(m)	14.94	15.78	0.4362
[Mn(CO)$_3${MeTe(CH$_2$)$_3$TeMe}I]	2016(s)	1947(m)	1908(m)	14.95	15.74	0.4272
[Mn(CO)$_3${PhTe(CH$_2$)$_3$TePh}Cl]	2025(s)	1957(m)	1917(m)	15.08	15.89	0.4245
[Mn(CO)$_3${PhTe(CH$_2$)$_3$TePh}Br]	2024(s)	1959(m)	1914(m)	15.02	15.91	0.4117
[Mn(CO)$_3$(TeMe$_2$)$_2$Cl]	2017(s)	1942(m)	1907(m)	14.97	15.69	0.4565
[Mn(CO)$_3$(SeMe$_2$)$_2$Cl]	2027(s)	1948(s)	1916(s)	15.14	15.80	0.4773
[Mn(CO)$_3$(SMe$_2$)$_2$Cl]	2034(s)	1954(s)	1920(s)	15.20	15.91	0.4868
[Mn(CO)$_3${*o*-C$_6$H$_4$(SeMe)$_2$}Cl][b]	2037	1964	1924	15.22	16.03	0.4551
[Mn(CO)$_3${*o*-C$_6$H$_4$(SeMe)$_2$}Br][b]	2035	1963	1924	15.21	16.01	0.4481
[Mn(CO)$_3${*o*-C$_6$H$_4$(SeMe)$_2$}I][b]	2030	1960	1924	15.21	15.95	0.4329
[Mn(CO)$_3${MeSe(CH$_2$)$_3$SeMe}Cl][b]	2032	1955	1917	15.13	15.91	0.4741
[Mn(CO)$_3${MeSe(CH$_2$)$_3$SeMe}Br][b]	2030	1954	1918	15.15	15.88	0.4661
[Mn(CO)$_3${MeSe(CH$_2$)$_3$SeMe}I][b]	2025	1951	1918	15.14	15.82	0.4507
[Mn(CO)$_3${*o*-C$_6$H$_4$(SMe)$_2$}Cl][c]	2041	1965	1927	15.28	16.06	0.4707
[Mn(CO)$_3${*o*-C$_6$H$_4$(SMe)$_2$}Br][c]	2039	1965	1927	15.27	16.05	0.4592
[Mn(CO)$_3${*o*-C$_6$H$_4$(SMe)$_2$}I][c]	2035	1963	1928	15.29	16.01	0.4441
[Mn(CO)$_3${MeS(CH$_2$)$_3$SMe}Cl][c]	2036	1954	1923	15.27	15.91	0.4947
[Mn(CO)$_3${MeS(CH$_2$)$_3$SMe}Br][c]	2034	1955	1924	15.27	15.91	0.4779
[Mn(CO)$_3${MeS(CH$_2$)$_3$SMe}I][c]	2031	1957	1927	15.29	15.91	0.4487
[Re(CO)$_3${*o*-C$_6$H$_4$(TeMe)$_2$}Cl]	2032(s)	1951(m)	1908(m)	15.00	15.87	0.5012
[Re(CO)$_3${*o*-C$_6$H$_4$(TeMe)$_2$}Br]	2032(s)	1952(m)	1908(m)	14.99	15.88	0.4966
[Re(CO)$_3${MeTe(CH$_2$)$_3$TeMe}Cl]	2028(s)	1942(m)	1899(m)	14.89	15.76	0.5277
[Re(CO)$_3${MeTe(CH$_2$)$_3$TeMe}Br]	2028(s)	1943(m)	1901(m)	14.91	15.77	0.5212
[Re(CO)$_3${*o*-C$_6$H$_4$(SeMe)$_2$}Br]	2038(s)	1953(s)	1911(s)	15.07	15.93	0.5238
[Re(CO)$_3${MeSe(CH$_2$)$_3$SeMe}Cl][d]	2034	1938	1906	15.07	15.74	0.5710
[Re(CO)$_3${MeSe(CH$_2$)$_3$SeMe}Br][d]	2038	1942	1906	15.06	15.81	0.5771
[Re(CO)$_3${MeSe(CH$_2$)$_3$SeMe}I][d]	2036	1944	1906	15.03	15.82	0.5572
[Re(CO)$_3${*o*-C$_6$H$_4$(SMe)$_2$}Br]	2041(s)	1957(s)	1913(s)	15.09	15.99	0.5211
[Re(CO)$_3${MeS(CH$_2$)$_3$SMe}Cl][d]	2037	1945	1912	15.14	15.83	0.5516
[Re(CO)$_3${MeS(CH$_2$)$_3$SMe}Br][d]	2042	1950	1914	15.16	15.91	0.5566
[Re(CO)$_3${MeS(CH$_2$)$_3$SMe}I][d]	2038	1948	1912	15.12	15.87	0.5446

[a] in $CHCl_3$ solution, [b] frequency data from reference 14, [c] frequency data from reference 15, [d] frequency data from reference 22.

Examination of the data in Table 2.8 shows that factors such as the halogen present, the chelate ring size and the R groups on the group 16 donor have some influence, but the most significant trend is observed with changes in the group 16 donor atom. These data suggest that the CO bonds weaken in the order S → Se → Te, and with significantly larger changes between Se and Te than between S and Se. These observations are found for both the manganese and rhenium complexes. The rationalisation for this observed trend is that as group 16 is descended more electron density is transferred to the metal centre, hence resulting in increased π-acceptance by the carbonyl groups. There is little evidence that π bonding (either donation or acceptance) plays any significant role in the group 16 donor-metal bond,[29, 32] and therefore the primary contribution to this trend is increased σ-donation as group 16 is descended and electronegativity of the chalcogen decreases. In Sn(IV) metal halide systems, there is some evidence for stronger binding by Se over S, but tellurium ligands appear to bind more weakly as the metal oxidation state increases,[32] probably due to poorer overlap between the large Te σ-donor orbital and the contracted metal orbitals. However, the present studies in low-valent carbonyl systems, where mismatch of the Te orbitals with the expanded metal orbitals is less likely to be significant, are consistent with very good donation from Te, resulting in an anomalously large increase in σ-donation from Se to Te. These results are thus entirely in accord with the theoretical predictions of Schumann and co-workers.[36]

Upon changing from manganese to rhenium little change is observed in the value of k_2, however the value of k_1 is generally smaller for the rhenium complexes. A decrease of *ca.* 0.1 millidynes $Å^{-1}$ is observed for thio- and selenoether complexes, with a smaller decrease of *ca.* 0.05 millidynes $Å^{-1}$ for telluroether complexes. Therefore, increased back bonding to the carbonyl groups is observed in the rhenium complexes, compared to the manganese complexes. In order to establish whether this increased back bonding is due to the group 16 ligands, the $^{125}Te\{^1H\}$ and $^{77}Se\{^1H\}$ NMR spectra may be inspected. Generally, the NMR shifts are less positive in the rhenium complexes than manganese analogues. Therefore, less σ-donation from the chalcogen is observed in rhenium complexes and so the decrease in k_1 on going from manganese to rhenium may be contributed to the increased electron density on rhenium.

2.3 Conclusions

The bidentate telluroether ligands, L-L, {L-L = $MeTe(CH_2)_3TeMe$ and *o*-$C_6H_4(TeMe)_2$} have been reacted with $[Mn(CO)_5X]$ (X = Cl, Br or I) and $[Re(CO)_5X]$ (X = Cl or Br) to give the complexes *fac*-$[M(CO)_3(L\text{-}L)X]$ (M = Mn or Re). The single crystal X-ray structures of $[Mn(CO)_3\{o\text{-}C_6H_4(TeMe)_2\}Cl]$ and $[Re(CO)_3\{o\text{-}C_6H_4(TeMe)_2\}Cl]$ have confirmed that these complexes exist as the *fac* isomers, with a distorted octahedral geometry about the Mn and Re metal centres and the chelating telluroether ligand adopting the *meso-2* arrangement. The monodentate complexes $[Mn(CO)_3(EMe_2)_2Cl]$ (E = S, Se, Te) have also been synthesised and it has been shown that whereas the thio- and selenoether complexes exist as the *fac-* isomers in solution, the telluroether complex is a mixture of both the *fac-* and the *mer-trans-* isomers.

Comparison of selected spectroscopic and crystallographic data for these complexes with those reported for the analogous thio- and selenoether complexes in the literature have provided information concerning the bonding properties of group 16 donor atoms to low valent carbonyl systems.

The manganese-55 NMR data for analogous complexes have shown that $\delta(^{55}Mn)$ is shifted to low frequency, indicating that the manganese nucleus experiences greater shielding, upon descending group 16 (Table 2.9).

Table 2.9. Chemical shift range for the complexes *fac*-$[Mn(CO)_3(L\text{-}L)X]$.

Ligand type	Manganese-55 chemical shift range[a]/ ppm
Thioether	67 to -567
Selenoether	-175 to -698
Telluroether	-435 to -1146

[a] relative to external $KMnO_4$ in water.

In addition to this, comparison of the ratio $\delta(^{125}Te)/\delta(^{77}Se)$ for these complexes with other group 16 compounds reported in the literature has shown the tellurium-125 chemical shifts for *fac*-$[Mn(CO)_3(L\text{-}L)X]$ to be much more positive than expected, thereby indicating increased σ-donation from the telluroether ligands. Crystallographic data corroborate this evidence, with comparison of the Mn-E (E = S, Se, Te) bond lengths in *fac*-$[Mn(CO)_3(L\text{-}L)X]$ with other group 16 complexes indicating that the Mn-Te bond is *ca.* 0.02 Å shorter than expected.

Finally, force constant calculations for the carbonyl groups have shown that the CO bonds weaken in the order S → Se → Te, with significantly larger changes between Se and Te than between S and Se.

The data therefore all suggest that σ-donation increases in the order S < Se << Te as a result of the decreasing electronegativity of the chalcogen atom as group 16 is descended.

2.4 Experimental

The ditelluroether ligands were made as described previously.[39, 40] Manganese(I) and rhenium(I) carbonyl halides were prepared by the literature methods.[41, 42] The reactions were protected from light by wrapping the reaction flask in foil and the isolated manganese complexes were stored in foil wrapped ampoules in a refrigerator. All compounds were synthesised by the same general procedure, with slight modifications for X = Cl, Br or I, examples of which are described.

fac-$[Mn(CO)_3\{o\text{-}C_6H_4(TeMe)_2\}Cl]$. To a solution of $[Mn(CO)_5Cl]$ (60 mg, 2.6 x 10^{-4} mol) in $CHCl_3$ (40 cm^3) was added the ditelluroether ligand (9.4 mg, 2.6 x 10^{-4} mol) and the solution stirred at room temperature. Removing aliquots of the solution and recording their IR spectra was used to monitor the progress of the reaction and after 16 hours, the carbonyl bands of $[Mn(CO)_5Cl]$ had been replaced by three new vibrations. The solution was concentrated under vacuum to *ca.* 2 cm^3, cooled in an ice-bath, and cold light petroleum ether (40-60 °C) (10 cm^3) added to precipitate the yellow product. The precipitate was collected, rinsed with cold petroleum ether (1 cm^3) and dried *in vacuo*. Yield 111 mg, 80 %. Analysis: Calculated for $C_{11}H_{10}ClMnO_3Te_2$: %C, 24.6; %H, 1.9. Found: %C, 24.7; %H, 2.2. ^1H NMR ($CDCl_3$, 300 K): δ 2.23 (s), 2.51 (s) (DL), 2.32 (s) (*meso*) (3H, $TeCH_3$), 7.5 - 7.8 (m, 2H, C_6H_4). $^{13}C\{^1H\}$ NMR ($CH_2Cl_2/CDCl_3$, 300 K): δ -2.3, -2.6, -4.4 ($TeCH_3$), 126.5, 130.7, 139.5 (C_6H_4), 220 - 223 (CO). FAB MS (3-NOBA), *m/z* = 538, 503, 454; calc. for $[Mn(CO)_3\{o\text{-}C_6H_4(^{130}TeMe)_2\}^{35}Cl]^+$ 540, $[Mn(CO)_3\{o\text{-}C_6H_4(^{130}TeMe)_2\}]^+$ 505, $[Mn\{o\text{-}C_6H_4(^{130}TeMe)_2\}^{35}Cl]^+$ 456. IR/cm^{-1} 3028(w), 2962(w), 2009(s), 1944(s), 1891(s), 1441(w), 1451(s), 1258(w), 1218(w), 1081(w), 850(w), 757(s), 666(m), 631(m), 608(m), 514(m), 486(w), 425(w), 321(w), 270(w), 245(w), 221(w), 197(w), 189(w).

fac-$[Mn(CO)_3\{MeTe(CH_2)_3TeMe\}Cl]$ was prepared similarly to give a yellow solid (49 %). Analysis: Calculated for $C_8H_{12}ClMnO_3Te_2$: %C, 19.1; %H, 2.4. Found: %C, 19.1; %H, 2.2. ^1H NMR ($CDCl_3$, 300 K): δ 1.7 - 1.9 (br, 1H, $CH_2CH_2CH_2$), 2.12 (s), 2.19 (s), 2.22 (s), 2.27 (s) ($TeCH_3$, 3H), 2.7 - 3.2 (br, 2H, $TeCH_2$). $^{13}C\{^1H\}$ NMR ($CH_2Cl_2/CDCl_3$, 300 K): δ -9.7, -10.5, -12.1, -12.6 ($TeCH_3$), 6.9, 8.0, 8.4 ($TeCH_2$), 26.0 ($CH_2CH_2CH_2$), 216 - 226 (CO). FAB MS (3-NOBA), *m/z* = 508, 469, 420; calc. for $[Mn(CO)_3\{Me^{130}Te(CH_2)_3{}^{130}TeMe\}^{35}Cl]^+$ 506, $[Mn(CO)_3\{Me^{130}Te(CH_2)_3{}^{130}TeMe\}]^+$ 471,

$[Mn\{Me^{130}Te(CH_2)_3{}^{130}TeMe\}^{35}Cl]^+$ 422. IR/cm^{-1} 2969(w), 2918(w), 2007(s), 1920(s), 1892(s), 1412(m), 1356(s), 1260(w), 1227(w), 1189(w), 1096(m), 995(m), 846(m), 718(w), 668(s), 631(m), 615(s), 513(m), 272(w), 219(w), 200(w), 191(w).

fac-$[Mn(CO)_3\{PhTe(CH_2)_3TePh\}Cl]$ was prepared similarly to give a yellow powder (54 %). Analysis: Calculated for $C_{18}H_{16}ClMnO_3Te_2$: %C, 34.5; %H, 2.6. Found: %C, 33.9; %H, 2.7. ^1H NMR ($CDCl_3$, 300 K): δ 1.6 - 1.9 (br, 1H, $CH_2CH_2CH_2$), 3.0 - 3.4 (br, 2H, $TeCH_2$), 7.4 - 7.7 (br, 5H, TePh). $^{13}C\{^1H\}$ NMR ($CH_2Cl_2/CDCl_3$, 300 K): decomposes see text. FAB MS (3-NOBA), *m/z* = 593, 544; calc. for $[Mn(CO)_3\{Ph^{130}Te(CH_2)_3{}^{130}TePh\}]^+$ 595, $[Mn\{Ph^{130}Te(CH_2)_3{}^{130}TePh\}^{35}Cl]^+$ 546 IR/cm^{-1} 3020(w), 2983(w), 2009(s), 1919(s), 1892(s), 1568(w), 1470(w), 1431(m), 1356(s), 1095(s), 1016(w), 996(w), 834(w), 734(m), 689(m), 666(m), 627(m), 612(m), 537(m), 453(w), 216(w), 194(w).

fac-$[Mn(CO)_3\{o\text{-}C_6H_4(TeMe)_2\}Br]$ was prepared similarly from $[Mn(CO)_5Br]$ and the ligand in $CHCl_3$ heated to 50 °C for 4 hours to give an orange solid (57 %). Analysis: Calculated for $C_{11}H_{10}BrMnO_3Te_2$: %C, 22.8; %H, 1.7. Found: %C, 22.4; %H, 1.8. ^1H NMR ($CDCl_3$, 300 K): δ 2.22 (s), 2.56 (s) (DL), 2.30 (s) (*meso*) (3H, $TeCH_3$), 7.5 - 7.8 (m, 2H, C_6H_4). $^{13}C\{^1H\}$ NMR ($CH_2Cl_2/CDCl_3$, 300 K): δ -2.2, -1.0, 1.6 ($TeCH_3$), 127.0, 131.2, 140.5 (C_6H_4), 220 - 223 (CO). FAB MS (3-NOBA), *m/z* = 582, 498; calc. for $[Mn(CO)_3\{o\text{-}C_6H_4(^{130}TeMe)_2\}^{79}Br]^+$ 584, $[Mn\{o\text{-}C_6H_4(^{130}TeMe)_2\}^{79}Br]^+$ 500. IR/cm^{-1} 2921(w), 2852(w), 2041(s), 1953(s), 1926(s), 1901(s), 1437(m), 1357(s), 1216(w), 1094(s), 987(m), 835(m), 767(m), 666(m), 613(m), 535(m), 522(m), 323(w), 296(w), 207(w).

fac-$[Mn(CO)_3\{MeTe(CH_2)_3TeMe\}Br]$ was prepared similarly to give an orange solid (38 %). Analysis: Calculated for $C_8H_{12}BrMnO_3Te_2$: %C, 17.6; %H, 2.2. Found: %C, 17.9; %H, 2.3. ^1H NMR ($CDCl_3$, 300 K): δ 1.7 - 2.0 (br, 1H, $CH_2CH_2CH_2$), 2.12 (s), 2.20 (s), 2.22 (s), 2.29 (s) (3H, $TeCH_3$), 2.7 - 3.3 (br, 2H, $TeCH_2$). $^{13}C\{^1H\}$ NMR ($CH_2Cl_2/CDCl_3$, 300 K): δ -11.8, -10.6, -10.0, -8.7 ($TeCH_3$), 7.6, 8.3, 8.8 ($TeCH_2$), 25.4, 25.9 ($CH_2CH_2CH_2$), 215 - 221 (CO). FAB MS (3-NOBA), *m/z* = 548, 464; calc. for $[Mn(CO)_3\{Me^{130}Te(CH_2)_3{}^{130}TeMe\}^{79}Br]^+$ 550, $[Mn\{Me^{130}Te(CH_2)_3{}^{130}TeMe\}^{79}Br]^+$ 466. IR/cm^{-1} 2944(w), 2922(w), 2006(s), 1926(s), 1896(s), 1357(s), 1260(w), 1095(s), 834(m), 802(m), 667(m), 615(m), 535(m), 220(w).

fac-[$Mn(CO)_3\{PhTe(CH_2)_3TePh\}Br$] was prepared similarly to produce a yellow solid (60 %). Analysis: Calculated for $C_{18}H_{16}BrMnO_3Te_2$: %C, 32.2; %H, 2.4. Found: %C, 32.7; %H, 2.3. ^1H NMR ($CDCl_3$, 300 K): δ 1.6 - 1.9 (br, 1H, $CH_2CH_2CH_2$), 2.9 - 3.4 (br, 2H, $TeCH_2$), 7.4 - 7.7 (br, 5H, TePh). $^{13}C\{^1H\}$ NMR ($CH_2Cl_2/CDCl_3$, 300 K): decomposes see text. FAB MS (3-NOBA), *m/z* = 672, 588; calc. for $[Mn(CO)_3\{Ph^{130}Te(CH_2)_3{}^{130}TePh\}^{79}Br]^+$ 674, $[Mn\{Ph^{130}Te(CH_2)_3{}^{130}TePh\}^{79}Br]^+$ 590. IR/cm^{-1} 3100(w), 2990(w), 2008(s), 1920(s), 1893(s), 1569(w), 1430(w), 1357(s), 1259(w), 1095(s), 996(m), 834(m), 735(m), 689(m), 664(m), 612(m), 538(m), 248(w), 219(w), 198(w).

fac-[$Mn(CO)_3\{o\text{-}C_6H_4(TeMe)_2\}I$] was prepared similarly with a reaction time of 18 hours in refluxing $CHCl_3$, to give an orange solid (58 %). Analysis: Calculated for $C_{11}H_{10}IMnO_3Te_2$: %C, 21.1; %H, 1.6. Found: %C, 20.7; %H, 1.3. ^1H NMR ($CDCl_3$, 300 K): δ 2.17 (s), 2.67 (s) (DL), 2.19 (*meso*) (3H, $TeCH_3$), 7.6 - 7.8 (m, 2H, C_6H_4). $^{13}C\{^1H\}$ NMR ($CH_2Cl_2/CDCl_3$, 300 K): δ -1.2, 0.8, 2.4 ($TeCH_3$), 128.2, 131.5, 140.5 (C_6H_4), 218 - 226 (CO). FAB MS (3-NOBA), *m/z* = 627, 544, 501; calc. for $[Mn(CO)_3\{o\text{-}C_6H_4(^{130}TeMe)_2\}I]^+$ 632, $[Mn\{o\text{-}C_6H_4(^{130}TeMe)_2\}I]^+$ 548, $[Mn(CO)_3\{o\text{-}C_6H_4(^{130}TeMe)_2\}]^+$ 505. IR/cm^{-1} 2928(w), 2023(s), 1950(s), 1926(s), 1902(s), 1357(s), 1215(m), 1094(s), 984(m), 834(m), 757(m), 664(m), 612(m), 537(m), 322(w), 298(w), 242(w), 220(w), 204(w).

fac-[$Mn(CO)_3\{MeTe(CH_2)_3TeMe\}I$] was prepared similarly using a 9 hour reaction time to give an orange solid (40 %). Analysis: Calculated for $C_8H_{12}IMnO_3Te_2.CHCl_3$: %C, 15.2; %H, 1.8. Found: %C, 15.1; %H, 1.8. ^1H NMR ($CDCl_3$, 300 K): δ 1.8 - 2.0 (br, 1H, $CH_2CH_2CH_2$), 2.12 (s), 2.18 (s), 2.27 (s) (3H, $TeCH_3$), 2.7 - 3.3 (br, 2H, $TeCH_2$). $^{13}C\{^1H\}$ NMR ($CH_2Cl_2/CDCl_3$, 300 K): δ -10.7, -9.3, -8.0 ($TeCH_3$), 8.6, 9.0, 9.2 ($TeCH_2$), 24.4, 28.5 (CH_2CH_2), 215 - 226 (CO). FAB MS (3-NOBA), *m/z* = 595, 511, 467; calc. for $[Mn(CO)_3\{Me^{130}Te(CH_2)_3{}^{130}TeMe\}I]^+$ 598, $[Mn\{Me^{130}Te(CH_2)_3{}^{130}TeMe\}I]^+$ 514, $[Mn(CO)_3\{Me^{130}Te(CH_2)_3{}^{130}TeMe\}]^+$ 471. IR/cm^{-1} 2962(w), 2918(w), 1995(s), 1920(s), 1894(s), 1357(s), 1261(w), 1092(s), 987(m), 834(m), 664(m), 615(m), 535(m), 203(w), 195(w).

fac-[$Mn(CO)_3(SMe_2)_2Cl$]. To a solution of [$Mn(CO)_5Cl$] (0.113g, 0.5 mmol) in CH_2Cl_2 (10 cm^3) was added excess SMe_2 (100 mg, 1.6 x 10^{-3} mol) and the solution stirred at room temperature. The progress of the reaction was monitored by solution IR spectroscopy as

before and after 24 was judged complete. The solution was concentrated to *ca.* 2 cm^3 in a stream of nitrogen, cooled in an ice bath and cold petroleum ether (10 cm^3) added. The yellow precipitate was filtered off and dried briefly in a nitrogen stream. Note that the complex loses ligand when placed under vacuum and hence must not be vacuum dried. Yield 120 mg, 80 %. Analysis: Calculated for $C_7H_{12}ClMnO_3S_2$: %C, 28.1; %H, 4.0. Found: %C, 27.7; %H, 3.8. ^1H NMR ($CDCl_3$, 300 K): δ 2.4 (br, SCH_3). $^{13}C\{^1H\}$ NMR ($CH_2Cl_2/CDCl_3$, 300 K): δ 22.4 (SCH_3), 217 - 220 (CO). FAB MS (3-NOBA), *m/z* = 270, 242; calc. for $[Mn(CO)_2(SMe_2)_2{}^{35}Cl]^+$ 270, $[Mn(CO)(SMe_2)_2{}^{35}Cl]^+$ 242. IR/cm^{-1} 2924(w), 2023(s), 1918(br, s), 1357(s), 1095(s), 986(m), 833(w), 679(w), 624(w), 535(w), 203(w), 192(w).

fac-$[Mn(CO)_3(SeMe_2)_2Cl]$ was prepared similarly (83 %). Analysis: Calculated for $C_7H_{12}ClMnO_3Se_2$: %C, 21.4; %H, 3.1. Found: %C, 20.9; %H, 3.3. ^1H NMR ($CDCl_3$, 300 K): δ 2.5 (br, $SeCH_3$). $^{13}C\{^1H\}$ NMR ($CH_2Cl_2/CDCl_3$, 300 K): δ 12.8 ($SeCH_3$), 218 - 223 (CO). FAB MS (3-NOBA), *m/z* = 392, 308; calc. for $[Mn(CO)_3(^{80}SeMe_2)_2{}^{35}Cl]^+$ 394, $[Mn(^{80}SeMe_2)_2{}^{35}Cl]^+$ 310. IR/cm^{-1} 2995(w), 2929(w), 2017(s), 1923(s), 1895(s), 1423(m), 1356(s), 1288(m), 1265(w), 1098(m), 995(m), 969(w), 928(m), 874(w), 834(w), 679(s), 622(s), 531(m), 515(m), 273(m), 208(w), 186(w).

$[Mn(CO)_3(TeMe_2)_2Cl]$ (mixture of *fac* and *mer-trans*) was prepared similarly, except the final solution was concentrated under reduced pressure before precipitation of the product (64 %). Analysis: Calculated for $C_7H_{12}ClMnO_3Te_2$: %C, 17.2; %H, 2.5. Found: %C, 16.7; %H, 2.4. ^1H NMR ($CDCl_3$, 300 K): δ 2.28 (s), 2.11 (s) ($TeCH_3$). $^{13}C\{^1H\}$ NMR ($CH_2Cl_2/CDCl_3$, 300 K): δ -10.6, -9.5 ($TeCH_3$), 219 - 221 (CO). FAB MS (3-NOBA), *m/z* = 490, 427; calc. for $[Mn(CO)_3(^{130}TeMe_2)_2{}^{35}Cl]^+$ 494, $[Mn(CO)_2(^{130}TeMe_2)_2]^+$ 431. IR/cm^{-1} 2940(w), 2907(w), 1998(m), 1907(m), 1883(m), 1357(s), 1094(s), 986(m), 8349m), 672(w), 613(m), 536(m), 216(w), 192(w).

fac-$[Re(CO)_3\{o\text{-}C_6H_4(TeMe)_2\}Cl]$. A solution of the ditelluroether (109 mg, 3.0 x 10^{-4} mol) in $CHCl_3$ (40 cm^3) and $[Re(CO)_5Br]$ (110 mg, 3.0 x 10^{-4} mol) were refluxed together for 24 hours. Removing aliquots of the solution and recording their IR spectra was used to monitor the progress of the reaction. The solution was worked up as for the manganese analogue to yield a pale orange product. Yield 130 mg, 65 %. Analysis: Calculated for $C_{11}H_{10}ClO_3ReTe_2$: %C, 19.8; %H, 1.5. Found: %C, 19.6; %H, 1.3. ^1H NMR

($CDCl_3$, 300 K): δ 2.35 (s), 2.50 (s) (DL), 2.43 (s), 2.57 (s) (*meso*) (3H, $TeCH_3$), 7.5 - 7.9 (m, 2H, C_6H_4). $^{13}C\{^1H\}$ NMR ($CH_2Cl_2/CDCl_3$, 300 K): δ -4.7, -1.6 ($TeCH_3$), 124.5, 131.4, 140.4 (C_6H_4), 191 - 193 (CO). FAB MS (3-NOBA), *m/z* = 668, 633, 584; calc. for $[^{185}Re(CO)_3\{o\text{-}C_6H_4(^{130}TeMe)_2\}^{35}Cl]^+$ 670, $[^{185}Re(CO)_3\{o\text{-}C_6H_4(^{130}TeMe)_2\}]^+$ 635, $[Re\{o\text{-}C_6H_4(^{130}TeMe)_2\}^{35}Cl]^+$ 586. IR/cm^{-1} 2962(w), 2922(w), 2855(w), 2024(s), 1941(s), 1884(s), 1357(s), 1260(w), 1223(w), 1094(s), 985(m), 834(m), 758(m), 613(m), 532(m), 200(w), 183(w).

fac-$[Re(CO)_3\{MeTe(CH_2)_3TeMe\}Cl]$ was prepared similarly using a 12 hour reflux to give a cream coloured solid (63 %). Analysis: Calculated for $C_8H_{12}ClO_3ReTe_2$: %C, 15.2; %H, 1.9. Found: %C, 14.9; %H, 1.7. ^1H NMR ($CDCl_3$, 300 K): δ 2.05 - 2.20 (m, 1H, $CH_2CH_2CH_2$); 2.25 (s), 2.30 (s) (DL), 2.27 (s) (*meso*) (3H, $TeCH_3$), 2.80 - 3.5 (m, 2H, $TeCH_2$). $^{13}C\{^1H\}$ NMR ($CH_2Cl_2/CDCl_3$, 300 K): δ -11.8, -10.9, -9.5 ($TeCH_3$), 6.8, 9.1, 10.0, 10.5 ($TeCH_2$), 27.1, 27.8 (CH_2CH_2), 188 - 192 (CO). FAB MS (3-NOBA), *m/z* = 633, 599, 550; calc. for $[^{185}Re(CO)_3\{Me^{130}Te(CH_2)_3{}^{130}TeMe\}^{35}Cl]^+$ 636, $[^{185}Re(CO)_3\{Me^{130}Te(CH_2)_3{}^{130}TeMe\}]^+$ 601, $[^{185}Re\{Me^{130}Te(CH_2)_3{}^{130}TeMe\}^{35}Cl]^+$ 552. IR/cm^{-1} 2951(w), 2918(w), 2014(s), 1920(s), 1884(s), 1357(m), 1275(w), 1191(w), 1096(m), 849(m), 721(w), 630(m), 591(w), 512(w), 271(w), 194(w).

fac-$[Re(CO)_3\{o\text{-}C_6H_4(TeMe)_2\}Br]$ was prepared analogously to the chloro-complex to give a pale orange powder (62 %). Analysis: Calculated for $C_{11}H_{10}BrO_3ReTe_2$: %C, 18.6; %H, 1.4. Found: %C, 18.8; %H, 1.3. ^1H NMR ($CDCl_3$, 300 K): δ 2.32 (s), 2.58 (s) (DL), 2.40 (s) (*meso*) (3H, $TeCH_3$), 7.5 - 8.0 (m) (2H, C_6H_4). $^{13}C\{^1H\}$ NMR ($CH_2Cl_2/CDCl_3$, 300 K): δ -2.7, -1.2, -0.2 ($TeCH_3$), 124.0, 131.2, 140.6 (C_6H_4), 189 - 193 (CO). FAB MS (3-NOBA), *m/z* = 712, 656; calc. for $[^{185}Re(CO)_3\{o\text{-}C_6H_4(^{130}TeMe)_2\}^{79}Br]^+$ 714, $[^{185}Re(CO)\{o\text{-}C_6H_4(^{130}TeMe)_2\}^{79}Br]^+$ 658. IR/cm^{-1} 3055(w), 2951(w), 2024(s), 1932(s), 1893(s), 1356(s), 1258(w), 1223(w), 1094(s), 989(m), 834(m), 752(m), 612(m), 588(w), 516(w), 225(w), 215(w).

fac-$[Re(CO)_3\{MeTe(CH_2)_3TeMe\}Br]$ was prepared similarly using a 72 hour reflux (53 %). Analysis: Calculated for $C_8H_{12}BrO_3ReTe_2$: %C, 14.2; %H, 1.8. Found: %C, 14.3; %H, 2.0. ^1H NMR ($CDCl_3$, 300 K): δ 1.98 - 2.20 (m, 1H, $CH_2CH_2CH_2$), 2.24 (s), 2.30 (s) (DL), 2.34 (s) (*meso*) (3H, $TeCH_3$), 2.8 - 3.5 (m, 2H, $TeCH_2$). $^{13}C\{^1H\}$ NMR ($CH_2Cl_2/CDCl_3$,

300 K): δ -10.4, -10.3, -9.2, -8.5 ($TeCH_3$), 7.2, 9.3, 10.3, 10.5 ($TeCH_2$), 26.6, 27.1, 28.1 (CH_2CH_2), 188 - 192 (CO). FAB MS (3-NOBA), *m/z* = 678, 650; calc. for $[^{185}Re(CO)_3\{Me^{130}Te(CH_2)_3{}^{130}TeMe\}{}^{79}Br]^+$ 680, $[^{185}Re(CO)_2\{Me^{130}Te(CH_2)_3{}^{130}TeMe\}{}^{79}Br]^+$ 652. IR/cm^{-1} 2973(w), 2018(s), 1929(s), 1886(s), 1357(s), 1093(s), 985(m), 834(m), 613(m), 531(m), 198(m), 188(m).

fac-$[Re(CO)_3\{o\text{-}C_6H_4(SMe)_2\}Br]$ was prepared similarly to the ditelluroether complex (50 %). Analysis: Calculated for $C_{11}H_{10}BrO_3S_2Re$: %C, 25.4; %H, 1.9. Found: %C, 25.7; %H, 2.2. ^1H NMR ($CDCl_3$, 300 K): δ 3.07 (s, 3H, SCH_3), 7.5 - 7.8 (m, 2H, C_6H_4). $^{13}C\{^1H\}$ NMR ($CH_2Cl_2/CDCl_3$, 300 K): δ 29.0 - 33.0 (SCH_3), 131.5, 133.7, 136.8 (C_6H_4), 188 - 191 (CO). FAB MS (3-NOBA), *m/z* = 520, 492, 441; calc. for $[^{185}Re(CO)_3\{o\text{-}C_6H_4(SMe)_2\}{}^{79}Br]^+$ 518, $[^{185}Re(CO)_2\{o\text{-}C_6H_4(SMe)_2\}{}^{79}Br]^+$ 490, $[^{185}Re(CO)_3\{o\text{-}C_6H_4(SMe)_2\}]^+$ 439. IR/cm^{-1} 3000(s), 2922(w), 2037(s), 1940(s), 1914(s), 1457(w), 1425(m), 1356(s), 1259(w), 1211(w), 1095(s), 983(m), 833(w), 768(s), 632(m), 613(m), 518(m), 474(m), 203(w).

fac-$[Re(CO)_3\{o\text{-}C_6H_4(SeMe)_2\}Br]$ was prepared similarly to the ditelluroether complex using a 24 hour reflux (89 %). Analysis: Calculated for $C_{11}H_{10}BrO_3Se_2Re$: %C, 21.5; %H, 1.6. Found: %C, 21.2; %H, 1.8. ^1H NMR ($CDCl_3$, 300 K): δ 2.68 (s), 2.93 (s), 2.79 (s), 2.98 (s) (3H, $SeCH_3$), 7.5 - 7.8 (m, 2H, C_6H_4). $^{13}C\{^1H\}$ NMR ($CH_2Cl_2/CDCl_3$, 300 K): δ 17.9, 22.9, 23.1 ($SeCH_3$), 130.2, 131.5, 132.2, 132.7, 135.2 (C_6H_4), 188 - 192 (CO). FAB MS (3-NOBA), *m/z* = 612, 533; calc. for $[^{185}Re(CO)_3\{o\text{-}C_6H_4(^{80}SeMe)_2\}{}^{79}Br]^+$ 614, $[^{185}Re(CO)_3\{o\text{-}C_6H_4(^{80}SeMe)_2\}]^+$ 535. IR/cm^{-1} 3020(w), 2950(w), 2030(s), 1945(s), 1919(s), 1900(s), 1416(w), 1356(s), 1096(s), 991(w), 922(m), 833(w), 764(m), 634(w), 612(w), 515(m), 298(w), 203(w).

X-ray Crystallographic Studies

fac-$[Mn(CO)_3\{o\text{-}C_6H_4(TeMe)_2\}Cl]$ and *fac*-$[Re(CO)_3\{o\text{-}C_6H_4(TeMe)_2\}Cl]$. Details of the crystallographic data collection and refinement parameters are given in Table 2.1. The crystals were grown by the vapour diffusion of petroleum ether (40 - 60 °C) into solutions of the appropriate complex in $CHCl_3$. Data collection used a Rigaku AFC7S four circle diffractometer operating at 150 K, using graphite-monochromated Mo-K_α X-radiation (λ = 0.71073 Å). No significant crystal decay or movement was observed and for $[Mn(CO)_3\{o\text{-}$

$C_6H_4(TeMe)_2\}Cl]$ the data were corrected for absorption using psi scans (for $[Re(CO)_3\{o\text{-}C_6H_4(TeMe)_2\}Cl]$ psi scans did not give a satisfactory absorption correction and so DIFABS[43] was applied to the raw data with the complete model at isotropic convergence). The structures were solved by heavy atom methods[44] and developed by iterative cycles of full-matrix least-squares refinement[45] and difference Fourier syntheses which located one complete molecule in the asymmetric unit, showing the compounds to be isostructural. All non-hydrogen atoms were refined anisotropically while H-atoms were placed in fixed, calculated positions with d(C-H) = 0.96 Å.

2.5 References

[1] D. T. Hurd, G. W. Sentell, Jr. and F. J. Norton, *J. Am. Chem. Soc.,* 1949, **71**, 1899.

[2] E. O. Brimm, M. A. Lynch, Jr. and W. J. Sesny, *J. Am. Chem. Soc.,*1954, **76**, 3831.

[3] P. M. Treichel, in *Comprehensive Organometallic Chemistry*, G. Wilkinson, F. G. A. Stone and E. W. Abel (eds.), 1st edition, Pergamon, Oxford, 1982, Vol. 4, pp. 31.

[4] E. W. Abel and G. Wilkinson, *J. Chem. Soc.,* 1959, 1501.

[5] For example, see R. J. Angelici and F. Basolo, *J. Am. Chem. Soc.,* 1962, **84**, 2495.

[6] For example, see J. D. Korp, I. Bernal, J. L. Atwood, W. E. Hunter, F. Calderazzo and D. Vitali, *J. Chem. Soc., Chem. Commun.,* 1979, 576.

[7] For example, see A. M. Bond, R. Colton and M. J. McCormack, *Inorg. Chem.*, 1977, **16**, 155.

[8] S. J. A. Pope and G. Reid, *J. Chem. Soc., Dalton Trans.,* 1999, 1615.

[9] H. C. E. Mannerskantz and G. Wilkinson, *J. Chem. Soc.,* 1962, 4454.

[10] A. G. Osborne and M. H. B. Stiddard, *J. Chem. Soc.,* 1962, 4715.

[11] E. W. Abel and G. V. Hutson, *J. Inorg. Nucl. Chem.,*1969, **31**, 3333.

[12] W. Hieber and F. Stanner, *Chem. Ber.,* 1969, **102**, 2930.

[13] A. Belforte, F. Calderazzo, D. Vitali and P. F. Zanazzi, *Gazz. Chim. Ital.* 1985, **115**, 125.

[14] J. Connolly, G. W. Goodban, G. Reid and A. M. Z. Slawin, *J. Chem. Soc., Dalton Trans.,* 1998, 2225.

[15] J. Connolly, M. K. Davies and G. Reid, *J. Chem. Soc., Dalton Trans.,* 1998, 3833.

[16] W. Hieber and K. Wollmann, *Chem. Ber.,* 1962, **95**, 1552.

[17] P. Jaitner and W. Winder, *Inorg. Chim. Acta,* 1987, **134**, 201.

[18] A. P. Coleman, M. Ke, R. S. Dickson, G. B. Deacon and B. O. West, *Polyhedron*, 1994, **13**, 2301.

[19] W. Hieber, R. Schuh and H. Fuchs, *Z. Anorg. Allg. Chem.,* 1941, **248**, 243.

[20] E. Singleton, J. T. Moelwyn-Hughes and A. W. B. Garner, *J. Organomet. Chem.,* 1970, **21**, 449.

[21] R. H. Reimann and E. Singleton, *J. Organomet. Chem.,* 1973, **59**, 309.

[22] E. W. Abel, S. K. Bhargava, M. M. Bhatti, K. Kite, M. A. Mazid, K. G. Orrell, V. Sik, B. L. Williams, M. B. Hursthouse and K. M. A. Malik, *J. Chem. Soc., Dalton Trans.,* 1982, 2065.

[23] E. W. Abel, S. K. Bhargava, K. Kite, K. G. Orrell, Vladimir Sik and B. L. Williams, *J. Chem. Soc., Dalton Trans.,* 1984, 365.

[24] E. Abel, K. G. Orrell, S. P. Scanlan, D. Stephenson, T. Kemmitt and W. Levason, *J. Chem. Soc., Dalton Trans.*, 1991, 591.

[25] E. W. Abel, S. K. Bhargava and K. G. Orrell, *Prog. Inorg. Chem.*, 1984, **32**, 1.

[26] E. W. Abel, M. M. Bhatti, K. G. Orrell and V. Sik, *J. Organomet. Chem.*, 1981, **208**, 195; E. W. Abel, S. K. Bhargava, M. M. Bhatti, M. A. Mazid, K. G. Orrell, V. Sik, M. B. Hursthouse and K. M. A. Malik, *J. Organomet. Chem.*,1983, **250**, 373.

[27] N. J. Holmes, W. Levason and M. Webster, *J. Organomet. Chem.*, 1998, **568**, 213.

[28] A. R. J. Genge, W. Levason and G. Reid, *J. Chem. Soc., Dalton Trans.*, 1997, 4549.

[29] H. Schumann, A. A. Arif, A. L. Rheingold, C. Janiak R. Hoffmann and N. Kuhn, *Inorg. Chem.*, 1991, **30**, 1618.

[30] F. Calderazzo, E. A. C. Lucken and D. F. Williams, *J. Chem. Soc. A*, 1967, 154.

[31] S. Onaka, T. Miyamoto and Y. Sasaki, *Bull. Chem. Soc. Jp.*, 1971, **44**, 1851.

[32] E. G. Hope and W. Levason, *Coord. Chem. Rev.*, 1993, **122**, 109.

[33] T. Kemmitt, W. Levason and M. Webster, *Inorg. Chem.*, 1989, **28**, 692.

[34] N. P. Luthra and J. D. Odom, in *The Chemistry of Organic Selenium and Tellurium Compounds*, S. Patai and Z. Rappoport (eds), Wiley, New York, 1986, Vol. 1, Chap. 6.

[35] T. Kemmitt and W. Levason, *Inorg. Chem.*, 1990, **29**, 731.

[36] N. Kuhn and H. Schumann, *J. Organomet. Chem.*, 1984, **276**, 55; N. Kuhn, H. Schumann and E. Zauder, *J. Organomet. Chem.*, 1987, **327**, 17; N. Kuhn, H. Schumann, M. Winter and E. Zauder, *Chem. Ber.*, 1988, **121**, 111.

[37] F. A. Cotton, *Inorg. Chem.*, 1964, **3**, 702.

[38] J. Dalton, I. Paul, J. G. Smith and F. G. A. Stone, *J. Chem. Soc. (A)*, 1968, 1208.

[39] E. G. Hope, T. Kemmitt and W. Levason, *Organometallics*, 1988, **7**, 78.

[40] T. Kemmitt and W. Levason, *Organometallics*, 1989, **8**, 1303.

[41] K. J. Reimer and A. Shaver, *Inorg. Synth.*, 1979, **19**, 158.

[42] S. P. Schmidt, W. C. Trogler and F. Basolo, *Inorg. Synth.*, 1990, **28**, 160.

[43] N. Walker and D. Stuart, *Acta Crystallogr., Sect. A.*, 1983, **39**, 158.

[44] PATTY, The DIRDIF Program System, P. T. Beurskens, G. Admiraal, G. Beurskens, W. P. Bosman, S. Garcia-Granda, R. O. Gould, J. M. M. Smits, C. Smykalla. Technical Report of the Crystallography Laboratory, University of Nijmegen, The Netherlands, 1992.

[45] TeXsan: Crystal Structure Analysis Package, Molecular Structure Corporation, Texas, 1995.

Chapter 3

Manganese(I) Tricarbonyl Group 16 Tripodal Complexes

3.1 Introduction

Hexacarbonylmanganese(I), $[Mn(CO)_6]^+$, is the parent compound of a large group of cationic manganese(I) species of the type $[Mn(CO)_{6-x}(L)_x]^+$ (L = neutral ligand). Like the halo-manganese carbonyls described in Chapter 2, the manganese is in oxidation state +1 with a $3d^6$ configuration, therefore diamagnetic (low spin) octahedral complexes that are kinetically inert are generally obtained. Although the presence of π-acceptor ligands is required to stabilise the low oxidation state of manganese, generally the extent of π-bonding between the metal and the carbonyls is small. This is illustrated by the relatively high ν(CO) stretching frequency for $[Mn(CO)_6]^+$ at 2090 cm^{-1} (in THF) which may be compared to the analogous ν(CO) values for the isoelectronic species $[Cr(CO)_6]$ and $[V(CO)_6]^-$ at 1996 (in CCl_4) and 1859 cm^{-1} (in THF) respectively.[1] Therefore, carbonyl substitution is quite easy to accomplish due to the relative weakness of the metal carbonyl bonds.

Numerous complexes have been synthesised, ranging from $[Mn(CO)_5L]^+$ to $[Mn(CO)(L)_5]^+$ usually with L being a phosphine ligand, although other group 15 ligands such as arsines, stibines and nitriles have attracted some interest.[2] These complexes may be prepared by a variety of routes including direct reaction of a metal carbonyl halide with added ligand,[3] reaction of metal carbonyl halide, a ligand and halide acceptor,[4] displacement of other anionic ligands[5] and ligand displacement from other cationic metal complexes.[6] Group 16 ligands have not received such detailed study, with oxygen donors (generally solvent molecules such as THF, Me_2CO,[13] MeOH and H_2O)[7] forming complexes of the type $[Mn(CO)_5L]^+$ probably the most studied of this group. The bis-substituted complexes $[Mn(CO)_4(PPh_3)L]^+$ (L = SMe_2, SH_2, OH_2)[8] and the telluroether complex $[Mn(CO)_4(TePh_2)_2]^+$ have also been synthesised.[9]

Complexes of the type $[Mn(CO)_3(L_3)]^+$ where L_3 is a tridentate ligand are of particular interest to this study with *fac*-$[Mn(CO)_3\{MeC(CH_2AsMe_2)_3\}]^+$[10] and *fac*-$[Mn(CO)_3\{[9]aneS_3\}]^+$ being reported.[11]

The complexes *fac*-$[Mn(CO)_3(L_3)]^+$ {L_3 = [10]aneS$_3$, $MeS(CH_2)_2S(CH_2)_2SMe$, $MeSe(CH_2)_3Se(CH_2)_3SeMe$, $Ph_2P(CH_2)_2PPh(CH_2)_2PPh_2$ or $MeC(CH_2PPh_2)_3$} have also been synthesised by the Southampton research group as part of work conducted in parallel with that reported in this Chapter.[12]

There are no reported complexes of multidentate telluroether complexes and so their properties remain unexplored. Since the study of the complexes *fac*-[$Mn(CO)_3$(L-L)X] {X = Cl, Br or I; L-L = $MeTe(CH_2)_3TeMe$, $PhTe(CH_2)_3TePh$ or *o*-$C_6H_4(TeMe)_2$} and *fac*-[$Re(CO)_3$(L-L)X] {X = Cl or Br; L-L = $MeTe(CH_2)_3TeMe$ or *o*-$C_6H_4(TeMe)_2$} (Chapter 2),[16] clearly illustrated the superior donating ability of ditelluroether ligands to low valent metal carbonyl centres, the preparation of similar tritelluroether and related thio- and selenoether species should also provide an excellent probe into their spectroscopic properties and characteristics.

This Chapter discusses the chemistry of cationic manganese(I) tricarbonyl species with the tripodal ligands L^3 {L^3 = $MeC(CH_2EMe)_3$ (E = S, Se or Te) or $MeC(CH_2TePh)_3$} to generate species of the type *fac*-[$Mn(CO)_3(L^3)$][CF_3SO_3]. The rhenium selenoether complex *fac*-[$Re(CO)_3${$MeC(CH_2SeMe)_3$}][CF_3SO_3] has also been prepared for comparison. These complexes have been characterised by analysis, IR and multinuclear NMR (^1H, $^{13}C\{^1H\}$, ^{55}Mn, $^{77}Se\{^1H\}/^{125}Te\{^1H\}$) spectroscopy as well as ES^+ mass spectrometry and X-ray crystallographic studies on all five complexes. The spectroscopic and crystallographic data have been compared with similar complexes reported in the literature and any trends discussed.

3.2 Results and Discussion

Reaction of *fac*-$[Mn(CO)_3(Me_2CO)_3]^+$ [13] with one molar equivalent of L^3 {L^3 = $MeC(CH_2EMe)_3$ (E = S, Se or Te) or $MeC(CH_2TePh)_3$} in degassed acetone, followed by reduction of the solvent volume *in vacuo*, and precipitation with light petroleum ether (40 - 60 °C) afforded the complexes *fac*-$[Mn(CO)_3(L^3)][CF_3SO_3]$ as yellow solids. The reactions were monitored by solution IR of the carbonyl region and were deemed complete when the bands corresponding to *fac*-$[Mn(CO)_3(Me_2CO)_3]^+$ had been replaced by two new vibrations (A_1 + E) associated with the product, and indicative of a C_{3v} *fac*-tricarbonyl unit. The IR data of the isolated complexes are presented in Table 3.1. The thio- and selenoether complexes were stable in the solid state and in solution, although the telluroether complexes decomposed slowly in solution. The compound *fac*-$[Re(CO)_3\{MeC(CH_2SeMe)_3\}][CF_3SO_3]$ was prepared *via* a similar procedure from $[Re(CO)_5Br]$. Attempts to prepare the related telluroether complexes by various routes were unfortunately unsuccessful.

$$[Mn(CO)_5Br] + AgCF_3SO_3 + 3Me_2CO \longrightarrow \textit{fac}\text{-}[Mn(CO)_3(Me_2CO)_3][CF_3SO_3]$$

$$\textit{fac}\text{-}[Mn(CO)_3(Me_2CO)_3][CF_3SO_3] \xrightarrow{L^3} \textit{fac}\text{-}[Mn(CO)_3(L^3)][CF_3SO_3]$$

Table 3.1. Carbonyl stretching vibrations ($CHCl_3$) for the complexes *fac*-$[Mn(CO)_3(L^3)]^+$ and *fac*-$[Re(CO)_3\{MeC(CH_2SeMe)_3\}]^+$.

Complex	ν(CO)/cm^{-1}	
fac-	A_1	E
$[Mn(CO)_3\{MeC(CH_2SMe)_3\}][CF_3SO_3]$	2048	1968
$[Mn(CO)_3\{MeC(CH_2SeMe)_3\}][CF_3SO_3]$	2039	1962
$[Mn(CO)_3\{MeC(CH_2TeMe)_3\}][CF_3SO_3]$	2023	1947
$[Mn(CO)_3\{MeC(CH_2TePh)_3\}][CF_3SO_3]$	2028	1959
$[Re(CO)_3\{MeC(CH_2SeMe)_3\}][CF_3SO_3]$	2044	1952

Inspection of Table 3.1 shows the expected numerical shift in both the A_1 and E modes to low frequency as the donor is changed from S → Se → Te, consistent with increased π back bonding to CO (Chapter 2).[16] The values for the $MeC(CH_2TePh)_3$ complex are higher than those for $MeC(CH_2TeMe)_3$, indicating poorer σ donation in the former, consistent with the electron donating methyl groups being replaced by electron withdrawing phenyl groups.

The values for the thioether complex compare well with those reported in the literature for *fac*-$[Mn(CO)_3\{MeS(CH_2)_2S(CH_2)_2SMe\}][CF_3SO_3]$ (2047, 1968), although ν(CO) for the tripodal selenoether complex are noticeably higher than those quoted for *fac*-$[Mn(CO)_3\{MeSe(CH_2)_3Se(CH_2)_3SeMe\}][CF_3SO_3]$ (2029, 1945).[12]

The positive electrospray mass spectra of the complexes displayed prominent peaks assigned to $[Mn(CO)_3(L^3)]^+$ with the correct isotopic distribution confirming the identify of the complex cations formed. Other peaks corresponding to the fragmentation ions $[Mn(CO)(L^3)]^+$ and $[Mn(L^3)]^+$ were also observed. Elemental microanalyses showed a good match to the expected calculated values.

3.21 NMR Spectroscopy

Co-ordination of the tripodal ligands to the $[Mn(CO)_3]^+$ unit leads to the possible formation of two stereoisomers (invertomers); *syn* and *anti* (Figure 3.1). Like the manganese ditelluroether complexes (Chapter 2), these invertomers may easily be identified by NMR spectroscopy providing pyramidal inversion is slow. Therefore, the ^1H, $^{13}C\{^1H\}$, ^{55}Mn and $^{77}Se\{^1H\}$ or $^{125}Te\{^1H\}$ NMR spectra have been recorded for these species.

Figure 3.1. The two invertomers possible for the complexes *fac*-$[Mn(CO)_3\{MeC(CH_2ER)_3\}]^+$ (E = S or Se; R = Me; E = Te, R = Me or Ph, carbon backbone omitted for clarity).

syn *anti*

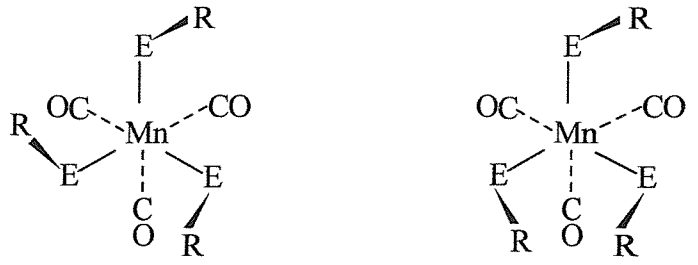

The ^1H NMR spectra were rather uninformative due to the resonances associated with the ligands being broadened by the ^{55}Mn quadrupole. Generally just one signal was observed for δ(EMe) and δ(ECH_2) (E = S or Te) indicating that *syn* isomer is dominant in solution for the telluroether complexes. However, the presence of just one resonance for the thioether complex is expected to be due to fast inversion occurring on the NMR time scale.[14] The presence of the *anti* invertomer would be expected to give rise to three signals in the NMR spectra, however generally just two are observed due to the coincidence of two of the resonances. For the complex $[Mn(CO)_3\{MeC(CH_2SeMe)_3\}][CF_3SO_3]$ three δ($SeCH_3$) resonances (2.27, 2.32, 2.38 ppm) were observed, consistent with the presence of both the *syn* (1 resonance) and *anti* (2 resonances) invertomers, although the two peaks associated with the *anti* invertomer were of very low intensity (approximately 5 %) (Figure 3.2).

Table 3.2. Selected ^{55}Mn, $^{77}Se\{^1H\}$ and $^{125}Te\{^1H\}$ NMR Data.

Complex	$\delta^{77}Se\{^1H\}$[a]	$\delta^{125}Te\{^1H\}$[b]	$\delta^{55}Mn$[c]
fac-$[Mn(CO)_3\{MeC(CH_2SMe)_3\}]^+$	-	-	-477(5000)
fac-$[Mn(CO)_3\{MeC(CH_2SeMe)_3\}]^+$	48	-	-721(3610)
fac-$[Mn(CO)_3\{MeC(CH_2TeMe)_3\}]^+$	-	112	-1509(1200)
fac-$[Mn(CO)_3\{MeC(CH_2TePh)_3\}]^+$	-	353	-1320(2100)
fac-$[Re(CO)_3\{MeC(CH_2SeMe)_3\}]^+$	23	-	-

[a] in $CH_2Cl_2/CDCl_3$ solution at 300 K, relative to external neat $SeMe_2$. [b] in $CH_2Cl_2/CDCl_3$ solution at 300 K, relative to neat external $TeMe_2$. [c] in $CH_2Cl_2/CDCl_3$ solution at 300 K, relative to external $KMnO_4$ in water, $w_{1/2}$ (Hz) in parentheses.

The $^{13}C\{^1H\}$ NMR spectra showed similar behaviour, with just one signal each for the EMe, CH_2 and MeC groups being observed. The resonances corresponding to δ(CO) were very broad, spanning several ppm, due to the large manganese quadrupole moment.

The $^{77}Se\{^1H\}$ NMR spectra for the two selenoether complexes showed just one signal (Table 3.2) which is consistent with the ligand having the *syn* configuation, and all three Se donors being equivalent, as deduced from ^1H and ^{13}C NMR spectroscopy. The *syn* isomer is also apparent for the two telluroether complexes, with again just one signal being observed in the $^{125}Te\{^1H\}$ NMR spectra (Table 3.2).

Generally for analogous complexes, the $\delta(^{125}Te)/\delta(^{77}Se)$ ratio is approximately 1.7 - 1.8.[15] However, for the manganese species reported here a ratio of *ca.* 2.3 is found. This is therefore, considerably higher than expected and suggests that there is more electron density associated with the Mn atom in the cationic tritelluroether complex compared to the selenoether analogue, and is consistent with the trend reported in Chapter 2.[16]

Figure 3.2. δ($SeCH_3$) region of the ^1H NMR spectrum (300 MHz, $CDCl_3$, 300 K) of *fac*-[$Mn(CO)_3${$MeC(CH_2SeMe)_3$}][CF_3SO_3], showing the presence of *syn* and *anti* invertomers.

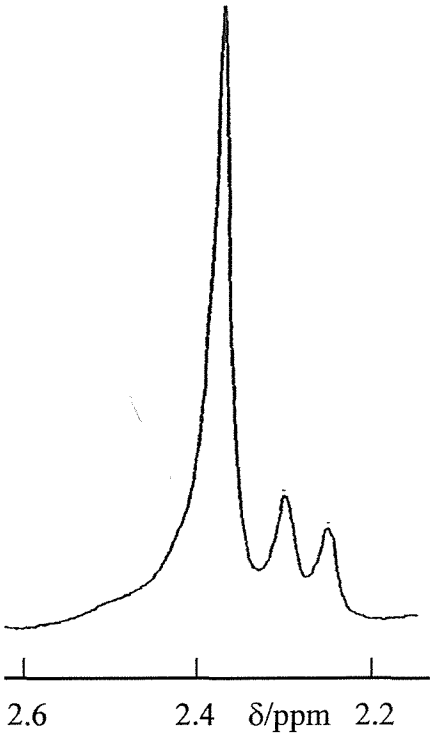

Our studies on manganese carbonyl halide complexes have shown that ^{55}Mn NMR spectroscopy is a sensitive probe of the subtle differences in bonding properties of group 15 and 16 ligands (Chapter 2).[16, 17] Similar studies on the manganese complexes reported here have been undertaken in order that comparisons with the neutral carbonyl halide derivatives (Chapter 2) can be made. One broad resonance was observed for each complex in the ^{55}Mn NMR spectra, indicating the presence of just one species. Data obtained from ^1H, $^{13}C\{^1H\}$ and $^{77}Se\{^1H\}/^{125}Te\{^1H\}$ NMR spectroscopy indicate this species being the *syn* rather than the *anti* invertomer. However, for the thioether complex, the observation of just one signal probably indicates fast pyramidal inversion. For the homologous series *fac*-[$Mn(CO)_3${$MeC(CH_2EMe)_3$}]$^+$, there is a very noticeable low frequency shift down the series δ(^{55}Mn) -477 (E = S), -721 (E = Se) and -1509 (E = Te), while *fac*-[$Mn(CO)_3${$MeC(CH_2TePh)_3$}]$^+$ gives δ(^{55}Mn) = -1320, i.e. less shielded than for the Me-substituted analogue and consistent with ν(CO) data.

Comparing the data for the cationic species with those reported previously for the neutral complexes (Chapter 2), shows that $\delta(^{55}Mn)$ follows the same trend with donor type, exhibiting a shift to low frequency along the series S → Se → Te. Further, for a particular donor type $\delta(^{55}Mn)$ for the cationic species are considerably to low frequency of the neutral species. These trends may be attributed to increased σ-donation down group 16 as electronegativity decreases, along with enhanced σ-donation in the cationic species as a consequence of the positive charge on Mn. Unsurprisingly, for the cationic phosphine and arsine complexes reported, $\delta(^{55}Mn)$ are *ca.* -1750, i.e. to low frequency of even the tripodal telluroether complex *fac*-$[Mn(CO)_3\{MeC(CH_2TeMe)_3\}]^+$, highlighting the superior coordinating properties of group 15 ligands compared to group 16.[12]

Manganese-55 NMR spectroscopic data have been reported for the thioether complexes *fac*-$[Mn(CO)_3([9]aneS_3)]^+$, *fac*-$[Mn(CO)_3([10]aneS_3)]^+$ and *fac*-$[Mn(CO)_3\{MeS(CH_2)_2S(CH_2)_2SMe\}]^+$ at δ -963, -764 and -696 respectively.[12] The manganese atom becomes less shielded in going from the superior $[9]aneS_3$ ligand to $[10]aneS_3$, with a similar trend observed with substitution of a macrocylic with an acyclic thioether ligand, $MeS(CH_2)_2S(CH_2)_2SMe$. The tripodal thioether complex has $\delta(^{55}Mn)$ = -477, i.e. to high frequency of all these complexes consistent with the presence of three 6-membered chelate rings, compared to 5-membered chelate rings for the facultative thioether complex.

The selenoether complex, *fac*-$[Mn(CO)_3\{MeSe(CH_2)_3Se(CH_2)_3SeMe\}]^+$ has $\delta(^{55}Mn)$ = -560, this is to high frequency of the tripodal selenoether complex reported here and indicates the superior donating ability of a tripodal ligand compared with its acyclic analogue.

3.22 Crystallographic Studies

To authenticate the geometry around the Mn(I) centre and establish trends in the bond lengths and angles, crystals suitable for single crystal X-ray crystallography were grown for each of the complexes reported here *via* the vapour diffusion of light petroleum ether into a solution of the appropriate complex in CH_2Cl_2. Previous to this study, the only structurally characterised species of the form *fac*-$[Mn(CO)_3(L_3)]^+$ where L_3 is a tridentate thio- seleno- or telluroether ligand were where L_3 = $[9]aneS_3$,[11] $[10]aneS_3$ or $MeS(CH_2)_2S(CH_2)_2SMe$.[12]

The structures of $[Mn(CO)_3\{MeC(CH_2EMe)_3\}]^+$ (E = S or Se) (Figures 3.3 and 3.4. Tables 3.3 to 3.7) show a facially bound tripodal ligand in the *syn* form, with the Me substituents adopting a propeller like arrangement, consistent with the dominant isomer observed in solution by NMR spectroscopy.

Figure 3.3. X-ray crystal structure of *fac*-$[Mn(CO)_3\{MeC(CH_2SMe)_3\}]^+$ with numbering scheme adopted. Ellipsoids are drawn at 40 % probability and H-atoms omitted for clarity.

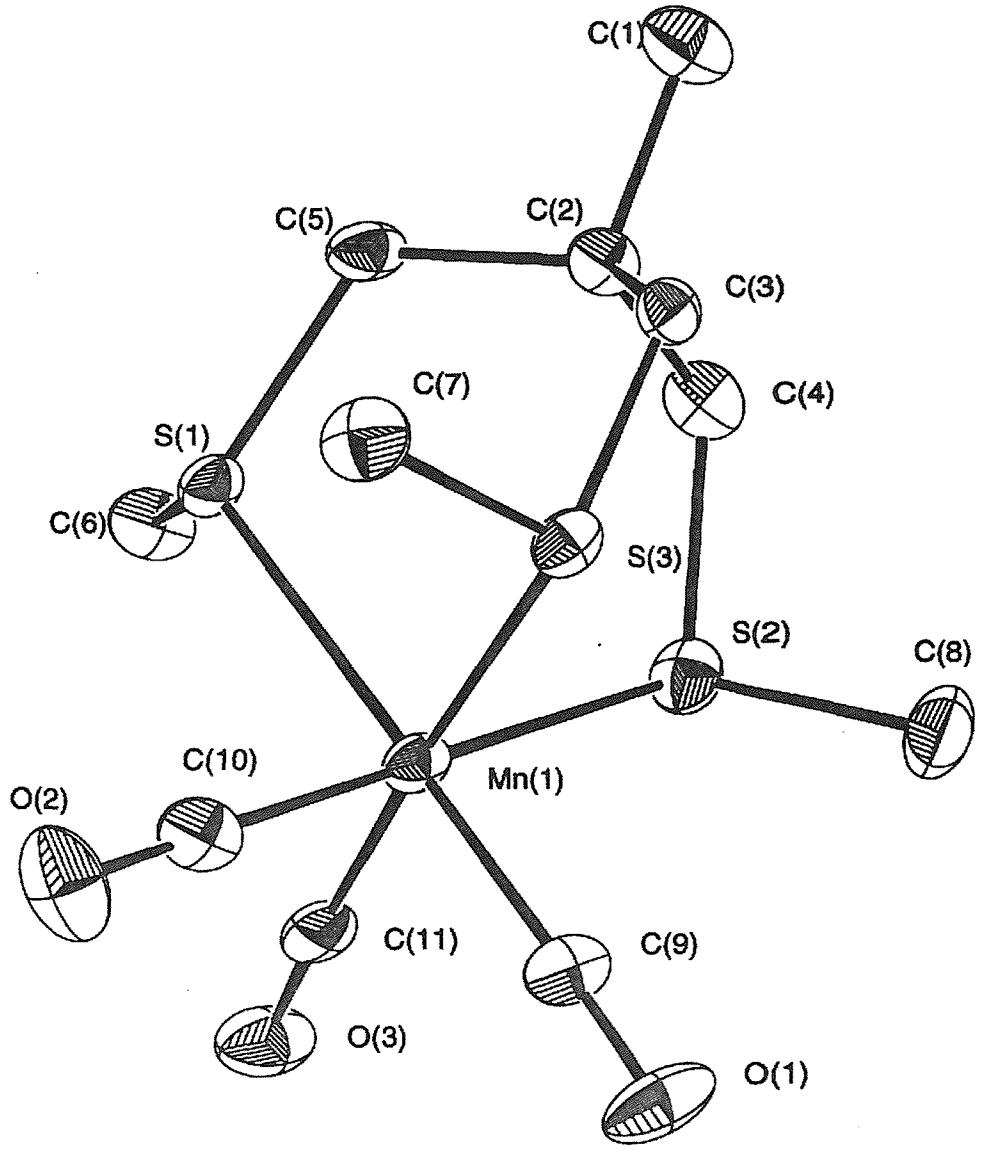

Table 3.3. Crystallographic data collection and refinement parameters for the complexes $[Mn(CO)_3(L^3)][CF_3SO_3]$ and $[Re(CO)_3\{MeC(CH_2SeMe)_3\}][CF_3SO_3]$.

	fac-$[Mn(CO)_3\{MeC(CH_2SMe)_3\}][CF_3SO_3]$	*fac*-$[Mn(CO)_3\{MeC(CH_2SeMe)_3\}][CF_3SO_3]$	*fac*-$[Mn(CO)_3\{MeC(CH_2TeMe)_3\}][CF_3SO_3]$	*fac*-$[Mn(CO)_3\{MeC(CH_2TePh)_3\}][CF_3SO_3]$	*fac*-$[Re(CO)_3\{MeC(CH_2SeMe)_3\}][CF_3SO_3]$
Formula	$C_{12}H_{18}F_3MnO_6S_4$	$C_{12}H_{18}F_3MnO_6SSe_3$	$C_{12}H_{18}F_3MnO_6STe_3$	$C_{27}H_{24}F_3MnO_6STe_3$	$C_{12}H_{18}F_3O_6ReSSe_3$
Formula weight	498.44	639.14	785.06	971.28	770.41
Crystal System	Triclinic	Triclinic	Monoclinic	Monoclinic	Triclinic
Space group	$P\bar{1}$	$P\bar{1}$	$P2_1/m$	$P2_1/n$	$P\bar{1}$
a, Å	9.190(1)	9.403(3)	8.989(3)	13.216(3)	12.584(1)
b, Å	12.085(2)	12.139(5)	10.033(2)	15.662(2)	15.216(1)
c, Å	9.079(1)	9.124(4)	12.086(2)	16.050(4)	12.4563(8)
α/°	98.85(1)	100.15(3)	-	-	99.144(7)
β/°	94.78(1)	94.76(4)	104.85(1)	106.73(2)	98.605(6)
γ/°	81.450(10)	80.92(3)	-	-	101.545(7)
V, $Å^3$	983.3(2)	1010.5(7)	1053.6(4)	3181(1)	2266.2(3)
Z	2	2	2	4	4
D_{calc}, g/cm^3	1.683	2.100	2.474	2.028	2.258
μ(Mo-K_α), cm^{-1}	11.04	61.27	48.47	32.20	103.22
Unique obs. reflections	3469	3563	1977	5832	7951
Obs. reflections with $[I_o > 2\sigma(I_o)]$	2732	2538	1603	2933	4114
R	0.028	0.038	0.025	0.044	0.047
R_w	0.026	0.042	0.034	0.046	0.055

$R = \Sigma (|F_{obs}|_i - |F_{calc}|_i) / \Sigma |F_{obs}|_i$, $R_w = \sqrt{[\Sigma w_i (|F_{obs}|_i - |F_{calc}|_i)^2 / \Sigma w_i |F_{obs}|_i^2]}$

Table 3.4. Selected bond lengths for *fac*-$[Mn(CO)_3\{MeC(CH_2SMe)_3\}]^+$.

Atom	Atom	Distance/Å	Atom	Atom	Distance/Å
Mn(1)	S(1)	2.3481(8)	Mn(1)	S(2)	2.3487(9)
Mn(1)	S(3)	2.3579(8)	Mn(1)	C(9)	1.806(3)
Mn(1)	C(10)	1.805(3)	Mn(1)	C(11)	1.816(3)
S(1)	C(5)	1.824(3)	S(1)	C(6)	1.800(3)
S(2)	C(4)	1.819(3)	S(2)	C(8)	1.810(3)
S(3)	C(3)	1.832(3)	S(3)	C(7)	1.810(3)

Table 3.5. Selected bond angles for *fac*-$[Mn(CO)_3\{MeC(CH_2SMe)_3\}]^+$.

Atom	Atom	Atom	Angle(°)	Atom	Atom	Atom	Angle(°)
S(1)	Mn(1)	S(2)	91.63(3)	S(1)	Mn(1)	S(3)	88.12(3)
S(1)	Mn(1)	C(9)	175.8(1)	S(1)	Mn(1)	C(10)	88.19(9)
S(1)	Mn(1)	C(11)	93.45(9)	S(2)	Mn(1)	S(3)	88.77(3)
S(2)	Mn(1)	C(9)	91.2(1)	S(2)	Mn(1)	C(10)	177.8(1)
S(2)	Mn(1)	C(11)	86.9(1)	S(3)	Mn(1)	C(9)	88.90(9)
S(3)	Mn(1)	C(10)	93.4(1)	S(3)	Mn(1)	C(11)	175.4(1)
C(9)	Mn(1)	C(10)	89.1(1)	C(9)	Mn(1)	C(11)	89.8(1)
C(10)	Mn(1)	C(11)	90.9(1)	Mn(1)	S(1)	C(5)	111.33(9)
Mn(1)	S(1)	C(6)	108.0(1)	C(5)	S(1)	C(6)	102.0(1)
Mn(1)	S(2)	C(4)	110.4(1)	Mn(1)	S(2)	C(8)	108.3(1)
C(4)	S(2)	C(8)	101.6(1)	Mn(1)	S(3)	C(3)	110.83(9)
Mn(1)	S(3)	C(7)	109.8(1)	C(3)	S(3)	C(7)	101.5(1)

Figure 3.4. X-ray crystal structure of *fac*-$[Mn(CO)_3\{MeC(CH_2SeMe)_3\}][CF_3SO_3]$ with numbering scheme adopted. Ellipsoids are drawn at 40 % probability and H-atoms omitted for clarity.

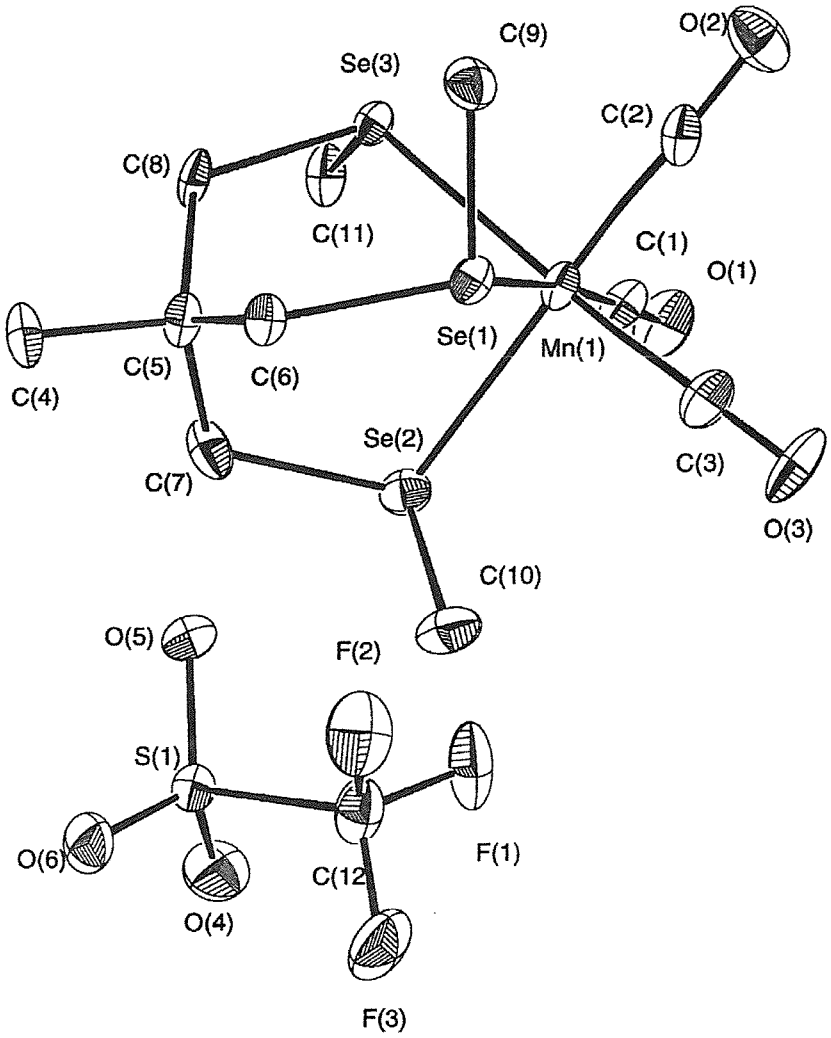

Table 3.6. Selected bond lengths for *fac*-$[Mn(CO)_3\{MeC(CH_2SeMe)_3\}]^+$.

Atom	Atom	Distance/Å	Atom	Atom	Distance/Å
Se(1)	Mn(1)	2.464(1)	Se(1)	C(6)	1.981(7)
Se(1)	C(9)	1.945(7)	Se(2)	Mn(1)	2.459(1)
Se(2)	C(7)	1.974(8)	Se(2)	C(10)	1.946(8)
Se(3)	Mn(1)	2.449(1)	Se(3)	C(8)	1.975(7)
Se(3)	C(11)	1.934(7)	Mn(1)	C(1)	1.821(8)
Mn(1)	C(2)	1.793(8)	Mn(1)	C(3)	1.804(8)

Table 3.7. Selected bond angles for *fac*-$[Mn(CO)_3\{MeC(CH_2SeMe)_3\}]^+$.

Atom	Atom	Atom	Angle(°)	Atom	Atom	Atom	Angle(°)
Mn(1)	Se(1)	C(6)	109.1(2)	Mn(1)	Se(1)	C(9)	107.9(2)
C(6)	Se(1)	C(9)	98.9(3)	Mn(1)	Se(2)	C(7)	109.5(2)
Mn(1)	Se(2)	C(10)	106.2(3)	C(7)	Se(2)	C(10)	98.1(4)
Mn(1)	Se(3)	C(8)	109.4(2)	Mn(1)	Se(3)	C(11)	104.7(2)
C(8)	Se(3)	C(11)	100.2(3)	Se(1)	Mn(1)	Se(2)	89.19(5)
Se(1)	Mn(1)	Se(3)	89.18(4)	Se(1)	Mn(1)	C(1)	175.3(2)
Se(1)	Mn(1)	C(2)	93.5(2)	Se(1)	Mn(1)	C(3)	87.6(2)
Se(2)	Mn(1)	Se(3)	91.45(4)	Se(2)	Mn(1)	C(1)	86.5(2)
Se(2)	Mn(1)	C(2)	177.2(2)	Se(2)	Mn(1)	C(3)	90.8(3)
Se(3)	Mn(1)	C(1)	92.7(2)	Se(3)	Mn(1)	C(2)	87.7(2)
Se(3)	Mn(1)	C(3)	176.0(2)	C(1)	Mn(1)	C(2)	90.9(3)
C(1)	Mn(1)	C(3)	90.7(3)	C(2)	Mn(1)	C(3)	90.2(4)

The structure of $[Mn(CO)_3\{MeC(CH_2TeMe)_3\}][CF_3SO_3]$ revealed the cation and anion both disordered across a crystallographic mirror plane (Figure 3.5. Tables 3.3 and 3.8 to 3.9). In the cation, the central Mn centre is coordinated to three mutually *fac* carbonyl ligands and all three Te donors. However, the disorder leads to two alternative but equally occupied sites for each of the Te-bound Me groups, and hence it is not possible to establish which diastereoisomer occurs in the solid state.

Figure 3.5. X-ray crystal structure of *fac*-$[Mn(CO)_3\{MeC(CH_2TeMe)_3\}]^+$ with numbering scheme adopted. Ellipsoids are drawn at 40 % probability and H-atoms omitted for clarity. The figure shows the *syn* arrangement established spectroscopically in solution, although it can not be certain which isomer occurs in the solid state due to the disorder.

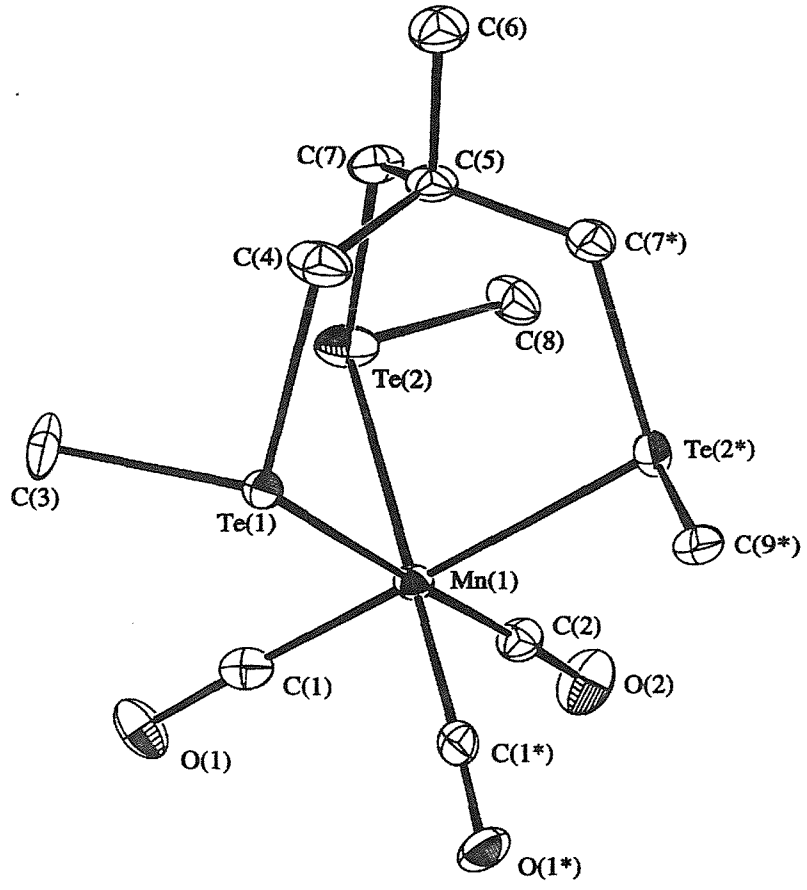

Table 3.8. Selected bond lengths for *fac*-$[Mn(CO)_3\{MeC(CH_2TeMe)_3\}]^+$.

Atom	Atom	Distance/Å	Atom	Atom	Distance/Å
Te(1)	Mn(1)	2.601(1)	Te(1)	C(3)	2.10(1)
Te(1)	C(3)	2.10(1)	Te(1)	C(4)	2.165(8)
Te(2)	Mn(1)	2.6063(8)	Te(2)	C(7)	2.162(5)
Te(2)	C(8)	2.05(1)	Te(2)	C(9)	1.97(1)
Mn(1)	C(1)	1.795(6)	Mn(1)	C(1)	1.795(6)
Mn(1)	C(2)	1.790(8)			

Table 3.9. Selected bond angles for *fac*-$[Mn(CO)_3\{MeC(CH_2TeMe)_3\}]^+$.

Atom	Atom	Atom	Angle(°)	Atom	Atom	Atom	Angle(°)
Mn(1)	Te(1)	C(3)	106.4(3)	Mn(1)	Te(1)	C(3)	106.4(3)
Mn(1)	Te(1)	C(4)	108.0(2)	C(3)	Te(1)	C(3)	140.9(7)
C(3)	Te(1)	C(4)	94.8(4)	C(3)	Te(1)	C(4)	94.8(4)
Mn(1)	Te(2)	C(7)	107.9(2)	Mn(1)	Te(2)	C(8)	109.5(3)
Mn(1)	Te(2)	C(9)	106.9(3)	C(7)	Te(2)	C(8)	99.6(4)
C(7)	Te(2)	C(9)	99.6(4)	C(8)	Te(2)	C(9)	130.8(5)
Te(1)	Mn(1)	Te(2)	90.08(3)	Te(1)	Mn(1)	Te(2)	90.08(3)
Te(1)	Mn(1)	C(1)	89.1(2)	Te(1)	Mn(1)	C(1)	89.1(2)
Te(1)	Mn(1)	C(2)	178.1(2)	Te(2)	Mn(1)	Te(2)	89.31(4)
Te(2)	Mn(1)	C(1)	90.6(2)	Te(2)	Mn(1)	C(1)	179.1(2)
Te(2)	Mn(1)	C(2)	88.6(2)	Te(2)	Mn(1)	C(1)	179.1(2)
Te(2)	Mn(1)	C(1)	90.6(2)	Te(2)	Mn(1)	C(2)	88.6(2)
C(1)	Mn(1)	C(1)	89.4(3)	C(1)	Mn(1)	C(2)	92.2(2)
C(1)	Mn(1)	C(2)	92.2(2)				

The complex $[Re(CO)_3\{MeC(CH_2SeMe)_3\}][CF_3SO_3]$ (Figure 3.7. Tables 3.13 to 3.14) shows a similar arrangement to its manganese analogue, adopting the *syn* form in the solid state, again consistent with solution NMR spectroscopy.

The Mn-S distances obtained for the thioether complex compared well with similar thioether complexes reported in the literature, $[Mn(CO)_3([9]aneS_3)]_3[PF_6]_2Br{\cdot}2H_2O$ (Mn-S = 2.314(4) - 2.341(4) Å),[11] *fac*-$[Mn(CO)_3([10]aneS_3)]^+$ (Mn-S = 2.303(5) - 2.405(6) Å) and *fac*-$[Mn(CO)_3\{MeS(CH_2)_2S(CH_2)_2SMe\}]^+$ (Mn-S = 2.320(3) - 2.402(4) Å).[12]

There are no reported structural data for cationic manganese(I) or rhenium(I) selenoether complexes in the literature, although *d*(M-Se) may be compared with those in the neutral species *fac*-$[Mn(CO)_3\{MeSe(CH_2)_2SeMe\}Cl]$ (Mn-Se = 2.481(3), 2.467(3) Å), *fac*-$[Mn(CO)_3\{MeSe(CH_2)_3SeMe\}Cl]$ (Mn-Se = 2.474(2), 2.482(2) Å)[18] and *fac*-$[Re(CO)_3\{MeSe(CH_2)_2SeMe\}I]$ (Re-Se = 2.593(1), 2.597(1) Å).[19]

Similarly, there are no reported structural data for cationic telluroether complexes of manganese(I). However, the data may be compared with the complex *fac*-$[Mn(CO)_3\{o\text{-}C_6H_4(TeMe)_2\}Cl]$ (Mn-Te = 2.598(1), 2.613(1) Å) (Chapter 2).[16]

The range of Mn-E distances and E-Mn-E angles observed for each complex are shown in Table 3.10. Comparing the structural data for the homologous series $[Mn(CO)_3\{MeC(CH_2EMe)_3\}]^+$ (E = S, Se or Te) shows an increase in *d*(Mn-E) according to the series S < Se < Te, in accord with the increasing covalent radii. In the absence of structural data on a much wider range of analogous systems, it is not possible to be certain whether the subtle changes in bonding down the group are reflected in the measured structural parameters. In fact it is likely that the differences are within the error limits of X-ray analyses.

Table 3.10. Range of Mn-E Distances and E-Mn-E Angles.

Complex	Mn-E/Å	E-Mn-E/(°)
$[Mn(CO)_3\{MeC(CH_2SMe)_3\}]^+$	2.3481(8) - 2.3579(8)	88.12(3) - 91.63(3)
$[Mn(CO)_3\{MeC(CH_2SeMe)_3\}]^+$	2.449(1) - 2.464(1)	89.18(4) - 91.45(4)
$[Mn(CO)_3\{MeC(CH_2TeMe)_3\}]^+$	2.601(1) - 2.6063(8)	89.31(4) - 90.08(3)
$[Mn(CO)_3\{MeC(CH_2TePh)_3\}]^+$	2.615(2) - 2.643(2)	86.07(6) - 94.49(6)
$[Re(CO)_3\{MeC(CH_2SeMe)_3\}]^+$	2.579(3) - 2.594(2)[a]	87.09(8) - 89.08(8)[b]

[a] Re-Se. [b] Se-Re-Se.

The structure of the complex *fac*-$[Mn(CO)_3\{MeC(CH_2TePh)_3\}][CF_3SO_3]$ shows the cation in a distorted octahedral geometry (Figure 3.6. Tables 3.11 to 3.12) with the Ph groups adopting the *syn* arrangement. The Mn-Te distances in the Me- substituted species are shorter (*ca.* 0.025 Å) than those for the Ph-substituted analogue (Table 3.10), and although this is consistent with the Me-substituted tripod being a better σ-donor ligand, steric effects may also have an effect.

Figure 3.6. X-ray crystal structure of *fac*-$[Mn(CO)_3\{MeC(CH_2TePh)_3\}]^+$ with numbering scheme adopted. Ellipsoids are drawn at 40 % probability and H-atoms omitted for clarity.

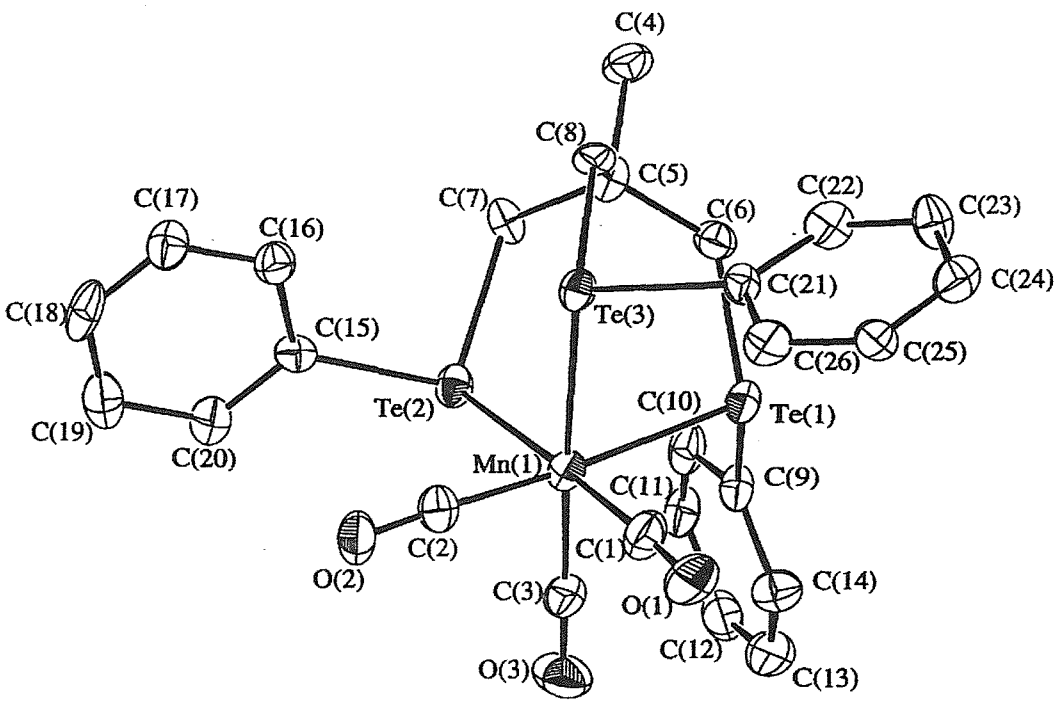

Table 3.11. Selected bond lengths for *fac*-$[Mn(CO)_3\{MeC(CH_2TePh)_3\}]^+$.

Atom	Atom	Distance/Å	Atom	Atom	Distance/Å
Te(1)	Mn(1)	2.627(2)	Te(1)	C(6)	2.16(1)
Te(1)	C(9)	2.14(1)	Te(2)	Mn(1)	2.615(2)
Te(2)	C(7)	2.16(1)	Te(2)	C(15)	2.13(1)
Te(3)	Mn(1)	2.643(2)	Te(3)	C(8)	2.16(1)
Te(3)	C(21)	2.14(1)	Mn(1)	C(1)	1.80(1)
Mn(1)	C(2)	1.80(1)	Mn(1)	C(3)	1.83(1)

Table 3.12. Selected bond angles for *fac*-[Mn(CO)$_3${MeC(CH$_2$TePh)$_3$}]$^+$.

Atom	Atom	Atom	Angle(°)	Atom	Atom	Atom	Angle(°)
Mn(1)	Te(1)	C(6)	108.3(3)	Mn(1)	Te(1)	C(9)	102.3(3)
C(6)	Te(1)	C(9)	100.3(5)	Mn(1)	Te(2)	C(7)	108.2(3)
Mn(1)	Te(2)	C(15)	105.6(3)	C(7)	Te(2)	C(15)	97.5(5)
Mn(1)	Te(3)	C(8)	107.3(3)	Mn(1)	Te(3)	C(21)	104.0(3)
C(8)	Te(3)	C(21)	96.0(5)	Te(1)	Mn(1)	Te(2)	87.68(6)
Te(1)	Mn(1)	Te(3)	86.07(6)	Te(1)	Mn(1)	C(3)	92.1(4)
Te(1)	Mn(1)	C(2)	175.6(4)	Te(1)	Mn(1)	C(1)	92.0(5)
Te(2)	Mn(1)	Te(3)	94.49(6)	Te(2)	Mn(1)	C(1)	176.7(5)
Te(2)	Mn(1)	C(2)	88.4(4)	Te(2)	Mn(1)	C(3)	87.1(4)
Te(3)	Mn(1)	C(1)	88.8(5)	Te(3)	Mn(1)	C(2)	92.4(4)
Te(3)	Mn(1)	C(3)	177.5(4)	C(1)	Mn(1)	C(2)	92.0(6)
C(1)	Mn(1)	C(3)	89.6(6)	C(2)	Mn(1)	C(3)	89.6(6)

Figure 3.7. X-ray crystal structure of *fac*-$[Re(CO)_3\{MeC(CH_2SeMe)_3\}]^+$ with numbering scheme adopted. Ellipsoids are drawn at 40 % probability and H-atoms omitted for clarity.

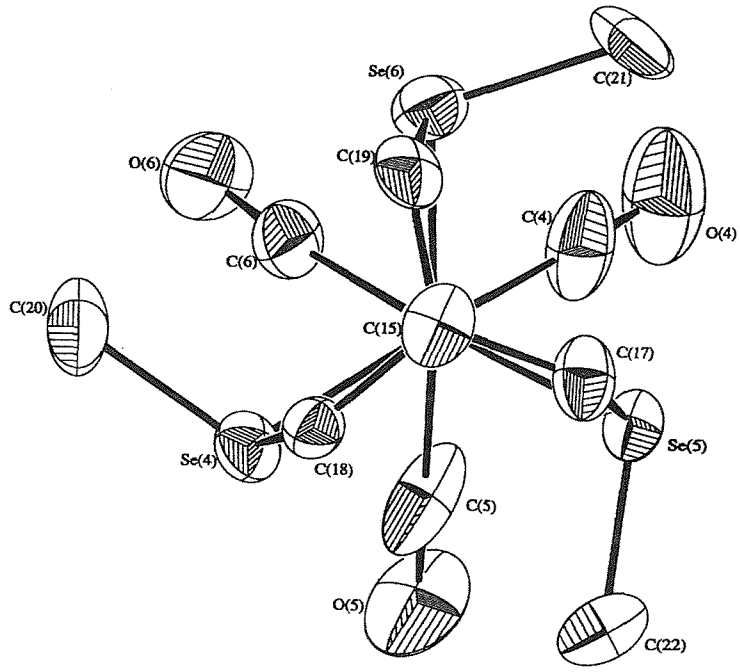

Table 3.13. Selected bond lengths for *fac*-$[Re(CO)_3\{MeC(CH_2SeMe)_3\}]^+$.

Atom	Atom	Distance/Å	Atom	Atom	Distance/Å
Re(1)	Se(1)	2.588(3)	Re(1)	Se(2)	2.579(2)
Re(1)	Se(3)	2.587(2)	Re(1)	C(1)	1.91(2)
Re(1)	C(2)	1.86(2)	Re(1)	C(3)	1.86(3)
Re(2)	Se(4)	2.579(3)	Re(2)	Se(5)	2.594(2)
Re(2)	Se(6)	2.578(3)	Re(2)	C(4)	1.93(3)
Re(2)	C(5)	1.98(3)	Re(2)	C(6)	1.95(3)
Se(1)	C(11)	1.95(2)	Se(1)	C(13)	1.93(2)
Se(2)	C(9)	1.97(2)	Se(2)	C(12)	1.94(2)
Se(3)	C(10)	1.99(2)	Se(3)	C(14)	1.93(2)
Se(4)	C(18)	1.98(2)	Se(4)	C(20)	1.92(2)
Se(5)	C(17)	1.97(2)	Se(5)	C(22)	1.95(3)
Se(6)	C(19)	1.98(2)	Se(6)	C(21)	1.97(3)

Table 3.14. Selected bond angles for *fac*-$[Re(CO)_3\{MeC(CH_2SeMe)_3\}]^+$.

Atom	Atom	Atom	Angle(°)	Atom	Atom	Atom	Angle(°)
Se(1)	Re(1)	Se(2)	87.94(8)	Se(1)	Re(1)	Se(3)	87.96(8)
Se(1)	Re(1)	C(1)	87.2(7)	Se(1)	Re(1)	C(2)	91.2(7)
Se(1)	Re(1)	C(3)	177.4(6)	Se(2)	Re(1)	Se(3)	87.76(7)
Se(2)	Re(1)	C(1)	91.9(6)	Se(2)	Re(1)	C(2)	178.6(6)
Se(2)	Re(1)	C(3)	89.7(6)	Se(3)	Re(1)	C(1)	175.1(7)
Se(3)	Re(1)	C(2)	91.1(7)	Se(3)	Re(1)	C(3)	90.9(6)
C(1)	Re(1)	C(2)	89.2(9)	C(1)	Re(1)	C(3)	94.0(9)
C(2)	Re(1)	C(3)	91.1(10)	Se(4)	Re(2)	Se(5)	87.68(8)
Se(4)	Re(2)	Se(6)	89.08(8)	Se(4)	Re(2)	C(4)	176.8(9)
Se(4)	Re(2)	C(5)	86.8(9)	Se(4)	Re(2)	C(6)	93.7(8)
Se(5)	Re(2)	Se(6)	87.09(8)	Se(5)	Re(2)	C(4)	89.9(7)
Se(5)	Re(2)	C(5)	94.2(6)	Se(5)	Re(2)	C(6)	176.1(7)
Se(6)	Re(2)	C(4)	92.9(10)	Se(6)	Re(2)	C(5)	175.6(9)
Se(6)	Re(2)	C(6)	89.3(7)	C(4)	Re(2)	C(5)	91(1)
C(4)	Re(2)	C(6)	88(1)	C(5)	Re(2)	C(6)	89.5(9)
Re(1)	Se(1)	C(11)	108.7(6)	Re(1)	Se(1)	C(13)	105.1(8)
C(11)	Se(1)	C(13)	100.1(9)	Re(1)	Se(2)	C(9)	108.5(5)
Re(1)	Se(2)	C(12)	104.3(7)	C(9)	Se(2)	C(12)	100.1(10)
Re(1)	Se(3)	C(10)	108.8(6)	Re(1)	Se(3)	C(14)	104.7(7)
C(10)	Se(3)	C(14)	98.8(9)	Re(2)	Se(4)	C(18)	108.9(6)
Re(2)	Se(4)	C(20)	107.7(9)	C(18)	Se(4)	C(20)	99.3(9)
Re(2)	Se(5)	C(17)	108.5(6)	Re(2)	Se(5)	C(22)	107.5(7)
C(17)	Se(5)	C(22)	97.1(10)	Re(2)	Se(6)	C(19)	108.6(6)
Re(2)	Se(6)	C(21)	104.9(8)	C(19)	Se(6)	C(21)	98(1)

3.3 Conclusions

The complexes *fac*-$[Mn(CO)_3(L^3)][CF_3SO_3]$ {L^3 = $MeC(CH_2SMe)_3$, $MeC(CH_2SeMe)_3$, $MeC(CH_2TeMe)_3$ or $MeC(CH_2TePh)_3$} and *fac*-$[Re(CO)_3\{MeC(CH_2SeMe)_3\}][CF_3SO_3]$ have been prepared as yellow solids in good yields *via* the reaction of $[Mn(CO)_3(Me_2CO)_3]^+$ or $[Re(CO)_3(Me_2CO)_3]^+$ with L^3 in acetone.

NMR and IR spectroscopic data have confirmed the identity of these complexes in solution, showing that the *syn* isomer is the dominant species, as well as providing further information on the relative bonding properties of these group 16 ligands. Manganese-55 NMR spectroscopy has shown that for a given donor type $\delta(^{55}Mn)$ lies significantly to low frequency compared to those for the neutral *fac*-$[Mn(CO)_3(L\text{-}L)X]$ (X= Cl, Br or I, L-L = dithio-, diseleno or ditelluroether) species (Chapter 2).

The manganese-55 NMR spectroscopic data for the series *fac*-$[Mn(CO)_3\{MeC(CH_2EMe)_3\}]^+$ (E = S, Se or Te) have also shown that $\delta(^{55}Mn)$ is shifted to low frequency, indicating that the manganese nucleus experiences greater shielding, upon descending group 16. In addition to this, comparison of the ratio $\delta(^{125}Te)/\delta(^{77}Se)$ for the complexes *fac*-$[Mn(CO)_3\{MeC(CH_2SeMe)_3\}]^+$ and *fac*-$[Mn(CO)_3\{MeC(CH_2TeMe)_3\}]^+$ with other group 16 compounds reported in the literature has shown the tellurium-125 chemical shift of telluroether complex to be more positive than expected, thereby indicating increased σ-donation from the telluroether ligand. Thus, the same trend of σ-donation increasing in the order S < Se << Te, described in Chapter 2, has been observed.

The single crystal X-ray structures of all five complexes have confirmed that the manganese or rhenium atom is bonded to all three donors of the tripodal ligand with a distorted octahedral geometry at the metal. The *syn* invertomer is observed for all complexes in the solid state, although for the complex *fac*-$[Mn(CO)_3\{MeC(CH_2TeMe)_3\}][CF_3SO_3]$ the invertomer could not be identified due to disorder.

3.4 Experimental

The compounds $[Mn(CO)_5Br]$,[20] $[Re(CO)_5Br]$,[21] *fac*-$[Mn(CO)_3(Me_2CO)_3][CF_3SO_3]$,[13] $MeC(CH_2SMe)_3$,[22] $MeC(CH_2SeMe)_3$[23] and $MeC(CH_2TeMe)_3$[24] were prepared *via* the literature procedures. The synthesis of the ligand $MeC(CH_2TePh)_3$ is described in Chapter 7, along with improved syntheses for the thio- and selenoether tripod ligands. The reactions were protected from light by wrapping the reaction flask in foil and the isolated manganese complexes were stored in foil wrapped ampoules in a refrigerator.

fac-$[Mn(CO)_3\{MeC(CH_2SMe)_3\}][CF_3SO_3]$. A solution of *fac*-$[Mn(CO)_3(Me_2CO)_3][CF_3SO_3]$ was prepared by treatment of $[Mn(CO)_5Br]$ (55 mg, 2.0×10^{-4} mol) with $AgCF_3SO_3$ (56 mg, 2.2×10^{-4} mol) in refluxing acetone for 1 hour, and subsequent removal of the precipitated AgBr by filtration to yield a yellow solution. $MeC(CH_2SeMe)_3$ (42 mg, 2.0×10^{-4} mmol) was dissolved in acetone (1 cm^3) and added to the reaction mixture. Removing aliquots of the solution and recording their IR spectra was used to monitor the progress of the reaction. After 16 hours the carbonyl bands of $[Mn(CO)_3(Me_2CO)_3]^+$ had been replaced by two new vibrations and the reaction was deemed to be complete. The solvent was removed *in vacuo* and CH_2Cl_2 (2 cm^3) added to dissolve the residue, followed by addition of ice cold light petroleum ether (40 - 60 °C) to precipitate a yellow powder. Yield 65 mg, 65 %. Analysis: Calculated for $C_{12}H_{18}F_3MnO_6S_4.CH_2Cl_2$: %C, 26.8; %H, 3.4. Found: %C, 27.0; %H, 3.5. ^1H NMR ($CDCl_3$, 300 K): δ 1.15 (s, 1H, CCH_3), 2.22 (s, 3H, SCH_3), 2.90 (s, 2H, SCH_2). $^{13}C\{^1H\}$ NMR ($CH_2Cl_2/CDCl_3$, 300 K): δ 25.5 (SCH_3), 31.2 (CCH_3), 36.2 (C), 39.4 (SCH_2), 214 - 217 (CO). ^{55}Mn NMR ($CH_2Cl_2/CDCl_3$, 300 K): δ -477 ($w_{1/2}$ = 5000 Hz). ES^+ (MeCN), *m/z* = 349; calc. for $[Mn(CO)_3\{MeC(CH_2SMe)_3\}]^+$ 349. IR/cm^{-1} 2963(w), 2047(s), 1953(s), 1424(m), 1359(m), 1262(s), 1233(m), 1154(s), 1096(s), 1031(s), 864(w), 803(m), 760(m), 666(m), 640(s), 622(m), 574(w), 524(m).

fac-$[Mn(CO)_3\{MeC(CH_2SeMe)_3\}][CF_3SO_3]$ was prepared similarly to give a yellow product (47 %). Analysis: Calculated for $C_{12}H_{18}F_3MnO_6SSe_3$: %C, 22.5; %H, 2.8. Found: %C, 23.2; %H, 3.0. ^1H NMR ($CDCl_3$, 300 K): δ 1.27 (s, 1H, CCH_3), 2.27 (s), 2.32 (s) (*anti*), 2.38 (s) (*syn*) (3H, $SeCH_3$), 2.70 (s, 2H, $SeCH_2$). $^{13}C\{^1H\}$ NMR ($CH_2Cl_2/CDCl_3$, 300 K): δ 16.1 ($SeCH_3$), 32.2 (CCH_3), 34.8 ($SeCH_2$), 38.3 (C), 215 - 218 (CO). ^{55}Mn NMR ($CH_2Cl_2/CDCl_3$, 300 K): δ -721 ($w_{1/2}$ = 3610 Hz). $^{77}Se\{^1H\}$ NMR ($CH_2Cl_2/CDCl_3$, 300 K):

δ 48. ES^+ (MeCN), *m/z* = 491, 435, 407; calc. for $[Mn(CO)_3\{MeC(CH_2{}^{80}SeMe)_3\}]^+$ 493, $[Mn(CO)\{MeC(CH_2{}^{80}SeMe)_3\}]^+$ 437, $[Mn\{MeC(CH_2{}^{80}SeMe)_3\}]^+$ 409. IR/cm^{-1} 2036(s), 1966(s), 1940(s), 1356(s), 1265(s), 1232(w), 1163(m), 1150(m), 1690(w), 1028(s), 995(w), 915(w), 833(w), 680(w), 663(w), 638(s), 618(m), 572(w), 555(w), 523(m), 279(w), 202(w), 191(w).

fac-$[Mn(CO)_3\{MeC(CH_2TeMe)_3\}][CF_3SO_3]$ was prepared similarly to give an orange product (78 %). Analysis: Calculated for $C_{12}H_{18}F_3MnO_6STe_3$: %C, 18.3; %H, 2.3. Found: %C, 18.9; %H, 2.6. ^1H NMR ($CDCl_3$, 300 K): δ 1.58 (s, 1H, CCH_3), 2.19 (s, 3H, $TeCH_3$), 3.00 (s, 2H, $TeCH_2$). $^{13}C\{^1H\}$ NMR ($CH_2Cl_2/CDCl_3$, 300 K): δ -8.3 ($TeCH_3$), 23.7 ($TeCH_2$), 29.4 (CCH_3), 39.5 (C), 217 - 222 (CO). ^{55}Mn NMR ($CH_2Cl_2/CDCl_3$, 300 K): δ -1509 ($w_{1/2}$ = 1200 Hz). $^{125}Te\{^1H\}$ NMR ($CH_2Cl_2/CDCl_3$, 300 K): δ 112. ES^+ (MeCN), *m/z* = 639, 583, 555; calc. for $[Mn(CO)_3\{MeC(CH_2{}^{130}TeMe)_3\}]^+$ 643, $[Mn(CO)\{MeC(CH_2{}^{130}TeMe)_3\}]^+$ 587, $[Mn\{MeC(CH_2{}^{130}TeMe)_3\}]^+$ 559. IR/cm^{-1} 2962(w), 2013(s), 1946(s), 1919(s), 1357(s), 1262(m), 1150(w), 1094(s), 1026(w), 834(m), 664(w), 636(m), 614(m), 535(m), 204(w), 188(w).

fac-$[Mn(CO)_3\{MeC(CH_2TePh)_3\}][CF_3SO_3]$ was prepared similarly to give an orange product (65 %). Analysis: Calculated for $C_{27}H_{24}F_3MnO_6STe_3$: %C, 33.3; %H, 2.5. Found: %C, 34.3; %H, 2.7. ^1H NMR ($CDCl_3$ 300 K): δ 1.20 (s, 1H, CCH_3), 2.8 - 3.8 (br, 2H, $TeCH_2$), 7.4 - 7.7 (m, 5H, TePh). $^{13}C\{^1H\}$ NMR ($CH_2Cl_2/CDCl_3$, 300 K): δ 20.5 ($TeCH_2$), 31.3 (CCH_3), 40.2 (C), 128 - 139 (TePh), 215 - 220 (CO). ^{55}Mn NMR ($CH_2Cl_2/CDCl_3$, 300 K): δ -1320 ($w_{1/2}$ = 2100 Hz). $^{125}Te\{^1H\}$ NMR ($CH_2Cl_2/CDCl_3$, 300 K): δ 353. ES^+ (MeCN), *m/z* = 824; calc. for $[Mn(CO)_3\{MeC(CH_2{}^{130}TePh)_3\}]^+$ 829. IR/cm^{-1} 3061(w), 2962(w), 2929(w), 2021(s), 1946(s), 1572(w), 1475(w), 1434(m), 1361(m), 1262(s), 1161(m), 1096(m), 1031(s), 998(m), 834(w), 803(w), 734(w), 690(w), 638(m), 614(m), 519(m), 453(m).

fac-$[Re(CO)_3\{MeC(CH_2SeMe)_3\}][CF_3SO_3]$. A solution of *fac*-$[Re(CO)_3(Me_2CO)_3][CF_3SO_3]$ was prepared by treatment of $[Re(CO)_5Br]$ (60 mg, 1.5 x 10^{-4} mol) with $AgCF_3SO_3$ (38 mg, 1.5 x 10^{-4} mol) in refluxing acetone for 4 hours. After cooling, the precipitated AgBr was removed by filtration and $MeC(CH_2SeMe)_3$ (52 mg, 1.5 x 10^{-4} mol) added to the reaction mixture which was then refluxed for a further 48 hours. The solvent was reduced *in vacuo* to 2 cm^3 and ice cold light petroleum ether (40 - 60 °C) added

to precipitate a white powder. Yield 30 mg, 26 %. Analysis: Calculated for $C_{12}H_{18}F_3O_6ReSSe_3$: %C, 18.7; %H, 2.3. Found: %C, 19.2; %H, 1.6. ^1H NMR ($CDCl_3$, 300 K): δ 1.33 (s, 1H, CCH_3), 2.31 (s, 3H, $SeCH_3$), 2.62 (s, 2H, $SeCH_2$). $^{13}C\{^1H\}$ NMR ($CH_2Cl_2/CDCl_3$, 300 K): δ 31.0 ($SeCH_3$), 34.9 (CCH_3), 40.4 ($SeCH_2$), 42.9 (C), 187.5 (CO). $^{77}Se\{^1H\}$ NMR ($CH_2Cl_2/CDCl_3$, 300 K): δ 23. ES^+ (MeCN), *m/z* = 621; calc. for $[^{185}Re(CO)_3\{MeC(CH_2{}^{80}SeMe)_3\}]^+$ 623. IR/cm^{-1} 2973(w), 2039(s), 1956(sh), 1940(s), 1357(s), 1260(s), 1226(w), 1154(m), 1092(m), 1029(s), 991(w), 834(w), 674(m), 668(m), 638(w), 516(m), 470(w).

X-ray Crystallographic Studies

Details of the crystallographic data collection and refinement parameters are given in Table 3.3. The crystals were grown by vapour diffusion of petroleum ether (40 - 60 °C) into solutions of the complexes in CH_2Cl_2. Data collection used a Rigaku AFC7S four circle diffractometer operating at 150 K (except for $[Re(CO)_3\{MeC(CH_2SeMe)_3\}][CF_3SO_3]$, 298 K) using graphite-monochromated Mo-K_α X-radiation (λ = 0.71073 Å). No significant crystal decay or movement was observed and the data were corrected for absorption using psi scans. The structures were solved by heavy atom methods[25] and expanded using Fourier techniques.[26] All calculations were performed using the teXsan crystallographic software package of Molecular Structure Corporation.[27]

fac-$[Mn(CO)_3\{MeC(CH_2SMe)_3\}][CF_3SO_3]$, *fac*-$[Mn(CO)_3\{MeC(CH_2SeMe)_3\}][CF_3SO_3]$ and *fac*-$[Mn(CO)_3\{MeC(CH_2TePh)_3\}][CF_3SO_3]$. All non-hydrogen atoms were refined anisotropically while H-atoms were placed in fixed, calculated positions with *d*(C-H) = 0.96 Å.

fac-$[Mn(CO)_3\{MeC(CH_2TeMe)_3\}][CF_3SO_3]$. The cation and anion were both disordered across a crystallographic mirror plane, although this disorder was successfully modelled. In the cation Mn(1), Te(1), O(2), C(2) and C(4) lie on the plane, although there are two equally populated alternative positions for each of the terminal Me substituents. The disorder in the triflate anion also leads to two equally populated arrangements, such that S(1), F(1) and O(3) lie on the mirror plane and are common to both, with one 50 % occupied triflate defined by S(1), O(3), O(4), O(5), F(1), F(2), F(3) and C(10), while the other is defined by S(1), O(3),

O(4), O(5*), C(10*), F(1), F(2*) and F(3*). All non-hydrogen atoms were refined anisotropically while H-atoms were placed in fixed, calculated positions with d(C-H) = 0.96 Å.

fac-[$Re(CO)_3${$MeC(CH_2SeMe)_3$}][CF_3SO_3]. Data were collected at 298 K and hence thermal parameters are higher than for the other structures. The structure shows two independent cations and two anions in the asymmetric unit. Both triflate anions show some disorder. In one case, the three F atoms are disordered through rotation about the C_3 axis. This was modelled successfully using alternative sites for each in a 50:50 ratio. In the other anion the O atoms are disordered *via* rotation about the C-S bond, giving two alternative sites in a 70:30 ratio. The F atoms in this molecule also show some disorder, although attempts to refine these with split occupancies were unsuccessful, hence these were refined anisotropically with high thermal parameters. The Re, Se, S, C and the fully occupied F and O atoms were refined anisotropically and H atoms included in fixed, calculated positions.

3.5 References

[1] W. Beck and R. E. Nitzschmann, *Z. Naturforsch., Teil, B,* 1962, **17**, 577.

[2] P. M. Treichel, in *Comprehensive Organometallic Chemistry*, G. Wilkinson, F. G. A. Stone, E. W. Abel (eds.), 1st edition, Pergamon, Oxford, 1982, Vol. 4, 31.

[3] W. Hieber and W. Schropp, Jr., *Z. Naturforsch., Teil B,* 1959, **14**, 460.

[4] T. Kruck and M. Noack, *Chem. Ber.,* 1963, **96**, 3028.

[5] F. L. Wimmer and M. R. Snow, *Aust. J. Chem.,* 1978, **31**, 267.

[6] D. Drew, D. J. Darensbourg and M. Y. Darensbourg, *Inorg. Chem.,* 1975, **14**, 1579.

[7] R. Mews, *Angew. Chem., Int. Ed. Engl.,* 1975, **14**, 640; 1977, **16**, 56.

[8] P. J. Harris, S. A. R. Knox, R. J. McKinney and F. G. A. Stone, *J. Chem. Soc., Dalton Trans.,* 1978, 1009.

[9] T. Kruck and M. Noack, *Chem. Ber.,* 1964, **97**, 1693.

[10] R. S. Nyholm, M. R. Snow and M. H. B. Stiddard, *J. Chem. Soc.,* 1965, 6564.

[11] H. Elias, G. Schmidt, H. -J Kuppers, M. Saher, K. Weighardt, B. Nuber and J. Weiss, *Inorg. Chem.,* 1989, **28**, 3021.

[12] J. Connolly, A. R. J. Genge, W. Levason, S. D. Orchard, S. J. A. Pope and G. Reid, *J. Chem. Soc., Dalton Trans.,* 1999, 2343.

[13] R. Usón, V. Riera, J. Gimeno, M. Laguna and M. P. Gamasa, *J. Chem. Soc., Dalton Trans.,* 1979, 996.

[14] J. Connolly, G. W. Goodban, G. Reid and A. M. Z. Slawin, *J. Chem. Soc., Dalton Trans.,* 1998, 2225.

[15] N. P. Luthra and J. D. Odom, in *The Chemistry of Organic Selenium and Tellurium Compounds,* S. Patai and Z. Rappoport (eds), Wiley, New York, 1986, Vol. 1, Chap. 6.

[16] W. Levason, S. D. Orchard and G. Reid, *Organometallics,* 1999, **18**, 1275.

[17] S. J. A. Pope and G. Reid, *J. Chem. Soc., Dalton Trans.,* 1999, 1615.

[18] J. Connolly, M. K. Davies and G. Reid, *J. Chem. Soc., Dalton Trans.,* 1998, 3833.

[19] E. W. Abel, S. K. Bhargava, K. Kite, K. G. Orrell, V. Sik and B. L. Williams, *J. Chem. Soc., Dalton Trans.,* 1984, 365.

[20] K. J. Reimer and A. Shaver, *Inorg. Synth.,* 1979, **19**, 158.

[21] S. P. Schmidt, W. C. Trogler and F. Basolo, *Inorg. Synth.,* 1990, **28**, 160.

[22] R. Ali, S. J. Higgins and W. Levason, *Inorg. Chim. Acta,* 1984, **84**, 65.

[23] D. J. Gulliver, E. G. Hope, W. Levason, S. G. Murray, D. M. Potter and G. L. Marshall, *J. Chem. Soc., Perkin Trans. II,* 1984, 429.

[24] E. G. Hope, T. Kemmitt and W. Levason, *Organometallics,* 1988, 7, 78.

[25] PATTY, The DIRDIF Program System, P. T. Beurskens, G. Admiraal, G. Beurskens, W. P. Bosman, S. Garcia-Granda, R. O. Gould, J. M. M. Smits, C. Smykalla. Technical Report of the Crystallography Laboratory, University of Nijmegen, The Netherlands, 1992.

[26] DIRDIF94, The DIRDIF-94 program system, P. T. Beurskens, G. Admiraal, G. Beurskens, W. P. Bosman, R. de Gelder, R. Israel and J. M. M. Smits. Technical Report of the Crystallography Laboratory, University of Nijmegen, The Netherlands, 1994.

[27] TeXsan: Crystal Structure Analysis Package, Molecular Structure Corporation, Texas, 1995.

Chapter 4

Homoleptic Platinum and Group 11 Metal Complexes

4.1 Introduction

The results of our studies into the bonding properties of telluroether ligands (Chapters 2 and 3) to low valent metal centres, along with the fact that, apart from the manganese(I) tritelluroether complexes discussed in Chapter 3, the coordination chemistry of multidentate telluroethers remained unexplored, promoted the investigation into homoleptic platinum group and group 10 metal complexes with the seleno- and telluroether tripodal ligands. However, in order to gain initial information on the properties of such homoleptic telluroether complexes the preparation of Pd(II) and Pt(II) bis(ditelluroether) species was investigated since there have been few reports of such systems. Indeed, as discussed in Chapter 1, most work has concentrated on the preparation of platinum metal halide complexes with a 1:1 metal:ditelluroether ratio including $[M(L\text{-}L)X_2]$ (M = Pd or Pt; L-L = $RTe(CH_2)_3TeR$, R = Me or Ph, or $o\text{-}C_6H_4(TeMe)_2$; X = Cl, Br or I),[1, 2] $[Ir(L\text{-}L)X_4]^-$,[2] and $[\{Ir(L\text{-}L)Cl_3\}_n]$.[3] Far fewer complexes with a 2:1 ditelluroether:metal ratio are known, examples being limited to some unstable cobalt(III) complexes,[4] and a range of homoleptic copper(I) and silver(I) complexes of the type $[M(L\text{-}L)_2]^+$, where L-L is a dithio-, diseleno- or ditelluroether ligand.[5, 6] Since the presence of halide co-ligands is expected to influence the properties of telluroether complexes significantly, the preparation of homoleptic species with Pd(II) and Pt(II) metal centres should enable the ditelluroether ligands to be studied in a new coordination environment.

In contrast to telluroether chemistry, the preparation of bis(dithioether) complexes with palladium and platinum is well established. The complexes $[M(L\text{-}L)_2][ClO_4]_2$ {M = Pd or Pt; L-L = $RS(CH_2)_nSR$ (R = Me or Ph, n = 2 or 3), *cis*-RSCH=CHSR and $o\text{-}C_6H_4(SR)_2$} have been prepared *via* the reaction of $Ag[ClO_4]$ with $[MCl_2(NCMe)_2]$ and subsequent addition of ligand.[7] These complexes were found to have low barriers to inversion due to the high *trans* influence of S compared to halide ligands. More recently, bis(diselenoether) complexes with Pd and Pt have also been studied. The preparation of the complexes $[M\{MeSe(CH_2)_3SeMe\}_2]^{2+}$ (M = Pd or Pt) have been reported *via* the reaction of the ligand with MCl_2 in refluxing MeCN in the presence of $TlPF_6$.[8] A few platinum metal complexes have also been described with the tripodal selenoether ligand $MeC(CH_2SeMe)_3$, including $[M\{MeC(CH_2SeMe)_3\}Cl_2]$ (M = Pd or Pt), $[M\{MeC(CH_2SeMe)_3\}Cl_3]$ (M = Rh or Ir) and $[Ru\{MeC(CH_2SeMe)_3\}Cl_3]$,[9] however no homoleptic species have yet been reported.

Reported here are the results of a study into the chemistry of the ligands $MeC(CH_2TeR)_3$ (R = Me and Ph) and, for comparison, $MeC(CH_2SeMe)_3$ with the platinum group and group 11 metals with the aim to form homoleptic species and probe the coordination modes adopted by these ligands on a variety of metal ions with differing stereochemical properties.

The homoleptic platinum and palladium complexes with ditelluroether ligands $[M(L\text{-}L)_2]^{2+}$ {M = Pd or Pt; L-L = $RTe(CH_2)_3TeR$ (R = Me or Ph) and *o*-$C_6H_4(TeMe)_2$} have also been synthesised for comparison.

These complexes have been characterised by analysis, IR and multinuclear NMR (^1H, $^{77}Se\{^1H\}/^{125}Te\{^1H\}$) spectroscopy as well as electrospray mass spectrometry. X-ray crystallographic studies have also been conducted on five of the complexes to confirm their identity and reveal their structures in the solid state.

4.2 Results and Discussion

4.21 Bis(ditelluroether) complexes of Pd and Pt

Reaction of $[M(NCMe)_2Cl_2]$ (M = Pd or Pt) with 2 mol. equiv. of ditelluroether ligand, L-L {L-L = $RTe(CH_2)_3TeR$ (R = Me or Ph) or *o*-$C_6H_4(TeMe)_2$}, and 2 mol. equiv. of $TlPF_6$ in MeCN affords the complexes $[M(L\text{-}L)_2][PF_6]_2$ as yellow or orange solids in high yield, after removal of the precipitated TlCl through filtration, reduction of the solvent volume *in vacuo* and addition of diethyl ether. Previously, the reaction of $[M(NCMe)_2Cl_2]$ with a large excess of ditelluroether had been shown to give $[M(L\text{-}L)Cl_2]$ as the only product,[1, 2] thereby necessitating the use of $TlPF_6$. Longer reaction times at room temperature were employed, rather than refluxing the reaction mixture, since dealkylation of the telluroether ligand was liable to occur.

4.211 NMR Spectroscopic Data

Coordinated ditelluroethers exist as two diastereoisomers, *meso* (with *syn* R groups) and DL (with *anti* R groups).[10, 11] Proton and especially $^{125}Te\{^1H\}$ NMR spectroscopies have proved very useful in assigning structures to many ditelluroether complexes. The possible combinations of *meso* and DL ditelluroethers for planar $M(L\text{-}L)_2$ moieties result in five possible isomers (invertomers) containing eight distinct tellurium centres, although all isomers need not be present in significant amounts in a given solution.

Figure 4.1. The possible invertomers for the complex $[M\{o\text{-}C_6H_4(TeMe)_2\}_2]^{2+}$.

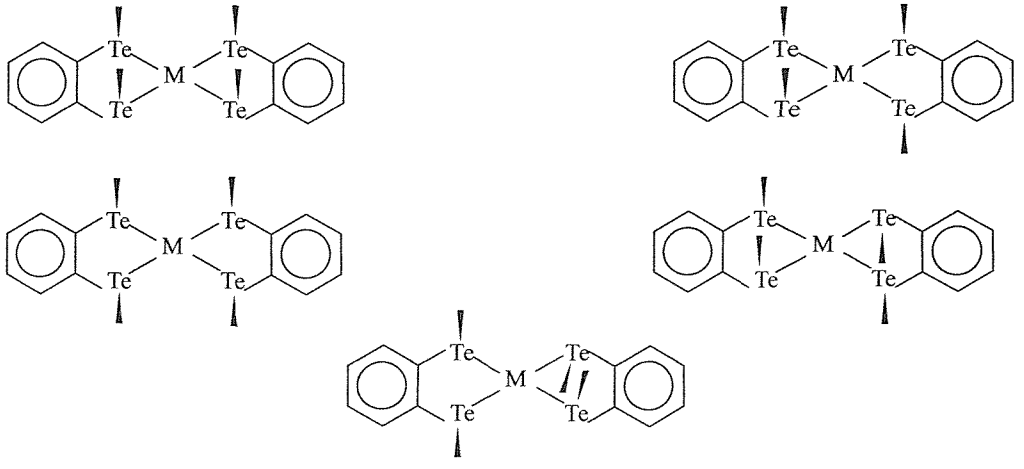

However, for the species discussed here the Te-*trans*-Te arrangement significantly lowers inversion barriers for pyramidal inversion, due to the high *trans* influence of tellurium. At room temperature the ^{1}H NMR spectra of all complexes showed broad features, sometimes with ill-defined splittings, thereby indicating that inversion processes were taking place on the ^{1}H NMR timescale. Similarly at 300 K, the $^{125}Te\{^{1}H\}$ NMR spectra showed very broad features typical of systems near to coalescence (Table 4.1).

Table 4.1. $^{125}Te\{^{1}H\}$ NMR data for the complexes $[M(L\text{-}L)_2]^{2+}$.

Complex	$\delta^{125}Te\{^{1}H\}$[a]/ppm
$[Pd\{MeTe(CH_2)_3TeMe\}_2]^{2+}$	198 - 219
$[Pd\{PhTe(CH_2)_3TePh\}_2]^{2+}$	485, 580, 605
$[Pd\{o\text{-}C_6H_4(TeMe)_2\}_2]^{2+}$	770 - 825
$[Pt\{MeTe(CH_2)_3TeMe\}_2]^{2+}$	195, 196, 200, 201
$[Pt\{PhTe(CH_2)_3TePh\}_2]^{2+}$	570 - 580
$[Pt\{o\text{-}C_6H_4(TeMe)_2\}_2]^{2+}$	692, 720

[a] in $Me_2CO/CDCl_3$ solution at 300 K, relative to neat external $TeMe_2$.

On cooling the spectra sharpened and for the platinum complexes individual resonances were resolved, but even at 210 K inversion still led to significant broadening and ^{195}Pt satellites were not resolved. Consistent with this, none of the platinum complexes exhibited a ^{195}Pt NMR spectrum at ambient temperature, but on cooling a solution of $[Pt\{o\text{-}C_6H_4(TeMe)_2\}_2]^{2+}$ to 210 K broad resonances appeared at δ -4790 and -4760. These shifts may be compared with those obtained for $[Pt\{MeSe(CH_2)_3SeMe\}_2]^{2+}$ (δ -4677, -4663 and -4657)[8] and $[Pt([8]aneSe_2)_2]^{2+}$ (δ -4606).[16]

4.212 X-ray Crystal Structure of [Pd{o-C$_6$H$_4$(TeMe)$_2$}$_2$][PF$_6$]$_2$·MeCN

Since NMR spectroscopic data revealed little structural information, due to the fluxional nature of these complexes, a single crystal X-ray diffraction study was undertaken on the species [Pd{*o*-C$_6$H$_4$(TeMe)$_2$}$_2$][PF$_6$]$_2$·MeCN, grown *via* the vapour diffusion of diethyl ether into a solution of the complex in MeCN. The structure (Figure 4.2, Tables 4.2 - 4.4) revealed a square planar cation with the Pd atom on an inversion centre, coordinated to two *meso* ditelluroether ligands. Two PF_6^- anions and a disordered MeCN molecule were also present in the asymmetric unit. The Te-Pd-Te angles are close to 90°, with *d*(Pd-Te) markedly longer than those in [Pd{PhTe(CH$_2$)$_3$TePh}Br$_2$] (2.528(1), 2.525(1) Å)[1] and thus consistent with the relative *trans* influence of Te > Br.

Attempts to oxidise the $[Pt(L\text{-}L)_2]^{2+}$ species to Pt^{IV} using Cl_2 in CCl_4 were unsuccessful, with the $^{125}Te\{^1H\}$ NMR spectrum showing signals corresponding to chlorinated ligand. This contrasts with the successful oxidation of [Pt(L-L)X$_2$] to stable [Pt(L-L)X$_4$] (L-L = dithio- or diselenoether) analogues,[12, 13] but is consistent with attempts to oxidise the dichloro-ditelluroether species.[1] Treatment of either of the palladium or platinum cations with LiCl in MeCN, monitored by UV/Vis spectroscopy, resulted in displacement of one ditelluroether and the formation of the corresponding [M(L-L)Cl$_2$] species.[1, 2] A similar result was found for the complexes $[M\{MeSe(CH_2)_3SeMe\}_2]^{2+}$ (M = Pd or Pt).[8]

Figure 4.2. X-ray crystal structure of [Pd{*o*-C$_6$H$_4$(TeMe)$_2$}$_2$]$^{2+}$ with numbering scheme adopted. Ellipsoids are drawn at 40 % probability and H-atoms omitted for clarity.

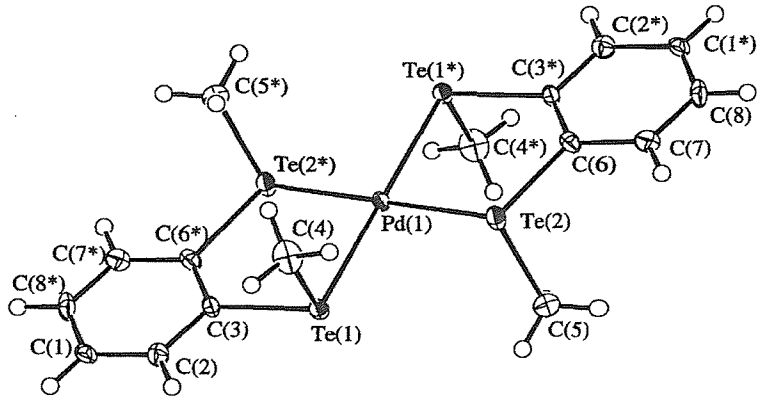

Table 4.2. Crystallographic Data Collection and Refinement Parameters.

	$[Pt\{MeC(CH_2SeMe)_3\}_2][PF_6]_2$	$[Ru\{MeC(CH_2SMe)_3\}_2]$ $[CF_3SO_3]_2$	$[Ru\{MeC(CH_2SeMe)_3\}_2]$ $[CF_3SO_3]_2$	$[Ag\{MeC(CH_2SeMe\}_3]$ $[CF_3SO_3]$	$[Pd\{o\text{-}C_6H_4(TeMe)_2\}_2]$ $[PF_6]_2 \cdot MeCN$
Formula	$C_{16}H_{36}F_{12}P_2PtSe_6$	$C_{18}H_{36}F_6O_6RuS_8$	$C_{18}H_{36}F_6O_6RuS_2Se_6$	$C_9H_{18}AgF_3O_3SSe_3$	$C_{18}H_{23}F_{12}NPdTe_4$
Formula weight	1187.24	820.02	1101.42	608.04	1160.11
Crystal System	Monoclinic	Triclinic	Triclinic	Monoclinic	Triclinic
Space group	$P2_1/n$	$P\bar{1}$	$P\bar{1}$	$P2_1/n$	$P\bar{1}$
a, Å	12.272(10)	8.658(3)	8.8436(5)	8.120(3)	8.9645(6)
b, Å	18.563(9)	11.533(3)	11.6692(15)	15.374(3)	18.896(6)
c, Å	15.285(7)	8.659(2)	8.7056(8)	14.071(2)	8.9325(5)
α/°	-	108.33(2)	107.369(9)	-	94.536(6)
β/°	113.18(3)	91.53(3)	91.648(7)	93.86(2)	95.649(5)
γ/°	-	106.01(2)	106.530(7)	-	99.533(7)
V, $Å^3$	3200(2)	782.8(4)	815.62(14)	1752.6(7)	1478.0(2)
Z	4	1	1	4	2
D_{calc}, g/cm^3	2.463	1.739	2.242	2.304	2.607
μ(Mo-K_α), cm^{-1}	113.69	11.02	73.68	75.27	46.94
Unique obs. reflections	5828	2762	2875	3228	5223
Obs. reflections with $[I_o > 2\sigma(I_o)]$	3435	2061	2263	2288	4284
R	0.054	0.048	0.037	0.046	0.031
R_w	0.049	0.050	0.101	0.060	0.035

$R = \Sigma (|F_{obs}|_i - |F_{calc}|_i) / \Sigma |F_{obs}|_i$, $R_w = \sqrt{[\Sigma w_i (|F_{obs}|_i - |F_{calc}|_i)^2 / \Sigma w_i |F_{obs}|_i^2]}$

Table 4.3. Selected bond lengths for $[Pd\{o\text{-}C_6H_4(TeMe)_2\}_2]^{2+}$.

Atom	Atom	Distance/Å	Atom	Atom	Distance/Å
Te(1)	Pd(1)	2.5716(4)	Te(1)	C(3)	2.120(7)
Te(1)	C(4)	2.132(8)	Te(2)	Pd(1)	2.5789(5)
Te(2)	C(5)	2.112(9)	Te(2)	C(6)	2.116(7)
Te(3)	Pd(2)	2.5732(5)	Te(3)	C(12)	2.112(9)
Te(3)	C(13)	2.120(7)	Te(4)	Pd(2)	2.5781(5)
Te(4)	C(10)	2.118(7)	Te(4)	C(11)	2.136(8)

Table 4.4. Selected bond angles for $[Pd\{o\text{-}C_6H_4(TeMe)_2\}_2]^{2+}$.

Atom	Atom	Atom	Angle(°)	Atom	Atom	Atom	Angle(°)
Pd(1)	Te(1)	C(3)	102.3(2)	Pd(1)	Te(1)	C(4)	98.3(2)
C(3)	Te(1)	C(4)	93.6(3)	Pd(1)	Te(2)	C(5)	100.5(2)
Pd(1)	Te(2)	C(6)	102.4(2)	C(5)	Te(2)	C(6)	92.8(3)
Pd(2)	Te(3)	C(12)	99.4(3)	Pd(2)	Te(3)	C(13)	103.2(2)
C(12)	Te(3)	C(13)	92.8(3)	Pd(2)	Te(4)	C(10)	102.7(2)
Pd(2)	Te(4)	C(11)	99.7(2)	C(10)	Te(4)	C(11)	93.6(3)
Te(1)	Pd(1)	Te(2)	89.98(1)	Te(3)	Pd(2)	Te(4)	90.33(1)

4.22 Bis(tripodal) complexes of the Platinum and Group 11 Metals

4.221 Palladium and Platinum

The preparation of homoleptic seleno- and telluroether Pd(II) and Pt(II) complexes with the tripodal ligands is of interest since the formation of square planar complexes with a free donor atom available on each ligand may lead to the stabilisation of unusual oxidation states. Such chemistry has been observed in the oxidation of $[Pd([9]aneS_3)_2]^{2+}$ to give the tetragonally distorted octahedral complex $[Pd([9]aneS_3)_2]^{3+}$.[14]

The target complexes $[M(L^3)_2][PF_6]_2$ (M = Pd or Pt; L^3 = $MeC(CH_2SeMe)_3$, $MeC(CH_2TeMe)_3$ or $MeC(CH_2TePh)_3$) were conveniently synthesised in moderate yield by the reaction of $[MCl_2(NCMe)_2]$ with two molar equivalents of ligand and $TlPF_6$ in MeCN. The selenoether complexes are stable in solution, however the products containing $MeC(CH_2TeMe)_3$ appear to decompose in solution over a few hours.

The NMR spectra of these species were expected to be complex due to the presence of five possible isomers (invertomers) containing eight distinct tellurium environments[5] with further complexity anticipated from the presence of both free and coordinated chalcogen functions. Considering this, the ^{1}H NMR spectra at 300 K for all six complexes were surprisingly simple, showing just one signal each for the ECH_3, ECH_2 (E = Se or Te) and CCH_3 groups. This indicates that these complexes are probably fluxional in solution at room temperature, the dynamic processes involving the arms of the tripod rapidly flipping on and off the metal centre.

Figure 4.3. ^{1}H NMR spectrum (300 MHz, CD_3CN, 300 K) of $[Pt\{MeC(CH_2TePh)_3\}_2][PF_6]_2$.

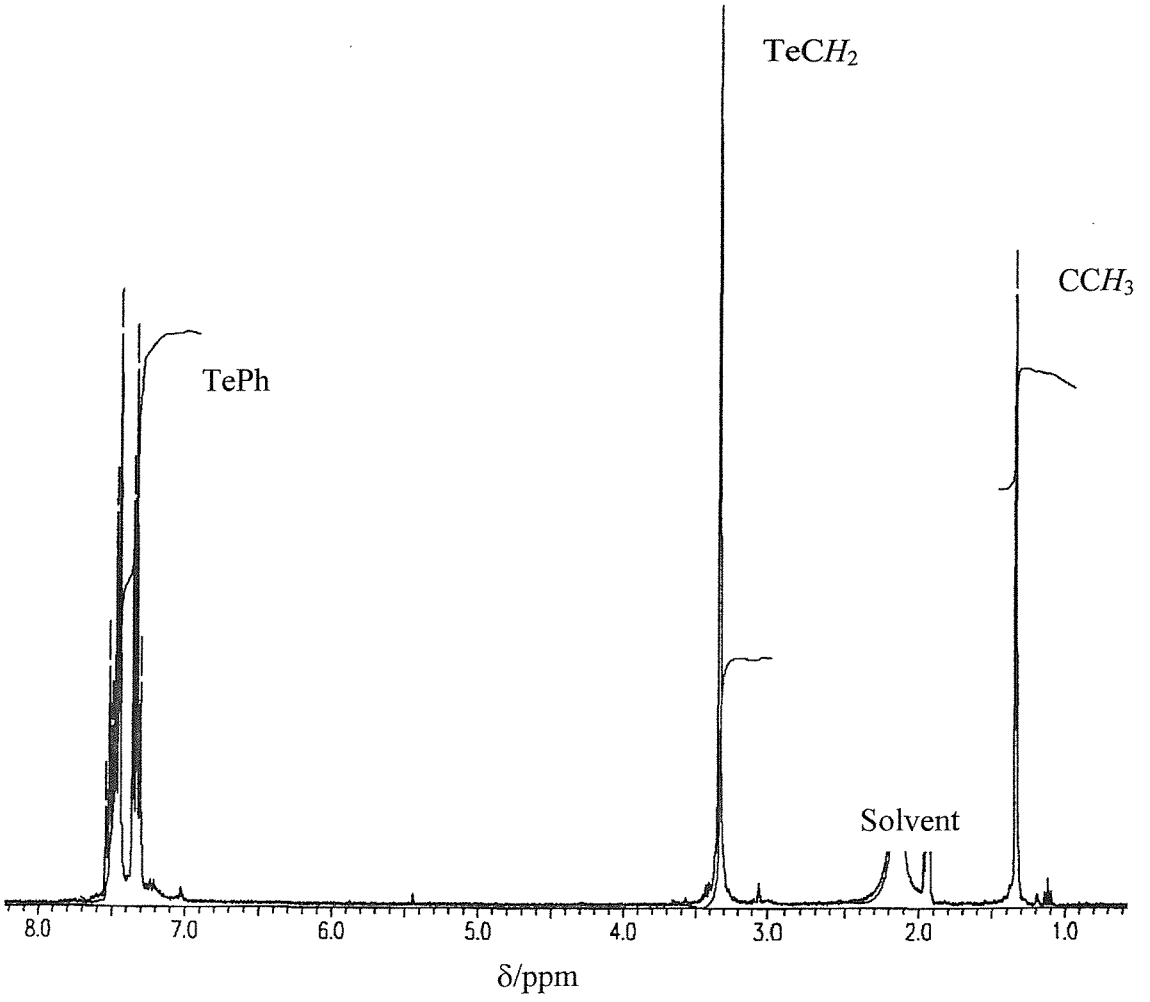

In order to study this dynamic behaviour further, VT ^{1}H NMR studies were conducted on the complexes $[M\{MeC(CH_2TeMe)_3\}_2][PF_6]_2$ (M = Pd or Pt). However, the spectra showed only a broadening of the resonances even at 180 K, indicating that fluxional processes were still rapid on the NMR timescale.

Variable temperature $^{77}Se\{^{1}H\}$ or $^{125}Te\{^{1}H\}$ NMR studies were also undertaken. At 300 K, the $^{77}Se\{^{1}H\}$ spectrum of $[Pd\{MeC(CH_2SeMe)_3\}_2][PF_6]_2$ exhibited a broad feature at δ 110 and for $[Pt\{MeC(CH_2SeMe)_3\}_2][PF_6]_2$ at δ 144. At 220 K, these signals were significantly sharper, with $w_{1/2}$ *ca.* 200 Hz, indicating a slowing of the dynamic processes, although the low-temperature limiting spectra were not obtained. The Pd complex showed three signals at δ 157, 147 (coordinated Se) and 32 (uncoordinated Se). The Pt complex gave more information showing five signals at δ 150, 149, 143, 142 and 34 with the signals corresponding to coordinated Se of similar intensity, probably indicating the up, up, up, down invertomer (Figure 4.4). The coupling to ^{195}Pt was not observed in these spectra even at 220 K, since the lines are still relatively broad, and indicates that $^{1}J_{Pt\text{-}Se}$ is within the line width of the resonances. This is consistent with similar reported complexes such as $[Pt([16]aneSe_4)]^{2+}$ where $^{1}J_{Pt\text{-}Se}$ was observed to be *ca.* 90 Hz.[8]

Figure 4.4. $^{77}Se\{^{1}H\}$ NMR spectrum (68.7 MHz, $Me_2CO/CDCl_3$, 220 K) of $[Pt\{MeC(CH_2SeMe)_3\}_2][PF_6]_2$.

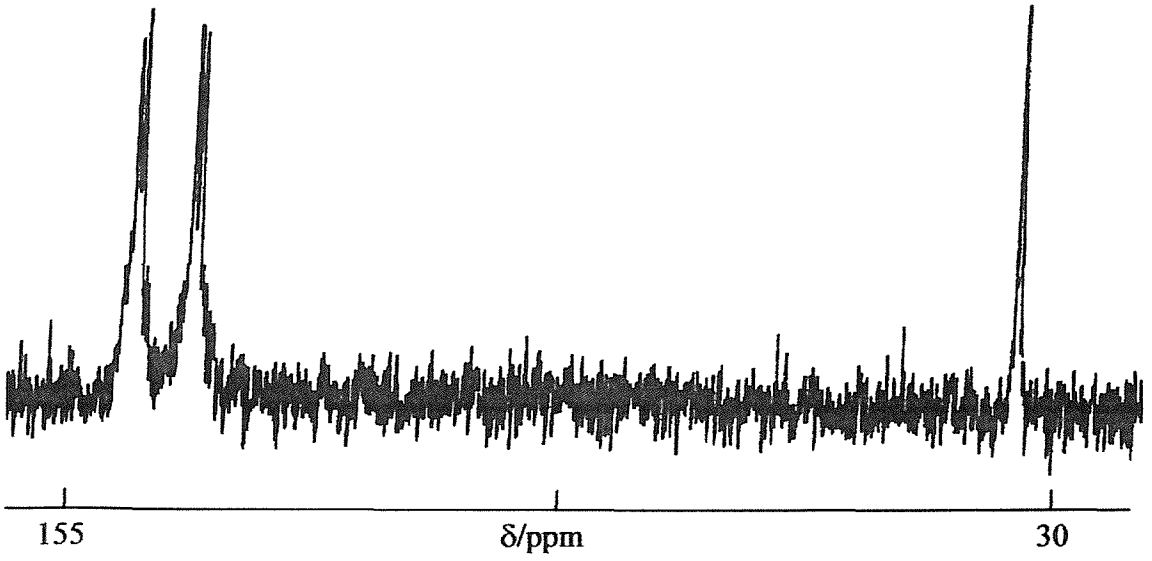

The ^{195}Pt NMR spectrum for $[Pt\{MeC(CH_2SeMe)_3\}_2]^{2+}$, at 220 K, showed a major signal at δ -4630 and a minor signal at δ -4888, this compares with δ -4750 for $[Pt([16]aneSe_4]^{2+}$ and δ -4677 for $[Pt\{MeSe(CH_2)_3SeMe\}_2]^{2+}$ and is therefore consistent with a Se_4 donor set at Pt(II).[15]

The complexes $[M\{MeC(CH_2TePh)_3\}_2][PF_6]_2$ (M = Pd or Pt) showed no signals in the $^{125}Te\{^1H\}$ spectra at room temperature although, broad signals were observed at 190 K at δ 528 and 561 for M = Pd. For M = Pt resonances associated with the uncoordinated chalcogen (δ 395) and coordinated chalcogen atoms (δ 512, 518, 542 and 547) were observed.

No signals were observed at either 300 K or 190 K for the complexes $[M\{MeC(CH_2TeMe)_3\}_2][PF_6]_2$ in the $^{125}Te\{^1H\}$ or ^{195}Pt NMR spectra. As there is no inherent reason for this, it is presumably due to decomposition in solution during the relatively long data accumulation.

4.222 X-ray Crystal Structure of $[Pt\{MeC(CH_2SeMe)_3\}_2][PF_6]_2$

Due to the dynamic nature of these complexes in solution, structural information *via* NMR spectroscopy was limited. Therefore in order to gain further insight into the structure of these d^8 complexes a single crystal X-ray diffraction study was undertaken on the complex $[Pt\{MeC(CH_2SeMe)_3\}_2][PF_6]_2$. Suitable crystals were grown from the vapour diffusion of diethyl ether into a solution of the complex in acetone. The structure (Figure 4.5, Tables 4.2, 4.5 - 4.6) reveals a square planar Se_4 donor set around the Pt(II) metal centre with the methyl groups on both ligands adopting a DL configuration, and the uncoordinated arm of each tripod pointing away from, and thus not interacting with, the Pt(II) centre, on opposite sides of the metal. The *d*(Pt-Se) (2.425(2) - 2.435(2) Å) are slightly longer than those observed for $[Pt([16]aneSe_4)]^{2+}$ (2.417(3) - 2.420(3) Å) and $[Pt\{MeSe(CH_2)_3SeMe\}_2]^{2+}$ (2.414(2) - 2.421(2) Å).[15, 16] The angles around the central Pt atom do not deviate significantly from 90 or 180° reflecting the good match of the six-membered chelate rings formed by the ligand and the *cis* angles required for the square planar geometry. The very flexible nature of the uncoordinated arms is also apparent from the crystal structure, which shows disorder in this region due to the presence of different conformations (see Experimental Section).

Figure 4.5. X-ray crystal structure of $[Pt\{MeC(CH_2SeMe)_3\}_2]^{2+}$ with numbering scheme adopted. Ellipsoids are drawn at 40 % probability and H-atoms omitted for clarity. The figure shows the major conformation.

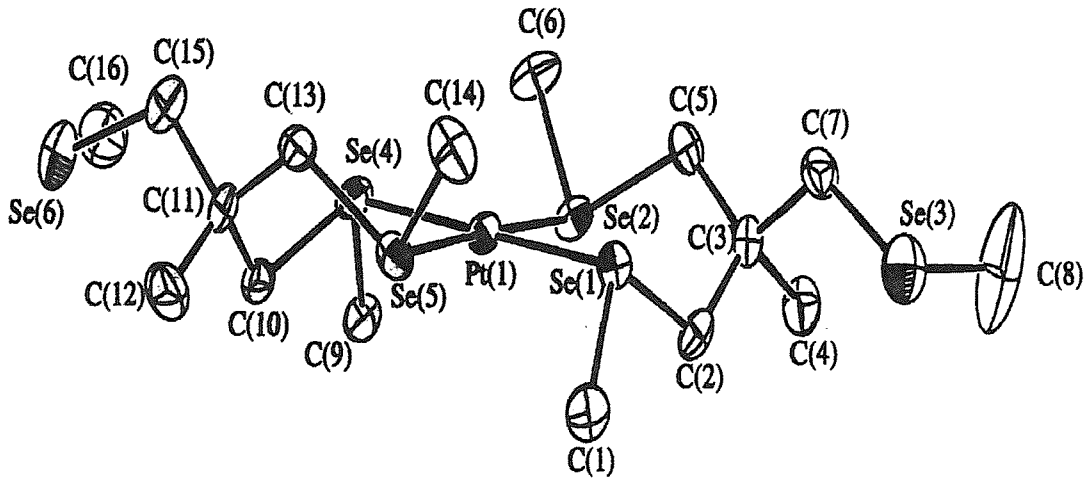

Table 4.5. Selected bond lengths for $[Pt\{MeC(CH_2SeMe)_3\}_2]^{2+}$.

Atom	Atom	Distance/Å	Atom	Atom	Distance/Å
Pt(1)	Se(1)	2.426(2)	Pt(1)	Se(2)	2.430(2)
Pt(1)	Se(4)	2.425(2)	Pt(1)	Se(5)	2.435(2)
Se(1)	C(1)	1.93(2)	Se(1)	C(2)	1.96(1)
Se(2)	C(5)	1.98(2)	Se(2)	C(6)	1.95(2)
Se(3)	C(7)	1.96(2)	Se(3)	C(8)	1.93(3)
Se(4)	C(10)	1.99(2)	Se(4)	C(9)	1.94(1)
Se(5)	C(14)	1.96(2)	Se(5)	C(13)	1.97(2)
Se(6)	C(15)	1.96(3)	Se(6)	C(16)	2.03(3)

Table 4.6. Selected bond angles for $[Pt\{MeC(CH_2SeMe)_3\}_2]^{2+}$.

Atom	Atom	Atom	Angle(°)	Atom	Atom	Atom	Angle(°)
Se(1)	Pt(1)	Se(2)	90.40(7)	Se(1)	Pt(1)	Se(4)	179.66(5)
Se(1)	Pt(1)	Se(5)	89.03(7)	Se(2)	Pt(1)	Se(4)	89.58(7)
Se(2)	Pt(1)	Se(5)	177.51(5)	Se(4)	Pt(1)	Se(5)	91.01(7)
Pt(1)	Se(1)	C(1)	103.6(7)	Pt(1)	Se(1)	C(2)	102.6(5)
C(1)	Se(1)	C(2)	95.2(6)	Pt(1)	Se(2)	C(5)	103.3(4)
Pt(1)	Se(2)	C(6)	105.3(5)	C(5)	Se(2)	C(6)	95.6(7)
C(7)	Se(3)	C(8)	102(1)	Pt(1)	Se(4)	C(9)	102.1(5)
Pt(1)	Se(4)	C(10)	102.8(6)	C(9)	Se(4)	C(10)	95.2(6)
Pt(1)	Se(5)	C(13)	101.8(5)	Pt(1)	Se(5)	C(14)	103.6(6)
C(13)	Se(5)	C(14)	94.2(8)	Se(1)	C(2)	C(3)	112.8(8)
C(15)	Se(6)	C(16)	98(1)				

4.223 Ruthenium

There are no examples of homoleptic hexaseleno- or hexatelluroether coordination in octahedral metal complexes, with typically two or more of the six coordination sites being occupied by halide co-ligands, which greatly influence the metal ion properties. This section reports the preparation of the first homoleptic hexaseleno- and hexatelluroether complexes, $[Ru(L^3)_2]^{2+}$ {L^3 = $MeC(CH_2EMe)_3$, E = S, Se or Te and $MeC(CH_2TePh)_3$}.

Reaction of $[Ru(dmf)_6][CF_3SO_3]_3$ with two mol. equiv. of L^3 in refluxing methanol affords the complexes $[Ru(L^3)_2][CF_3SO_3]_2$ as yellow solids. The electrospray mass spectra showed peaks with the correct isotopic distribution for the doubly charged species $[Ru(L^3)_2]^{2+}$, with IR spectroscopy showing peaks associated with the coordinated tripod ligands and the uncoordinated $CF_3SO_3^-$ anions.

The electronic spectra of $[Ru\{MeC(CH_2EMe)_3\}_2][CF_3SO_3]_2$ (E = S or Se) showed two *d-d* transitions, $^1A_{1g} \rightarrow {}^1T_{1g}$ and $^1A_{1g} \rightarrow {}^1T_{2g}$ at 27 530 and 31 730 cm $^{-1}$ for E = S, and 25 975 and 29 940 cm^{-1} for E = Se, as well as intense charge transfer transitions at higher energy. This leads to approximate values of 10 *Dq* and *B* of 26 500 and 260 cm^{-1} for the thioether complex and 25 000 and 250 cm^{-1} for the selenoether species.[17] These values may be compared with $[Ru(H_2O)_6]^{2+}$ (17 700 and 425), $[Ru(en)_3]^{2+}$ (25 450 and 390)[17] and

$[Ru([9]aneS_3)_2]^{2+}$ (28 400 and 290 cm^{-1}).[18] These data therefore indicate that the thio- and selenoether tripods, like [9]aneS$_3$, are strong field ligands with a high degree of covalent character in the Ru-Se bonds. The electronic spectra for the telluroether complexes showed charge transfer transitions tailing into the visible region, thus obscuring the metal centred transitions and preventing detailed analysis.

The $^{77}Se\{^1H\}$ and $^{125}Te\{^1H\}$ NMR shifts for these complexes are showed in Table 4.7.

Table 4.7. $^{77}Se\{^1H\}$ and $^{125}Te\{^1H\}$ NMR data for the complexes $[Ru(L^3)_2]^{2+}$.

Complex	$\delta(^{77}Se)^a$ or $\delta(^{125}Te)^b$	$\Delta(^{77}Se)^a$ or $\Delta(^{125}Te)^b$
$[Ru\{MeC(CH_2SeMe)_3\}_2]^{2+}$	120	96
$[Ru\{MeC(CH_2TeMe)_3\}_2]^{2+}$	204	182
$[Ru\{MeC(CH_2TePh)_3\}_2]^{2+}$	481	94

[a] in $MeNO_2/CDCl_3$ solution at 300 K, relative to neat external $SeMe_2$. [b] in $MeNO_2/CDCl_3$ solution at 300 K, relative to neat external $TeMe_2$.

Inspection of Table 4.7 shows just one resonance is observed for each of the complexes. Given that pyramidal inversion at an Ru-SeR_2 or Ru-TeR_2 unit is expected to be slow, the observation of only one resonance in each case indicates that each coordinated ligand adopts a *syn* configuration.[19] The coordination shift for the $MeC(CH_2TePh)_3$ complex is noticeably smaller than that observed for the $MeC(CH_2EMe)_3$ (E = Se or Te) complexes, indicating poorer σ-donation from the phenyl-substituted ligand. ^1H NMR spectroscopy also indicated the presence of just the *syn* invertomer, with one signal being observed for δ(EMe). However in order to confirm that pyramidal inversion is slow in these species, VT ^1H NMR studies were conducted on the complex $[Ru\{MeC(CH_2SeMe)_3\}_2][CF_3SO_3]_2$. No change in the spectrum was observed as the temperature was lowered to 180 K suggesting, although not confirming, that these complexes are not undergoing fast inversion on the ^1H NMR timescale.

An important feature to note is the relative ease of formation of these homoleptic Ru(II) complexes using the tripodal ligands. All previously reported seleno- and telluroether Ru(II) complexes have incorporated co-ligands such as halides, and homoleptic thioether coordination has only been achieved through the use of macrocyclic ligands.

4.224 X-ray Crystal Structure of $[Ru\{MeC(CH_2EMe)_3\}][CF_3SO_3]_2$ (E = S or Se)

Since the complexes reported in this section represent the first homoleptic hexaseleno- and hexatelluroether complexes, single crystal X-ray diffraction studies were undertaken on the thio- and selenoether species. Unfortunately, attempts to obtain crystals of the telluroether species were unsuccessful. Crystals of both complexes were grown *via* the vapour diffusion of diethyl ether into a solution of the appropriate complex in $MeNO_2$. The data collected for the complexes at 150 K gave rather broad peaks and did not refine satisfactorily. Data collection was therefore repeated at a slower scan-speed at room temperature, yielding better quality data.

The structure of the selenoether complex (Figure 4.6, Tables 4.2, 4.8 - 4.9) shows an ordered centrosymmetric $[Ru\{MeC(CH_2SeMe)_3\}_2]^{2+}$ cation with the Ru occupying a crystallographic inversion centre, giving a half cation and one $CF_3SO_3^-$ anion in the asymmetric unit. Within the cation, the Ru^{II} centre is coordinated to two tridentate, facially bound selenoether ligands, to give a slightly distorted octahedral arrangement with *d*(Ru-Se) = 2.4701(7) - 2.4808(7) Å. The Se-Ru-Se angles involved in the six membered chelate rings are close to 90°, with the Me substituents oriented in the propeller-like arrangement associated with the *syn* configuration, consistent with $^{77}Se\{^1H\}$ NMR spectroscopy. The Ru-Se distances compare with 2.396(1) - 2.465(1) Å in *cis*-$[RuCl_2([16]aneSe_4)]$ and 2.465(3) - 2.479(3) Å in *trans*-$[RuCl(PPh_3)([16]aneSe_4)]^+$.[19]

Figure 4.6. X-ray crystal structure of $[Ru\{MeC(CH_2SeMe)_3\}_2]^{2+}$ with numbering scheme adopted. Ellipsoids are drawn at 40 % probability and H-atoms omitted for clarity.

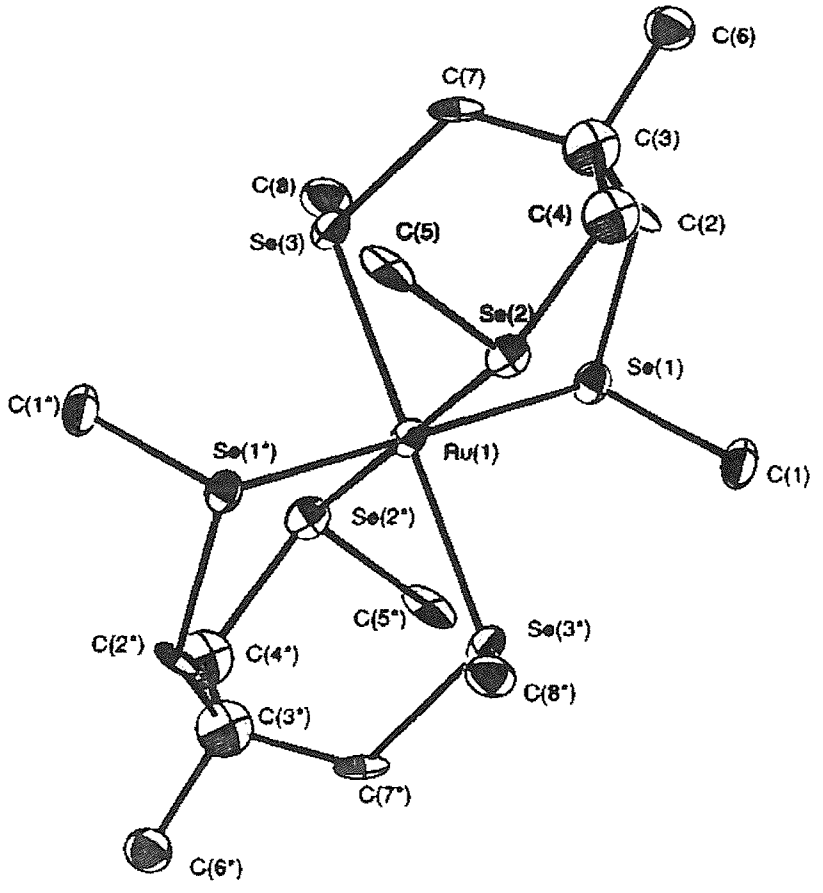

Table 4.8. Selected bond lengths for $[Ru\{MeC(CH_2SeMe)_3\}_2]^{2+}$.

Atom	Atom	Distance/Å	Atom	Atom	Distance/Å
Ru(l)	Se(l)	2.4808(7)	Se(l)	C(2)	1.975(6)
Ru(l)	Se(2)	2.4701(7)	Se(2)	C(5)	1.968(7)
Ru(l)	Se(3)	2.4781(6)	Se(3)	C(8)	1.958(7)
Se(l)	C(1)	1.953(7)	Se(3)	C(7)	1.970(7)
Se(2)	C(4)	1.968(7)			

Table 4.9. Selected bond angles for $[Ru\{MeC(CH_2SeMe)_3\}_2]^{2+}$.

Atom	Atom	Atom	Angle(°)	Atom	Atom	Atom	Angle(°)
Se(1)	Ru(1)	Se(2)	89.81(2)	C(1)	Se(1)	C(2)	98.1(3)
Se(1)	Ru(1)	Se(3)	90.99(2)	C(1)	Se(1)	Ru(1)	109.1(3)
Se(2)	Ru(1)	Se(3)	92.44(2)	C(8)	Se(3)	Ru(1)	109.8(2)
Ru(1)	Se(1)	C(2)	109.3(2)	C(7)	Se(3)	Ru(1)	109.59(19)
C(6)	Se(2)	C(5)	97.8(3)	C(8)	Se(3)	C(7)	97.5(3)
C(5)	Se(2)	Ru(1)	109.2(2)	C(6)	Se(2)	Ru(1)	108.1(3)

The crystal structure of $[Ru\{MeC(CH_2SMe)_3\}_2][CF_3SO_3]_2$ (Figure 4.7, Tables 4.2, 4.10 - 4.11) shows this compound to be isostructural with $[Ru\{MeC(CH_2SeMe)_3\}_2][CF_3SO_3]_2$, revealing an ordered centrosymmetric cation with the Ru occupying a crystallographic inversion centre and coordinated to two tridentate, facially bound thioether ligands in a *syn* configuration. The *d*(Ru-S) (2.375(2), 2.373(2), 2.367(2) Å) are slightly longer than those for $[Ru([9]aneS_3)_2]$, *d*(Ru-S) = 2.3272(14) - 2.3357(14) Å, probably due to the superior ligand properties of the macrocyclic ligand.[20] The S-Ru-S bond angles involved in the six-membered chelate rings are very close to 90°.

Figure 4.7. X-ray crystal structure of $[Ru\{MeC(CH_2SMe)_3\}_2]^{2+}$ with numbering scheme adopted. Ellipsoids are drawn at 40 % probability and H-atoms omitted for clarity.

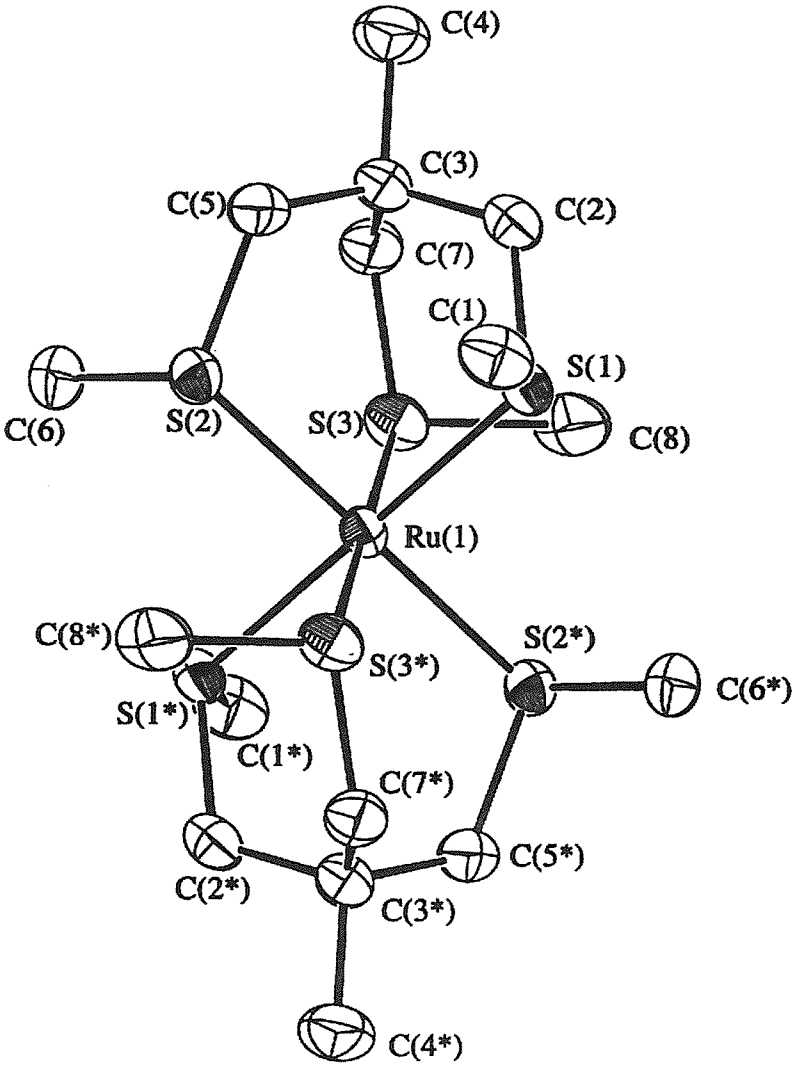

Table 4.10. Selected bond lengths for $[Ru\{MeC(CH_2SMe)_3\}_2]^{2+}$.

Atom	Atom	Distance/Å	Atom	Atom	Distance/Å
Ru(l)	S(1)	2.375(2)	S(1)	C(2)	1.841(7)
Ru(l)	S(2)	2.373(2)	S(2)	C(6)	1.810(8)
Ru(l)	S(3)	2.367(2)	S(3)	C(8)	1.813(8)
S(1)	C(1)	1.800(7)	S(3)	C(7)	1.826(7)
S(2)	C(5)	1.829(7)			

Table 4.11. Selected bond angles for $[Ru\{MeC(CH_2SMe)_3\}_2]^{2+}$.

Atom	Atom	Atom	Angle(°)	Atom	Atom	Atom	Angle(°)
S(1)	Ru(1)	S(2)	91.19(6)	Ru(1)	S(1)	C(1)	111.5(3)
S(1)	Ru(1)	S(3)	92.48(6)	C(1)	S(1)	C(2)	101.1(3)
S(2)	Ru(1)	S(3)	89.84(6)	Ru(1)	S(2)	C(6)	111.0(3)
Ru(1)	S(1)	C(2)	111.2(2)	Ru(1)	S(3)	C(7)	110.5(2)
Ru(1)	S(2)	C(5)	111.1(2)	C(7)	S(3)	C(8)	100.5(3)
C(5)	S(2)	C(6)	101.1(3)	Ru(1)	S(3)	C(8)	110.9(3)

4.225 Rhodium and Iridium

The complexes $[Rh(L\text{-}L)_2Cl_2][PF_6]$ {L-L = $RTe(CH_2)_3TeR$ (R = Me or Ph) or *o*-$C_6H_4(TeMe)_2$}, have been recently prepared by this research group as an extension of the homoleptic bis(ditelluroether) palladium and platinum chemistry discussed in Section 4.21. These medium oxidation complexes were formed in high yield from the reaction of $RhCl_3.3H_2O$ with two mol. equiv. of L-L.[21] In light of these results and the ease of preparation of the homoleptic ruthenium(II) complexes with the tripodal ligands, we were interested to ascertain if we could extend the investigation into homoleptic species to medium oxidation complexes. Therefore, the preparation of hexaseleno- and hexatelluroether complexes with rhodium(III) and iridium(III) centres, which has previously not been achieved, was investigated.

Reaction of $[Rh(OH_2)_6]^{3+}$ with 2 mol. equiv. of $MeC(CH_2SeMe)_3$ and addition of excess NH_4PF_6 affords $[Rh\{MeC(CH_2SeMe)_3\}_2][PF_6]_3$ as a red powder. The IR spectrum showed the presence of the coordinated ligand and the PF_6^- anion, with the ^1H NMR spectrum indicating the presence of both *syn* and *anti* invertomers. The electrospray mass spectrum gave one cluster of peaks centred at *m/z* = 395, which corresponds to the ion $[Rh\{MeC(CH_2SeMe)_3\}\{MeC(CH_2SeMe)_2(CH_2Se)\}]^{2+}$, therefore indicating that dealkylation of the tripositive cation has occurred during ionisation to produce the dipositive cation. The isotope pattern confirmed this assignment, providing a very good match with the calculated pattern. The $^{77}Se\{^1H\}$ NMR spectrum at 300 K showed several resonances but these did not show any coupling to ^{103}Rh, therefore the sample was cooled to 200 K whereupon doublets were observed in the range of δ 126 to 159 with $^1J_{Rh\text{-}Se}$ approximately 43 Hz. This Rh-Se

coupling constant is consistent with related species such as *trans*-$[RhCl_2([8]aneSe_2)_2][BF_4]$ (42 Hz) and *cis*-$[RhCl_2([16]aneSe_4)][PF_6]$ (36 Hz, 37 Hz).[22]

Attempts to prepare the related telluroether complexes *via* similar methods were unsuccessful, probably due to facile decomposition or dealkylation occurring as a consequence of the higher oxidation state of the metal compared to the Ru(II) complexes. This has been observed for other systems.[23]

The Ir(III) complex $[Ir\{MeC(CH_2SeMe)_3\}_2][PF_6]_3$ was prepared by the reaction of $MeC(CH_2SeMe)_3$ with the Ir(I) precursor $[IrCl(C_8H_{14})_2]_2$ to give a yellow solid *via* the oxidation of Ir(I) by HBF_4. Interestingly, similar reaction conditions using the ligand $[9]aneS_3$ gave the hydride analogue, $[IrH([9]aneS_3)_2][BF_4]_2$, which may be converted to $[Ir([9]aneS_3)_2]^{3+}$ by treatment with HNO_3.[24] The ^1H NMR spectrum indicated the presence of the selenoether ligand with IR spectroscopy showing peaks assigned to the ligand and PF_6^- anion. Interestingly, the electrospray mass spectrum showed the same behaviour as the rhodium complex, one cluster of peaks corresponding to the dication $[Ir\{MeC(CH_2SeMe)_3\}\{MeC(CH_2SeMe)_2(CH_2Se)\}]^{2+}$, being observed at *m/z* = 439. Therefore, dealkylation has again occurred during the ionisation process. The $^{77}Se\{^1H\}$ NMR spectrum showed peaks at δ 77, 87, 109 entirely reasonable shifts compared to the previous complexes. Like the rhodium species, attempts to prepare the analogous telluroether complexes by similar methods were unsuccessful and hence this chemistry was not pursued.

4.226 Copper and Silver

The self-assembly of complex structures is an area of chemistry receiving much attention in the literature. Both copper(I) and silver(I) metal centres have played key roles in the construction of such supramolecular arrays and our research group recently reported a range of homoleptic dithio-, diseleno- and ditelluroether complexes with these metals.[25] The crystal structures of several of these compounds revealed highly unusual structural features, including a three dimensional infinite lattice for the complex $[Ag_n(PhSCH_2CH_2CH_2SPh)_{2n}]^{n+}$.[26] Since we were interested in studying the tripodal ligands in new homoleptic coordination environments, including extended structures, their chemistry with the Cu(I) and Ag(I) ions was investigated.

The reaction of $[Cu(NCMe)_4][PF_6]$ with two mol. equiv. of L^3 (L^3 = $MeC(CH_2SeMe)_3$, $MeC(CH_2TeMe)_3$ or $MeC(CH_2TePh)_3$) gave the species $[Cu(L^3)_2][PF_6]$ as pale yellow

products. The electrospray mass spectra showed peaks corresponding to the ion $[Cu(L^3)]^+$ for all complexes, however the ion $[Cu(L^3)_2]^+$ was only observed for the $MeC(CH_2TeMe)_3$ complex. This behaviour is common for other systems and has been attributed to the labile nature of these d^{10} complexes, which liberate ligand readily in the mass spectrometer.[5] Elemental analyses confirmed the identity of the complexes as the bis-ligand species.

The ^1H NMR spectra were rather uninformative, showing only the presence of the coordinated ligand, indicating that rapid exchange processes such as reversible intramolecular chelate ring-opening and pyramidal inversion are probably occurring in solution. Similar behaviour was observed for the bis-bidentate complexes, for example $[Cu\{MeSeCH_2CH_2SeMe\}_2][PF_6]$.[5] Attempts to obtain ^{63}Cu, $^{77}Se\{^1H\}$ or $^{125}Te\{^1H\}$ NMR spectra were unsuccessful, even at low temperature, again illustrating the rapid and complex dynamic behaviour of these species in solution.

Recently, the structures of Ag(I) complexes with thioether cages[27] and with the tripodal phosphine, $CH_3C(CH_2PPh_2)_3$, have been reported reflecting the interest in the unique structural features associated with this chemistry.[28] This, together with the structures previously identified for the bidentate group 16 ligand complexes of Ag(I),[26] prompted the investigation into the coordination chemistry of the group 16 tripod ligands with this ion. Reaction of 2 mol. equiv. of L^3 (L^3 = $MeC(CH_2SeMe)_3$, $MeC(CH_2TeMe)_3$ or $MeC(CH_2TePh)_3$) with $Ag[CF_3SO_3]$ gave white, light sensitive powders, after reduction of the solvent *in vacuo* and addition of diethyl ether.

The ^1H NMR spectra of the Ag(I) complexes showed similar behaviour to the Cu(I) compounds, and so provided little structural information. Elemental analyses gave information as to the stoichiometry, revealing that although the telluroether complexes are the expected $[Ag\{MeC(CH_2TeR)_3\}_2][CF_3SO_3]$ (R = Me or Ph) species, the isolated selenoether product was in fact the 1:1 complex, $[Ag\{MeC(CH_2SeMe)_3\}][CF_3SO_3]$. The electrospray mass spectra of all three complexes showed peaks corresponding to the ion $[Ag(L^3)_2]^+$. Unfortunately, the $^{77}Se\{^1H\}$ or $^{125}Te\{^1H\}$ NMR spectra could not be obtained even at low temperature.

4.227 X-ray Crystal Structure of $[Ag\{MeC(CH_2SeMe)_3\}][CF_3SO_3]$

Since the crystal structures of the bidentate group 16 complexes revealed extended structures, the structures of these tripod derivatives were of particular interest. Colourless crystals of the selenoether complex $[Ag\{MeC(CH_2SeMe)_3\}][CF_3SO_3]$ were grown by the

vapour diffusion of diethyl ether into a solution of 2 mol. equiv. of $MeC(CH_2SeMe)_3$ and 1 mol. equiv. of $Ag[CF_3SO_3]$ in dry CH_2Cl_2, under a N_2 atmosphere. The structure of $[Ag\{MeC(CH_2SeMe)_3\}][CF_3SO_3]$ shows an infinite chain lattice (Figures 4.8 - 4.9, Table 4.2, 4.12- 4.13) *via* bidentate coordination of $MeC(CH_2SeMe)_3$ to one Ag(I) and monodentate coordination to an adjacent Ag(I), resulting in a distorted trigonal planar geometry around each Ag atom. The electrospray mass spectrum of these crystals was identical to that of the bulk solid, giving a cluster of peaks for $[Ag\{MeC(CH_2SeMe)_3\}_2]^+$. This species may be expected as a fragment of the crystallographically identified linear chain polymer involving a 1:1 Ag:selenoether ratio, since the selenoether ligands are effectively bridging Ag ions. The *d*(Ag-Se) (2.544(1), 2.607(2), 2.678(1) Å) vary by over 0.1 Å, with the two longer bonds in the chelate. Similar behaviour was observed for $[Ag_n\{\mu\text{-}o\text{-}C_6H_4(SeMe)_2\}_n\{o\text{-}C_6H_4(SeMe)_2\}_n]^{n+}$ where bond lengths varied from 2.587(1) - 2.861(1) Å.[25] The Ag-Se bond distances are comparable to those observed for $[Ag(MeSeCH_2CH_2SeMe)_2][BF_4]$ (*d*(Ag-Se) = 2.610(1) - 2.638(1) Å).[6] The Se-Ag-Se bond angle involved in the six-membered chelate ring is 94.36(4)° with the two angles to the Se attached to the next Ag(I) at 126.09(5)° and 139.55(5)°. The Me substituents are again orientated in the *syn* configuration.

After this work had been submitted for publication, a paper was published reporting the formation of one-dimensional copper(I) coordination polymers based on the tridentate thioether ligand $MeSi(CH_2SMe)_3$ of the formula $[Cu_3\{MeSi(CH_2SMe)_3\}_2Br_3]$.[29] The structure revealed tetrahedral Cu(I) with the thioether ligands exhibiting two different coordination modes namely unidentate:bidentate and bidentate:bidentate, again illustrating the flexibility and unique coordination chemistry of these tripodal ligands.

Figure 4.8. X-ray crystal structure of $[Ag\{MeC(CH_2SeMe)_3\}_2]^+$ with numbering scheme adopted, showing the local geometry around Ag^+ ion. Ellipsoids are drawn at 40 % probability and H-atoms omitted for clarity.

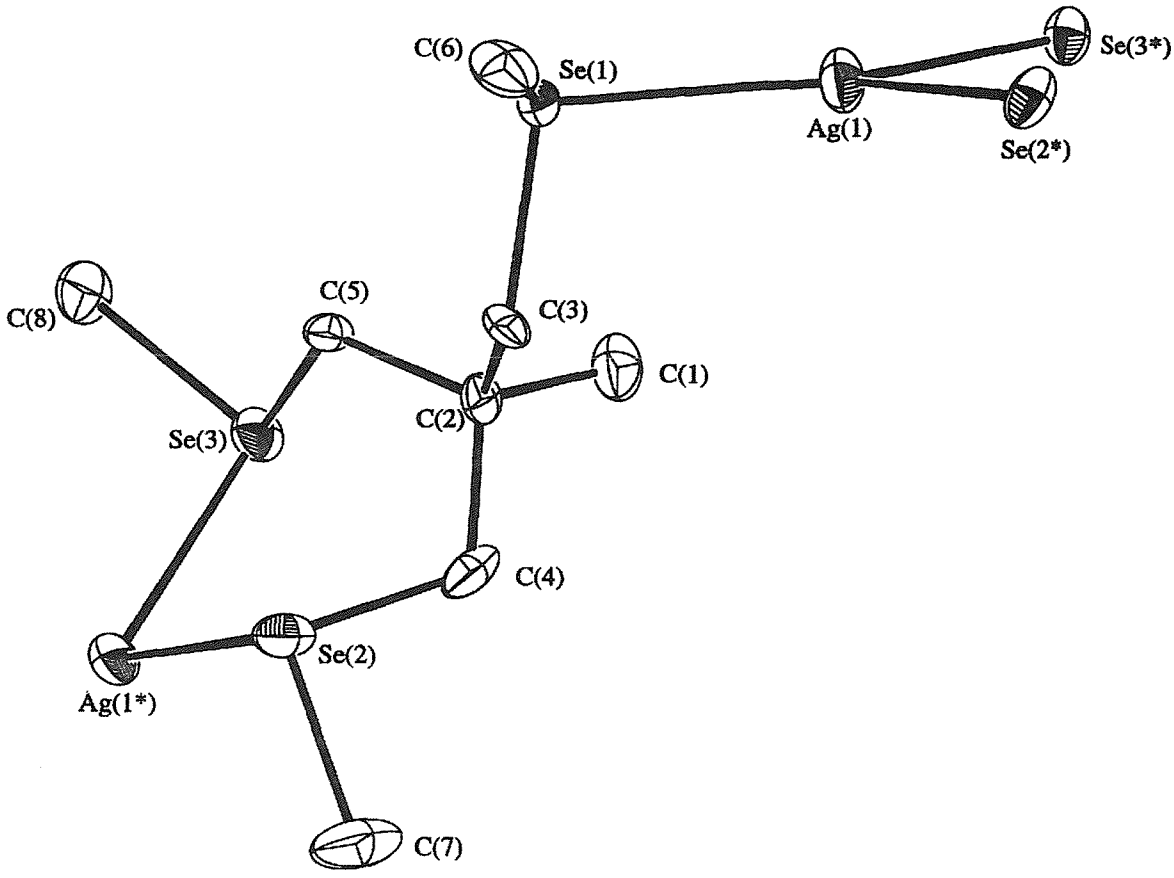

Table 4.12. Selected bond lengths for $[Ag\{MeC(CH_2SeMe)_3\}]^+$.

Atom	Atom	Distance/Å	Atom	Atom	Distance/Å
Ag(1)	Se(1)	2.544(1)	Ag(1)	Se(2)	2.678(1)
Ag(1)	Se(3)	2.607(2)	Se(1)	C(3)	1.97(1)
Se(1)	C(6)	1.94(1)	Se(2)	C(4)	1.96(1)
Se(2)	C(7)	1.95(1)	Se(3)	C(5)	1.963(9)
Se(3)	C(8)	1.97(1)			

Figure 4.9. X-ray crystal structure of $[Ag\{MeC(CH_2SeMe)_3\}_2]^+$ with numbering scheme adopted, showing extended structure. Ellipsoids are drawn at 40 % probability and H-atoms omitted for clarity.

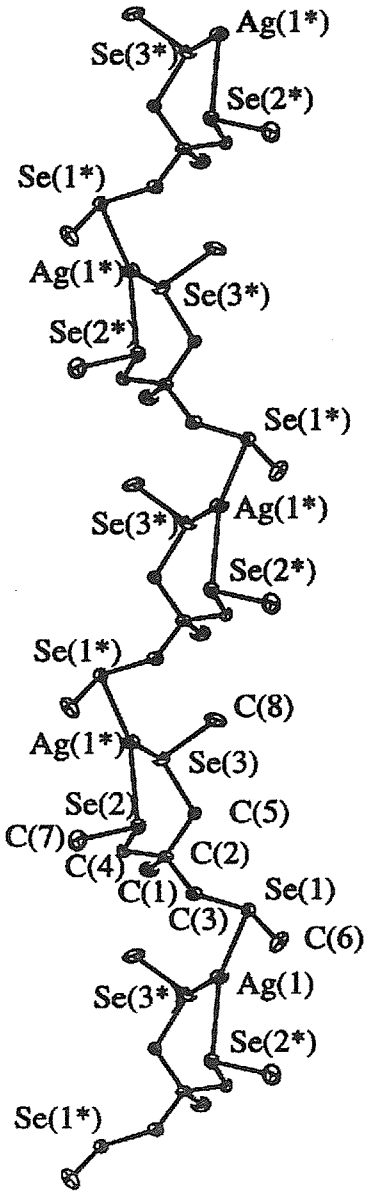

Table 4.13. Selected bond angles for $[Ag\{MeC(CH_2SeMe)_3\}]^+$.

Atom	Atom	Atom	Angle(°)	Atom	Atom	Atom	Angle(°)
Se(1)	Ag(1)	Se(2)	126.09(5)	Se(1)	Ag(1)	Se(3)	139.55(5)
Se(2)	Ag(1)	Se(3)	94.36(4)	Ag(1)	Se(1)	C(3)	102.5(3)
Ag(1)	Se(1)	C(6)	98.9(4)	C(3)	Se(1)	C(6)	95.9(5)
Ag(1)	Se(2)	C(4)	92.1(3)	Ag(1)	Se(2)	C(7)	104.8(4)
C(4)	Se(2)	C(7)	95.9(6)	Ag(1)	Se(3)	C(5)	95.9(3)
Ag(1)	Se(3)	C(8)	101.7(3)	C(5)	Se(3)	C(8)	94.9(5)

4.228 Electrochemistry

The macrocylic ligand [9]aneS$_3$ has been shown to stabilise unusual oxidation states in homoleptic platinum group metal complexes, such as $[Rh([9]aneS_3)_2]^{2+}$ obtained *via* the electrochemical reduction of the Rh(III) complex[30] and the $[M([9]aneS_3)_2]^{3+}$ (M = Pd and Pt) species obtained from the oxidation of the M(II) species.[14, 31] In order to investigate the ability of these tripodal ligands to stabilise other less common oxidation states, the electrochemical behaviour of all of the platinum group metal complexes was investigated by cyclic voltammetry over the range + 1.8 V to –1.8 V in MeCN solution at room temperature. The redox responses were rather uninformative; revealing only very broad, irreversible processes which shift potential upon varying the scan-rate. The absence of any reversible redox processes for the Ru(II) complexes is in accord with the large ligand field splitting observed for these species. After this work had been published the homoleptic Ru(II)-diphosphine and Ru(II)-diarsine complexes $[Ru(L\text{-}L)_3][CF_3SO_3]_2$ (L-L = $Me_2P(CH_2)_nPMe_2$, n = 1 and 2; *o*-$C_6H_4(AsMe_2)_2$) were reported. Electrochemical studies on these complexes also failed to show an oxidation wave to the respective Ru(III) species.[32]

4.3 Conclusions

The preparation of homoleptic ditelluroether complexes of Pd(II) and Pt(II) has shown that the presence of halide co-ligands greatly affects the properties of the metal ion, and are not necessarily required to form stable platinum metal complexes with telluroether ligands.

The extension of this chemistry to the group 16 tripod ligands, $MeC(CH_2SeMe)_3$, $MeC(CH_2TeMe)_3$ and $MeC(CH_2TePh)_3$ has illustrated the versatility of these ligands with a variety of medium oxidation state transition metal ions. In particular, the various coordination modes that they may adopt to accommodate metal ion requirements has been demonstrated. For the Ru(II), Rh(III) and Ir(III) complexes facial tridentate coordination, for Pd(II) and Pt(II) bidentate coordination with one uncoordinated arm, and for the Ag(I) selenoether complex both bi- and monodentate coordination to two different Ag(I) centres is observed. The homoleptic selenoether and telluroether coordination achieved for the complexes in this work contrasts with the much more familiar halo-derivatives known for the platinum metal ions. In particular the ease of formation of the hexaseleno- and hexatelluroether Ru(II) species illustrates the excellent ligand properties of these group 16 tripods in comparison to the bidentate ligands where such coordination has not been achieved. The fact that the telluroether complexes could not be isolated for Rh(III) and Ir(III) is perhaps more as a consequence of the harsh reaction conditions employed, to avoid halide coordination, and resulting in dealkylation, rather than the stability of the final complexes.

4.4 Experimental

4.41 Bis(ditelluroether) complexes of Pd and Pt

The ligands $MeTe(CH_2)_3TeMe$, $PhTe(CH_2)_3TePh$ and *o*-$C_6H_4(TeMe)_2$ were prepared *via* the literature procedures.[33, 34]

$[Pd\{MeTe(CH_2)_3TeMe\}_2][PF_6]_2$. $[PdCl_2(NCMe)_2]$ (82 mg, 3.2 x 10^{-4} mol) and $TlPF_6$ (226 mg, 6.5 x 10^{-4} mol) were stirred at room temperature for 30 minutes under a dinitrogen atmosphere in MeCN (30 cm^3). $MeTe(CH_2)_3TeMe$ (221 mg, 6.8 x 10^{-4} mol) in MeCN (5 cm^3) was then added and the reaction stirred at room temperature for 18 hours to give a yellow solution and fine white precipitate. The solution was filtered to remove the TlCl, reduced to *ca.* 2 cm^3 *in vacuo* and diethyl ether (10 cm^3) added to precipitate a yellow solid. Yield 220 mg, 65 %. Analysis: Calculated for $C_{10}H_{24}F_{12}P_2PdTe_4$: %C, 11.42; %H, 2.28. Found: %C, 11.39; %H, 2.28. ^1H NMR (CD_3CN, 300 K): δ 2.27 (br, 1H, $CH_2CH_2CH_2$), 2.37 (s, 3H, $TeCH_3$), 2.93 (m, 2H, $TeCH_2$). IR/cm^{-1} 2957(w), 2924(w), 1425(w), 1357(s), 1279(s), 1212(w), 1095(m), 987(m), 832(s), 739(w), 709(m), 613(w), 556(s).

$[Pd\{PhTe(CH_2)_3TePh\}_2][PF_6]_2$ was prepared similarly to give an orange powder (70 %). Analysis: Calculated for $C_{30}H_{32}F_{12}P_2PdTe_4$: %C, 27.72; %H, 2.46. Found: %C, 27.93; %H, 2.27. ^1H NMR (CD_3CN, 300 K): δ 2.58 (br, 1H, $CH_2CH_2CH_2$), 3.13 (br, 2H, $TeCH_2$), 7.58 (m, 5H, TePh). IR/cm^{-1} 1570(w), 1470(w), 1432(w), 1357(s), 1260(w), 1210(w), 1093(s), 1018(w), 996(m), 840(s), 728(m), 686(m), 615(w), 557(s), 452(w).

$[Pd\{o\text{-}C_6H_4(TeMe)_2\}_2][PF_6]_2$ was prepared similarly to give a yellow solid (80 %). Analysis: Calculated for $C_{16}H_{20}F_{12}P_2PdTe_4$: %C, 17.16; %H, 1.79. Found: %C, 17.59; %H, 1.78. ^1H NMR (CD_3CN, 300 K): δ 2.60 (s, 3H, $TeCH_3$), 7.81 (m, 2H, *o*-C_6H_4). IR/cm^{-1} 1356(s), 1093(s), 985(m), 834(s), 756(m), 613(w), 556(m).

$[Pt\{MeTe(CH_2)_3TeMe\}_2][PF_6]_2$. $PtCl_2(NCMe)_2$ (60 mg, 0.23 mmol) and $TlPF_6$ (170 mg, 0.47 mmol) were stirred at room temperature for 30 minutes under a dinitrogen atmosphere in MeCN (30 cm^3). $MeTe(CH_2)_3TeMe$ (180 mg, 0.55 mmol) in MeCN (5 cm^3) was then added and the reaction stirred at room temperature for 48 hours to give a yellow solution and

fine white precipitate. The solution was filtered to remove the TlCl, reduced to *ca.* 2 cm^3 *in vacuo* and diethyl ether (10 cm^3) added to precipitate a yellow solid. Yield 210 mg, 80 %. Analysis: Calculated for $C_{10}H_{24}F_{12}P_2PtTe_4$: %C, 10.53; %H, 2.11. Found: %C, 11.00; %H, 2.01. ^1H NMR (CD_3CN, 300 K): δ 2.24 (m, 1H, $CH_2CH_2CH_2$), 2.43 (s, 3H, $TeCH_3$), 3.02 (m, 2H, $TeCH_2$). IR/cm^{-1} 2922(w), 2853(w), 1357(s), 1262(vw), 1228(w), 1205(w), 1092(s), 986(w), 834(s), 613(w), 557(s).

$[Pt\{PhTe(CH_2)_3TePh\}_2][PF_6]_2$ was prepared similarly to give an orange powder (76 %). Analysis: Calculated for $C_{30}H_{32}F_{12}P_2PtTe_4$: %C, 25.95; %H, 2.31. Found: %C, 25.98; %H, 2.08. ^1H NMR (CD_3CN, 300 K): δ 2.52 (br, 1H, $CH_2CH_2CH_2$), 3.20 (br, 2H, $TeCH_2$), 7.58 (m, 5H, TePh). IR/cm^{-1} 3070(w), 1569(w), 1471(w), 1357(m), 1210(w), 1093(m), 1015(w), 996(m), 838(s), 732(m), 689(m), 613(w), 557(s), 453(w).

$[Pt\{o\text{-}C_6H_4(TeMe)_2\}_2][PF_6]_2$ was prepared similarly to give a light brown solid (75 %). Analysis: Calculated for $C_{16}H_{20}F_{12}P_2PtTe_4$: %C, 15.90; %H, 1.66. Found: %C, 15.86; %H, 1.59. ^1H NMR (CD_3CN, 300 K): δ 2.60 (s, 3H, $TeCH_3$), 7.84 (m, 2H, *o*-C_6H_4). IR/cm^{-1} 1357(s), 1261(w), 1092(s), 987(m), 839(s), 743(m), 613(m), 557(s).

4.42 Bis(tripodal) complexes of the Platinum and Group 11 Metals

The complexes $[Cu(NCMe)_4][PF_6]$,[35] $[IrCl(C_8H_{14})_2]_2$[36] and $[Ru(dmf)_6][CF_3SO_3]_3$[37] were prepared by the literature procedures, as were the ligands $MeC(CH_2SMe)_3$,[38] $MeC(CH_2SeMe)_3$,[39] $MeC(CH_2TeMe)_3$.[33] Improved syntheses for the thio- and selenoether ligands are detailed in Chapter 7, along with the synthesis of $MeC(CH_2TePh)_3$.

$[Pd\{MeC(CH_2SeMe)_3\}_2][PF_6]_2$. $[PdCl_2(NCMe)_2]$ (25 mg, 9.6 x 10^{-5} mol) and $TlPF_6$ (70 mg, 2.0 x 10^{-4} mol) were stirred in MeCN (40 cm^3) for 15 min. under a dinitrogen atmosphere. $Me(CH_2SeMe)_3$ (68 mg, 1.9 x 10^{-4} mol) in CH_2Cl_2 (5 cm^3) was then added and the reaction stirred at room temperature for 18 hours to give a yellow solution and fine white precipitate of TlCl. The solution was filtered, reduced to *ca.* 2 cm^3 *in vacuo* and diethyl ether (10 cm^3) added to precipitate a yellow solid. Yield 60 mg, 57 %. Analysis: Calculated for $C_{16}H_{36}F_{12}P_2PdSe_6$: %C, 17.5; %H, 3.3. Found: %C, 17.1; %H, 3.1. ^1H NMR (CD_3CN, 300 K): δ 1.34 (s, 1H, CCH_3), 2.41 (s, 3H, $SeCH_3$), 3.13 (s, 2H, $SeCH_2$). $^{77}Se\{^1H\}$ NMR

($Me_2CO/CDCl_3$, 300 K): δ 110(br); (220 K): δ 32 (uncoordinated SeMe), 147, 157 (coordinated SeMe). IR/cm^{-1} 2940(w), 2918(w), 1464(w), 1405(sh), 1357(s), 1272(w), 1261(w), 1095(s), 988(w), 841(s), 613(w), 559(s). UV/vis (MeCN)/cm^{-1} (ε_{mol} mol^{-1} dm^3 cm^{-1}) 26 880 (8420), 33 160 (18 130).

$[Pd\{MeC(CH_2TeMe)_3\}_2][PF_6]_2$ was prepared similarly to give a brown solid (38 %). Analysis: Calculated for $C_{16}H_{36}F_{12}P_2PdTe_6$: %C, 13.8; %H, 2.6. Found: %C, 13.1; %H, 2.3. ^1H NMR (CD_3CN, 300 K): δ 1.39 (s, 1H, CCH_3), 2.35 (s, 3H, $TeCH_3$), 3.15 (s, 2H, $TeCH_2$). IR/cm^{-1} 2940(w), 1356(s), 1092(s), 988(m), 838(s), 613(w), 557(m). UV/vis (MeCN)/cm^{-1} (ε_{mol} mol^{-1} dm^3 cm^{-1}) 24650sh (4970), 29 800sh (10 280), 36 870 (18 300).

$[Pd\{MeC(CH_2TePh)_3\}_2][PF_6]_2$ was prepared similarly to give an orange solid (65 %). Analysis: Calculated for $C_{46}H_{48}F_{12}P_2PdTe_6$: %C, 31.3; %H, 2.5. Found: %C, 31.3; %H 2.5. ^1H NMR (CD_3CN, 300 K): δ 1.33 (s, 1H, CCH_3), 3.33 (s, 2H, $TeCH_2$), 7.30 – 7.55 (m, 5H, TePh). $^{125}Te\{^1H\}$ NMR ($Me_2CO/CDCl_3$, 190 K): δ 528, 561. IR/cm^{-1} 3061(w), 1570(w), 1476(w), 1434(w), 1359(s), 1267(w), 1096(s), 1024(w), 997(m), 837(s), 733(m), 690(m), 613(w), 558(m), 453(m). UV/vis (MeCN)/cm^{-1} (ε_{mol} mol^{-1} dm^3 cm^{-1}) 26 940 (19 510), 37 650sh (23 160).

$[Pt\{MeC(CH_2SeMe)_3\}_2][PF_6]_2$. $PtCl_2$ (25 mg, 9.4 x 10^{-5} mol) was refluxed in MeCN for 2 hours to give a light yellow solution of $[PtCl_2(NCMe)_2]$. $TlPF_6$ (66 mg, 1.9 x 10^{-4} mol) and $Me(CH_2SeMe)_3$ (68 mg, 1.9 x 10^{-4} mol) in CH_2Cl_2 (5 cm^3) were then added and the reaction stirred at room temperature for 48 hours to give a yellow solution and fine white precipitate of TlCl. The solution was filtered to remove the TlCl, reduced to *ca.* 2 cm^3 *in vacuo* and diethyl ether (10 cm^3) added to precipitate a pale yellow solid. Yield 56 mg, 50 %. Analysis: Calculated for $C_{16}H_{36}F_{12}P_2PtSe_6$: %C, 16.2; %H, 3.0. Found: %C, 15.9; %H, 3.1. ^1H NMR (CD_3CN, 300 K): δ 1.33 (s, 1H, CCH_3), 2.48 (s, 3H, $SeCH_3$), 3.25 (s, 2H, $SeCH_2$). $^{77}Se\{^1H\}$ NMR ($Me_2CO/CDCl_3$, 300 K): δ 144(br); (220 K): δ 33.7 (uncoordinated SeMe), 141.8, 142.6, 149.5, 150.3 (coordinated SeMe). ^{195}Pt NMR ($Me_2CO/CDCl_3$, 220 K): δ -4888, –4630. IR/cm^{-1} 2951(w), 2918(w), 1405(sh), 1357(m), 1095(m), 986(w), 834(s), 613(w), 559(s). UV/vis (MeCN)/cm^{-1} (ε_{mol} mol^{-1} dm^3 cm^{-1}) 28 500 (1300), 33 560 (6310).

$[Pt\{MeC(CH_2TeMe)_3\}_2][PF_6]_2$ was prepared similarly to give a brown solid (28 %). Analysis: Calculated for $C_{16}H_{36}F_{12}P_2PtTe_6$: %C, 13.0; %H, 2.4. Found: %C, 13.4; %H, 2.2. ^1H NMR (CD_3CN, 300 K): δ 1.39 (s, 1H, CCH_3), 2.26 (s, 3H, $TeCH_3$), 3.27 (s, 2H, $TeCH_2$). IR/cm^{-1} 2929(w), 2895(w), 1358(s), 1097(s), 991(m), 836(s), 613(w), 558(m). UV/vis (MeCN)/cm^{-1} (ε_{mol} mol^{-1} dm^3 cm^{-1}) 30 560sh (8630), 36 870 (20 350).

$[Pt\{MeC(CH_2TePh)_3\}_2][PF_6]_2$ was prepared similarly to give an orange solid (20 %). Analysis: Calculated for $C_{46}H_{48}F_{12}P_2PtTe_6$: %C, 29.8; %H, 2.6. Found: %C, 29.8; %H, 2.4. ^1H NMR (CD_3CN, 300 K): δ 1.30 (s, 1H, CCH_3), 3.42 (s, 2H, $TeCH_2$), 7.35 – 7.55 (m, 5H, TePh). $^{125}Te\{^1H\}$ NMR ($Me_2CO/CDCl_3$, 190 K): δ 395 (uncoordinated TePh), 512, 518, 542, 547 (coordinated TePh). IR/cm^{-1} 3017(w), 1572(w), 1474(w), 1435(w), 1359(s), 1267(w), 1096(s), 997(m), 836(s), 734(m), 690(m), 613(w), 557(s), 453(m). UV/vis (MeCN)/cm^{-1} (ε_{mol} mol^{-1} dm^3 cm^{-1}) 32 050 (19 360), 37 760sh (32 350).

$[Ru\{MeC(CH_2SMe)_3\}_2][CF_3SO_3]_2$. $[Ru(dmf)_6][CF_3SO_3]_3$ (70 mg, 7.1 x 10^{-5} mol) was added to a solution of $MeC(CH_2SeMe)_3$ (33 mg, 1.6 x 10^{-4} mol) in MeOH (40 cm^3). The reaction was refluxed under an atmosphere of dinitrogen for 24 hours to give a yellow solution. Reduction of the solvent volume *in vacuo* to 1 cm^3 and addition a diethyl ether gave a light yellow solid. Yield 40 mg, 69 %. Analysis Calculated for $C_{18}H_{36}F_6O_6RuS_8$: %C, 26.4; %H, 4.4. Found: %C, 26.0; %H, 4.1. ^1H NMR (CD_3NO_2, 300 K): δ 1.28 (s, 1H, CCH_3), 2.47 (s, 3H, SCH_3), 2.85 (s, 2H, SCH_2). ES^+ (MeCN), *m/z* = 671, 261; calc. for $([^{102}Ru\{MeC(CH_2SMe)_3\}_2][CF_3SO_3])^+$ 671, $[^{102}Ru\{MeC(CH_2SMe)_3\}_2]^{2+}$ 261. IR/cm^{-1} 2984(w), 2940(w), 1463(w), 1423(m), 1358(w), 1262(s), 1227(m), 1167(m), 1151(m), 1097(w), 1032(s), 976(m), 874(w), 812(w), 756(w), 721(w), 639(s), 573(w), 518(m), 429(w). UV/vis (MeCN)/cm^{-1} (ε_{mol} mol^{-1} dm^3 cm^{-1}) 27 530 (160), 31 730 (180), 35 210 (1990), 43 480 (18 590).

$[Ru\{MeC(CH_2SeMe)_3\}_2][CF_3SO_3]_2$ was prepared similarly to give a yellow solid (42 %). Analysis: Calculated for $C_{18}H_{36}F_6O_6RuS_2Se_6$: %C, 19.6; %H, 3.3. Found: %C, 19.9; %H, 3.2. ^1H NMR (CD_3NO_2, 300 K): δ 1.46 (s, 1H, CCH_3), 2.51 (s, 3H, $SeCH_3$), 2.6 – 2.9 (br, 2H, $SeCH_2$). $^{77}Se\{^1H\}$ NMR ($MeNO_2/CDCl_3$, 300 K): δ 120. ES^+ (MeCN), *m/z* = 953, 403; calc. for $([^{102}Ru\{MeC(CH_2{}^{80}SeMe)_3\}_2][CF_3SO_3])^+$ 959, $[^{102}Ru\{MeC(CH_2{}^{80}SeMe)_3\}_2]^{2+}$ 405. IR/cm^{-1} 1461(w), 1416(w), 1359(m), 1261(s), 1227(m), 1167(m), 1151(m), 1099(w),

1032(s), 921(m), 897(m), 834(w), 757(w), 639(s), 573(m), 518(m). UV/vis (MeCN)/cm^{-1} (ε_{mol} mol^{-1} dm^3 cm^{-1}) 25 930 (220), 29 900 (230), 39 800 (38 230).

$[Ru\{MeC(CH_2TeMe)_3\}_2][CF_3SO_3]_2$ was prepared similarly to give a brown solid (33 %). Analysis: Calculated for $C_{18}H_{36}F_6O_6RuS_2Te_6$: %C, 15.5; %H, 2.6. Found: %C, 15.2; %H, 2.7. ^1H NMR (CD_3NO_2, 300 K): δ 1.71 (s, 1H, CCH_3), 2.38 (s, 3H, $TeCH_3$), 2.5 – 2.7 (br, 2H, ($TeCH_2$). $^{125}Te\{^1H\}$ NMR ($MeNO_2/CDCl_3$, 300 K) δ 204. ES^+ (MeCN), *m/z* = 547; calc. for $[^{102}Ru\{MeC(CH_2{}^{130}TeMe)_3\}_2]^{2+}$ 555. IR/cm^{-1} 2962(w), 2907(w), 1360(s), 1271(s), 1232(sh), 1161(m), 1095(m), 1032(m), 834(m), 759(w), 639(s), 616(sh), 574(w), 517(m). UV/vis (MeCN)/cm^{-1} (ε_{mol} mol^{-1} dm^3 cm^{-1}) 26 890sh (2450), 35 800 (22 000), 41 800 (28 100).

$[Ru\{MeC(CH_2TePh)_3\}_2][CF_3SO_3]_2$ was prepared similarly to give a brown solid (49 %). Analysis: Calculated for $C_{48}H_{48}F_6O_6RuS_2Te_6$: %C, 32.6; %H, 2.7. Found: %C, 32.2; %H, 1.8. ^1H NMR (CD_3NO_2, 300 K): δ 1.67 (s, 3H, CCH_3), 2.5 – 3.6 (br, 6H, $TeCH_2$), 7.2 – 7.6 (m, 15H, TePh). $^{125}Te\{^1H\}$ NMR ($MeNO_2/CDCl_3$, 300 K) δ 481. ES^+ (MeCN), *m/z* = 734; calc. for $[^{102}Ru\{MeC(CH_2{}^{130}TePh)_3\}_2]^{2+}$ 741. IR/cm^{-1} 2918(w), 1570(w), 1476(w), 1432(w), 1359(s), 1278(s), 1258(s), 1160(m), 1085(m), 1030(s), 996(m), 835(w), 738(s), 690(m), 637(s), 517(m), 453(m). UV/vis (MeCN)/cm^{-1} (ε_{mol} mol^{-1} dm^3 cm^{-1}) 25 720 (1330), 32 720 (29 000), 35 310 (33 990).

$[Rh\{MeC(CH_2SeMe)_3\}_2][PF_6]_3$. $AgNO_3$ (56 mg, 3.3 x 10^{-4} mol) was added to a solution of $RhCl_3.3H_2O$ (29 mg, 1.1 x 10^{-4} mol) in H_2O (15 cm^3) and the mixture refluxed for 2 hours. The precipitated AgCl was filtered off to leave a yellow solution to which was added $MeC(CH_2SeMe)_3$ (78 mg, 2.2 x 10^{-4} mol) in MeOH (25 cm^3) and the mixture refluxed for 24 hours. Addition of NH_4PF_6 (65 mg, 4.0 x 10^{-4} mol) gave a fine red precipitate. Yield 45 mg, 33 %. Analysis: Calculated for $C_{16}H_{36}F_{18}P_3RhSe_6$: %C, 15.5; %H, 2.9. Found: %C, 16.0; %H, 2.6. ^1H NMR (CD_3CN, 300 K): δ 1.40 (s, 1H, CCH_3), 2.39(s), 2.49(s), 2.54(s), 2.61(s) (3H, $SeCH_3$), 2.80 – 2.85 (br, 2H, $SeCH_2$). $^{77}Se\{^1H\}$ NMR ($MeNO_2/CDCl_3$, 300 K) δ 117.3, 134.8, 147.5, 152.1. $^{77}Se\{^1H\}$ NMR ($MeNO_2/CDCl_3$, 200 K, $^1J_{Rh\text{-}Se}$ in parenthesis) δ 126.2 (d, 43 Hz), 136.6 (d, 42 Hz), 137.2 (d, 43 Hz), 155.3 (d, 43 Hz), 159.0 (d, 42 Hz). ES^+ (MeCN), *m/z* = 395; calc. for $[^{103}Rh\{MeC(CH_2{}^{80}SeMe)_3\}\{MeC(CH_2{}^{80}SeMe)_2(CH_2{}^{80}Se)\}]^{2+}$ 398. IR/cm^{-1} 2963(w), 1460(w), 1358(s), 1264(w), 1096(s), 988(m), 836(s), 743(w), 671(w),

614(m), 558(s). UV/vis (MeCN)/cm^{-1} (ε_{mol} mol^{-1} dm^3 cm^{-1}) 21 180 (1720), 32 570 (62 200), 39 060 (68 110).

$[Ir\{MeC(CH_2SeMe)_3\}_2][PF_6]_3$. $[IrCl(C_8H_{14})_2]_2$ (34 mg, 3.8 x 10^{-5} mol) was added to $MeC(CH_2SeMe)_3$ (62 mg, 1.8 x 10^{-4} mol) and 40 % HBF_4 (0.5 cm^3) in a mixture of water (20 cm^3) and methanol (10 cm^3) and the reaction refluxed for 18 hours to give a yellow solution. After cooling, excess NH_4PF_6 (59 mg, 3.6 x 10^{-4} mol) was added and the solvent removed *in vacuo*. The residue was dissolved in $MeNO_2$ (5 cm^3), filtered and diethyl ether (20 cm^3) added to give a light yellow precipitate. Yield 55 mg, 46 %. Analysis: Calculated for $C_{16}H_{36}F_{18}P_3IrSe_6$: %C, 14.5; %H, 2.7. Found: %C, 14.0; %H, 2.5. ^1H NMR (CD_3CN, 300 K): δ 1.35 (s, 1H, CCH_3), 2.44 - 2.60 (m, 3H, $SeCH_3$), 2.80 – 3.05 (br, 2H, $SeCH_2$). $^{77}Se\{^1H\}$ NMR ($MeNO_2/CDCl_3$, 300 K) δ 77.6, 87.4, 109.1. ES^+ (MeCN), *m/z* = 439; calc. for $[^{193}Ir\{MeC(CH_2{}^{80}SeMe)_3\}\{MeC(CH_2{}^{80}SeMe)_2(CH_2{}^{80}Se)\}]^{2+}$ 443. IR/cm^{-1} 2929(w), 1359(s), 1087(s), 839(s), 557(m). UV/vis (MeCN)/cm^{-1} (ε_{mol} mol^{-1} dm^3 cm^{-1}) 40 850 (19 250), 45 290 (23 150).

$[Cu\{MeC(CH_2SeMe)_3\}_2][PF_6]$. $[Cu(NCMe)_4][PF_6]$ (37 mg, 9.9 x 10^{-5} mol) was added to a solution of $MeC(CH_2SeMe)_3$ (75 mg, 2.1 x 10^{-4} mol) in dry CH_2Cl_2 (35 cm^3) and the reaction stirred for 1 hour and refluxed for 10 minutes. After cooling the solvent volume was reduced *in vacuo* to 5 cm^3 and diethyl ether (15 cm^3) added to precipitate a pale yellow solid. Yield 74 mg, 82 %. Analysis: Calculated for $C_{16}H_{36}CuF_6PSe_6.CH_2Cl_2$: %C, 20.5; %H, 3.8. Found: %C, 19.9; %H, 3.7. ^1H NMR ($CDCl_3$, 300 K): δ 1.25 (s, 1H, CCH_3), 2.22 (s, 3H, $SeCH_3$), 2.88 (s, 2H, $SeCH_2$). ES^+ (MeCN), *m/z* = 456, 415; calc. for $[^{63}Cu\{MeC(CH_2{}^{80}SeMe)_3\}(NCMe)]^+$ 458, $[^{63}Cu\{MeC(CH_2{}^{80}SeMe)_3\}]^+$ 417. IR/cm^{-1} 2929(w), 2267(w), 1359(s), 1092(s), 991(m), 835(s), 727(m), 614(w), 559(m), 447(w).

$[Cu\{MeC(CH_2TeMe)_3\}_2][PF_6]$ was prepared similarly to give a yellow solid (75 %). Analysis: Calculated for $C_{16}H_{36}CuF_6PTe_6$: %C, 16.0; %H, 3.0. Found: %C, 15.9; %H, 3.0. ^1H NMR ($CDCl_3$, 300 K): δ 1.27 (s, 1H, CH_3C), 2.02 (s, 3H, $TeCH_3$), 2.98 (s, 2H, $TeCH_2$). ES^+ (MeCN), *m/z* = 1058, 602, 563; calc. for $[^{63}Cu\{MeC(CH_2{}^{130}TeMe)_3\}_2]^+$ 1071, $[^{63}Cu\{MeC(CH_2{}^{130}TeMe)_3\}(NCMe)]^+$ 608, $[^{63}Cu\{MeC(CH_2{}^{130}TeMe)_3\}]^+$ 567. IR/cm^{-1} 2951(w), 1360(s), 1223(w), 1090(s), 991(m), 841(s), 728(m), 610(w), 558(m), 477(w).

$[Cu\{MeC(CH_2TePh)_3\}_2][PF_6]$ was prepared similarly to give a yellow solid (44 %). Analysis: Calculated for $C_{46}H_{48}CuF_6PTe_6$: %C, 35.1; %H, 3.1. Found: %C, 34.6; %H, 2.2. ^1H NMR ($CDCl_3$, 300 K): δ 1.25 (s, 1H, CCH_3), 3.13 (s, 2H, $TeCH_2$), 7.21 - 7.61 (m, 5H, TePh). ES^+ (MeCN), *m/z* = 749; calc. for $[^{63}Cu\{MeC(CH_2{}^{130}TePh)_3\}]^+$ 753. IR/cm^{-1} 3050(w), 2951(w), 1572(m), 1474(m), 1433(s), 1360(s), 1261(w), 1223(w), 1095(s), 1017(m), 998(m), 839(s), 732(s), 690(s), 655(w), 614(w), 558(m), 479(w), 453(w).

$[Ag\{MeC(CH_2SeMe)_3\}][CF_3SO_3]$. $Ag[CF_3SO_3]$ (20 mg, 7.8 x 10^{-5} mol) was added to a solution of $MeC(CH_2SeMe)_3$ (56 mg, 1.6 x 10^{-4} mol) in dry CH_2Cl_2 (30 cm^3) and the reaction stirred for 1 hour. The solvent volume was reduced *in vacuo* to 5 cm^3 and diethyl ether added to give a white solid. Yield 26 mg, 55 %. Analysis: Calculated for $C_9H_{18}AgF_3O_3SSe_3$: %C, 17.8; %H, 3.0. Found: %C, 17.8; %H, 2.7. ^1H NMR ($CDCl_3$, 300 K): δ 1.29 (s, 1H, CCH_3), 2.29 (s, 3H, $SeCH_3$), 2.01 (s, 2H, $SeCH_2$). ES^+ (MeCN), *m/z* = 808; calc. for $[^{107}Ag\{MeC(CH_2{}^{80}SeMe)_3\}_2]^+$ 815. IR/cm^{-1} 2962(w), 2907(w), 1410(m), 1362(s), 1274(s), 1232(m), 1162(m), 1090(s), 1037(s), 990(m), 908(m), 835(w), 760(w), 643(s), 557(w), 524(w).

$[Ag\{MeC(CH_2TeMe)_3\}_2][CF_3SO_3]$ was prepared similarly to give a pale yellow solid (63 %). Analysis: Calculated for $C_{17}H_{36}AgF_3O_3STe_6$: %C, 16.3; %H, 2.9. Found: %C, 16.0; %H, 2.1. ^1H NMR ($CDCl_3$, 300 K): δ 1.30 (s, 1H, CCH_3), 2.18 (s, 3H, $TeCH_3$), 3.05 (s, 2H, $TeCH_2$). ES^+ (MeCN), *m/z* = 1104, 609; calc. for $[^{107}Ag\{MeC(CH_2{}^{130}TeMe)_3\}_2]^+$ 1115, $[^{107}Ag\{MeC(CH_2{}^{130}TeMe)_3\}]^+$ 611. IR/cm^{-1} 2951(w), 2918(w), 1362(m), 1264(s), 1233(m), 1162(m), 1095(m), 1039(m), 835(m), 759(w), 645(s), 571(w), 522(w).

$[Ag\{MeC(CH_2TePh)_3\}_2][CF_3SO_3]$ was prepared similarly to give a pale yellow solid (29 %). Analysis: Calculated for $C_{47}H_{48}AgF_3O_3STe_6.CH_2Cl_2$: %C, 33.7; %H, 2.9. Found: %C, 33.3; %H, 2.8. ^1H NMR ($CDCl_3$, 300 K): δ 1.23 (s, 1H, CCH_3), 2.39 (s, 2H, $TeCH_2$), 7.00 - 7.65 (m, 5H, TePh). ES^+ (MeCN), *m/z* = 1477; calc. for $[^{107}Ag\{MeC(CH_2{}^{130}TePh)_3\}_2]^+$ 1487. IR/cm^{-1} 3063(w), 2957(w), 1572(m), 1473(m), 1432(m), 1370(m), 1263(s), 1233(m), 1161(s), 1064(w), 1039(m), 1017(m), 998(m), 910(w), 835(w), 790(w), 730(s), 690(s), 637(s), 573(w), 516(w), 454(m).

X-ray Crystallographic Studies

Details of the crystallographic data collection and refinement parameters are given in Table 4.2. The crystals were grown by vapour diffusion of diethyl ether into solutions of the complexes in acetonitrile for $[Pd\{o\text{-}C_6H_4(TeMe)_2\}_2][PF_6]_2 \cdot MeCN$, acetone for $[Pt\{MeC(CH_2SeMe)_3\}_2][PF_6]_2$, nitromethane for $[Ru\{MeC(CH_2EMe)_3\}_2][CF_3SO_3]_2$ (E = S or Se) and dichloromethane for $[Ag\{MeC(CH_2SeMe)_3\}][CF_3SO_3]$. Data collection used a Rigaku AFC7S four-circle diffractometer operating at 150 K, except $[Ru\{MeC(CH_2SMe)_3\}_2][CF_3SO_3]_2$ and $[Ru\{MeC(CH_2SeMe)_3\}_2][CF_3SO_3]_2$ for which data were collected at 298 K, using graphite-monochromated Mo-K_α X-radiation (λ = 0.71073 A). No significant crystal decay or movement was observed. The structures were solved by heavy atom Patterson methods[40] and developed by iterative cycles of full-matrix least-squares refinement and difference Fourier syntheses.[41]

$[Pd\{o\text{-}C_6H_4(TeMe)_2\}_2][PF_6]_2 \cdot MeCN$. The structure shows two independent half cations with inversion symmetry, two PF_6^- anions on general positions and two disordered half MeCN solvent molecules in the asymmetric unit. The latter are disordered across inversion centres such that the methyl C atom of one form is superimposed on the cyano C atom of the other form and *vice versa* with the inversion centre at the midpoint of this C-C vector. The H atoms associated with the MeCN molecules were not located from the difference map and therefore were omitted from the final structure factor calculation. All non-hydrogen atoms were refined anisotropically while H-atoms, apart from those associated with the MeCN molecules, were placed in fixed, calculated positions with d(C-H) = 0.96 Å.

$[Pt\{MeC(CH_2SeMe)_3\}_2][PF_6]_2$. Some disorder was identified within the uncoordinated arms of the triselenoether ligands in $[Pt\{MeC(CH_2SeMe)_3\}_2][PF_6]_2$. Alternative sites were identified for C(15), Se(6) and C(16) giving relative occupancies of 60%:40%, while within the other free arm, an alternative location was identified for C(8) giving a 70%:30% occupancy. This disorder model refined reasonably successfully.[42] All non-H-atoms, except for the partially occupied C atoms, were refined anisotropically and H atoms were placed in fixed, calculated positions (except for the H atoms associated with the disordered C atoms which were not located and were omitted from the final structure factor calculation).

$[Ru\{MeC(CH_2SeMe)_3\}_2][CF_3SO_3]_2$. While the centrosymmetric cation is ordered, the $CF_3SO_3^-$ anion, which occupies a general position, has high thermal parameters, particularly those associated with the F and O atoms. Attempts to model this disorder by refining partial site occupancies were not successful, hence the atoms were refined with unit occupancies and high thermal parameters. While low temperature data collection would normally be expected to reduce the thermal motion and improve the structure quality, a data set from a different crystal collected previously at 150 K gave broad peaks and a significantly poorer fit to the data. All non-H atoms were refined anisotropically while H-atoms were placed in fixed, calculated positions with d(C-H) = 0.96 Å.

$[Ru\{MeC(CH_2SMe)_3\}_2][CF_3SO_3]_2$ and $[Ag\{MeC(CH_2SeMe)_3\}][CF_3SO_3]$. All non-H atoms were refined anisotropically while H-atoms were placed in fixed, calculated positions with d(C-H) = 0.96 Å.

4.5 References

[1] T. Kemmitt, W. Levason and M. Webster, *Inorg. Chem.*, 1989, **28**, 692.

[2] T. Kemmitt and W. Levason, *Inorg. Chem.*, 1990, **29**, 731.

[3] R. A. Cipriano, W. Levason, R. A. S. Mould. D. Pletcher and N. A. Powell, *J. Chem. Soc., Dalton Trans.*, 1988, 2677.

[4] J. L. Brown, T. Kemmitt and W. Levason, *J. Chem. Soc., Dalton Trans.*, 1990, 1513.

[5] J. R. Black and W. Levason, *J. Chem. Soc., Dalton Trans.*, 1994, 3225.

[6] J. R. Black, N. R. Champness, W. Levason and G. Reid, *J. Chem. Soc., Dalton Trans.*, 1995, 3439.

[7] F. R. Hartley, W. Levason, C. A. McAuliffe, S. G. Murray and H. E. Soutter, *Inorg. Chem. Acta,* 1979, **35**, 265.

[8] N. R. Champness, P. F. Kelly, W. Levason, G. Reid, A. M. Z. Slawin and D. J. Williams, *Inorg. Chem.*, 1995, **34**, 651.

[9] E. G. Hope, W. Levason, G. L. Marshall and S. G. Murray, *J. Chem. Soc., Dalton Trans.*, 1985, 2185.

[10] E. W. Abel, K. G. Orrell, S. P. Scanlan, D. Stevenson, T. Kemmitt and W. Levason, *J. Chem. Soc., Dalton Trans.*, 1991, 591.

[11] E. W. Abel, S. K. Bhargava and K. G. Orrell, *Prog. Inorg. Chem.*, 1984, **32**, 1.

[12] D. J. Gulliver, W. Levason, K. G. Smith, M. J. Selwood and S. G. Murray, *J. Chem. Soc., Dalton Trans.*, 1980, 1872.

[13] E. G. Hope, W, Levason, M. Webster and S. G. Murray, *J. Chem. Soc., Dalton Trans.*, 1986, 1003.

[14] A. J. Blake, A. J. Holder, T. I. Hyde and M. Schröder, *J. Chem. Soc., Chem. Commun.*, 1987, 987.

[15] N. R. Champness, P. F. Kelly, W. Levason, G. Reid, A. M. Z. Slawin and D. J. Williams, *Inorg. Chem.*, 1995, **34**, 651.

[16] N. R. Champness, W. Levason, J. J. Quirk and G. Reid, *Polyhedron,* 1995, **14**, 2753.

[17] A. P. B. Lever, *Inorganic Electronic Spectroscopy,* Elsevier, Amsterdam, 2nd edn., 1984.

[18] S. C. Rawle, T. J. Sewell and S. R. Cooper, *Inorg. Chem.*, 1987, **26**, 3769.

[19] W. Levason, J. J. Quirk, G. Reid and S. M. Smith, *J. Chem. Soc., Dalton Trans.*, 1997, 3719.

[20] M. N. Bell, A. J. Blake, M. Schröder, H. -J. Küppers and K. Wieghardt, *Angew. Chem. Int. Ed. Engl.,* 1987, **26**, 250.

[21] W. Levason, S. D. Orchard, G. Reid and V. -A. Tolhurst, *J. Chem. Soc., Dalton Trans.,* 1999, 2071.

[22] W. Levason, J. J. Quirk and G. Reid, *J. Chem. Soc., Dalton Trans.,* 1996, 3713.

[23] T. Kemmitt, W. Levason, M. D. Spicer and M. Webster, *Organometallics,* 1990, **9**, 1181.

[24] A. J. Blake, R. O. Gould, A. J. Holder, T. I. Hyde, G. Reid and M. Schröder, *J. Chem. Soc., Dalton Trans.,* 1990, 1759.

[25] J. R. Black, N. R. Champness, W. Levason and G. Reid, *Inorg. Chem.,* 1996, **35**, 4432.

[26] J. R. Black, N. R. Champness, W. Levason and G. Reid, *J. Chem. Soc., Chem. Commum.,* 1995, 1277.

[27] R. Alberto, D. Angst, U. Abram, K. Ortner, T. A. Kaden and A. P. Schubiger, *J. Chem. Soc., Chem. Commun.,* 1999, 1513.

[28] S. T. James, D. M. P. Mingos, A. J. P. White and D. J. Williams, *J. Chem. Soc., Chem. Commum.,* 1998, 2323.

[29] T. E. Concolino, L. M. Liable-Sands, E. E. Pullen, D. Rabinovich, A. L. Rheingold, L. M. Tran and H. W. Yim, *Inorg. Chem.,* 1999, **38**, 6234.

[30] A. J. Blake, R. O. Gould, A. J. Holder, T. I. Hyde and M. Schröder, *J. Chem. Soc., Dalton Trans.,* 1988, 1861.

[31] A. J. Blake, R. O. Gould, A. J. Holder, T. I. Hyde, A, J, Lavery, M. O. Odulate and M. Schröder, *J. Chem. Soc., Chem. Commun.,* 1987, 118.

[32] A. A. La Pensée, S. J. Higgins, C. A. Stuart and J. F. Bickley, *Inorg. Chem. Commun.,* 1999, **2**, 524.

[33] E. G. Hope, T. Kemmitt and W. Levason, *Organometallics*, 1988, **7**, 78.

[34] T. Kemmitt and W. Levason, *Organometallics,* 1989, **8**, 1303.

[35] G. J. Kubas, *Inorg. Synth.*, 1979, **19**, 90.

[36] J. L. Herde, J. C. Lambert and C. V. Senoff, *Inorg. Synth.*, 1974, **15**, 18.

[37] R. J. Judd, R. Cao, M. Biner, T. Armbruster, H. -B. Burgi, A. E. Merbach and A. Ludi, *Inorg. Chem.,* 1995, **34**, 5080.

[38] R. Ali, S. J. Higgins and W. Levason, *Inorg. Chim. Acta.,* 1984, **84**, 65.

[39] D. J. Gulliver, E. G. Hope, W. Levason, G. L. Marshall, S. G. Murray and D. M. Potter, *J. Chem. Soc., Perkin Trans. II,* 1984, 429.

[40] PATTY, The DIRDIF Program System, P.T. Beurskens, G. Admiraal, G. Beurskens, W.P. Bosman, S. Garcia-Granda, R.O. Gould, J.M.M. Smits and C. Smykalla, Technical Report of the Crystallography Laboratory, University of Nijmegen, The Netherlands, 1992.

[41] TeXsan: Crystal Structure Analysis Package, Molecular Structure Corporation, Texas, 1995.

[42] SHELXS86, Program for crystal structure solution, G.M. Sheldrick, *Acta Crystallogr. Sect. A,* 1990, **46**, 467.

Chapter 5

Rhodium and Iridium Organometallic Group 16 Tripodal Complexes

5.1 Introduction

The organometallic chemistry of both rhodium and iridium, although well established, is still an area of intense interest, both academically and industrially as a result of the rich coordination chemistry both metals show, along with the catalytic properties that many of their complexes exhibit. This catalytic activity may be attributed to the availability of both the +1 and +3 formal oxidation states for the metal centre, which are readily interconverted *via* oxidative addition, and reductive elimination. Indeed two of the most interesting catalysts discovered, $[RhCl(PPh_3)_3]$ and $[IrCl(CO)(PPh_3)_2]$ involve these metals,[1, 2] and it was these complexes that sparked off the growth in rhodium and iridium organometallic chemistry involving phosphine donor ligands.

The reactions of the triphos ligand, $MeC(CH_2PPh_2)_3$, with a range of rhodium and iridium organometallic precursors are of particular interest to this study. Intensive studies into the catalytic properties of such complexes have been undertaken over the past decade, including the modelling of the hydrodesulfurisation process.[3, 4] More recently it has been shown that the mononuclear zwitterionic Rh(I) complexes [(sulfos)Rh(cod)] and $[(sulfos)Rh(CO)_2]$ (sulfos = $^-O_3S(C_6H_4)CH_2C(CH_2PPh_2)_3$) are effective catalysts for the hydrogenation of styrene to ethylbenzene and the hydroformylation of 1-hexene to aldehydes or alcohols.[5] The flexibility of the triphos ligand has also been illustrated in the complex [RhH(CO)(triphos)] which has been shown to be a catalyst for olefin hydroformylation *via* the dissociation and re-association of one phosphine arm.[6]

The preparation of group 16 organometallic complexes has received increased interest during the past decade, although these species have generally involved thioether ligands. Various rhodium(I) and iridium(I) complexes with the macrocyclic ligand $[9]aneS_3$ have been reported as part of a study into the properties of the small ring macrocycle.[7, 8] The extension of this chemistry to study the role of group 16 organometallics as catalysts has included the application of iridium(I) complexes containing dithioether ligands for asymmetric hydrogenation.[9] The reactions of monodentate heterocyclic organotellurium ligands with the pentamethylcyclopentadienylrhodium(III) dichloride dimer have also been reported as potential models for the initial steps in heterogeneously catalysed hydrodesulfurisation.[10, 11] However the preparation of organometallic complexes with seleno- or telluroether ligands is generally limited to carbonyl containing species.

An investigation into the species *fac*-$[M(CO)_3(L\text{-}L)X]$ (M = Mn or Re; X = Cl, Br or I; L-L = dithio-, diseleno- or ditelluroether) probing the relative donating abilities of group 16

ligands was discussed in Chapter 2 and revealed that, in agreement with theoretical predictions by Schumann and co-workers,[12] telluroether ligands are significantly better σ-donors to low valent metal centres than their lighter analogues.[13] Further, our studies into the preparation of homoleptic platinum metal species with the tripodal ligands illustrated the versatility of these ligands in adopting various coordination modes to accommodate the metal ion requirements (Chapter 4). Described here is the preparation of group 16 tripodal ligand complexes of rhodium and iridium involving co-ligands other than carbonyls.

This Chapter reports the results of a study into the chemistry of the ligands, L^3, {L^3 = $MeC(CH_2TeR)_3$ (R = Me and Ph) and, for comparison, $MeC(CH_2SeMe)_3$} with the species $[M(cod)Cl]_2$ and $[M(C_5Me_5)Cl_2]_2$ (M = Rh or Ir) to give the complexes $[M(cod)(L^3)][PF_6]$ and $[M(C_5Me_5)(L^3)][PF_6]_2$ respectively. These precursors were chosen since they provide convenient sources of the metal ions in oxidation state +1 and +3 respectively and thus the effect of metal oxidation state on the donor properties of these ligands may be established. The metal oxidation states also have different geometrical requirements and hence the flexible nature of the tripodal ligands may be studied.

These complexes have been characterised by analysis, IR and multinuclear NMR (^1H, $^{13}C\{^1H\}$, $^{77}Se\{^1H\}/^{125}Te\{^1H\}$) spectroscopy as well as ES^+ mass spectrometry. X-ray crystallographic studies on four of the M(I) complexes are also described. The bonding trends for the chalcogen ligands to low and medium oxidation state metals are discussed along with the reaction chemistry of the Rh(I) and Ir(I) complexes with H_2.

5.2 Results and Discussion

5.21 Rhodium(I) and Iridium(I) Complexes

Reaction of $[M(cod)Cl]_2$ (M = Rh or Ir) with two molar equivalents of L^3 (L^3 = $MeC(CH_2ER)_3$, E = Se, R = Me; E = Te, R = Me or Ph) and two molar equivalents of NH_4PF_6 at room temperature in CH_2Cl_2 affords a yellow (selenoether) or orange brown (telluroether) solution, from which the complexes $[M(cod)(L^3)][PF_6]$ may be isolated after removal of the precipitated NH_4Cl, reduction of the solvent volume *in vacuo* and addition of diethyl ether. IR spectroscopy on the isolated products showed peaks consistent with the free PF_6^- anion, coordinated L^3 and cod ligands. The electrospray mass spectra confirmed the identity of the cation, showing clusters of peaks, with the correct isotopic distribution, corresponding to $[M(cod)(L^3)]^+$ in each case.

5.211 NMR Spectroscopy

As discussed in Chapters 1 and 3, coordination of selenium or tellurium to a metal centre leads to chirality at the chalcogen atom and hence the potential presence of both the *syn* and *anti* invertomers. For these d^8 complexes, further complexity is anticipated from the geometry at the metal centre since the donor atoms on the tripod ligand are likely to be inequivalent. Considering this, the ^1H NMR spectra at 300 K for all six complexes were suprisingly simple, showing just one signal each for the EMe, CH_2 and MeC groups, along with one signal for the cod-CH and cod-CH_2 groups. This indicates that these complexes are probably fluxional in solution at room temperature. Similar behaviour was observed for the d^8 square planar species $[M(L^3)_2]^{2+}$ (M = Pd or Pt) (Chapter 4). The $^{13}C\{^1H\}$ NMR spectra were also recorded in order to study the cod ligand. As in the ^1H NMR spectra, just one signal was observed for each set of chemically equivalent carbons in the free cod or tripod ligand (Figure 5.1). This behaviour is consistent with $^{13}C\{^1H\}$ and ^1H NMR data reported for the complex $[Rh(cod)([9]aneS_3)][PF_6]$.[14] The $^{13}C\{^1H\}$ NMR shifts of δ(cod-CH) for $[M(cod)L^3]^+$ are presented in Table 5.1.

Table 5.1. $^{13}C\{^1H\}$ NMR δ(cod-CH) shift ($CH_2Cl_2/CDCl_3$, 300 K) for the complexes $[M(cod)(L^3)][PF_6]$.

Complex	δ(cod-CH)
$[Rh(cod)\{MeC(CH_2SeMe)_3\}]^+$	80.8
$[Rh(cod)\{MeC(CH_2TeMe)_3\}]^+$	76.4
$[Rh(cod)\{MeC(CH_2TePh)_3\}]^+$	79.3
$[Ir(cod)\{MeC(CH_2SeMe)_3\}]^+$	62.3
$[Ir(cod)\{MeC(CH_2TeMe)_3\}]^+$	61.8
$[Ir(cod)\{MeC(CH_2TePh)_3\}]^+$	64.3

Inspection of Table 5.1 shows that the cod-CH resonance is shifted to lower frequency and hence is more shielded in the complex $[Rh(cod)\{MeC(CH_2TeMe)_3\}][PF_6]$ compared to the other rhodium species. This supports the superior σ-donor properties of the ligand $MeC(CH_2TeMe)_3$ to low valent metals, resulting in increased π-back bonding from Rh to the $\pi^*(C=C)$ orbitals, compared to the $MeC(CH_2SeMe)_3$ and $MeC(CH_2TePh)_3$ ligands. For the iridium complexes δ(cod-CH) are shifted to low frequency compared to the rhodium analogues, indicating greater nuclear shielding from the heavier Ir nucleus. However the $^{13}C\{^1H\}$ NMR spectra again show that the cod-CH group is more shielded in the $MeC(CH_2TeMe)_3$ complex than the other two species, although the effect is less pronounced than that observed for the rhodium analogues. Interestingly, the δ(cod-CH) resonances for the $MeC(CH_2TeMe)_3$ complexes are shifted to lower frequency than those observed for the complexes $[M(cod)([9]aneS_3)]^+$ (M = Rh and Ir) where δ(cod-CH) = 78.3 and 63.0 respectively, again illustrating the superior donating abilities of $MeC(CH_2TeMe)_3$.[14, 15]

In order to gain further information on the structure of these complexes in solution, $^{77}Se\{^1H\}/^{125}Te\{^1H\}$ NMR spectra were recorded. At room temperature, the $^{77}Se\{^1H\}$ and $^{125}Te\{^1H\}$ NMR data (Table 5.2) show that for all six complexes only one resonance is observed. This again indicates that the complexes are fluxional in solution at room temperature and thus all three arms of the tripod ligand appear equivalent.

Table 5.2. $^{77}Se\{^1H\}$ and $^{125}Te\{^1H\}$ NMR ($CH_2Cl_2/CDCl_3$, 300 K) data for the complexes $[M(cod)(L^3)][PF_6]$.

Complex	$\delta(^{77}Se\{^1H\})^a$	$\delta(^{125}Te\{^1H\})^b$	$\Delta(^{77}Se)^c$	$\Delta(^{125}Te)^c$	$\delta(Te)/\delta(Se)$
$[Rh(cod)\{MeC(CH_2EMe)_3\}]^+$	78.2	188.3 (79 Hz)	53.8	166.3	2.4
$[Rh(cod)\{MeC(CH_2TePh)_3\}]^+$	-	455.2	-	68.2	-
$[Ir(cod)\{MeC(CH_2EMe)_3\}]^+$	58.7	145.0	34.3	123.0	2.5
$[Ir(cod)\{MeC(CH_2TePh)_3\}]^+$	-	420.2	-	33.2	-

[a] Relative to neat external $SeMe_2$. [b] Relative to neat external $TeMe_2$, $^1J_{Te\text{-}Rh}$ in parenthesis. [c] $\delta_{complex} - \delta_{free\ ligand}$.

Rhodium coupling is only observed for the $MeC(CH_2TeMe)_3$ complex with a doublet in the $^{125}Te\{^1H\}$ NMR spectrum ($^1J_{Te\text{-}Rh} = 79$ Hz), indicating that ligand dissociation does not occur during the fluxional process. When compared to the rhodium complexes, the ^{77}Se and ^{125}Te resonances are shifted to low frequency in the iridium complexes, again indicating greater nuclear shielding from the heavier Ir nucleus.

In order to try to distinguish the different tellurium environments, the $^{125}Te\{^1H\}$ NMR spectra were also recorded at 210 K for the samples $[Rh(cod)\{MeC(CH_2TeR)_3\}][PF_6]$ (R = Me or Ph). However, no change from the room temperature spectrum was observed for the $MeC(CH_2TeMe)_3$ complex, although for the $MeC(CH_2TePh)_3$ complex a broadening of the resonance was detected.

As discussed in Chapter 1, for many comparable organo-selenium and -tellurium compounds the ^{77}Se and ^{125}Te chemical shifts show very consistent trends and often the $\delta(^{125}Te)/\delta(^{77}Se)$ ratio is 1.7-1.8.[16] However, in our study of dithio-, diseleno- and ditelluroether complexes of manganese carbonyl halides (Chapter 2) we found that the ^{125}Te chemical shifts for the coordinated telluroethers were much more positive than expected, either by comparison with the ^{77}Se chemical shifts in the selenoether analogues, or by comparisons with the same ligands bound to medium oxidation state metal centres.[13] Thus we were interested to compare this ratio in the Rh(I) and Ir(I) complexes reported here. Although the range of complexes is more limited, the same trend is observed with $\delta(^{125}Te)/\delta(^{77}Se)$ being 2.4 for the rhodium complexes and 2.5 for the iridium complexes, indicating superior σ-donation by the telluroether ligand (Table 5.2).

Figure 5.1. $^{13}C\{^1H\}$ **NMR spectrum (90.1 MHz, $CH_2Cl_2/CDCl_3$, 300 K) of $[Ir(cod)\{MeC(CH_2SeMe)_3\}][PF_6]$.**

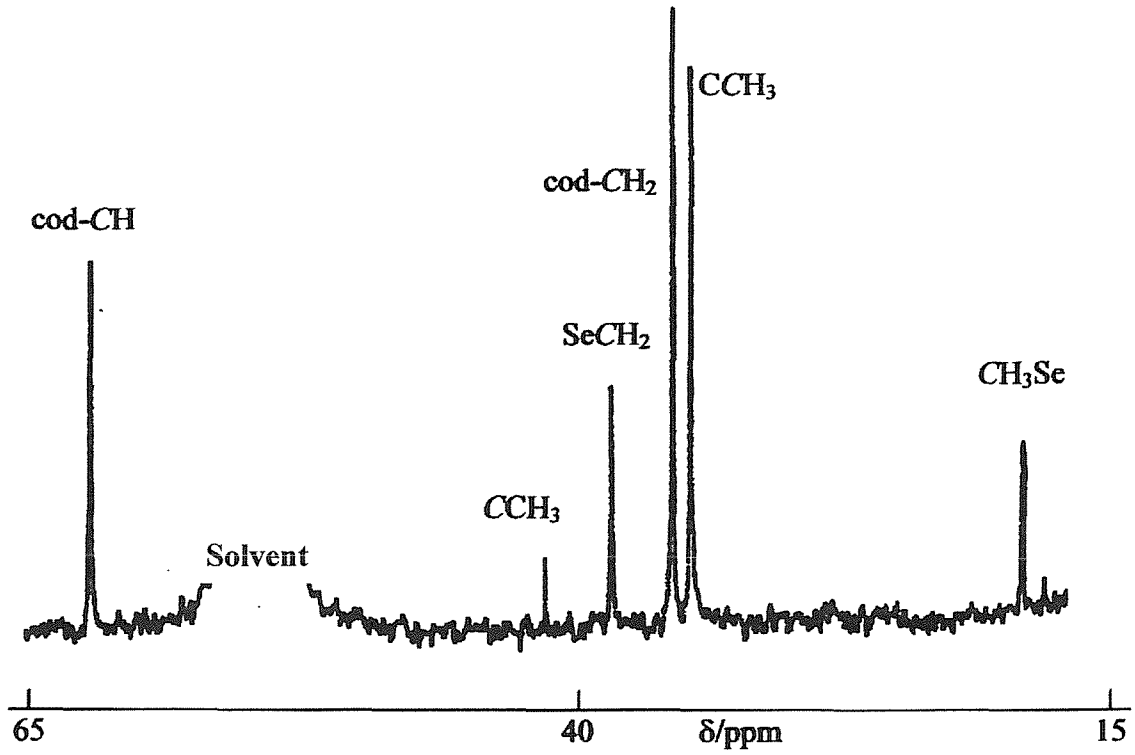

The preparation of the cyclooctene complexes $[M(C_8H_{14})_2(L^3)]^+$ (M = Rh or Ir) was also investigated *via* the reaction of $[M(C_8H_{14})_2Cl]_2$ with two molar equiv. of L^3 and NH_4PF_6 in CH_2Cl_2. For rhodium, a mixture of unidentified products was isolated that decomposed rapidly. The iridium complexes were slightly more stable with the electrospray mass spectra showing a cluster of peaks corresponding to $[Ir(C_8H_{14})(L^3)]^+$, and IR spectroscopy displaying bands assigned to the tripodal ligand, cyclooctene and PF_6^-. However, the ^1H NMR spectra showed broad peaks indicating decomposition and elemental analyses were consistently poor, and hence these species were not pursued.

5.212 Crystallographic Studies

Due to the dynamic nature of these complexes, limited structural information was obtained from NMR spectroscopy, therefore particular emphasis was placed on obtaining X-ray crystallographic data on these complexes in order to ascertain their structural characteristics in the solid state. Since the metal centre in these species has a d^8 configuration, a square planar geometry may be expected with one of the tripod arms uncoordinated, as observed for the complex $[Pt\{MeC(CH_2SeMe)_3\}_2]^{2+}$ (Chapter 4). However, for Rh(I) and Ir(I), although square planar complexes predominate, 5-coordination also occurs, with the relative stability of five- and four coordinate species dependent on the ligands involved.

Yellow or orange crystals of the complexes $[Rh(cod)\{MeC(CH_2SeMe)_3\}][PF_6]$, $[Rh(cod)\{MeC(CH_2TeMe)_3\}][PF_6]$, $[Ir(cod)\{MeC(CH_2SeMe)_3\}][PF_6]$ and $[Ir(cod)\{MeC(CH_2TePh)_3\}][PF_6]$ were grown *via* the vapour diffusion of diethyl ether into a solution of the appropriate complex in MeCN (rhodium) or Me_2CO (iridium). The structure of the complex $[Rh(cod)\{MeC(CH_2TeMe)_3\}][PF_6]$ (Figure 5.2, Tables 5.3 - 5.5) shows the Rh(I) centre coordinated to the cod and to all three arms of the tripodal ligand, with the methyl groups on the tripodal ligand adopting the *syn* arrangement. Hence, a five coordinate complex cation is obtained. Since both ligands in these complexes are constrained, regular trigonal bipyramidal or square planar geometries are not expected. Analysis of the bond lengths around the metal centre gives *d*(Rh-Te) = 2.6226(8), 2.5786(8) and 2.6924(7) Å, thus one Rh-Te bond is notably longer than the other two. The Te-Rh-Te angles do not deviate significantly from 90°, with the Te-Rh-cod angles ranging from 83.5(3) to 167.9(2)°. Thus, the structure may best be described as square pyramidal with the longer Rh-Te bond axial and the shorter bonds being *trans* to the cod ligand.

Table 5.3. Crystallographic Data Collection and Refinement Parameters.

	[Rh(cod){MeC($CH_2SeMe)_3$}][PF_6]	[Rh(cod){MeC($CH_2TeMe)_3$}][PF_6]	[Ir(cod){MeC($CH_2SeMe)_3$}][PF_6]	[Ir(cod){MeC($CH_2TePh)_3$}][PF_6]·0.5Me_2CO
Formula	$C_{16}H_{30}F_6PRhSe_3$	$C_{16}H_{30}F_6PRhTe_3$	$C_{16}H_{30}F_6PIrSe_3$	$C_{32.5}H_{39}F_6IrO_{0.5}PTe_3$
Formula weight	707.16	853.08	796.48	1157.65
Crystal System	Monoclinic	Monoclinic	Monoclinic	Monoclinic
Space group	$P2_1/n$	$C2/c$	$P2_1/n$	$C2/c$
a, Å	12.857(3)	27.203(3)	12.889(4)	22.330(4)
b, Å	12.278(3)	14.998(4)	12.274(6)	14.57(2)
c, Å	14.514(3)	12.658(3)	14.492(3)	23.67(1)
β/°	105.40(2)	114.75(1)	105.28(2)	107.55(2)
V, $Å^3$	2209.0(7)	4689(1)	2211(7)	7342(10)
Z	4	8	4	8
D_{calc}, g/cm^3	2.126	2.416	2.392	2.094
μ(Mo-K_α), cm^{-1}	58.38	45.02	111.15	60.81
Unique obs. reflections	4098	4303	4102	6732
Obs. reflections with $[I_o > 2\sigma(I_o)]$	1792	2906	3014	5221
R	0.048	0.028	0.038	0.041
R_w	0.054	0.034	0.049	0.058

$R = \Sigma (|F_{obs}|_i - |F_{calc}|_i) / \Sigma |F_{obs}|_i$, $R_w = \sqrt{[\Sigma w_i (|F_{obs}|_i - |F_{calc}|_i)^2 / \Sigma w_i |F_{obs}|_i^2]}$

Figure 5.2. X-ray crystal structure of $[Rh(cod)\{MeC(CH_2TeMe)_3\}]^+$ with numbering scheme adopted. Ellipsoids are drawn at 40 % probability and H-atoms omitted for clarity.

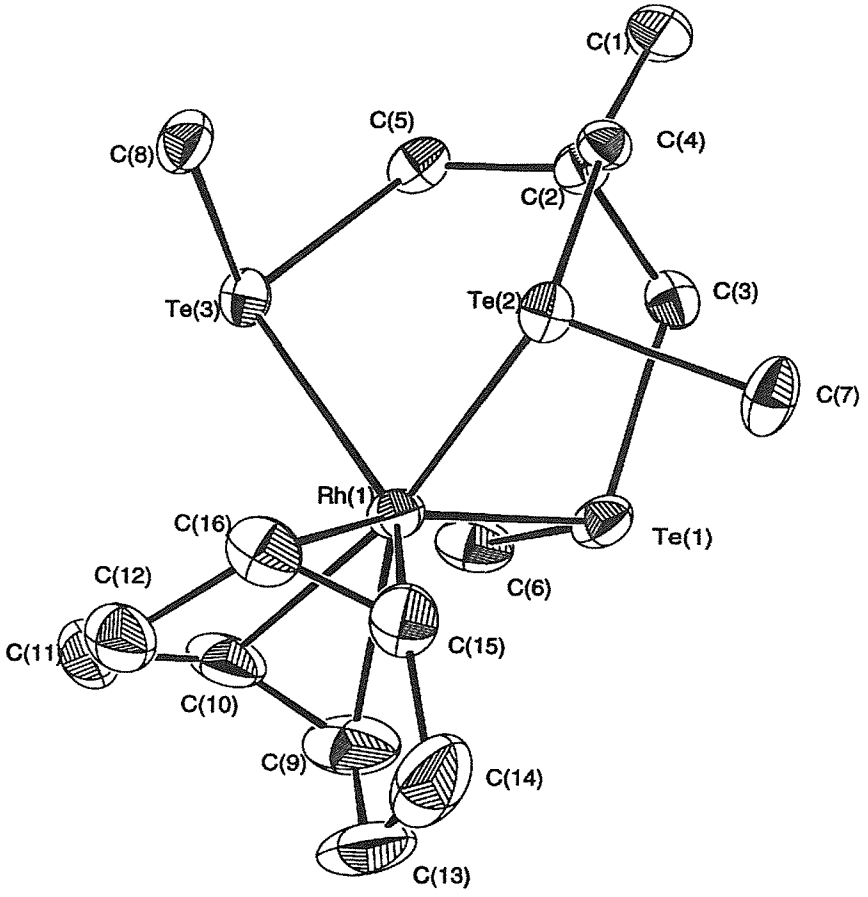

Table 5.4. Selected bond lengths for $[Rh(cod)\{MeC(CH_2TeMe)_3\}]^+$.

Atom	Atom	Distance/Å	Atom	Atom	Distance/Å
Te(1)	Rh(1)	2.6226(8)	Te(1)	C(3)	2.156(7)
Te(1)	C(6)	2.147(8)	Te(2)	Rh(1)	2.5786(8)
Te(2)	C(4)	2.158(7)	Te(2)	C(7)	2.118(8)
Te(3)	Rh(1)	2.6924(7)	Te(3)	C(5)	2.156(7)
Te(3)	C(8)	2.151(8)	Rh(1)	C(9)	2.219(9)
Rh(1)	C(10)	2.178(8)	Rh(1)	C(15)	2.167(8)
Rh(1)	C(16)	2.135(8)			

Table 5.5. Selected bond angles for $[Rh(cod)\{MeC(CH_2TeMe)_3\}]^+$.

Atom	Atom	Atom	Angle(°)	Atom	Atom	Atom	Angle(°)
Rh(1)	Te(1)	C(3)	107.9(2)	Rh(1)	Te(1)	C(6)	102.9(2)
C(3)	Te(1)	C(6)	94.9(3)	Rh(1)	Te(2)	C(4)	108.9(2)
Rh(1)	Te(2)	C(7)	105.4(3)	C(4)	Te(2)	C(7)	95.4(3)
Rh(1)	Te(3)	C(5)	104.9(2)	Rh(1)	Te(3)	C(8)	106.4(2)
C(5)	Te(3)	C(8)	95.8(3)	Te(1)	Rh(1)	Te(2)	89.26(2)
Te(1)	Rh(1)	Te(3)	92.25(2)	Te(1)	Rh(1)	C(9)	85.5(2)
Te(1)	Rh(1)	C(10)	101.0(2)	Te(1)	Rh(1)	C(15)	126.7(2)
Te(1)	Rh(1)	C(16)	164.5(2)	Te(2)	Rh(1)	Te(3)	87.11(2)
Te(2)	Rh(1)	C(9)	152.8(3)	Te(2)	Rh(1)	C(10)	167.9(2)
Te(2)	Rh(1)	C(15)	83.5(3)	Te(2)	Rh(1)	C(16)	90.7(2)
Te(3)	Rh(1)	C(9)	119.8(3)	Te(3)	Rh(1)	C(10)	86.1(3)
Te(3)	Rh(1)	C(15)	139.5(3)	Te(3)	Rh(1)	C(16)	103.2(2)
C(9)	Rh(1)	C(10)	36.5(4)	C(9)	Rh(1)	C(15)	78.5(4)
C(9)	Rh(1)	C(16)	87.5(3)	C(10)	Rh(1)	C(15)	95.3(4)
C(10)	Rh(1)	C(16)	81.1(3)	C(15)	Rh(1)	C(16)	38.0(3)
Rh(1)	C(9)	C(13)	113.4(8)	Te(1)	C(3)	C(2)	121.4(5)
Rh(1)	C(10)	C(11)	108.1(5)	Te(2)	C(4)	C(2)	121.3(5)
Rh(1)	C(15)	C(16)	69.8(5)	Te(3)	C(5)	C(2)	123.4(5)
Rh(1)	C(16)	C(15)	72.2(5)	Rh(1)	C(9)	C(10)	70.1(5)
Rh(1)	C(16)	C(12)	114.0(6)	Rh(1)	C(10)	C(9)	73.3(6)
Rh(1)	C(15)	C(14)	112.9(9)				

The two selenoether complexes $[Rh(cod)\{MeC(CH_2SeMe)_3\}][PF_6]$ and $[Ir(cod)\{MeC(CH_2SeMe)_3\}][PF_6]$ (Figures 5.3 and 5.4, Tables 5.3, 5.6 - 5.9) are isostructural with *d*(Rh-Se) = 2.479(2), 2.483(2) and 2.635(2) Å and *d*(Ir-Se) = 2.570(1), 2.481(1) and 2.478(1) Å. The Se-M-Se bond angles are approximately 90°. The complex $[Ir(cod)\{MeC(CH_2TePh)_3\}][PF_6]$ (Figure 5.5, Tables 5.10 and 5.11) has *d*(Ir-Te) = 2.6033(8), 2.6062(7) and 2.661(1) Å with again Te-Ir-Te not significantly deviating from 90°. Hence these complexes show similar structural features to $[Rh(cod)\{MeC(CH_2TeMe)_3\}]^+$ i.e. a distorted square pyramidal geometry with the axial M-E (E = Se or Te) bond significantly

longer than the M-E bonds *trans* to cod. The R groups on the chalcogen atoms adopt the *syn* arrangement in each example.

Figure 5.3. X-ray crystal structure of $[Rh(cod)\{MeC(CH_2SeMe)_3\}]^+$ with numbering scheme adopted. Ellipsoids are drawn at 40 % probability and H-atoms omitted for clarity.

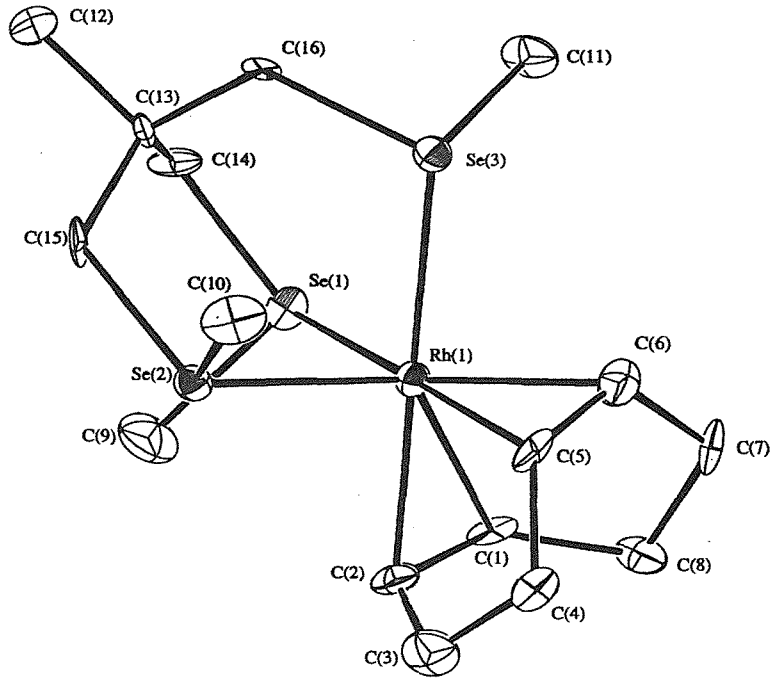

Table 5.6. Selected bond lengths for $[Rh(cod)\{MeC(CH_2SeMe)_3\}]^+$.

Atom	Atom	Distance/Å	Atom	Atom	Distance/Å
Rh(l)	Se(l)	2.479(2)	Rh(1)	Se(2)	2.635(2)
Rh(l)	Se(3)	2.483(2)	Rh(l)	C(1)	2.18(1)
Rh(l)	C(2)	2.13(1)	Rh(l)	C(5)	2.13(1)
Rh(l)	C(6)	2.17(2)	Se(l)	C(9)	1.96(2)
Se(l)	C(14)	1.96(1)	Se(2)	C(10)	1.94(2)
Se(2)	C(15)	1.99(1)	Se(3)	C(11)	1.97(1)
Se(3)	C(16)	1.96(1)			

Table 5.7. Selected bond angles for $[Rh(cod)\{MeC(CH_2SeMe)_3\}]^+$.

Atom	Atom	Atom	Angle(°)	Atom	Atom	Atom	Angle(°)
Se(1)	Rh(1)	Se(2)	89.64(7)	Se(1)	Rh(1)	Se(3)	90.55(7)
Se(1)	Rh(1)	C(1)	86.6(4)	Se(1)	Rh(1)	C(2)	96.1(5)
Se(1)	Rh(1)	C(5)	174.4(4)	Se(1)	Rh(1)	C(6)	138.3(4)
Se(2)	Rh(1)	Se(3)	85.29(6)	Se(2)	Rh(1)	C(1)	127.6(4)
Se(2)	Rh(1)	C(2)	90.3(5)	Se(2)	Rh(1)	C(5)	94.9(5)
Se(2)	Rh(1)	C(6)	129.8(4)	Se(3)	Rh(1)	C(1)	146.9(4)
Se(3)	Rh(1)	C(2)	172.0(5)	Se(3)	Rh(1)	C(5)	93.1(4)
Se(3)	Rh(1)	C(6)	81.3(4)	C(1)	Rh(1)	C(2)	38.6(6)
C(1)	Rh(1)	C(5)	88.0(6)	C(1)	Rh(1)	C(6)	79.1(6)
C(2)	Rh(1)	C(5)	80.6(6)	C(2)	Rh(1)	C(6)	96.6(6)
C(5)	Rh(1)	C(6)	38.6(6)	Rh(1)	Se(1)	C(9)	104.6(5)
Rh(1)	Se(1)	C(14)	110.0(4)	C(9)	Se(1)	C(14)	98.5(7)
Rh(1)	Se(2)	C(10)	107.6(5)	Rh(1)	Se(2)	C(15)	108.1(4)
C(10)	Se(2)	C(15)	99.8(7)	Rh(1)	Se(3)	C(11)	108.0(5)
Rh(1)	Se(3)	C(16)	109.9(4)	C(11)	Se(3)	C(16)	100.2(6)
Rh(1)	C(1)	C(8)	115(1)	Rh(1)	C(1)	C(2)	68.6(8)
Rh(1)	C(2)	C(1)	72.8(9)	Rh(1)	C(2)	C(3)	110(1)
Rh(1)	C(5)	C(6)	72.3(9)	Rh(1)	C(5)	C(4)	115(1)
Rh(1)	C(6)	C(5)	69.1(9)	Rh(1)	C(6)	C(7)	111(1)
Se(2)	C(15)	C(13)	118.1(10)	Se(1)	C(14)	C(13)	120(1)
Se(3)	C(16)	C(13)	121.5(10)				

Figure 5.4. X-ray crystal structure of $[Ir(cod)\{MeC(CH_2SeMe)_3\}]^+$ with numbering scheme adopted. Ellipsoids are drawn at 40 % probability and H-atoms omitted for clarity.

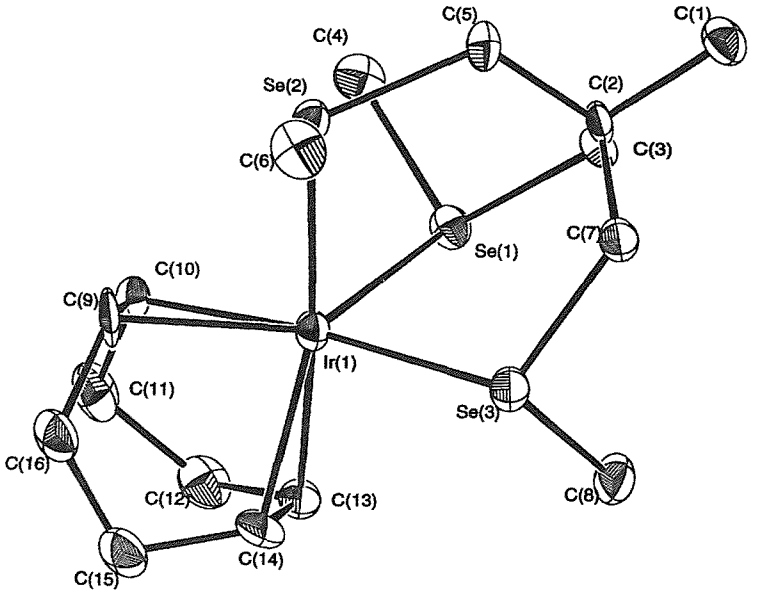

Table 5.8. Selected bond lengths for $[Ir(cod)\{MeC(CH_2SeMe)_3\}]^+$.

Atom	Atom	Distance/Å	Atom	Atom	Distance/Å
Ir(1)	Se(1)	2.570(1)	Ir(1)	Se(2)	2.481(1)
Ir(1)	Se(3)	2.478(1)	Ir(1)	C(9)	2.17(1)
Ir(1)	C(10)	2.13(1)	Ir(1)	C(13)	2.15(1)
Ir(1)	C(14)	2.19(1)	Se(1)	C(3)	1.97(1)
Se(1)	C(4)	1.94(1)	Se(2)	C(5)	1.97(1)
Se(2)	C(6)	1.96(1)	Se(3)	C(7)	1.96(1)
Se(3)	C(8)	1.95(1)			

Table 5.9. Selected bond angles for $[Ir(cod)\{MeC(CH_2SeMe)_3\}]^+$.

Atom	Atom	Atom	Angle(°)	Atom	Atom	Atom	Angle(°)
Se(1)	Ir(1)	Se(2)	86.44(4)	Se(1)	Ir(1)	Se(3)	90.21(4)
Se(1)	Ir(1)	C(9)	131.4(4)	Se(1)	Ir(1)	C(10)	95.7(3)
Se(1)	Ir(1)	C(13)	90.2(3)	Se(1)	Ir(1)	C(14)	126.5(3)
Se(2)	Ir(1)	Se(3)	90.79(4)	Se(2)	Ir(1)	C(9)	81.3(3)
Se(2)	Ir(1)	C(10)	92.8(3)	Se(2)	Ir(1)	C(13)	172.2(3)
Se(2)	Ir(1)	C(14)	146.9(3)	Se(3)	Ir(1)	C(9)	136.5(4)
Se(3)	Ir(1)	C(10)	173.2(3)	Se(3)	Ir(1)	C(13)	96.3(3)
Se(3)	Ir(1)	C(14)	85.8(3)	C(9)	Ir(1)	C(10)	38.9(5)
C(9)	Ir(1)	C(13)	95.8(5)	C(9)	Ir(1)	C(14)	78.7(5)
C(10)	Ir(1)	C(13)	80.5(4)	C(10)	Ir(1)	C(14)	88.0(4)
C(13)	Ir(1)	C(14)	37.8(5)	Ir(1)	Se(1)	C(3)	107.7(3)
Ir(1)	Se(1)	C(4)	106.5(4)	C(3)	Se(1)	C(4)	99.6(5)
Ir(1)	Se(2)	C(5)	109.4(3)	Ir(1)	Se(2)	C(6)	107.5(4)
C(5)	Se(2)	C(6)	100.2(5)	Ir(1)	Se(3)	C(7)	108.9(3)
Ir(1)	Se(3)	C(8)	105.0(4)	C(7)	Se(3)	C(8)	98.3(5)
Se(2)	C(5)	C(2)	121.5(8)	Se(1)	C(3)	C(2)	121.1(7)
Ir(1)	C(9)	C(10)	69.3(6)	Se(3)	C(7)	C(2)	121.8(8)
Ir(1)	C(14)	C(15)	114.4(8)	Ir(1)	C(9)	C(16)	113.1(8)
Ir(1)	C(10)	C(11)	116.0(7)	Ir(1)	C(10)	C(9)	71.9(6)
Ir(1)	C(13)	C(12)	110.7(7)	Ir(1)	C(13)	C(14)	72.8(7)
Ir(1)	C(14)	C(13)	69.4(6)				

Figure 5.5. X-ray crystal structure of $[Ir(cod)\{MeC(CH_2TePh)_3\}]^+$ with numbering scheme adopted. Ellipsoids are drawn at 40 % probability and H-atoms omitted for clarity.

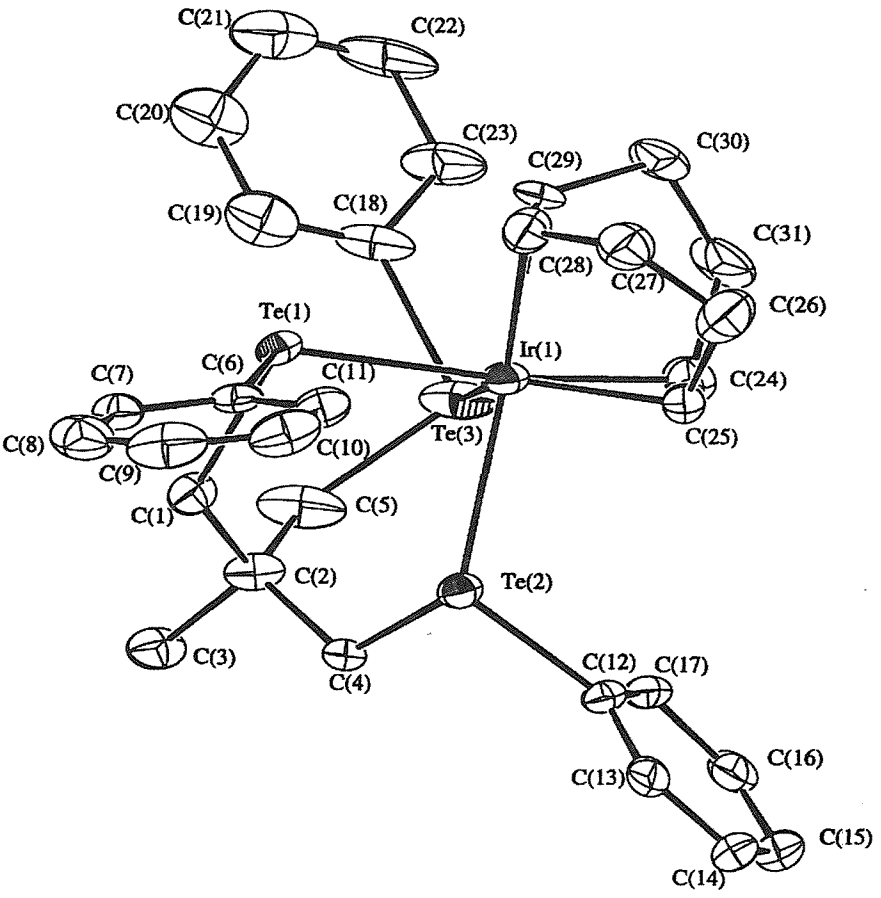

Table 5.10. Selected bond lengths for $[Ir(cod)\{MeC(CH_2TePh)_3\}]^+$.

Atom	Atom	Distance/Å	Atom	Atom	Distance/Å
Ir(1)	Te(1)	2.6033(8)	Ir(1)	Te(2)	2.6062(7)
Ir(1)	Te(3)	2.661(1)	Ir(1)	C(24)	2.19(1)
Ir(1)	C(25)	2.17(1)	Ir(1)	C(28)	2.19(1)
Ir(1)	C(29)	2.165(10)	Te(1)	C(1)	2.169(10)
Te(1)	C(6)	2.129(9)	Te(2)	C(4)	2.16(1)
Te(2)	C(12)	2.124(9)	Te(3)	C(5)	2.17(1)
Te(3)	C(18)	2.12(1)			

Table 5.11. Selected bond angles for $[Ir(cod)\{MeC(CH_2TePh)_3\}]^+$.

Atom	Atom	Atom	Angle(°)	Atom	Atom	Atom	Angle(°)
Te(1)	Ir(1)	Te(2)	84.70(2)	Te(1)	Ir(1)	Te(3)	87.39(3)
Te(1)	Ir(1)	C(24)	168.4(5)	Te(1)	Ir(1)	C(25)	152.5(5)
Te(1)	Ir(1)	C(28)	85.3(3)	Te(1)	Ir(1)	C(29)	92.3(3)
Te(2)	Ir(1)	Te(3)	95.93(3)	Te(2)	Ir(1)	C(24)	104.0(4)
Te(2)	Ir(1)	C(25)	87.8(3)	Te(2)	Ir(1)	C(28)	128.4(4)
Te(2)	Ir(1)	C(29)	166.7(4)	Te(3)	Ir(1)	C(24)	84.1(5)
Te(3)	Ir(1)	C(25)	119.8(5)	Te(3)	Ir(1)	C(28)	134.0(4)
Te(3)	Ir(1)	C(29)	96.9(4)	C(24)	Ir(1)	C(25)	37.7(6)
C(24)	Ir(1)	C(28)	94.9(5)	C(24)	Ir(1)	C(29)	80.9(4)
C(25)	Ir(1)	C(28)	78.7(4)	C(25)	Ir(1)	C(29)	89.0(4)
C(28)	Ir(1)	C(29)	38.3(5)	Ir(1)	Te(1)	C(1)	106.1(3)
Ir(1)	Te(1)	C(6)	108.2(3)	C(1)	Te(1)	C(6)	93.8(4)
Ir(1)	Te(2)	C(4)	105.9(2)	Ir(1)	Te(2)	C(12)	109.7(3)
C(4)	Te(2)	C(12)	93.1(4)	Ir(1)	Te(3)	C(5)	106.6(3)
Ir(1)	Te(3)	C(18)	104.2(3)	C(5)	Te(3)	C(18)	97.0(5)
Te(2)	C(4)	C(2)	118.7(6)	Te(1)	C(1)	C(2)	122.2(7)
Te(1)	C(6)	C(7)	117.6(7)	Te(3)	C(5)	C(2)	121.5(9)
Te(2)	C(12)	C(13)	117.9(8)	Te(1)	C(6)	C(11)	122.1(8)
Te(3)	C(18)	C(19)	124.3(9)	Te(2)	C(12)	C(17)	121.5(7)
Te(3)	C(18)	C(23)	116(1)	Ir(1)	C(24)	C(31)	109.5(9)
Ir(1)	C(24)	C(25)	70.5(8)	Ir(1)	C(25)	C(24)	71.8(9)
Ir(1)	C(25)	C(26)	114.9(8)	Ir(1)	C(28)	C(29)	70.0(6)
Ir(1)	C(28)	C(27)	112.7(8)	Ir(1)	C(29)	C(28)	71.7(6)
Ir(1)	C(29)	C(30)	114.4(8)				

Since these complexes represent the first structurally characterised seleno- or telluroether rhodium(I) or iridium(I) complexes reported, no direct comparisons from the literature are available. Structural data for a series of Cu(I), Ag(I) or Sn(IV) complexes have shown an increase in M-E of *ca.* 0.15 Å from E = Se to E = Te consistent with the difference in radii of

Se verses Te.[17] However, comparison of the structural data for the complexes $[Mn(CO)_3(L\text{-}L)X]$ (L-L = diseleno or ditelluroether, X = Cl, Br or I) discussed in Chapter 2, showed a smaller increase in M-E of 0.13 Å.[13] For the low valent complexes reported in this Chapter the increase in M-E is again smaller than expected (*ca.* 0.1 Å), consistent with all of the spectroscopic data indicating greater σ-donation from Te compared to Se.

5.213 Reactivity of Rh(I) and Ir(I) complexes with H_2

The generation of transition metal hydride species is of interest due to their role in many catalytic hydrogenation processes. We were interested in establishing whether these new Rh(I) and Ir(I) complexes would react with H_2 gas to form such species. In order to study this reaction, H_2 was bubbled through solutions of the complexes in CD_2Cl_2 at 0 °C and the ^1H NMR (360 MHz) spectra recorded immediately under an atmosphere of H_2 gas at 0 °C and at -50 °C. Weak hydride resonances were only observed for the complex $[Ir(cod)\{MeC(CH_2SeMe)_3\}]^+$ at δ -13.01, -13.04 and -13.40 at 0 °C, which became more intense as the temperature was lowered to -50 °C. No change was observed in the spectra for the other complexes. These shifts are consistent with those obtained for iridium hydride complexes obtained *via* the reaction of $[Ir(cod)\{(+)\text{-}RiSSR_2\}]^+$ {(+)-RiSSR$_2$ = 1,2-*O*-isopropylidene-3,5-bis(methylsulfanyl)-, 1,2-*O*-isopropylidene-3,5-bis(isopropylsulfanyl)- and 1,2-*O*-isopropylidene-3,5-bis(phenylsulfanyl)-α-D-(+)-ribofuranose with H_2.[9]

5.22 Rhodium(III) and Iridium(III) Complexes

The extension of this chemistry to Rh(III) and Ir(III) metal centres was undertaken in order to study the properties of medium oxidation state organometallic complexes involving seleno- and telluroether ligands. Reaction of $[M(C_5Me_5)Cl_2]_2$ (M = Rh or Ir) with 2 mol. equiv. of L^3 and 4 mol. equiv. of $TlPF_6$ in refluxing MeOH afforded an orange solution and white precipitate of TlCl. After removal of the TlCl by filtration and reduction of the solvent volume *in vacuo*, the complexes $[M(C_5Me_5)(L^3)][PF_6]_2$ were isolated as orange solids, upon addition of diethyl ether. The IR spectra showed the expected bands corresponding to the coordinated tripod ligand, C_5Me_5 and uncoordinated PF_6^- anion. The electrospray mass spectra showed clusters of peaks with the correct isotopic distribution for $[Rh(C_5Me_5)(L^3)]^{2+}$ (Figure 5.6) however for the iridium complexes the fragment $[Ir(C_5Me_5)(L^3)Cl]^+$ was

observed, probably due to the presence of chloride ions in the mass spectrometer. An X-ray data set was collected on a very small crystal of $[Ir(C_5Me)_5\{MeC(CH_2SeMe)_3\}][PF_6]_2$, but the data were too weak to afford a satisfactory refinement, although the expected pseudo-octahedral heavy atom framework was confirmed.

The ^1H NMR spectra showed sharp peaks corresponding to the coordinated tripod and C_5Me_5 ligands. Since inversion at an Rh(III)-Se/TeR_2 unit is expected to be slow (Chapter 4) the observation of just one peak for the Rh complexes for δ(EMe) indicates that the *syn* invertomer is dominant in solution. For the complexes $[Ir(C_5Me_5)\{MeC(CH_2EMe)_3\}]^{2+}$ the ^1H NMR spectra showed one δ(EMe) signal for E = Te, indicating the *syn* invertomer, however for E = Se, two signals were observed corresponding to the *anti* isomer.

The $^{77}Se\{^1H\}$ and $^{125}Te\{^1H\}$ NMR spectra showed one doublet for each of the three rhodium complexes (Table 5.12), consistent with the presence of just the *syn* invertomer in solution.

Figure 5.6. Electrospray mass spectrum of $[Rh(C_5Me_5)\{MeC(CH_2SeMe)_3\}]^{2+}$ showing the isotopic pattern for the peak $[Rh(C_5Me_5)\{MeC(CH_2SeMe)_3\}]^{2+}$ with calculated isotope pattern. The half-mass peaks were not observed in the spectrum due to the resolution of the spectrometer.

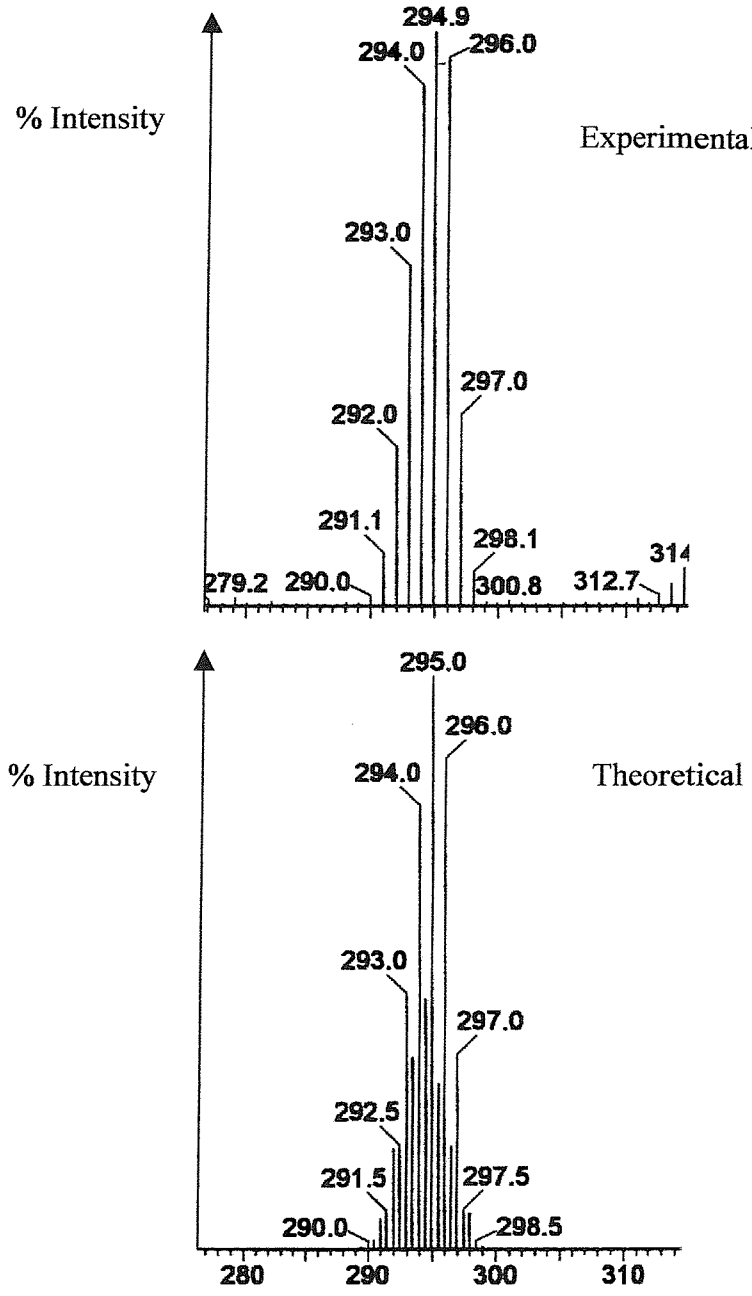

Table 5.12. $^{13}C\{^1H\}$ and $^{77}Se\{^1H\}$/ $^{125}Te\{^1H\}$ NMR (MeCN/$CDCl_3$, 300 K) data for the complexes $[M(C_5Me_5)(L^3)][PF_6]_2$.

Complex	$\delta(^{77}Se)^a$	$\delta(^{125}Te)^b$	$\delta(C_5Me_5)$
$[Rh(C_5Me_5)\{MeC(CH_2SeMe)_3\}]^{2+}$	126.6 (34)	-	100.2
$[Rh(C_5Me_5)\{MeC(CH_2TeMe)_3\}]^{2+}$	-	270.5 (91)	104.2
$[Rh(C_5Me_5)\{MeC(CH_2TePh)_3\}]^{2+}$	-	481.6 (91)	106.2
$[Ir(C_5Me_5)\{MeC(CH_2SeMe)_3\}]^{2+}$	98.1, 102.3	-	93.8
$[Ir(C_5Me_5)\{MeC(CH_2TeMe)_3\}]^{2+}$	-	214.5	98.5
$[Ir(C_5Me_5)\{MeC(CH_2TePh)_3\}]^{2+}$	-	394.2, 409.5, 449.1	94.4

[a] Relative to external neat $SeMe_2$. $^1J_{Rh\text{-}Se}$ in parenthesis. [b] Relative to external neat $TeMe_2$, $^1J_{Te\text{-}Rh}$ in parenthesis.

In the iridium systems, one resonance was observed in the $^{125}Te\{^1H\}$ NMR spectrum for the $MeC(CH_2TeMe)_3$ complex, indicating the presence of the *syn* invertomer, with two resonances being observed in the $^{77}Se\{^1H\}$ NMR spectrum for the $MeC(CH_2SeMe)_3$ complex of 2:1 intensity, indicating the *anti* invertomer. The $MeC(CH_2TePh)_3$ complex exhibited three resonances, consistent with the presence of both the *syn* and *anti* invertomers in solution.

Comparing the ^{77}Se and ^{125}Te NMR shifts for L^3 with those for the cod complexes, a significant shift to high frequency is observed, as would be expected due to the higher oxidation state of the metal centre causing deshielding of the chalcogen donor. Upon changing from Rh to Ir, $\delta(^{77}Se)$ and $\delta(^{125}Te)$ are shifted to low frequency as observed for the Rh(I) and Ir(I) complexes. The ratio $\delta(^{125}Te)/\delta(^{77}Se)$ for these +3 oxidation state complexes is expected to be nearer the norm of 1.7-1.8. This is indeed observed, with $\delta(^{125}Te)/\delta(^{77}Se)$ = 2.1 for both the rhodium and iridium species with $MeC(CH_2EMe)_3$ (E = Se or Te). Thus, telluroether donation is less effective here compared to the Rh(I) and Ir(I) cod complexes.

For the rhodium systems, coupling between rhodium and selenium or tellurium was observed in the form of doublets in the $^{125}Te\{^1H\}$ or $^{77}Se\{^1H\}$ NMR spectra (Figure 5.7). The value of $^1J_{Rh\text{-}Se}$ found for the selenoether complex (34 Hz) is lower than that observed for other Rh(III) selenoether complexes such as $[Rh\{MeC(CH_2SeMe)_3\}Cl_3]$ (*syn* 41 Hz, *anti* 39 Hz),[18] $[Rh\{MeC(CH_2SeMe)_3\}_2][PF_6]_3$ (43 Hz), *trans*-$[RhCl_2([8]aneSe_2)_2][BF_4]$ (42 Hz) and *cis*-$[RhCl_2([16]aneSe_4)][PF_6]$ (36 Hz, 37 Hz).[19] In contrast, the $^1J_{Te\text{-}Rh}$ values observed for the telluroether complexes (Table 5.12) are larger than that found for the $[Rh(cod)\{MeC(CH_2TeMe)_3\}]^+$ complex and those reported for the complexes

$[Rh(L\text{-}L)_2Cl_2][PF_6]$ (L-L = $MeTe(CH_2)_3TeMe$, $PhTe(CH_2)_3TePh$ or *o*-$C_6H_4(TeMe)_2$) where $^1J_{Te\text{-}Rh}$ ranged from 50 - 70 Hz.[20] For comparable complexes the ^1J(Te-X)/^1J(Se-X) ratio is generally *ca.* 2-3 and this trend is observed for the $MeC(CH_2EMe)_3$ complexes with ^1J(Te-Rh)/^1J(Rh-Se) = 2.6.[16]

Figure 5.7. $^{125}Te\{^1H\}$ NMR spectrum (113.6 MHz, $CH_2Cl_2/CDCl_3$, 300 K) of $[Rh(C_5Me_5)\{MeC(CH_2TeMe)_3\}][PF_6]_2$.

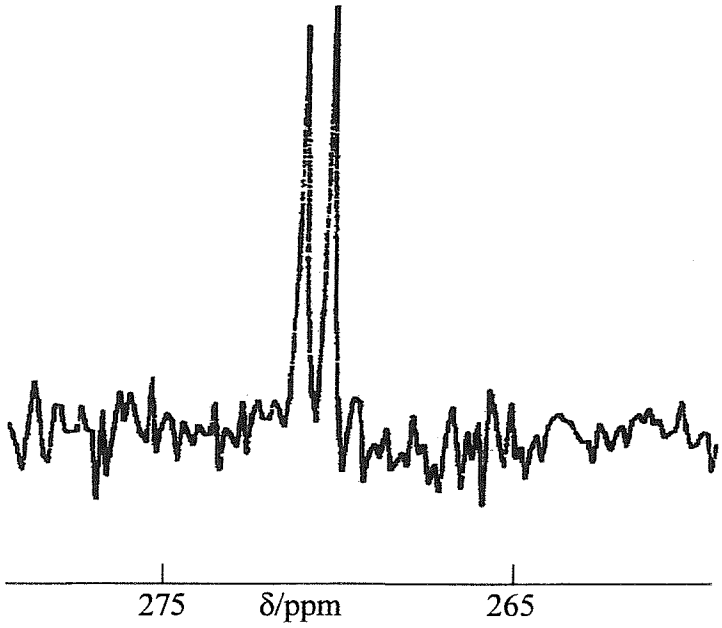

The $^{13}C\{^1H\}$ NMR spectra were recorded to examine changes at the C_5Me_5 group. Comparison of shifts for the Rh and Ir complexes shows that upon changing the metal centre from Rh to Ir, a shift to low frequency is again observed. Interestingly, $\delta(C_5Me_5)$ is shifted to high frequency upon changing the donor from Se to Te. This trend is observed for both the rhodium and iridium complexes and indicates that the C_5Me_5 ligand is more shielded in the selenoether complex than in the telluroether complex. Hence, as the donor is changed from Se to Te, less electron density is transferred to the metal, resulting in increased σ-donation by the C_5Me_5 group. This indicates that for these medium oxidation state complexes, selenium is a stronger σ-donor than tellurium, probably due to poorer overlap between the large Te σ-donor orbital and the contracted metal *d* orbitals.

5.3 Conclusions

The low and medium oxidation state organometallic complexes $[M(cod)(L^3)][PF_6]$ and $[M(C_5Me_5)(L^3)][PF_6]_2$ (M = Rh or Ir, L^3 = $MeC(CH_2SeMe)_3$, $MeC(CH_2TeR)_3$, R = Me or Ph) have been prepared. The M(I) complexes are dynamic in solution and VT NMR studies have failed to slow this fluxionality sufficiently to differentiate between the different chalcogen environments. X-ray crystallography has shown that the geometry of the ligands around the metal centre is best described as square pyramidal in the solid state with the axial M-E bond significantly longer than the equatorial M-E bonds.

The NMR spectroscopic data have been compared in order to ascertain the bonding properties of the chalcogen ligands. Comparison of the ratio $\delta(^{125}Te)/\delta(^{77}Se)$ for these complexes has shown the tellurium-125 chemical shift for the $[M(cod)\{MeC(CH_2TeMe)_3\}]^+$ complexes to be more positive than expected. The ^{13}C NMR shift for δ(cod-CH) has also indicated increased π-back bonding from the metal centre to the cod ligand in the complexes with the $MeC(CH_2TeMe)_3$ ligand. Thus a similar trend to that observed for the Mn(I) carbonyl complexes described in Chapters 2 and 3 is observed, with increased σ-donation from the telluroether ligand compared to the selenoether ligand.

In contrast, NMR spectroscopic data for the M(III) complexes have shown the ratio $\delta(^{125}Te)/\delta(^{77}Se)$ to be nearer the norm of 1.7 - 1.8 for these species. Further, the $^{13}C\{^1H\}$ NMR shift for $\delta(C_5Me_5)$ has shown increased σ-donation from the C_5Me_5 ligand to the metal centre in the telluroether complex compared to the selenoether system. These data indicate telluroether ligands are poorer σ-donors than selenoethers in medium oxidation state complexes, probably as a consequence of decreased overlap between the diffuse tellurium orbitals and contracted metal *d* orbitals.

5.4 Experimental

The complexes $[Rh(cod)Cl]_2$,[21] $[Ir(cod)Cl]_2$,[22] $[Rh(C_5Me_5)Cl_2]_2$ and $[Ir(C_5Me_5)Cl_2]_2$ were prepared by the literature procedures,[23] as were the ligands $MeC(CH_2SeMe)_3$[24] and $MeC(CH_2TeMe)_3$.[25] An improved synthesis for the selenoether ligand is detailed in Chapter 7, along with the synthesis of $MeC(CH_2TePh)_3$.

$[Rh(cod)\{MeC(CH_2SeMe)_3\}][PF_6]$. $[Rh(cod)Cl]_2$ (55 mg, 1.1 x 10^{-4} mol) was added to $MeC(CH_2SeMe)_3$ (80 mg, 2.2 x 10^{-4} mol) and NH_4PF_6 (39 mg, 2.4 x 10^{-4} mol) in CH_2Cl_2 (30 cm^3) and the mixture stirred at room temperature for 1 hour. The precipitated NH_4Cl removed by filtration, the solvent volume reduced to 2 cm^3 *in vacuo* and diethyl ether added (10 cm^3) to give an orange precipitate. Yield 105 mg, 68 %. Analysis: Calculated for $C_{16}H_{30}F_6PRhSe_3$: %C, 27.2; %H, 4.2. Found: %C, 26.6; %H, 3.7. ^1H NMR (CD_3CN, 300 K): δ 1.22 (s, 3H, CCH_3), 2.23 (s, 9H, $SeCH_3$), 2.40 (br, 8H, cod-CH_2), 2.68 (s, 6H, $SeCH_2$), 3.96 (br, 4H, cod-CH). $^{13}C\{^1H\}$ NMR ($CH_2Cl_2/CDCl_3$, 300 K): δ 13.5 ($SeCH_3$), 32.2 (CCH_3), 32.7 (cod-CH_2), 35.7 ($SeCH_2$), 80.8 (cod-CH). $^{77}Se\{^1H\}$ NMR ($CH_2Cl_2/CDCl_3$, 300 K): δ 78.2. ES^+ (MeCN), *m/z* = 561; calc for $[Rh(cod)\{MeC(CH_2{}^{80}SeMe)_3\}]^+$ 565. IR/cm^{-1} 3017(w), 2973(w), 2940(w), 2879(w), 2830(w), 1460(w), 1420(m), 1359(m), 1267(w), 1094(m), 926(m), 906(w), 845(s), 613(w), 557(m).

$[Rh(cod)\{MeC(CH_2TeMe)_3\}][PF_6]$ was prepared similarly to give a brown solid (67 %). Analysis: Calculated for $C_{16}H_{30}F_6PRhTe_3$: %C, 22.5; %H, 3.5. Found: %C, 22.0; %H, 3.2. ^1H NMR (CD_3CN, 300 K): δ 1.52 (s, 3H, CCH_3), 2.06 (s, 9H, $TeCH_3$), 2.43 (br, 8H, cod-CH_2), 2.51 (s, 6H, $TeCH_2$), 3.82 (br, 4H, cod-CH). $^{13}C\{^1H\}$ NMR ($CH_2Cl_2/CDCl_3$, 300 K): δ –10.5 ($TeCH_3$), 14.4 ($TeCH_2$), 31.6 (CCH_3), 32.3 (cod-CH_2), 76.4 (cod-CH). $^{125}Te\{^1H\}$ NMR ($CH_2Cl_2/CDCl_3$, 300 K): δ 188.3 ($^1J_{Te\text{-}Rh}$ = 79 Hz). ES^+ (MeCN), *m/z* = 709; calc for $[Rh(cod)\{MeC(CH_2{}^{130}TeMe)_3\}]^+$ 715. IR/cm^{-1} 1359(s), 1096(s), 987(m), 836(s), 613(w), 558(m).

$[Rh(cod)\{MeC(CH_2TePh)_3\}][PF_6]$ was prepared in a similar manner to give an orange solid (69 %). Analysis: Calculated for $C_{31}H_{36}F_6PRhTe_3.CH_2Cl_2$: %C, 34.2; %H, 3.2. Found: %C, 34.6; %H, 2.9. ^1H NMR (CD_3CN, 300 K): δ 1.58 (s, 3H, CCH_3), 2.60 (s, 8H, cod-CH_2), 2.73 (s, 6H, $TeCH_2$), 3.99 (s, 4H, cod-CH), 7.4 - 7.7 (m, 15H, TePh). $^{13}C\{^1H\}$ NMR

($CH_2Cl_2/CDCl_3$, 300 K): δ 20.4 ($TeCH_2$), 32.0 (CCH_3), 32.6 (cod-CH_2), 79.3 (cod-CH), 111.9, 129.7, 130.0, 135.2 (TePh). $^{125}Te\{^1H\}$ NMR ($CH_2Cl_2/CDCl_3$, 300 K): δ 455.2. ES^+ (MeCN), *m/z* = 895; calc for $[Rh(cod)\{MeC(CH_2{}^{130}TePh)_3\}]^+$ 901. IR/cm^{-1} 3050(w), 2951(w), 2896(w), 1571(w), 1474(m), 1433(w), 1405(w), 1359(m), 1262(w), 1235(w), 1094(m), 1016(w), 997(w), 840(s), 740(m), 693(m), 613(w), 558(s), 454(m).

$[Ir(cod)\{MeC(CH_2SeMe)_3\}][PF_6]$ was prepared similarly using $[Ir(cod)Cl]_2$ instead of $[Rh(cod)Cl]_2$ to give a yellow solid (66 %). Analysis: Calculated for $C_{16}H_{30}F_6IrPSe_3$: %C, 24.1; %H, 3.8. Found: %C, 23.9; %H, 3.4. ^1H NMR (CD_3CN, 300 K): δ 1.21 (s, 3H, CCH_3), 2.24 (br, 8H, cod-CH_2), 2.37 (s, 9H, $SeCH_3$), 2.65 (s, 6H, $SeCH_2$), 3.96 (br, 4H, cod-CH). $^{13}C\{^1H\}$ NMR ($CH_2Cl_2/CDCl_3$, 300 K): δ 16.6 ($SeCH_3$), 32.8 (CCH_3), 33.7 (cod-CH_2), 36.8 ($SeCH_2$), 40.1 (CCH_3), 62.3 (cod-CH). $^{77}Se\{^1H\}$ NMR ($CH_2Cl_2/CDCl_3$, 300 K): δ 58.7. ES^+ (MeCN), *m/z* = 651; calc for $[^{193}Ir(cod)\{MeC(CH_2{}^{80}SeMe)_3\}]^+$ 655. IR/cm^{-1} 2973(w), 2918(w), 2841(w), 1416(m), 1356(s), 1095(s), 991(m), 930(w), 905(w), 846(s), 613(w), 557(m).

$[Ir(cod)\{MeC(CH_2TeMe)_3\}][PF_6]$ was prepared similarly to give a brown solid (31 %). Analysis: Calculated for $C_{16}H_{30}F_6PIrTe_3$: %C, 20.4; %H, 3.2. Found: %C, 19.9; %H, 2.5. ^1H NMR (CD_3CN, 300 K): δ 1.47 (s, 3H, CCH_3), 2.11 (s, 9H, $TeCH_3$), 2.35 (br, 8H, cod-CH_2), 2.57 (s, 6H, $TeCH_2$), 3.42 (br, 4H, cod-CH). $^{13}C\{^1H\}$ NMR ($CH_2Cl_2/CDCl_3$, 300 K): δ –8.3 ($TeCH_3$), 14.0 ($TeCH_2$), 34.1 (CCH_3), 36.3 (cod-CH_2), 61.8 (cod-CH). $^{125}Te\{^1H\}$ NMR ($CH_2Cl_2/CDCl_3$, 300 K): δ 145.0. ES^+ (MeCN), *m/z* = 799; calc for $[^{193}Ir(cod)\{MeC(CH_2{}^{130}TeMe)_3\}]^+$ 805. IR/cm^{-1} 2962(w), 1359(s), 1261(w), 1091(s), 991(m), 841(s), 613(w), 557(m).

$[Ir(cod)\{MeC(CH_2TePh)_3\}][PF_6]$ was prepared in a similar manner to give an orange solid (64 %). Analysis: Calculated for $C_{31}H_{36}F_6PIrTe_3$: %C, 33.0; %H, 3.2. Found: %C, 32.5; %H, 2.5. ^1H NMR (CD_3CN, 300 K): δ 1.43 (s, 3H, CCH_3), 2.35 (s, 8H, cod-CH_2), 2.52 (s, 6H, $TeCH_2$), 3.82 (s, 4H, cod-CH), 7.4 - 7.7 (m, 15H, TePh). $^{13}C\{^1H\}$ NMR ($CH_2Cl_2/CDCl_3$, 300 K): δ 20.3 ($TeCH_2$), 33.3 (CCH_3), 36.7 (cod-CH_2), 64.3 (cod-CH), 111.9, 131.1, 135.4 (TePh). $^{125}Te\{^1H\}$ NMR ($CH_2Cl_2/CDCl_3$, 300 K): δ 420.2. ES^+ (MeCN), *m/z* = 985; calc for $[^{193}Ir(cod)\{MeC(CH_2{}^{130}TePh)_3\}]^+$ 991. IR/cm^{-1} 2995(w), 2951(w), 1571(w), 1474(w),

1434(w), 1359(s), 1236(w), 1092(s), 1016(w), 997(m), 842(s), 741(s), 693(m), 613(w), 558(s), 434(m).

In situ reaction of H_2 with Rh(I) and Ir(I) complexes:

In a typical preparation, hydrogen was bubbled through a solution of the complex in CD_2Cl_2 for 15 minutes at 0 °C. The solution was then transferred into a NMR spectrometer tube and placed under an atmosphere of H_2 and the ^1H NMR spectrum recorded (using a Bruker AM360 spectrometer operating at 360 MHz) at 0 °C and -50 °C.

$[Rh(C_5Me_5)\{MeC(CH_2SeMe)_3\}][PF_6]_2$. To a solution of $MeC(CH_2SeMe)_3$ (57 mg, 1.6 x 10^{-4} mol) in MeOH (40 cm^3) was added $TlPF_6$ (3.2 x 10^{-4} mol) and $[Rh(C_5Me_5)Cl_2]_2$ (50 mg, 8.1 x 10^{-5} mol). The reaction mixture was refluxed for 18 hours to give an orange solution and white precipitate of TlCl. After filtration and reduction of the solvent volume *in vacuo* to 2 cm^3, addition of diethyl ether (10 cm^3) produced a light orange solid, which was subsequently recrystallised from MeCN and diethyl ether. Yield 60 mg, 84 %. Analysis: Calculated for $C_{18}H_{33}F_{12}P_2RhSe_3$: %C, 24.6; %H, 3.8. Found: %C, 24.1; %H, 2.6. ^1H NMR ($(CD_3)_2CO$, 300 K): δ 1.00 (s, 3H, CCH_3), 1.43 (s, 15H, $C_5\mathit{Me}_5$), 2.62 (s, 9H, $SeCH_3$), 2.90 - 3.40 (br, 6H, $SeCH_2$). $^{13}C\{^1H\}$ NMR ($CH_3CN/CDCl_3$, 300 K): δ 8.1 ($C_5\mathit{Me}_5$), 14.4 ($SeCH_3$), 29.6 ($C\mathit{C}H_3$), 34.6 ($SeCH_2$), 40.4 ($\mathit{C}CH_3$), 100.2 (C_5Me_5). $^{77}Se\{^1H\}$ NMR ($CH_3CN/CDCl_3$, 300 K): δ 126.5 ($^1J_{Rh\text{-}Se}$ = 34 Hz). ES^+ (MeCN), *m/z* = 295; calc for $[Rh(C_5Me_5)\{MeC(CH_2{}^{80}SeMe)_3\}]^{2+}$ 296. IR/cm^{-1} 2907(w), 1361(m), 1096(m), 1023(w), 987(w), 838(s), 559(m).

$[Rh(C_5Me_5)\{MeC(CH_2TeMe)_3\}][PF_6]_2$ was prepared similarly to give a brown solid (75 %). Analysis: Calculated for $C_{18}H_{33}F_{12}P_2RhTe_3$: %C, 21.1; %H, 3.2. Found: %C, 21.4; %H, 2.6. ^1H NMR ($(CD_3)_2CO$, 300 K): δ 1.40 (s, 3H, CCH_3), 1.75 (s, 15H, $C_5\mathit{Me}_5$), 2.05 (s, 9H, $TeCH_3$), 2.45 (s, 6H, $TeCH_2$). $^{13}C\{^1H\}$ NMR ($CH_3CN/CDCl_3$, 300 K): δ -6.4 ($TeCH_3$), 9.3 ($C_5\mathit{Me}_5$), 17.9 ($TeCH_2$), 32.9 ($C\mathit{C}H_3$), 38.9 ($\mathit{C}CH_3$), 104.2 (C_5Me_5). $^{125}Te\{^1H\}$ NMR ($CH_3CN/CDCl_3$, 300 K): δ 270.5 ($^1J_{Te\text{-}Rh}$ = 91 Hz). ES^+ (MeCN), *m/z* = 368; calc for $[Rh(C_5Me_5)\{MeC(CH_2{}^{130}TeMe)_3\}]^{2+}$ 371. IR/cm^{-1} 1474(w), 1359(s), 1095(m), 839(s), 740(w), 614(w), 559(m).

$[Rh(C_5Me_5)\{MeC(CH_2TePh)_3\}][PF_6]_2$ was prepared similarly to give a light orange solid (70 %). Analysis: Calculated for $C_{33}H_{39}F_{12}P_2RhTe_3$: %C, 32.7; %H, 3.2. Found: %C, 32.5; %H, 2.5. ^1H NMR ($(CD_3)_2CO$, 300 K): δ 1.30 (s, 3H, CCH_3), 1.48 (s, 15H, $C_5\mathit{Me}_5$), 3.10 - 3.30 (br, 6H, $TeCH_2$), 7.4 - 7.7 (m, 15H, TePh). $^{13}C\{^1H\}$ NMR ($CH_3CN/CDCl_3$, 300 K): δ 10.4 ($C_5\mathit{Me}_5$), 26.1 (CCH_3), 33.4 ($TeCH_2$), 40.9 ($\mathit{C}CH_3$), 106.2 (C_5Me_5) 130 - 138 (TePh). $^{125}Te\{^1H\}$ NMR ($CH_3CN/CDCl_3$, 300 K): δ 481.6 ($^1J_{Te\text{-}Rh}$ = 91 Hz). ES^+ (MeCN), *m/z* = 461; calc for $[^{103}Rh(C_5Me_5)\{MeC(CH_2{}^{130}TePh)_3\}]^{2+}$ 464. IR/cm^{-1} 1359(s), 1096(s), 997(m), 839(s), 732(m), 690(w), 674(w), 558(m).

$[Ir(C_5Me_5)\{MeC(CH_2SeMe)_3\}][PF_6]_2$ was prepared similarly using $[Ir(C_5Me_5)Cl_2]_2$ instead of $[Rh(C_5Me_5)Cl_2]_2$ to give a yellow solid (65 %). Analysis: Calculated for $C_{18}H_{33}F_{12}IrP_2Se_3$: %C, 22.3; %H, 3.4. Found: %C, 22.8; %H, 3.4. ^1H NMR ($(CD_3)_2CO$, 300 K): δ 1.46 (s, 3H, CCH_3), 1.81 (s, 15H, $C_5\mathit{Me}_5$), 2.00, 2.15 (s, 9H, $SeCH_3$), 2.66 (s, 6H, $SeCH_2$). $^{13}C\{^1H\}$ NMR ($CH_3CN/CDCl_3$, 300 K): δ 7.9 ($C_5\mathit{Me}_5$), 13.4, 13.9 ($SeCH_3$), 31.3 (CCH_3), 35.8, 36.2, 36.4 ($SeCH_2$), 42.3 ($\mathit{C}CH_3$), 93.8 (C_5Me_5). $^{77}Se\{^1H\}$ NMR ($CH_3CN/CDCl_3$, 300 K): δ 98.1, 102.3. ES^+ (MeCN), *m/z* = 715; calc for $[^{193}Ir(C_5Me_5)\{MeC(CH_2{}^{80}SeMe)_3\}^{35}Cl]^+$ 717. IR/cm^{-1} 1461(w), 1359(m), 1096(m), 985(w), 837(s), 558(m).

$[Ir(C_5Me_5)\{MeC(CH_2TeMe)_3\}][PF_6]_2$ was prepared similarly to give a brown solid (55 %). Analysis: Calculated for $C_{18}H_{33}F_{12}IrP_2Te_3$: %C, 19.4; %H, 3.0. Found: %C, 19.0; %H, 2.5. ^1H NMR ($(CD_3)_2CO$, 300 K): δ 1.60 (s, 3H, CCH_3), 2.16 (s, 15H, $C_5\mathit{Me}_5$), 2.39 (s, 9H, $TeCH_3$), 3.0 - 3.5 (s, 6H, $TeCH_2$). $^{13}C\{^1H\}$ NMR ($CH_3CN/CDCl_3$, 300 K): δ -5.6 ($TeCH_3$), 8.8 ($C_5\mathit{Me}_5$), 15.6 ($TeCH_2$), 33.9 (CCH_3), 38.9 ($\mathit{C}CH_3$) 98.5 (C_5Me_5). $^{125}Te\{^1H\}$ NMR ($CH_3CN/CDCl_3$, 300 K): δ 214.5. ES^+ (MeCN), *m/z* = 861; calc for $[^{193}Ir(C_5Me_5)\{MeC(CH_2{}^{130}TeMe)_3\}^{35}Cl]^+$ 867. IR/cm^{-1} 2940(w), 1359(s), 1098(s), 986(m), 841(s), 740(w), 697(w), 615(w), 558(m).

$[Ir(C_5Me_5)\{MeC(CH_2TePh)_3\}][PF_6]_2$ was prepared similarly to give a light orange solid (60 %). Analysis: Calculated for $C_{33}H_{39}F_{12}IrP_2Te_3$: %C, 30.5; %H, 3.0. Found: %C, 30.3; %H, 2.3. ^1H NMR ($(CD_3)_2CO$, 300 K): δ 1.26 (s, 3H, CCH_3), 1.63 (s, 15H, $C_5\mathit{Me}_5$), 2.26 (s, 6H, $TeCH_2$), 7.2 - 7.8 (m, 15H, TePh). $^{13}C\{^1H\}$ NMR ($CH_3CN/CDCl_3$, 300 K): δ 8.2 ($C_5\mathit{Me}_5$), 25.2 ($TeCH_2$), 29.9 (CCH_3), 40.6 ($\mathit{C}CH_3$), 94.4 (C_5Me_5), 127 - 138 (TePh).

$^{125}Te\{^{1}H\}$ NMR ($CH_3CN/CDCl_3$, 300 K): δ 394.2, 409.5, 449.1. ES^+ (MeCN), *m/z* = 1047; calc for $[^{193}Ir(C_5Me_5)\{MeC(CH_2{}^{130}TePh)_3\}^{35}Cl]^+$ 1053. IR/cm^{-1} 3061(w), 1572(w), 1475(m), 1435(m), 1360(s), 1095(s), 998(m), 839(s), 737(m), 692(m), 558(m), 454(w).

X-ray Crystallographic Studies

$[Rh(cod)\{MeC(CH_2SeMe)_3\}][PF_6]$, $[Rh(cod)\{MeC(CH_2TeMe)_3\}][PF_6]$, $[Ir(cod)\{MeC(CH_2SeMe)_3\}][PF_6]$ and $[Ir(cod)\{MeC(CH_2TePh)_3\}][PF_6]$. Details of the crystallographic data collection and refinement parameters are given in Table 5.3. The crystals were grown by vapour diffusion of diethyl ether into solutions of the appropriate complexes in MeCN (for the Rh complexes) and Me_2CO (for the Ir complexes). Data collection used a Rigaku AFC7S four-circle diffractometer operating at 150 K, using graphite-monochromated Mo-K_α X-radiation (λ = 0.71073 Å). The data were corrected for absorption using psi-scans (except for $[Rh(cod)\{MeC(CH_2SeMe)_3\}]PF_6$ for which psi-scans did not provide a satisfactory correction, hence with the model at isotropic convergence, the data were corrected for absorption using DIFABS).[26] The structures were solved by heavy atom Patterson methods[27] and developed by iterative cycles of full-matrix least-squares refinement and difference Fourier syntheses.[28] All non-H-atoms were refined anisotropically and H atoms were placed in fixed, calculated positions with *d*(C-H) = 0.96 Å.

5.5 References

[1] J. F. Young, J. A. Osborne, F. H. Jardine and G. Wilkinson, *J. Chem. Soc., Chem. Commun.,* 1965, 131.

[2] L. Vaska and J. W. Di Luzio, *J. Am. Chem. Soc.,* 1961, **83**, 2784.

[3] C. Bianchini, A Meli, M. Peruzzini, F. Vizza, S. Moneti, V. Herrera and R. Sánchez-Delgado, *J. Am. Chem. Soc.,* 1994, **116**, 4370.

[4] C. Bianchini, P. Frediani, V. Herrera, M. V. Jiménez, A. Meli, L. Rincón, R. Sánchez-Delgado and F. Vizza, *J. Am. Chem. Soc.,* 1995, **117**, 4333.

[5] C. Bianchini, P. Frediani and V. Sernau, *Organometallics,* 1995, **14**, 5458.

[6] E. G. Thaler, K. Folting and K. G. Caulton, *J. Am. Chem. Soc.,* 1990, **112**, 2664.

[7] A. J. Blake, R. O. Gould, M. A. Halcrow and M. Schröder, *J. Chem. Soc., Dalton Trans.,* 1994, 2197.

[8] A. J. Blake, M. A. Halcrow and M. Schröder, *J. Chem. Soc., Dalton Trans.,* 1994, 1631.

[9] O. Pàmies, M. Diéguez, G. Net, A. Ruiz and C. Claver, *J. Chem. Soc., Dalton Trans.,* 1999, 3439.

[10] K. Badyal, W. R. McWhinnie, H. L. Chen and T. A. Hamor, *J. Chem. Soc., Dalton Trans.,* 1997, 1579.

[11] K. Badyal, W. R. McWhinnie, J. Homer and M. C. Perry, *J. Organomet. Chem.,* 1998, **555**, 279.

[12] H. Schumann, A. A. Arif, A. L. Rheingold, C. Janiak, R. Hoffmann and N. Kuhn, *Inorg. Chem.,* 1991, **30**, 1618.

[13] W. Levason, S. D. Orchard and G. Reid, *Organometallics,* 1999, **18**, 1275.

[14] A. J. Blake, R. O. Gould, M. A. Halcrow and M. Schröder, *J. Chem. Soc., Dalton Trans.,* 1994, 2197.

[15] A. J. Blake, M. A. Halcrow and M. Schröder, *J. Chem. Soc., Dalton Trans.,* 1994, 1613.

[16] N. P. Luthra and J. D. Odom, in *The Chemistry of Organic Selenium and Tellurium Compunds;* S. Patai and Z. Rappoport (eds.), Wiley, New York, 1986, Vol. 1, Chap. 6.

[17] A. R. J. Genge, W. Levason and G. Reid, *J. Chem. Soc., Dalton Trans.,* 1997, 4549.

[18] E. G. Hope, W. Levason, G. L. Marshall and S. G. Murray, *J. Chem. Soc., Dalton Trans.,* 1985, 2185.

[19] W. Levason, J. J. Quirk and G. Reid, *J. Chem. Soc., Dalton Trans.,* 1996, 3713.

[20] W. Levason, S. D. Orchard, G. Reid and V. -A. Tolhurst, *J. Chem. Soc., Dalton Trans.,* 1999, 2071.

[21] G. Giordano and R. H. Crabtree, *Inorg. Synth.,* 1979, **19**, 218.

[22] J. L. Herde, J. C. Lambert and C. V. Senoff, *Inorg. Synth.,* 1974, **15**, 18.

[23] J. W. Kang, K. Moseley and P. M. Maitlis, *J. Am. Chem. Soc.,* 1969, **91**, 5970.

[24] D. J. Gulliver, E. G. Hope, W. Levason, G. L. Marshall, S. G. Murray and D. M. Potter, *J. Chem. Soc., Perkin Trans. II,* 1984, 429.

[25] E. G. Hope, T. Kemmitt and W. Levason, *Organometallics,* 1988, **7**, 78.

[26] N. Walker and D. Stuart, *Acta Crystallogr. Sect. A,* 1983, **39**, 158.

[27] PATTY, The DIRDIF Program System, P.T. Beurskens, G. Admiraal, G. Beurskens, W.P. Bosman, S. Garcia-Granda, R.O. Gould, J.M.M. Smits and C. Smykalla, Technical Report of the Crystallography Laboratory, University of Nijmegen, The Netherlands, 1992.

[28] TeXsan: Crystal Structure Analysis Package, Molecular Structure Corporation, Texas, 1995.

Chapter 6

Ruthenium(II) Group 16 Tripodal Complexes

6.1 Introduction

Although ruthenium exhibits a wide range of oxidation states from VIII to -II, the most common are III and II. Indeed a wide range of Ru(II) complexes are known, with virtually all being octahedral, diamagnetic with a low spin t_{2g}^6 configuration. Catalytic processes utilising Ru(II) phosphine complexes have been an area of intense interest in recent years.[1]

The preparation of $MeC(CH_2PPh_2)_3$ (triphos) complexes with a range of platinum group metals have been reported.[2] Such species combine the excellent ligand properties associated with phosphine ligands along with the stereochemical constraints such tripodal ligands impose.[3] Bianchini and co-workers have reported much of this work, in addition to studies mimicking the hydrodesulfurisation (HDS) process with various metal centres including, for example, rhodium,[4] iridium,[5] and two component tungsten/rhodium systems.[6] HDS is important industrially since it is the mechanism by which sulfur is removed from crude petroleum to provide more processable and environmentally acceptable fuels. This work has included C-S bond cleavage of benzo[*b*]thiophene,[7] by the ruthenium(II) (tetrahydroborate)hydride complex [(triphos)RuH(BH_4)] and the first example of homogenous and chemoselective hydrogenolysis of benzo[*b*]thiophene to 2-ethylthiophenol effectively catalysed by the Ru(0) fragment [(triphos)RuH]$^-$, obtained *via* the thermolysis of the complex K[(triphos)RuH_3].[8] The ruthenium(II) tris(acetonitrile) complex [(triphos)Ru$(NCMe)_3$][BPh_4]$_2$ has played a key role in this chemistry since K[(triphos)RuH_3] is prepared *via* the reaction of KO^tBu with [(triphos)RuH(BH_4)] which is, in turn, obtained from [(triphos)Ru$(NCMe)_3$][BPh_4]$_2$ and $NaBH_4$. Recent work has also shown that this acetonitrile complex is an extremely efficient catalyst precursor for the regioselective hydrogenation of benzo[*b*]thiophene to 2,3-dihydrobenzo[*b*]-thiophene under mild reaction conditions.[9]

The chemistry of Ru(II) with thioether ligands, in particular the macrocyclic [9]aneS_3 has received considerable attention, with complexes such as [Ru([9]aneS_3)$_2$]$^{2+}$ and [RuCl([9]aneS_3)$(dmso)_2$]$^+$ being reported.[10] The species [$RuCl_2(PPh_3)$([9]aneS_3)][11] and [RuX(CS)(PPh_3)([9]aneS_3)][PF_6] (X = H, Cl, SCN and SC_6H_4Me-4) have also been prepared as part of an investigation in to organometallic macrocycle chemistry.[12] These studies have also reported the σ-vinyl and σ-aryl complexes [Ru$(CH{=}CH_2)(CO)(PPh_3)$([9]aneS_3)]$^+$ and [Ru$(C_6H_4$Me-4$)(CO)(PPh_3)$([9]aneS_3)]$^+$ although it should be noted that these species still

contain phosphine ligands which will of course also influence the properties of the complexes.[13]

The chemistry of ruthenium(II) with the heavier seleno- and telluroether ligands has generally been limited to the preparation and characterisation of bidentate analogues including the $[Ru(L\text{-}L)_2Cl_2]$ (L-L = bidentate seleno-[14] or telluroether ligand) and $[Ru(L\text{-}L)_2(PPh_3)Cl][PF_6]$ (L-L = bidentate telluroether) species.[15] The crystal structures of the macrocyclic *cis*-$[RuCl_2([16]aneSe_4)]$ and *trans*-$[RuCl(PPh_3)([16]aneSe_4)][PF_6]$ complexes have also been reported as part of a study into the chemistry of the tetraselenoether ligand.[16]

The successful preparation of low and medium oxidation state rhodium and iridium organometallic complexes with the group 16 tripodal ligands, L^3 {$L^3 = MeC(CH_2EMe)_3$ (E = Se or Te), $MeC(CH_2TePh)_3$} discussed in Chapter 5, along with their flexible coordination modes (Chapter 4) and changing bonding abilities (Chapters 3 and 5) led us to consider the ability these ligands to promote novel reaction chemistry. Our investigation into homoleptic platinum metal complexes with L^3 reported the synthesis of the complexes $[Ru(L^3)_2]^{2+}$ {L^3 = $MeC(CH_2EMe)_3$ (E = S, Se or Te) and $MeC(CH_2TePh)_3$} (Chapter 4). Considering the difficulty encountered in preparing similar diseleno- and ditelluroether analogues, these species were found to be remarkably robust. Therefore we were interested in synthesising piano-stool complexes containing the $[(L^3)Ru]^{2+}$ fragment in order to determine whether such species were sufficiently robust to support any subsequent reaction chemistry.

This Chapter reports an investigation into the preparation, characterisation and electrochemistry of the complexes $[RuCl_2(PPh_3)(L^3)]$ and $[RuCl_2(dmso)(L^3)]$ (L^3 = $MeC(CH_2SeMe)_3$, $MeC(CH_2TeMe)_3$ and $MeC(CH_2TePh)_3$). These complexes have been studied by analysis, IR and multinuclear NMR (^1H, $^{13}C\{^1H\}$, $^{31}P\{^1H\}$ and $^{77}Se\{^1H\}/^{125}Te\{^1H\}$) spectroscopy as well as ES^+ mass spectrometry and X-ray crystallographic studies on two of the complexes. The preparation of the tris(acetonitrile) complexes $[Ru(NCMe)_3\{MeC(CH_2ER)_3\}]^{2+}$ (E = Se, R = Me; E = Te, R = Ph) from the respective chloro-dmso species is also described, along with studies into the lability of the MeCN ligands and reaction of these complexes with $NaBH_4$.

6.2 Results and Discussion

6.21 Ruthenium(II) Dichloro-phosphine Complexes

The precursor $[RuCl_2(PPh_3)_3]$ has been used extensively in the preparation of Ru(II) derivatives with various ligands. Recently this research group has reported its reaction with bidentate telluroether ligands to form species of the type $[Ru(L\text{-}L)_2(PPh_3)Cl][PF_6]$ (L-L = $RTe(CH_2)_3TeR$, R = Me or Ph, and *o*-$C_6H_4(TeMe)_2$) as part of a study into the preparation of 1:2 metal:ditelluroether complexes.[15] We were interested in the preparation of group 16 tripodal complexes with $[RuCl_2(PPh_3)_3]$ and their reaction chemistry, since such species would allow the study of complexes containing both phosphine and group 16 tripodal ligands, and provide complexes containing the $[(L^3)Ru]^{2+}$ {L^3 = $MeC(CH_2EMe)_3$ (E = Se or Te) and $MeC(CH_2TePh)_3$} fragment, upon which further chemistry may be undertaken.

Reaction of $[RuCl_2(PPh_3)_3]$ with 1 mol. equiv. of L^3 in CH_2Cl_2 at room temperature for 18 hours gave an orange (selenoether) or brown (telluroether) solution. After reduction of the solvent volume *in vacuo* and addition of diethyl ether, the complexes $[RuCl_2(PPh_3)(L^3)]$ were obtained in good yield. The ES^+ mass spectra (MeCN solution) showed clusters of peaks with the correct *m/z* and isotope pattern for $[RuCl(NCMe)(PPh_3)(L^3)]^+$ where the loss of Cl^- has enabled ionisation, with replacement of this ligand by MeCN. A further cluster of peaks corresponding to $[RuCl(PPh_3)(L^3)]^+$ was also observed. Elemental analysis confirmed the identity of the complexes, showing good agreement with the expected values and confirming that triphenylphosphine oxide is not present in the isolated species.

Although apparently stable in the solid state, these complexes were found to be unstable in solution, even when thoroughly degassed with N_2, to give a green coloured solution, assigned to Ru(III) species. Since such species are paramagnetic, this led to complications when recording NMR spectra. To inhibit this process methanol (*ca.* 10 %) was added to solutions of the complexes in $CH_2Cl_2/CDCl_3$ before recording the NMR spectra since long accumulation times were necessary. The ^1H NMR spectra were recorded from freshly prepared solutions, under N_2.

The ^1H NMR spectra were expected to be fairly complicated, due to the different environments for the tripod donor arms, and the potential presence of both *syn* and *anti* invertomers, since inversion at an Ru(II)-Se/TeR_2 centre is expected to be slow (Chapter 4). Sharp resonances that may be assigned to PPh_3 and the tripod ligand were apparent for the selenoether complex, however only broad resonances, possibly associated with a

paramagnetic species, were observed for the telluroether complexes, hence individual environments were obscured and detailed analysis meaningless.

The $^{31}P\{^{1}H\}$ NMR spectra again revealed the reactivity of these complexes. Coordinated PPh_3, would generally be expected to have a signal at $\delta \approx 40$ for selenoether complexes[16] and $\delta \approx 50$ for telluroether complexes.[15] However for the telluroether complexes, only resonances assigned to oxidised triphenylphosphine were observed at approximately 26 ppm. This behaviour is common and has been observed in other ruthenium complexes, although the reaction appears to be extremely rapid for these species.[17] Attempts to run the spectra in $CH_2Cl_2/CDCl_3$ solution resulted in immediate decomposition and a meaningful $^{31}P\{^{1}H\}$ NMR spectrum could not be obtained due to the formation of paramagnetic species. The selenoether complex exhibited two resonances in the $^{31}P\{^{1}H\}$ NMR spectrum of approximate equal intensity at $\delta = 34.4$ and 35.2, shifts consistent with coordinated PPh_3 (Figure 6.1) and probably indicating the presence of two invertomers.

Figure 6.1. $^{31}P\{^{1}H\}$ NMR spectrum (145.8 MHz, $CH_2Cl_2/CDCl_3$/MeOH, 300K) of $[RuCl_2(PPh_3)\{MeC(CH_2SeMe)_3\}]$.

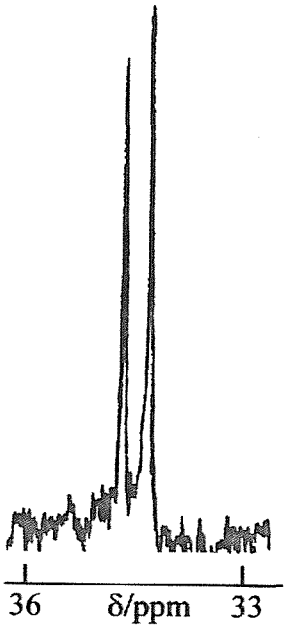

The $^{77}Se\{^1H\}$ and $^{125}Te\{^1H\}$ NMR spectra were also recorded, although the spectra for the tellurium complexes were of the decomposed species. The complex $[RuCl_2(PPh_3)\{MeC(CH_2SeMe)_3]$ showed seven signals, although $^2J_{Se\text{-}P}$ were poorly resolved, over the range of 100 ppm. This is consistent with the inequivalence of the tripod arms with both Se-*trans*-Cl and Se-*trans*-P environments, together with the presence of both the *syn* and *anti* invertomers. The $^{125}Te\{^1H\}$ NMR spectrum of $[RuCl_2(PPh_3)\{MeC(CH_2TePh)_3\}]$ showed similar behaviour although the range of signals was greater (> 200 ppm), again indicating the presence of a decomposition product. Considering this, the spectrum for $[RuCl_2(PPh_3)\{MeC(CH_2TeMe)_3\}]$ was surprisingly simple, exhibiting just two signals at δ = 340 and 336, although again these are obviously not due to the prepared complex. The lack of any coupling to phosphorus in these spectra confirmed the dissociation of PPh_3 in these species, verifying the reactivity of these complexes.

Interestingly the complexes $[RuCl_2(PPh_3)([9]aneS_3)]$, $[RuCl(PPh_3)([14]aneS_4)]^+$,[11] $[RuCl(PPh_3)([16]aneSe_4)]^+$ [14] have been observed to be stable in solution and therefore exhibit similar behaviour to $[RuCl_2(PPh_3)\{MeC(CH_2SeMe)_3\}]$, although the ditelluroether complexes $[RuCl(PPh_3)(L\text{-}L)_2]^+$ (L-L = $RTe(CH_2)_3TeR$, R = Me or Ph, and *o*-$C_6H_4(TeMe)_2$) decomposed on standing in CH_2Cl_2 solution in air, developing new $^{31}P\{^1H\}$ resonances consistent with the presence of $OPPh_3$.[15]

6.22 X-ray Crystal Structure of $[RuCl_2(PPh_3)\{MeC(CH_2SeMe)_3\}]$

Due to the instability of these complexes and the complex nature of the NMR spectroscopic data, it was felt particularly important to obtain the crystal structure of one of these species. Crystals of the complex $[RuCl_2(PPh_3)\{MeC(CH_2SeMe)_3\}]$ were grown *via* the slow diffusion of diethyl ether into a solution of the complex in $MeOH/CH_2Cl_2$ under N_2. The structure (Figure 6.2, Tables 6.1 - 6.3) shows Ru(II) coordinated to all three arms of the facially bound selenoether ligand, with the Cl^- and PPh_3 auxiliary ligands completing the distorted octahedral geometry, *d*(Ru-Se) = 2.429(1), 2.423(1) and 2.492(1) Å with the longer bond *trans* to PPh_3, consistent with the higher *trans* influence of PPh_3 compared to Cl^-, *d*(Ru-Cl) = 2.453(2) and 2.454(2) Å, *d*(Ru-P) = 2.336(2) Å. The majority of the angles around Ru(II) are close to the 90° or 180° expected for a regular octahedron, although the angle Se(1)-Ru(1)-P(1) = 99.91(6)°, is noticeably larger. The Ru-Se bond lengths compare well with those for *trans*-$[RuCl_2\{PhSe(CH_2)_2SePh\}_2]$ (2.433(1) - 2.460(1) Å)[18] and *trans*-

$[RuCl(PPh_3)([16]aneSe_4)]^+$ (2.465(3) - 2.497(3) Å), with the Ru-P and two Ru-Cl bond lengths also consistent with those found in *trans*-$[RuCl(PPh_3)([16]aneSe_4)]^+$ (d(Ru-P) = 2.307(6) Å; d(Ru-Cl) = 2.499(5) Å). The methyl substituents on the selenoether adopt the *syn* arrangement.

Figure 6.2. X-ray crystal structure of $[RuCl_2(PPh_3)\{MeC(CH_2SeMe)_3\}]$ with numbering scheme adopted. Ellipsoids are drawn at 40 % probability and H-atoms omitted for clarity.

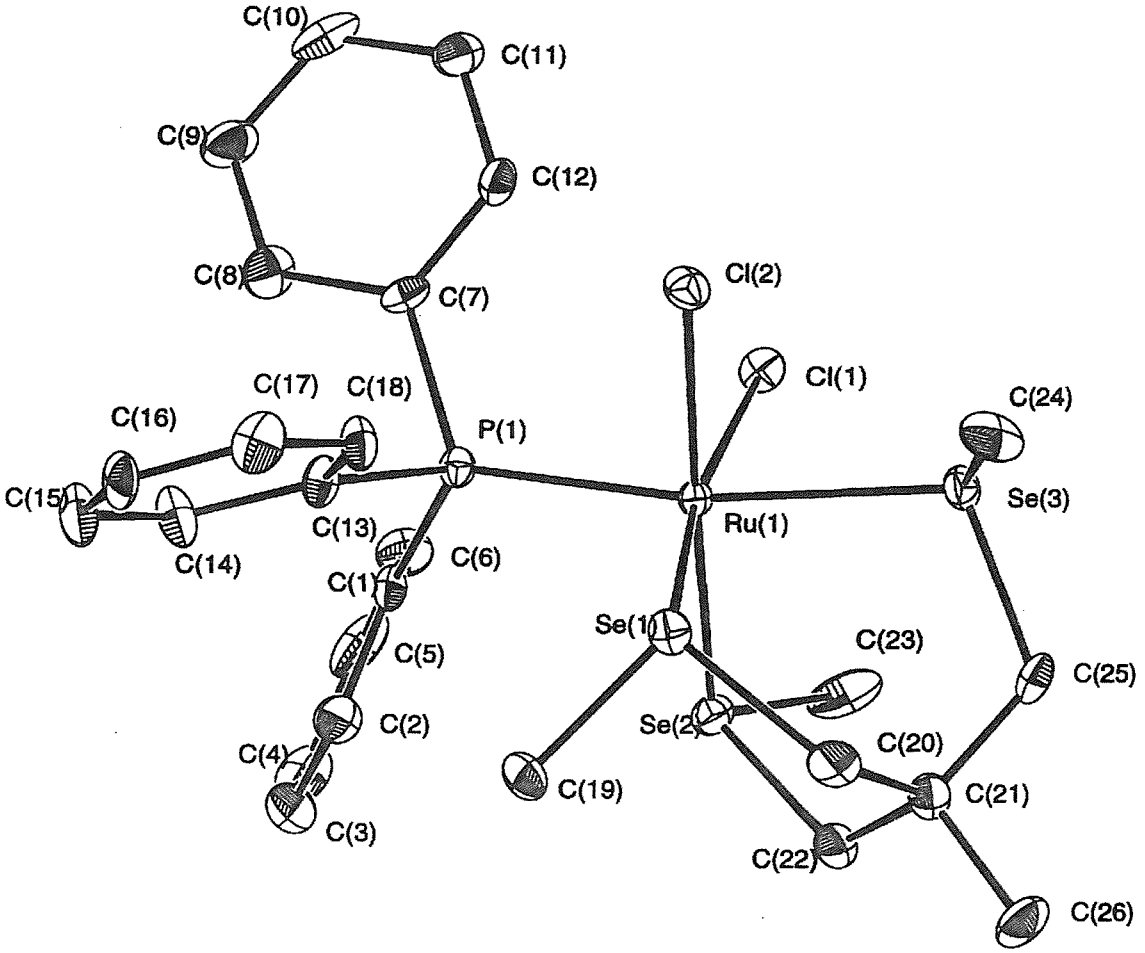

Table 6.1. Crystallographic data collection and refinement parameters for $[RuCl_2(PPh_3)\{MeC(CH_2SeMe)_3\}]$ and $[RuCl_2(dmso)\{MeC(CH_2SeMe)_3\}]$.

	$[RuCl_2(PPh_3)\{MeC(CH_2SeMe)_3\}]$	$[RuCl_2(dmso)\{MeC(CH_2SeMe)_3\}]$
Formula	$C_{26}H_{33}Cl_2PRuSe_3$	$C_{10}H_{24}Cl_2ORuSSe$
Formula weight	785.38	601.22
Crystal System	Orthorhombic	Monoclinic
Space group	*Pbca*	*Cc*
a, Å	16.001(7)	10.13(1)
b, Å	22.237(7)	13.486(6)
c, Å	15.686(5)	13.396(7)
β/°	-	101.49(5)
V, $Å^3$	5581(3)	1794(2)
Z	8	4
D_{calc}, g/cm^3	1.869	2.226
μ(Mo-K_α), cm^{-1}	47.39	73.63
Unique obs. reflections	5533	1733
Obs. reflections with $[I_o > 2\sigma(I_o)]$	2695	1417
R	0.036	0.040
R_w	0.037	0.054

$R = \Sigma (|F_{obs}|_i - |F_{calc}|_i) / \Sigma |F_{obs}|_i$, $R_w = \sqrt{[\Sigma w_i (|F_{obs}|_i - |F_{calc}|_i)^2 / \Sigma w_i |F_{obs}|_i^2]}$

Table 6.2. Selected bond lengths for $[RuCl_2(PPh_3)\{MeC(CH_2SeMe)_3\}]$.

Atom	Atom	Distance/Å	Atom	Atom	Distance/Å
Ru(1)	Se(1)	2.429(1)	Ru(1)	Se(2)	2.423(1)
Ru(1)	Se(3)	2.492(1)	Ru(1)	Cl(1)	2.453(2)
Ru(1)	Cl(2)	2.454(2)	Ru(1)	P(1)	2.336(2)
Se(1)	C(19)	1.945(8)	Se(1)	C(20)	1.992(8)
Se(2)	C(22)	1.974(8)	Se(2)	C(23)	1.941(9)
Se(3)	C(24)	1.955(9)	Se(3)	C(25)	1.961(8)
P(1)	C(1)	1.837(8)	P(1)	C(7)	1.860(8)
P(1)	C(13)	1.854(8)			

Table 6.3. Selected bond angles for $[RuCl_2(PPh_3)\{MeC(CH_2SeMe)_3\}]$.

Atom	Atom	Atom	Angle(°)	Atom	Atom	Atom	Angle(°)
Se(1)	Ru(1)	Se(2)	89.34(4)	Se(1)	Ru(1)	Se(3)	87.47(3)
Se(1)	Ru(1)	Cl(1)	171.07(6)	Se(1)	Ru(1)	Cl(2)	86.83(6)
Se(1)	Ru(1)	P(1)	99.91(6)	Se(2)	Ru(1)	Se(3)	93.53(4)
Se(2)	Ru(1)	Cl(1)	89.13(6)	Se(2)	Ru(1)	Cl(2)	175.60(6)
Se(2)	Ru(1)	P(1)	92.86(6)	Se(3)	Ru(1)	Cl(1)	83.85(5)
Se(3)	Ru(1)	Cl(2)	84.15(6)	Se(3)	Ru(1)	P(1)	170.29(6)
Cl(1)	Ru(1)	Cl(2)	94.33(7)	Cl(1)	Ru(1)	P(1)	88.95(7)
Cl(2)	Ru(1)	P(1)	89.94(7)	Ru(1)	Se(1)	C(19)	111.8(3)
Ru(1)	Se(1)	C(20)	107.8(2)	C(19)	Se(1)	C(20)	95.2(3)
Ru(1)	Se(2)	C(22)	108.8(2)	Ru(1)	Se(2)	C(23)	110.7(3)
C(22)	Se(2)	C(23)	95.8(3)	Ru(1)	Se(3)	C(24)	109.5(3)
Ru(1)	Se(3)	C(25)	108.9(2)	C(24)	Se(3)	C(25)	97.8(4)
Ru(1)	P(1)	C(1)	114.6(3)	Ru(1)	P(1)	C(7)	117.2(3)
Ru(1)	P(1)	C(13)	118.7(3)	C(1)	P(1)	C(7)	102.3(4)
C(1)	P(1)	C(13)	102.9(4)	C(7)	P(1)	C(13)	98.4(4)
P(1)	C(1)	C(2)	122.4(6)	P(1)	C(1)	C(6)	119.3(6)
P(1)	C(7)	C(8)	120.8(7)	P(1)	C(7)	C(12)	121.4(6)
P(1)	C(13)	C(14)	123.1(6)	P(1)	C(13)	C(18)	118.4(6)
Se(1)	C(20)	C(21)	121.2(6)	Se(3)	C(25)	C(21)	117.7(5)
Se(2)	C(22)	C(21)	121.5(6)				

As stated previously, these complexes were prepared in order to study the reaction chemistry of the $[Ru(L^3)]^{2+}$ fragment. Despite their obvious vulnerability to oxidation and dissociation of PPh_3, it was hoped that by replacement of the phosphine and chloride co-ligands with labile solvent molecules, such a $[Ru(L^3)]^{2+}$ system might be acquired. Unfortunately the reaction of $[RuCl_2(PPh_3)(L^3)]$ with 2 mol. equiv. of $Ag[CF_3SO_3]$ in refluxing MeCN led to the isolation of dark grey materials (which decomposed rapidly to black oily solids) that showed no selenium or tellurium isotope pattern in the electrospray mass spectra, hence indicating that the target complexes $[Ru(NCMe)_3(L^3)]^{2+}$ had not been obtained. Therefore, an alternative route was adopted.

6.23 Ruthenium(II) Dichloro-dmso Complexes

The sensitivity of the chloro-phosphine complexes was thought to be due to the presence of the phosphine ligand. Therefore, by using an alternative Ru(II) precursor these difficulties should be avoided. Similar work on complexes with $MeC(CH_2PPh_2)_3$ has shown that $[RuCl_2(dmso)_4]$ provides a convenient route into such chemistry, avoiding the use of phosphine co-ligands.[19]

Treatment of $[RuCl_2(dmso)_4]$ with 1 mol. equiv. of L^3 in toluene at 100 °C for 24 hours, affords the complexes $[RuCl_2(dmso)(L^3)]$. For the ligands $MeC(CH_2EMe)_3$ (E = Se or Te) the complexes are precipitated as orange (for $MeC(CH_2SeMe)_3$) or brown (for $MeC(CH_2TeMe)_3$) powders, which may be isolated by filtration and subsequent washing with diethyl ether. For $MeC(CH_2TePh)_3$ an orange solution is obtained and the complex is isolated *via* reduction of the solvent volume *in vacuo* to 5 cm^3 and addition of diethyl ether.

FAB mass spectrometry showed clusters of peaks with the correct *m/z* and isotope pattern for $[RuCl_2(dmso)\{MeC(CH_2EMe)_3\}]^+$ (E = Se or Te). However, for $[RuCl_2(dmso)\{MeC(CH_2TePh)_3\}]$ the molecular ion was not observed, but clusters of peaks were observed corresponding to $[RuCl\{MeC(CH_2TePh)_3\}]^+$. IR spectroscopy showed bands associated with the coordinated tripod, chloride (ν(Ru-Cl) at approximately 240 cm^{-1} *cf.* ν(Ru-Cl) for $[RuCl_2(CO)\{MeC(CH_2AsPh_2)_3\}]$ at 270 cm^{-1}) and dmso ligands (ν(SO) at approximately 1080 to 1090 cm^{-1}) indicative of S-bound dmso by comparison with similar complexes.[19] The ^1H NMR spectra were again complex due to the structural characteristics of these complexes. However, resonances associated with the tripod and dmso ligand were apparent and, in contrast to the previous dichloro-triphenylphosphine species, these complexes were found to be stable in solution. Elemental analysis confirmed the stoichiometry of these species.

Interestingly, for the reactions of $[RuCl_2(dmso)_4]$ with $MeC(CH_2EPh_2)_3$ (E = P or As) the chloro-bridge dimer $[Ru_2(\mu\text{-}Cl)_3\{MeC(CH_2EPh_2)_3\}_2]^+$ is obtained for E = P, although for E = As, $[RuCl_2(dmso)\{MeC(CH_2AsPPh_2)_3\}]$ is isolated.[19] However, spectroscopic information for the group 16 ligand complexes reported here confirms the preparation of the mononuclear species.

The $^{77}Se\{^1H\}$ or $^{125}Te\{^1H\}$ NMR spectra were also recorded. For the selenoether complex six resonances were observed (δ 168, 170, 218, 219, 229 and 244), with similar shifts to those observed for the dichloro- phosphine complex, showing the inequivalence of

the tripod donors (*trans*-dmso and *trans*-Cl) and the presence of both *syn* and *anti* invertomers. However since seven resonances are predicted for the presence of the three possible invertomers this indicates the coincidence of two of the *trans*-dmso signals. The $MeC(CH_2TeMe)_3$ complex was highly insoluble in non-coordinating solvents and hence the spectrum obtained was too weak to provide useful information. For the $MeC(CH_2TePh)_3$ complex three resonances were observed of similar intensity which may be assigned to the *anti* invertomer, in which the phenyl substituents on the tellurium atoms *trans* to Cl are pointing in opposite directions (Figure 6.3).

Figure 6.3. $^{125}Te\{^1H\}$ NMR spectrum (113.6 MHz, $CH_2Cl_2/CDCl_3$, 300K) of $[RuCl_2(dmso)\{MeC(CH_2TePh)_3\}]$.

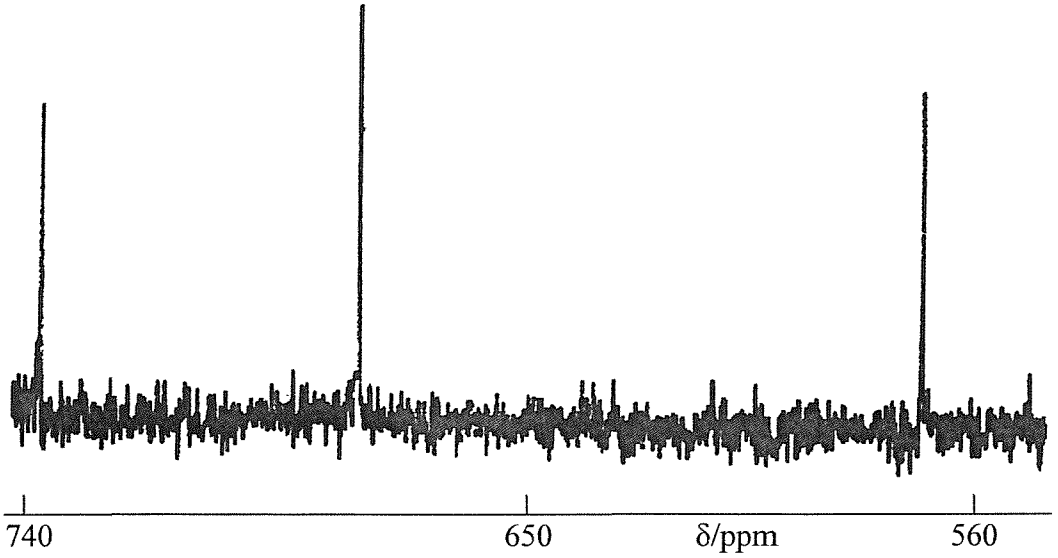

6.24 X-ray Crystal Structure of $[RuCl_2(dmso)\{MeC(CH_2SeMe)_3\}]$

Since we were interested in the further reaction chemistry of these systems, it was particularly important to establish their structure unambiguously. Crystals suitable for single crystal X-ray diffraction were grown of $[RuCl_2(dmso)\{MeC(CH_2SeMe)_3\}]$ *via* the slow evaporation of CH_2Cl_2 from a solution of the complex in $MeOH/CH_2Cl_2$. The structure (Figure 6.4, Tables 6.1, 6.4 - 6.5) shows the ruthenium coordinated to all three arms of the facial selenoether, with the methyl groups adopting the *syn* arrangement. The octahedral coordination sphere is completed by two chlorides and one dmso molecule, coordinated *via* the sulfur atom and thus consistent with the IR spectrum. Spectroscopic data for the complex

$[RuCl_2(dmso)\{MeC(CH_2AsPh_2)_3\}]$ also indicated sulfur bonding for the dmso molecule, although the crystal structure was not reported.[19] The *d*(Ru-Se) = 2.455(2), 2.417(2) and 2.466(2) Å and *d*(Ru-Cl) = 2.441(4) and 2.448(4) Å are comparable to those in $[RuCl_2(PPh_3)\{MeC(CH_2SeMe)_3\}]$ and $[Ru\{MeC(CH_2SeMe)_3\}_2]^{2+}$ (Chapter 4) with *d*(Ru-S) = 2.336 Å.

Figure 6.4. X-ray crystal structure of $[RuCl_2(dmso)\{MeC(CH_2SeMe)_3\}]$ with numbering scheme adopted. Ellipsoids are drawn at 40 % probability and H-atoms omitted for clarity.

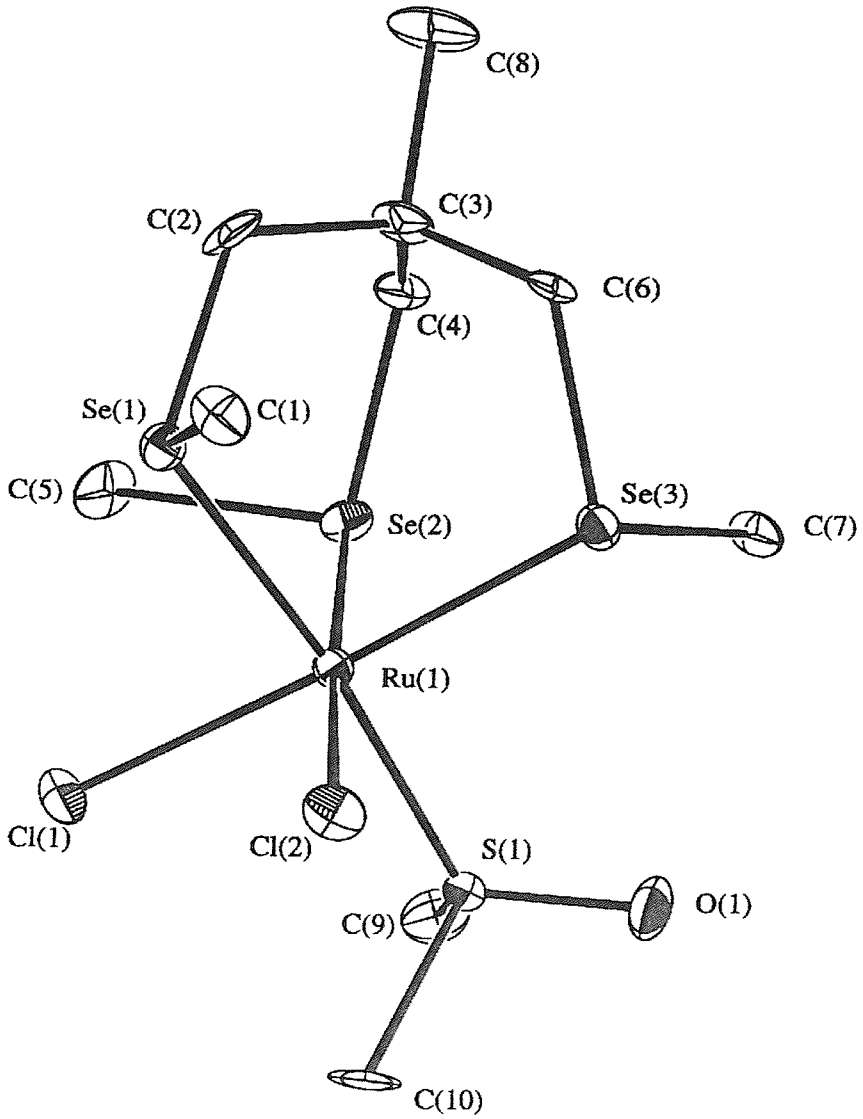

Table 6.4. Selected bond lengths for $[RuCl_2(dmso)\{MeC(CH_2SeMe)_3\}]$.

Atom	Atom	Distance/Å	Atom	Atom	Distance/Å
Ru(1)	Se(1)	2.455(2)	Ru(1)	Se(2)	2.417(2)
Ru(1)	Se(3)	2.466(2)	Ru(1)	Cl(1)	2.441(4)
Ru(1)	Cl(2)	2.448(4)	Ru(1)	S(1)	2.258(4)
Se(1)	C(1)	1.94(2)	Se(1)	C(2)	1.93(2)
Se(2)	C(4)	1.95(1)	Se(2)	C(5)	2.02(2)
Se(3)	C(6)	1.98(1)	Se(3)	C(7)	1.91(1)
S(1)	O(1)	1.49(1)	S(1)	C(9)	1.83(2)
S(1)	C(10)	1.80(2)	C(2)	C(3)	1.52(2)

Table 6.5. Selected bond angles for $[RuCl_2(dmso)\{MeC(CH_2SeMe)_3\}]$.

Atom	Atom	Atom	Angle(°)	Atom	Atom	Atom	Angle(°)
Se(1)	Ru(1)	Se(2)	91.29(6)	Se(1)	Ru(1)	Se(3)	91.75(8)
Se(1)	Ru(1)	Cl(1)	85.7(1)	Se(1)	Ru(1)	Cl(2)	89.4(1)
Se(1)	Ru(1)	S(1)	173.2(1)	Se(2)	Ru(1)	Se(3)	87.49(6)
Se(2)	Ru(1)	Cl(1)	92.77(10)	Se(2)	Ru(1)	Cl(2)	177.1(1)
Se(2)	Ru(1)	S(1)	92.6(1)	Se(3)	Ru(1)	Cl(1)	177.5(1)
Se(3)	Ru(1)	Cl(2)	89.7(1)	Se(3)	Ru(1)	S(1)	94.0(1)
Cl(1)	Ru(1)	Cl(2)	90.1(1)	Cl(1)	Ru(1)	S(1)	88.5(1)
Cl(2)	Ru(1)	S(1)	87.0(1)	Ru(1)	Se(1)	C(1)	111.2(5)
Ru(1)	Se(1)	C(2)	111.0(4)	C(1)	Se(1)	C(2)	98.3(7)
Ru(1)	Se(2)	C(4)	108.5(5)	Ru(1)	Se(2)	C(5)	105.8(5)
C(4)	Se(2)	C(5)	98.6(7)	Ru(1)	Se(3)	C(6)	106.3(5)
Ru(1)	Se(3)	C(7)	109.0(5)	C(6)	Se(3)	C(7)	96.4(7)
Ru(1)	S(1)	O(1)	117.5(5)	Ru(1)	S(1)	C(9)	113.7(6)
Ru(1)	S(1)	C(10)	110.9(6)	O(1)	S(1)	C(9)	107.0(8)
O(1)	S(1)	C(10)	107.1(8)	C(9)	S(1)	C(10)	98.7(8)
Se(1)	C(2)	C(3)	116.8(10)	Se(2)	C(4)	C(3)	121(1)
Se(3)	C(6)	C(3)	119(1)				

6.25 Ruthenium(II) Tris(acetonitrile) Complexes

The availability of labile or vacant sites in metal coordination spheres have long been recognised as essential features of reactive complexes. Such complexes may be obtained by the use of bulky ligands to give coordinatively unsaturated species[20] such as $[Pd(PCy_3)_2]$[21] (Cy = cyclohexyl) where four coordination is generally preferred, or by the use of potentially labile ligands such as phosphines, e.g. $[RhCl(PPh_3)_3]$[22] or solvent molecules.[23]

Soon after its synthesis was reported, the complex $[Ru(NCMe)_3\{MeC(CH_2PPh_2)_3\}]^{2+}$ was shown to yield the soluble complex $[RuH(BH_4)\{MeC(CH_2PPh_2)_3\}]$, upon reaction with $NaBH_4$,[24] which facilitates the cleavage of the C-S bond in benzo[*b*]thiophene to give 2-ethylthiophenolate, without the cooperation of either a multimetallic structure or externally added reagents.[7] We were therefore interested in obtaining the analogous tris(acetonitrile) complexes of the group 16 tripod ligands.

Reaction of $[RuCl_2(dmso)\{MeC(CH_2ER)_3\}]$ (E = Se, R = Me; E = Te, R = Ph) with 2 mol. equiv. of $Ag[CF_3SO_3]$ in refluxing MeCN for 2 hours afforded a light yellow solution and white precipitate. After removal of the AgCl through filtration, reduction of the solvent volume *in vacuo* and addition of diethyl ether, the complexes $[Ru(NCMe)_3\{MeC(CH_2ER)_3\}][CF_3SO_3]_2$ were obtained in good yield as yellow (selenoether) or orange (telluroether) solids. Unfortunately the analogous $MeC(CH_2TeMe)_3$ complex could not be isolated despite numerous attempts, including the use of $TlPF_6$ instead of $Ag[CF_3SO_3]$. The reasons for this are unclear but are perhaps due to facile dealkylation occurring.

The characterisation of these complexes was more straightforward due to the increased symmetry compared to the previous species. The ES^+ mass spectra showed clusters of peaks with the correct isotopic distribution corresponding to the doubly charged species $[Ru(NCMe)_3\{MeC(CH_2ER)_3\}]^{2+}$ and $[Ru(NCMe)_2\{MeC(CH_2ER)_3\}]^{2+}$. IR spectroscopy displayed peaks assigned to the tripod ligand and $CF_3SO_3^-$ anion, along with weak bands associated with coordinated MeCN (ν(CN) = 2310 cm^{-1}), with elemental analysis showing a good match with the calculated values.

^1H NMR spectroscopy showed signals assigned to the tripod ligand adopting the *syn* arrangement with a further resonance at δ 2.29 (telluroether) or δ 2.42 (selenoether) assigned to the coordinated MeCN molecules. This shift is comparable with that for the $MeC(CH_2PPh_2)_3$ complex where $\delta(CH_3CN)$ = 2.34. The $^{77}Se\{^1H\}$ and $^{125}Te\{^1H\}$ NMR

spectra (Figure 6.5) showed just one resonance again indicating the presence of just the *syn* invertomer, since fast inversion is unlikely with the weak *trans* donor MeCN. Both signals are to low frequency of the corresponding chloro-dmso species, consistent with the substitution of the electronegative chloride ligands with acetonitrile ligands, they are however to high frequency of the respective Ru(II) homoleptic seleno- and telluroether complexes discussed in Chapter 4.

Figure 6.5. $^{125}Te\{^{1}H\}$ NMR spectrum (113.6 MHz, MeCN/$CDCl_3$, 300K) of $[Ru(NCMe)_3\{MeC(CH_2TePh)_3\}][CF_3SO_3]_2$.

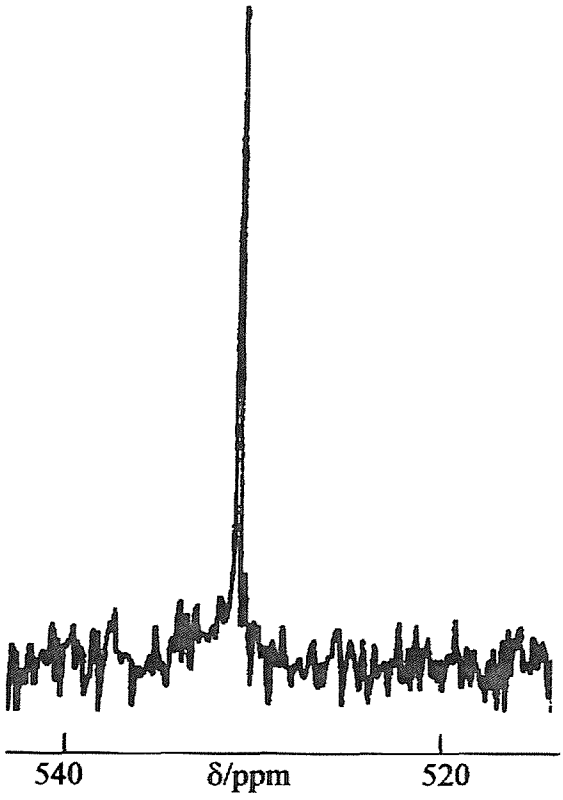

The reaction of $[RuCl_2(dmso)\{MeC(CH_2SeMe)_3\}]$ with two molar equivalents of $Ag[CF_3SO_3]$ in acetone was also studied, with the aim of preparing the tris(acetone) derivative $[Ru(OCMe_2)_3\{MeC(CH_2SeMe)_3\}]^{2+}$. The product obtained was found to be extremely unstable upon isolation, although the mass spectrum was recorded confirming its identity, with rapid oxidation to Ru(III) species occurring. However, this intermediate may be of use since it is stable in solution under N_2.

6.26 Reaction Chemistry of the Ruthenium(II) Tris(acetonitrile) Complexes

The principle aim of this research was to obtain a reactive $[Ru(L^3)]^{2+}$ fragment upon which further chemistry could be conducted. Therefore, we wished to confirm that the acetonitrile ligands could be substituted easily by other ligands, obviously a prerequisite if these complexes were to be able to carry out reaction chemistry.

Addition of one mol. equiv. of $MeC(CH_2SMe)_3$ to $[Ru(NCMe)_3\{MeC(CH_2SeMe)_3\}][CF_3SO_3]_2$ in methanol and subsequent reflux for 18 hours led to the isolation of the complex $[Ru\{MeC(CH_2SMe)_3\}\{MeC(CH_2SeMe)_3\}][CF_3SO_3]_2$, after reduction of the solvent volume *in vacuo* and addition of diethyl ether, as a light yellow solid in high yield. The complex $[Ru\{MeC(CH_2TePh)_3\}\{MeC(CH_2SeMe)_3\}][CF_3SO_3]_2$ was obtained similarly *via* the reaction of $[Ru(NCMe)_3\{MeC(CH_2TePh)_3\}][CF_3SO_3]_2$ with 1 mol. equiv. of $MeC(CH_2SeMe)_3$.

IR spectroscopy displayed peaks associated with the coordinated tripodal ligands and $CF_3SO_3^-$ anion, with the electrospray mass spectra showing clusters of peaks corresponding to the doubly charged cation. Elemental analysis showed a good match with the expected values.

The ^1H NMR spectra were complex due to the number of overlapping signals, however resonances associated with both ligands in the complex could be identified in each case. The $^{77}Se\{^1H\}$ and $^{125}Te\{^1H\}$ NMR spectra showed one resonance corresponding to the *syn* invertomer. For the thio- selenoether complex $\delta(^{77}Se\{^1H\}) = 123$ (Figure 6.6), a similar shift to the homoleptic complex $[Ru\{MeC(CH_2SeMe)_3\}_2]^{2+}$ discussed in Chapter 4. The seleno-telluroether complex shows $\delta(^{77}Se\{^1H\}) = 128$ and $\delta(^{125}Te\{^1H\}) = 485$, both shifts are consistent with those observed for the respective homoleptic Se_6 or Te_6 donor species reported in Chapter 4.

Crystals suitable for X-ray crystal diffraction were grown of $[Ru\{MeC(CH_2SMe)_3\}\{MeC(CH_2SeMe)_3\}][CF_3SO_3]_2$ *via* the vapour diffusion of diethyl ether into a solution of the complex in $MeNO_2$. Unfortunately, the complex crystallised in a centrosymmetric space group ($P\bar{1}$) with a half cation in the asymmetric unit, indicating that the structure was disordered and hence useful bond lengths could not be obtained.

Figure 6.6. $^{77}Se\{^{1}H\}$ NMR spectrum (68.7 MHz, $MeNO_2/CDCl_3$, 300K) of $[Ru\{MeC(CH_2SMe)_3\}\{MeC(CH_2SeMe)_3\}][CF_3SO_3]_2$.

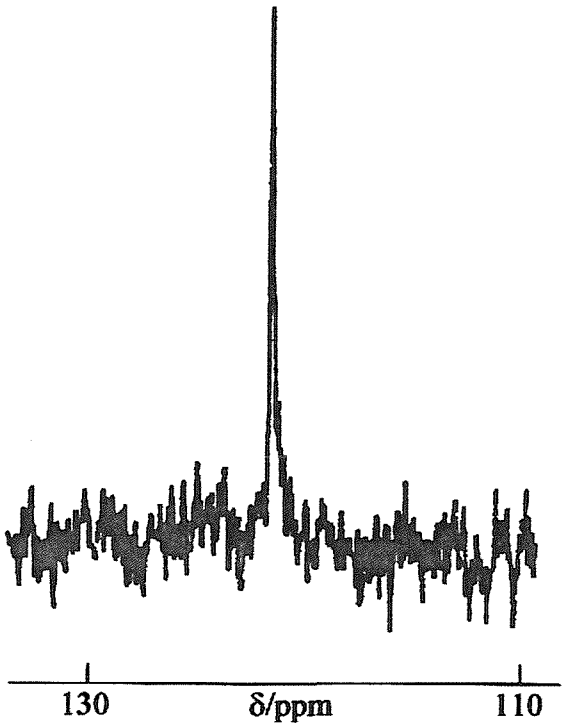

Having established the lability of the acetonitrile ligands and hence the availability of the $[Ru(L^3)]^{2+}$ fragment, we were interested to study the reaction of these species with $NaBH_4$ in the expectation of generating hydride species, so important for hydrogenation and hydrodesulfurisation catalysis. As stated previously, reaction of $[Ru(NCMe)_3\{MeC(CH_2PPh_2)_3\}]^{2+}$ with $NaBH_4$ gave the ruthenium(II) (tetrahydroborate)hydride complex, $[\{MeC(CH_2PPh_2)_3\}RuH(BH_4)]$.[24] Therefore, in order to study the reactivity of the group 16 donor complexes a similar reaction was undertaken.

Initially excess solid $NaBH_4$ was added slowly to a solution of $[Ru(NCMe)_3\{MeC(CH_2ER)_3\}][CF_3SO_3]_2$ (E = Se, R = Me; E = Te, R = Ph) in dry ethanol at room temperature. A gas was evolved immediately along with the precipitation of a black solid, which was filtered off. Attempts to identify this product were unsuccessful, with the mass spectrum and ^{1}H NMR spectrum showing no peaks that could be assigned to a tripod-containing product. It is likely that this product is ruthenium metal, obtained *via* the reduction of Ru(II) by $NaBH_4$ and dissociation of the ligands. This is obviously in contrast to the

chemistry observed with $MeC(CH_2PPh_2)_3$ and is probably as a result of the poorer σ-donor/π-acceptor ligand properties of the group 16 tripods compared to phosphine ligands, making ligand dissociation and liberation of ruthenium more probable.

In order to ascertain whether the products could be stabilised at low temperature, this reaction was repeated by slowly adding the $NaBH_4$ to a slurry of $[Ru(NCMe)_3\{MeC(CH_2ER)_3\}][CF_3SO_3]_2$ in ethanol at -78°C. No reaction was observed, probably due to the insolubility of the reactants in ethanol at this temperature, therefore the mixture was allowed to warm slowly. However, as soon as the reactants began to dissolve, a black precipitate was again observed, indicating decomposition to ruthenium metal.

This rather disappointing result does not necessarily exclude these complexes as potential catalysts, since the coordination of the substrate may well stabilise the Ru(II) centre and assist in keeping the tripodal ligand bound. It does however illustrate the differences between the coordination abilities of phosphine and group 16 donor ligands.

6.27 Electrochemistry

Cyclic voltammetry was used to investigate the electrochemistry of the complexes reported in this Chapter over the range - 0.75 V to + 1.0 V in CH_2Cl_2 solution at room temperature under an atmosphere of N_2. The Ru(II)/Ru(III) oxidation couple was of particular interest due to observation of the facile oxidation of the $[RuCl_2(PPh_3)(L^3)]$ complexes. The telluroether complexes of $[RuCl_2(dmso)(L^3)]$ and $[RuCl_2(PPh_3)(L^3)]$ generally showed just broad ill defined oxidation processes, which shifted potential upon varying scan-rate. However, for the selenoether derivatives quasi-reversible oxidations were observed at - 0.2 V for $[RuCl_2(dmso)\{MeC(CH_2SeMe)_3\}]$ and -0.1 V (*vs.* $Fc\text{-}Fc^+$ at 0.43 V) for $[RuCl_2(PPh_3)\{MeC(CH_2SeMe)_3\}]$. These potentials are similar to those obtained for the complexes *trans*-$[Ru\{PhSe(CH_2)_2SePh\}_2Cl_2]$ ($E_{1/2}$ = 0.16 V *vs.* $Fc\text{-}Fc^+$)[18] and *trans*-$[RuCl_2([16]aneSe_4)]$ ($E_{1/2}$ = 0.0 V *vs.* $Fc\text{-}Fc^+$).[16] The observation of ill defined potentials for the telluroether complexes is consistent with electrochemical studies on $[Ru(L\text{-}L)_2X_2]$ (L-L = ditelluroether, X = Cl, Br or I) complexes.[15]

6.3 Conclusions

The preparation of the complexes $[RuCl_2(PPh_3)(L^3)]$ (L^3 = $MeC(CH_2SeMe)_3$, $MeC(CH_2TeMe)_3$ and $MeC(CH_2TePh)_3$) has led to the observation of some unexpected chemistry. Although the selenoether complex is relatively stable, the instability of the telluroether complexes in solution, through facile oxidation of the metal centre and triphenylphosphine ligand has hindered the characterisation of these species, and their use in preparing $[Ru(L^3)]^{2+}$ fragments with labile solvent molecules occupying the remaining coordination sites. However, an alternative route into this chemistry has been devised through the preparation of the complexes $[RuCl_2(dmso)(L^3)]$ which are stable in solution. Reaction of these complexes with $Ag[CF_3SO_3]$ in refluxing MeCN has given the target species $[Ru(NCMe)_3\{MeC(CH_2ER)_3\}]^{2+}$ (E = Se, R = Me; E = Te, R = Ph) with the lability of the acetonitrile ligands being established *via* the preparation of the mixed-tripod Ru(II) complexes $[Ru\{MeC(CH_2SMe)_3\}\{MeC(CH_2SeMe)_3\}]^{2+}$ and $[Ru\{MeC(CH_2SeMe)_3\}\{MeC(CH_2TePh)_3\}]^{2+}$. The reaction of the tris(acetonitrile) complexes with $NaBH_4$ to give a hydride derivative, has instead led to decomposition of the complexes, with precipitation of ruthenium metal, even at low temperature.

Electrochemical studies have shown that the complexes $[RuCl_2(dmso)\{MeC(CH_2SeMe)_3\}]$ and $[RuCl_2(PPh_3)\{MeC(CH_2SeMe)_3\}]$ undergo quasi-reversible oxidations at low potentials.

6.4 Experimental

The complexes $[RuCl_2(PPh_3)_3]$[25] and $[RuCl_2(dmso)_4]$[26] were prepared *via* the literature procedures, as were the ligands $MeC(CH_2SMe)_3$,[27] $MeC(CH_2SeMe)_3$[28] and $MeC(CH_2TeMe)_3$.[29] Improved syntheses for the thio- and selenoether ligands are detailed in Chapter 7, along with the synthesis of $MeC(CH_2TePh)_3$.

$[RuCl_2(PPh_3)\{MeC(CH_2SeMe)_3\}]$. $[RuCl_2(PPh_3)_3]$ (208 mg, 2.2 x 10^{-4} mol) was added to $MeC(CH_2SeMe)_3$ (77 mg, 2.2 x 10^{-4} mol) in dry CH_2Cl_2 (40 cm^3) and the reaction stirred at room temperature for 18 hours to give an orange solution. This was reduced to *ca.* 2 cm^3 *in vacuo* and diethyl ether (10 cm^3) added to precipitate an orange solid. Yield 113 mg, 66 %. Analysis: Calculated for $C_{26}H_{33}Cl_2PRuSe_3$: %C, 39.8; %H, 4.2. Found: %C, 39.9; %H, 4.4. ^1H NMR ($CDCl_3$, 300 K): δ 1.37 (s, 1H, CCH_3), 1.6 - 2.0 (m, 3H, $SeCH_3$), 2.3 - 2.6 (m, 2H, $SeCH_2$), 7.2 - 8.2 (m, 5H, Ph). $^{77}Se\{^1H\}$ NMR (CH_2Cl_2/MeOH/$CDCl_3$, 300 K): δ 165, 168, 171, 245, 247, 272, 275. $^{31}P\{^1H\}$ NMR (CH_2Cl_2/MeOH/$CDCl_3$, 300 K): δ 35.2, 34.4. ES^+ (MeCN), *m/z* = 792, 751; calc. for $[^{102}Ru^{35}Cl(PPh_3)\{MeC(CH_2{}^{80}SeMe)_3\}(NCMe)]^+$ 794, $[^{102}Ru^{35}Cl(PPh_3)\{MeC(CH_2{}^{80}SeMe)_3\}]^+$ 753. IR/cm^{-1} 3050(w), 2962(w), 2940(w), 1481(m), 1433(m), 1358(s), 1090(s), 989(m), 907(w), 834(m), 746(m), 697(s), 614(w), 523(s), 499(m), 459(m), 422(m), 290(m), 216(m).

$[RuCl_2(PPh_3)\{MeC(CH_2TeMe)_3\}]$ was prepared similarly to give a light brown solid (61 %). Analysis: Calculated for $C_{26}H_{33}Cl_2PRuTe_3.CH_2Cl_2$: %C, 31.9; %H, 3.3. Found: %C, 31.9; %H, 3.5. ^1H NMR ($CDCl_3$, 300 K): see text. $^{125}Te\{^1H\}$ NMR (CH_2Cl_2/MeOH/$CDCl_3$, 300 K): δ 336, 340. $^{31}P\{^1H\}$ NMR (CH_2Cl_2/MeOH/$CDCl_3$, 300 K): δ 26.7. ES^+ (MeCN), *m/z* = 938, 897; calc. for $[^{102}Ru^{35}Cl(PPh_3)\{MeC(CH_2{}^{130}TeMe)_3\}(NCMe)]^+$ 944, $[^{102}Ru^{35}Cl(PPh_3)\{MeC(CH_2{}^{130}TeMe)_3\}]^+$ 903. IR/cm^{-1} 3051(w), 2922(w), 1481(m), 1432(s), 1360(s), 1267(w), 1217(w), 1190(w), 1090(s), 998(m), 835(s), 744(s), 697(s), 614(w), 526(s), 459(w), 309(m), 223(m).

$[RuCl_2(PPh_3)\{MeC(CH_2TePh)_3\}]$ was prepared similarly to give an orange solid (72 %). Analysis: Calculated for $C_{41}H_{39}Cl_2PRuTe_3$: %C, 44.1; %H, 3.5. Found: %C, 39.7; %H, 3.1. ^1H NMR ($CDCl_3$, 300 K): see text. $^{125}Te\{^1H\}$ NMR (CH_2Cl_2/MeOH/$CDCl_3$, 300 K): δ 566, 570, 741, 742, 770. $^{31}P\{^1H\}$ NMR (CH_2Cl_2/MeOH/$CDCl_3$, 300 K): δ 25.6. ES^+ (MeCN), *m/z*

= 1122, 1081; calc. for $[^{102}Ru^{35}Cl(PPh_3)\{MeC(CH_2{}^{130}TePh)_3\}(NCMe)]^+$ 1130, $[^{102}Ru^{35}Cl(PPh_3)\{MeC(CH_2{}^{130}TePh)_3\}]^+$ 1089. IR/cm^{-1} 3052(w), 1571(m), 1476(m), 1432(s), 1358(s), 1263(w), 1187(w), 1090(s), 1017(m), 998(m), 834(w), 797(w), 735(s), 694(s), 524(s), 456(m), 250(m).

$[RuCl_2(dmso)\{MeC(CH_2SeMe)_3\}]$. $[RuCl_2(dmso)_4]$ (40 mg, 8.3 x 10^{-5} mol) was added to dry toluene (40 cm^3) and heated to 100°C for 10 minutes. The resulting suspension was allowed to cool, and $MeC(CH_2SeMe)_3$ (29 mg, 8.3 x 10^{-5} mol) in toluene (5 cm^3) added and the mixture heated to 100°C for 24 hours. The resulting precipitate was filtered, washed with diethyl ether (10 cm^3) to give an orange solid. Yield 30 mg, 60 %. Analysis: Calculated for $C_{10}H_{24}Cl_2ORuSSe_3$: %C, 20.0; %H, 4.0. Found: %C, 20.3; %H, 3.8. ^{1}H NMR ($CDCl_3$, 300 K): δ 1.34 (s, 1H, CCH_3), 2.1 - 2.6 (m, 3H, $SeCH_3$), 2.61 (s, 2H, CH_3S), 3.35 - 3.51 (m, 2H, $SeCH_2$). ^{77}Se{^{1}H} NMR (CH_2Cl_2/$CDCl_3$, 300 K): δ 168, 170, 218, 219, 229, 244. FAB MS (3-NOBA), *m/z* = 601, 567, 523; calc. for $[^{102}Ru^{35}Cl_2(dmso)\{MeC(CH_2{}^{80}SeMe)_3\}]^+$ 604, $[^{102}Ru^{35}Cl(dmso)\{MeC(CH_2{}^{80}SeMe)_3\}]^+$ 569, $[^{102}Ru^{35}Cl_2\{MeC(CH_2{}^{80}SeMe)_3\}]^+$ 526. IR/cm^{-1} 2950(w), 1413(m), 1358(s), 1262(m), 1076(s), 1017(m), 924(w), 834(w), 802(w), 713(w), 678(w), 614(w), 540(w), 427(m), 238(m).

$[RuCl_2(dmso)\{MeC(CH_2TeMe)_3\}]$ was prepared similarly to give a brown solid (61 %). Analysis: Calculated for $C_{10}H_{24}Cl_2ORuSTe_3$: %C, 16.1; %H, 3.2. Found: %C, 16.5; %H, 3.5. ^{1}H NMR ($CDCl_3$, 300 K): δ 1.26 (s, 1H, CCH_3), 2.1 - 2.4 (m, 3H, $TeCH_3$), 2.63 (s, 2H, CH_3S), 3.40 - 3.55 (m, 2H, $TeCH_2$). ^{130}Te{^{1}H} NMR (CH_2Cl_2/$CDCl_3$, 300 K): see text. FAB MS (3-NOBA), *m/z* = 748; calc. for $[^{102}Ru^{35}Cl_2(dmso)\{MeC(CH_2{}^{130}TeMe)_3\}]^+$ 754. IR/cm^{-1} 2925(w), 1359(s), 1095(s), 1018(m), 996(m), 835(m), 682(w), 613(w), 536(w), 425(w), 236(m).

$[RuCl_2(dmso)\{MeC(CH_2TePh)_3\}]$ was prepared similarly except an orange solution was produced upon heating for 24 hours. The solvent volume was reduced *in vacuo* to 5 cm^3 and diethyl ether added to give an orange solid (69 %). Analysis: Calculated for $C_{25}H_{30}Cl_2ORuSTe_3$: %C, 32.2; %H, 3.2. Found: %C, 31.8; %H, 3.3. ^{1}H NMR ($CDCl_3$, 300 K): δ 1.26 (s, 1H, CCH_3), 2.57 (s, 2H, CH_3S), 3.10 - 3.50 (m, 2H, $TeCH_2$), 6.8 - 8.2 (m, 5H, TePh). ^{130}Te{^{1}H} NMR (CH_2Cl_2/$CDCl_3$, 300 K): δ 570, 677, 737. FAB MS (3-NOBA), *m/z* = 821; calc. for $[^{102}Ru^{35}Cl\{MeC(CH_2{}^{130}TePh)_3\}]^+$ 827. IR/cm^{-1} 3050(w), 2951(w), 1570(w),

1475(m), 1432(m), 1359(s), 1262(m), 1089(s), 1017(s), 998(s), 802(m), 740(m), 693(m), 612(w), 541(w), 455(w), 421(w), 253(m).

$[Ru(NCMe)_3\{MeC(CH_2SeMe)_3\}][CF_3SO_3]_2$. $[RuCl_2(dmso)\{MeC(CH_2SeMe)_3\}]$ (34 mg, 5.7 x 10^{-5} mol) was added to $Ag[CF_3SO_3]$ (29 mg, 1.1 x 10^{-4} mol) in MeCN (40 cm^3). The mixture was refluxed for 2 hours, cooled and filtered to remove the precipitated AgCl. The solvent volume was reduced *in vacuo* to 2 cm^3 and diethyl ether added to give a light yellow solid. Yield 40 mg, 80 %. Analysis: Calculated for $C_{16}H_{27}F_6N_3O_6RuS_2Se_3$: %C, 22.0; %H, 3.1; %N, 4.8. Found: %C, 21.9; %H, 3.2; %N, 4.8. ^1H NMR ($(CD_3)_2CO$, 300 K): δ 1.47 (s, 1H, CCH_3), 2.42 (s, 3H, $NCCH_3$), 2.51 (s, 3H, $SeCH_3$), 2.85 (m, 2H, $SeCH_2$). $^{77}Se\{^1H\}$ NMR ($MeCN/CDCl_3$, 300 K): δ 159. ES^+ (MeCN), *m/z* = 288, 267; calc. for $[^{102}Ru(NCMe)_3\{MeC(CH_2{}^{80}SeMe)_3\}]^{2+}$ 290, $[^{102}Ru(NCMe)_2\{MeC(CH_2{}^{80}SeMe)_3\}]^{2+}$ 269. IR/cm^{-1} 2312(w), 1360(s), 1263(s), 1225(m), 1150(m), 1098(m), 1032(m), 991(w), 836(w), 638(s), 518(w).

$[Ru(NCMe)_3\{MeC(CH_2TePh)_3\}][CF_3SO_3]_2$ was prepared similarly to give an orange solid (53 %). Analysis: Calculated for $C_{31}H_{33}F_6N_3O_6RuS_2Te_3$: %C, 30.9; %H, 2.7; %N, 3.5. Found: %C, 30.5; %H, 2.4, %N, 3.3. ^1H NMR ($(CD_3)_2CO$, 300 K): δ 1.91 (s, 1H, CCH_3), 2.29 (s, 3H, $NCCH_3$), 2.90 (s, 2H, $TeCH_2$), 7.5 - 7.8 (m, 5H, TePh). $^{125}Te\{^1H\}$ NMR ($MeCN/CDCl_3$, 300 K): δ 531. ES^+ (MeCN), *m/z* = 453, 432, 414; calc. for $[^{102}Ru(NCMe)_3\{MeC(CH_2{}^{130}TePh)_3\}]^{2+}$ 458, $[^{102}Ru(NCMe)_2\{MeC(CH_2{}^{130}TePh)_3\}]^{2+}$ 437, $[^{102}Ru(NCMe)\{MeC(CH_2{}^{130}TePh)_3\}]^{2+}$ 417. IR/cm^{-1} 2315(w), 1478(w), 1435(w), 1358(m), 1276(s), 1154(s), 1093(m), 1032(s), 998(m), 834(w), 745(m), 693(m), 638(s), 574(w), 518(m), 458(w).

$[Ru\{MeC(CH_2SMe)_3\}\{MeC(CH_2SeMe)_3\}][CF_3SO_3]_2$. $MeC(CH_2SMe)_3$ (17 mg, 7.9 x 10^{-5} mol) was added to $[Ru(NCMe)_3\{MeC(CH_2SeMe)_3\}][CF_3SO_3]_2$ (69 mg, 7.9 x 10^{-5} mol) in MeOH (30 cm^3) and the reaction mixture refluxed for 18 hours. After cooling the solvent volume was reduced *in vacuo* to 5 cm^3 and diethyl ether added to precipitate a light yellow solid. Yield 60 mg, 79 %. Analysis: Calculated for $C_{18}H_{36}F_6O_6RuS_5Se_3$: %C, 22.5; %H, 3.8. Found: %C, 22.5; %H, 3.5. ^1H NMR ($(CD_3)_2CO$, 300 K): δ 1.26 (s, 1H, $CH_3C(CH_2SCH_3)_3$), 1.38 (s, 1H, $CH_3C(CH_2SeCH_3)_3$), 2.34 (s, 3H, $SeCH_3$), 2.52 (s, 3H, SCH_3), 2.7-2.9 (m, 4H, $SeCH_2$, SCH_2). $^{77}Se\{^1H\}$ NMR ($MeNO_2/CDCl_3$, 300 K): δ 123. ES^+ (MeCN), *m/z* = 811,

331; calc. for $([^{102}Ru\{MeC(CH_2SMe)_3\}\{MeC(CH_2{}^{80}SeMe)_3\}][CF_3SO_3])^+$ 815, $[^{102}Ru\{MeC(CH_2SMe)_3\}\{MeC(CH_2{}^{80}SeMe)_3\}]^{2+}$ 333. IR/cm^{-1} 2940(w), 1461(w), 1420(m), 1358(m), 1262(s), 1227(m), 1166(m), 1096(m), 1032(s), 976(w), 639(s), 518(m).

$[Ru\{MeC(CH_2TePh)_3\}\{MeC(CH_2SeMe)_3\}][CF_3SO_3]_2$ was similarly prepared *via* the reaction of $[Ru(NCMe)_3\{MeC(CH_2TePh)_3\}][CF_3SO_3]_2$ with $MeC(CH_2SeMe)_3$ (73 %). Analysis: Calculated for $C_{33}H_{42}F_6O_6RuS_2Se_3Te_3$: %C, 27.6; %H, 2.9. Found: %C, 27.4; %H, 2.8. ^{1}H NMR ($(CD_3)_2CO$, 300 K): δ 1.16 (s, 2H, C*H*$_3$), 2.06 (s, 3H, $SeCH_3$), 2.4-2.9 (m, 4H, $SeCH_2$, $TeCH_2$), 7.5 - 8.0 (m, 5H, TePh). $^{77}Se\{^1H\}$ NMR ($MeNO_2/CDCl_3$, 300 K): δ 128. $^{125}Te\{^1H\}$ NMR ($MeNO_2/CDCl_3$, 300 K): δ 485. ES$^+$ (MeCN), *m/z* = 569; calc. for $[^{102}Ru\{MeC(CH_2{}^{130}TePh)_3\}\{MeC(CH_2{}^{80}SeMe)_3\}]^{2+}$ 573. IR/cm^{-1} 2929(w), 1572(w), 1476(w), 1433(w), 1358(s), 1262(s), 1224(m), 1156(m), 1096(m), 1030(s), 997(m), 910(w), 834(w), 738(m), 693(m), 638(s), 573(w), 518(m), 456(m).

X-ray Crystallographic Studies

$[RuCl_2(PPh_3)\{MeC(CH_2SeMe)_3\}]$ and $[RuCl_2(dmso)\{MeC(CH_2SeMe)_3\}]$. Details of the crystallographic data collection and refinement parameters are given in Table 6.1. The crystals were grown *via* the vapour diffusion of diethyl ether into a solution of $[RuCl_2(PPh_3)\{MeC(CH_2SeMe)_3\}]$ in CH_2Cl_2/MeOH and by the slow evaporation of CH_2Cl_2 from a solution of $[RuCl_2(dmso)\{MeC(CH_2SeMe)_3\}]$ in CH_2Cl_2/MeOH. Data collection used a Rigaku AFC7S four circle diffractometer operating at 150 K, using graphite-monochromated Mo-K_α X-radiation (λ = 0.71073 Å). No significant crystal decay or movement was observed. The structures were solved by heavy atom methods[30] and developed by iterative cycles of full-matrix least-squares refinement[31] and difference Fourier syntheses. All non-hydrogen atoms were refined anisotropically while H-atoms were placed in fixed, calculated positions with *d*(C-H) = 0.96 Å.

6.5 References

[1] M. Schröder and T. A. Stephenson, in *Comprehensive Coordination Chemistry*, G. Wilkinson, R. D. Gillard and J. A. McCleverty (eds.), Pergamon Press, Oxford, 1987, Vol. 4, pp. 279.

[2] H. A. Mayer and W. C. Kaska, *Chem. Rev.,* 1994, **94**, 1239.

[3] C. Bianchini, A. Meli, M. Peruzzini, F. Vizza and F. Zanobini, *Coord. Chem. Rev.* 1992, **120**, 193.

[4] C. Bianchini, P. Frediani, V. Herrera, M. V. Jiménez, A. Meli, L. Rincón, R. Sánchez-Delgado and F. Vizza, *J. Am. Chem. Soc.,* 1995, **117**, 4333.

[5] C. Bianchini, V. Herrera, A. Meli, S. Moneti, M. Peruzzi, R. Sánchez-Delgado and F. Vizza, *J. Am. Chem. Soc.,* 1994, **116**, 4370.

[6] C. Bianchini, M. V. Jiménez, A. Meli, S. Moneti, V. Patinec and F. Vizza, *Organometallics,* 1997, **16**, 5696.

[7] C. Bianchini, D. Masi, A. Meli, M. Peruzzini, F. Vizza and F. Zanobini, *Organometallics,* 1998, **17**, 2495.

[8] C. Bianchini, A. Meli, S. Moneti and F. Vizza, *Organometallics,* 1998, **17**, 2636.

[9] C. Bianchini, A. Meli, S. Moneti, W. Oberhauser, F. Vizza, V. Herrera, A. Fuentes and R. A. Sánchez-Delgado, *J. Am. Chem. Soc.,* 1999, **121**, 7071.

[10] M. N. Bell, A. J. Blake, H. -J. Küppers, M. Schröder and K. Wieghardt, *Angew. Chem. Int. Ed. Engl.,* 1987, **26**, 250.

[11] N. W. Alcock, J. C. Cannadine, G. R. Clark and A. F. Hill, *J. Chem. Soc., Dalton Trans.,* 1993, 1131.

[12] A. L. Hector and A. F. Hill, *Inorg. Chem.,* 1995, **34**, 3797.

[13] J. C. Cannadine, A. F. Hill, A. J. P. White, D. J. Williams and J. D. E. T. Wilton-Ely, *Organometallics,* 1996, **15**, 5409.

[14] N. R. Champness, W. Levason, S. R. Preece and M. Webster, *Polyhedron,* 1994, **13**, 881.

[15] W. Levason, S. D. Orchard, G. Reid and V. -A. Tolhurst, *J. Chem. Soc., Dalton Trans.,* 1999, 2071.

[16] W. Levason, J. J. Quirk, G. Reid and S. M. Smith, *J. Chem. Soc., Dalton Trans.,* 1997, 3719.

[17] B. A. Moyer, B. K. Sipe and T. J. Meyer, *Inorg. Chem.,* 1981, **20**, 1475.

[18] N. R. Champness, W. Levason, S. R. Preece and M. Webster, *Polyhedron*, 1994, **13**, 881.

[19] L. F. Rhodes, C. Sorato, L. M. Venanzi and F. Bachechi, *Inorg. Chem.,* 1988, **27**, 604.

[20] C. A. Tolman, *Chem. Rev.,* 1977, **77**, 313.

[21] A. Immirzi and A. Musco, *J. Chem. Soc., Chem. Commun.,* 1974, 400.

[22] J. A. Osborn, F. H. Jardine, J. F. Young and G. Wilkinson, *J. Chem. Soc., A*, 1966, 1711.

[23] J. R. Shapley, R. R. Schrock and J. A. Osborn, *J. Am. Chem. Soc.,* 1970, **92**, 6976.

[24] L. F. Rhodes and L. M. Venanzi, *Inorg. Chem.,* 1987, **26**, 2692.

[25] T. A. Stephenson and G. Wilkinson, *J. Inorg. Nucl. Chem.,* 1966, **28**, 945.

[26] I. P. Evans, A. Spencer and G. Wilkinson, *J. Chem. Soc., A,* 1973, 204.

[27] R. Ali, S. J. Higgins and W. Levason, *Inorg. Chim. Acta,* 1984, **84**, 65.

[28] D. J. Gulliver, E. G. Hope, W. Levason, G. L. Marshall, S. G. Murray and D. M. Potter, *J. Chem. Soc., Perkin Trans. II,* 1984, 429.

[29] E. G. Hope, T. Kemmitt and W. Levason, *Organometallics,* 1988, **7**, 78.

[30] PATTY, The DIRDIF Program System, P. T. Beurskens, G. Admiraal, G. Beurskens, W. P. Bosman, S. Garcia-Granda, R. O. Gould, J. M. M. Smits, C. Smykalla. Technical Report of the Crystallography Laboratory, University of Nijmegen, The Netherlands, 1992.

[31] TeXsan: Crystal Structure Analysis Package, Molecular Structure Corporation, Texas, 1995.

Chapter 7

Ligand Synthesis

7.1 Introduction

Despite organic tellurium compounds having a history dating back to 1840, it still remains a rather poorly understood area of modern chemistry. Much of the difficulty associated with this chemistry arises from the weakness of Te-H and Te-C bonds and was discussed in Chapter 1. Therefore, routes generally associated with the preparation of thio- and selenoether ligands can not be employed for telluroethers. Hence the analogous tellurium chemistry associated with thiols is almost unknown, and any reports of such isolated species should be treated with some caution. Similarly, the well-known reduction of RSeCN to RSe^- functions using $Na/NH_{3(l)}$ as a route to form a variety of multidentate and macrocyclic selenoether ligands is not successfully transferred into tellurium chemistry. The analogous tellurocyanates are generally extremely unstable and although systems such as $ArCH_2TeCN$ (Ar = 4-ClC_6H_4 and 4-$MeOC_6H_4$) are known, attempts to synthesise ditellurocyanates have failed.[1] Therefore the preparation of species such as $NaTe(CH_2)_3TeNa$ is far more challenging than first inspection would suggest. Indeed there are at least as many differences as similarities in the chemical behaviour of selenium and tellurium.

Further difficulties can also often arise from attempts to carry out further reaction chemistry with tellurium containing fragments since reaction at tellurium is frequently observed in preference to the required transformation. The sensitive nature of the isolated species should also not be underestimated since they are generally air and moisture sensitive, depositing tellurium upon exposure. Subsequently, purification of ligands is also surprisingly difficult if they may not be distilled *in vacuo* or recrystallised.

However, the preparation of new tellurium containing ligands is of great interest, as a consequence of the rich coordination chemistry these ligands possess and their enhanced σ-donor properties to low valent metal centres (Chapter 2) and therefore these synthetic difficulties need to be overcome. The preparation of tellurium containing macrocycles is of particular interest since these ligands will enable tellurium to be studied in a macrocyclic environment, and will lead to complexes with novel properties as a result of the enhanced kinetic and thermodynamic stability associated with the *Macrocyclic Effect*.[2] Such macrocyclic complexes may have applications in many diverse fields including:

- Catalysis: Electrochemical studies on thioether macrocyclic complexes have shown that unusual oxidation states may be accessed and stabilised that are not possible with their acyclic analogues. For example, the paramagnetic Pd(III) ion is stabilised in $[Pd([9]aneS_3)_2]^{3+}$.[3] The availability of these uncommon oxidation states suggests that such systems may well have potential in some electrocatalytic pathways. Recently the complex $[Rh(PPh_3)_2([9]aneS_3)][PF_6]$ has been shown to undergo ligand substitution and effectively catalyse the demercuration of bis(alkynyl)mercurials.[4]
- Biological Models: There is currently much interest in the role macrocyclic complexes play in nature since in many biological molecules the active metal centre is bound within a macrocyclic ring. Marcrocycles have been used to mimic the behaviour of certain biological systems such as Mo-nitrogenases, blue copper proteins and Ni-hydrogenases.[5, 6]
- Selectivity: Macrocycles, depending on their donor atoms and ring size are capable of extracting certain metal ions from a mixture. This is particularly true for the crown ethers and derivatives, where hard oxygen donors preferably bind group 1 and group 2 metals, for example [18]crown6 selectively binds K^+ over Na^+.[7]
- Tumour Imaging: The radiopharmaceutical industry has recently noted the potential for macrocycles as carriers for β and γ emitters such as ^{64}Cu. The strong coordinating ability of the macrocycle ensures that the metal centre remains complexed to the imaging agent.[8]

Unfortunately, the synthesis of macrocycles is generally more problematic than their corresponding acyclic derivatives. There are two major approaches that may be employed:

- High Dilution:- This technique involves the ring closure reaction being performed in conditions of high dilution in order that concentrations of the reagents in the vessel at any one time are very low. The disadvantages of this technique are that it may give low yields due to side reactions occurring, and usually leads to long reaction times which can cause difficulties when using air or moisture sensitive materials.
- Metal Template:- This technique requires the acyclic precursors to be coordinated to a metal centre, and hence in close proximity, favouring ring closure over polymerisation. The obvious disadvantage to this approach is that demetallation is then necessary to give the free macrocyclic ligand. Problems are also often encountered in identifying suitable metal templates since ion size is extremely

important. Sellmann and Zapf utilised this route in order to prepare [9]aneS_3 in high yield *via* the cyclisation of the open chain dithiolate, $^{-}S(CH_2)_2S(CH_2)_2S^{-}$, and 1,2-dibromoethane on the $Mo(CO)_3$ fragment.[9]

Just one homoleptic Te macrocycle, [12]aneTe_3, has been prepared, reflecting the synthetic difficulties in combining organo-tellurium and macrocyclic chemistry.[10]

There have been a few potentially useful intermediates reported such as $[o\text{-}C_6H_4Te_2]^{2-}$ prepared from the phenylenemercury hexamer[11] and $[1,2\text{-}C_5H_6Te_2]^{2-}$ which may be conveniently synthesised from 1,2-dibromocyclopentene, ^{t}BuLi and tellurium in THF.[12] These dianions, in theory, would allow for the preparation of new multidentate telluroether ligands.

This Chapter reports an investigation in the organic chemistry of tellurium, focusing on the preparation of new ligands. For convenience, it has been divided in to three sections. The first section will detail improved syntheses for the tripodal ligands $MeC(CH_2EMe)_3$ (E = S and Se) as well as the synthesis of the new ligand $MeC(CH_2TePh)_3$. The second section will report an investigation into the chemistry of dilithium 1,2-cyclopenteneditellurolate, an important potential precursor in the preparation of new ligands. Finally, the synthesis of new mixed donor thio-telluroether macrocycles will be discussed, along with the preparation of their Ag(I) complexes.

7.2 Results and Discussion

7.21 Synthesis of the Tripodal Ligands $MeC(CH_2EMe)_3$ (E = S or Se) and $MeC(CH_2TePh)_3$

The group 16 tripodal ligands $MeC(CH_2EMe)_3$ (E = S, Se and Te) have formed a major part of this research. Previous syntheses reported for the thio-[13] and selenoether[14] ligands have reported yields of 33 % and 27 % respectively, with the majority of the crude product being the mono- and di-substituted derivatives. Since the tribromo precursor, $MeC(CH_2Br)_3$, is time consuming to prepare, it was advantageous to maximise the yields of these ligands based on this reactant. This was achieved by using 6 molar equivalents of nucleophile, MeS^- or $MeSe^-$, and extending the reaction time to overnight reflux in dry ethanol or THF respectively. The tri-substituted ligand was the only product isolated in yields of 83 % (E = S) and 80 % (E = Se).

Despite the ligand $MeC(CH_2TeMe)_3$ being reported approximately 10 years ago,[15] the phenyl derivative is not known. Therefore, in order to investigate the properties of multidentate telluroethers further, a synthesis for this ligand was devised. The new tripodal ligand $MeC(CH_2TePh)_3$ was prepared *via* the addition of $MeC(CH_2Br)_3$ to 6 molar equivalents of PhTeLi in THF at -196 °C. The mixture was allowed to warm to room temperature, stirred for 18 hours, and refluxed for one hour to give a dark red solution. The mixture was worked up to give a dark red oil, the $^{125}Te\{^1H\}$ NMR spectrum of which gave two resonances at δ 385 and 417. The signal at δ 417 may be assigned to diphenyl ditelluride,[15] leading to an initial assignment of the second resonance to the product. Studies on RTeR' by O'Brien and co-workers have shown that the effects of R and R' are approximately additive and that stepwise deshielding of tellurium occurs with the replacement of the hydrogens in Me_2Te with other groups.[16] The $^{125}Te\{^1H\}$ for $MeC(CH_2TeMe)_3$ has been reported as δ 21,[15] and since the contribution to this shift of the methyl groups may be taken as 0 ppm, this shift may be attributed to the tripod backbone. A prediction for $MeC(CH_2TePh)_3$ therefore requires the contribution from Ph which may be taken to be 329 ppm (PhTeMe) or 342 ppm from Ph_2Te (685 ppm). Adding the contributions from the tripod backbone and an averaged Ph figure (336 ppm), the chemical shift for the ligand $MeC(CH_2TePh)_3$ may be predicted to be 357 ppm, and hence in good accord with the observed value considering the simplicity of this model.

In order to purify the product, the crude red oil was recrystallised twice from light petroleum ether to give a light orange solid, the $^{125}Te\{^1H\}$ NMR spectrum of which showed just one signal at δ 385, indicating that the diphenyl ditelluride had been removed. The ^1H and $^{13}C\{^1H\}$ NMR spectroscopic data are shown in Table 7.1, and confirmed the purity of the ligand, along with elemental analysis which showed a good match with the calculated values. The FAB mass spectrum also confirmed the required ligand had been prepared showing a cluster of peaks at *m/z* = 684 (calculated for $[MeC(CH_2{}^{130}TePh)_3]^+ = 690$).

Table 7.1. ^1H and $^{13}C\{^1H\}$ NMR ($CDCl_3$, 300 K) data for $MeC(CH_2TePh)_3$.

^1H NMR Data		$^{13}C\{^1H\}$ NMR Data	
1.20, s, 1H	CH_3	26.1 ($^1J_{Te\text{-}C}$ = 175 Hz)	$TeCH_2$
3.23, s, 2H	$TeCH_2$	28.7	CCH_3
7.1 - 7.7, m, 5H	*TePh*	39.7	CCH_3
		113	*ipso*-C
		139	*ortho*-C
		128, 129	*meta, para*-C

7.22 Investigation into the Chemistry of Cyclopentene 1,2-ditellurolate

The preparation of organic molecules containing two tellurolate functions is of great interest to this study. Such species would be convenient precursors for the preparation of multidentate and more importantly, macrocyclic telluroether ligands. However, such dianions, in contrast to thio- and selenoether chemistry, are synthetically challenging to prepare. This is as a result of a lack of compounds containing two tellurium atoms that may be exploited to synthesise such species, and also due to the weakness of Te-C bonds, leaving such anions prone to rapid decomposition *via* elimination of the carbon backbone and the formation of ditellurides. As discussed previously, routes such as the preparation of Te-H entities that are used extensively in the analogous thioether chemistry are not accessible, with attempts to prepare species such as RTeCN giving irreproducible results.

The bidentate telluroether ligands were prepared *via* the reaction of RTeLi with dibromoalkanes. An obvious extension of this chemistry would be the preparation, and subsequent reaction with tellurium, of dilithio- reagents. These species in themselves are not trivial to prepare but would allow, in theory for the preparation of ditellurolates. Two such

species have been reported in the literature, dilithium 1,2-benzeneditellurolate[11] and dilithium 1,2-cyclopenteneditellurolate although this chemistry has not been investigated in detail, with just the Pt(II) complexes $[Pt(Te_2C_5H_6)(PPh_3)_2]$ and $[Pt(Te_2C_6H_4)(PPh_3)_2]$ being reported (Figure 7.1)[17] along with their reaction with tetrachloroethene, as part of a study into designer organic metals, to give dibenzotetratellurafulvalene and hexamethylenetetratellurafulvalene (Figure 7.2).[18, 19]

Figure 7.1. Single crystal X-ray structure of $[Pt(Te_2C_6H_4)(PPh_3)_2]$.[17]

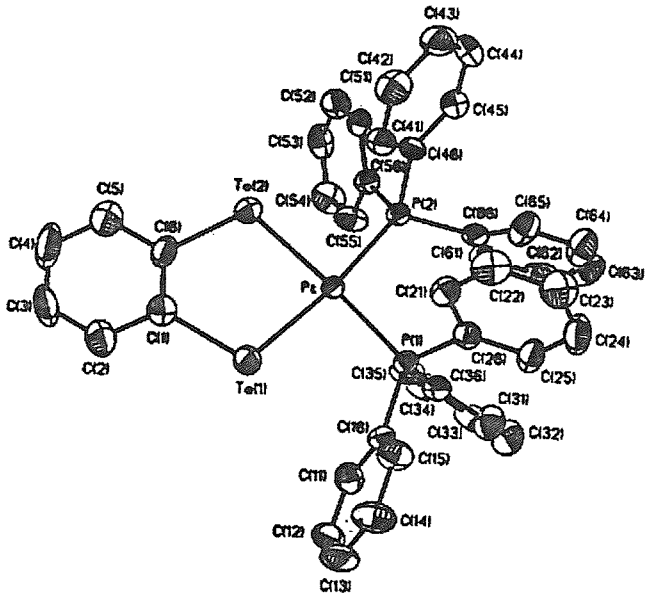

Figure 7.2. Single crystal X-ray structure of hexamethylenetetratellurafulvalene.[18]

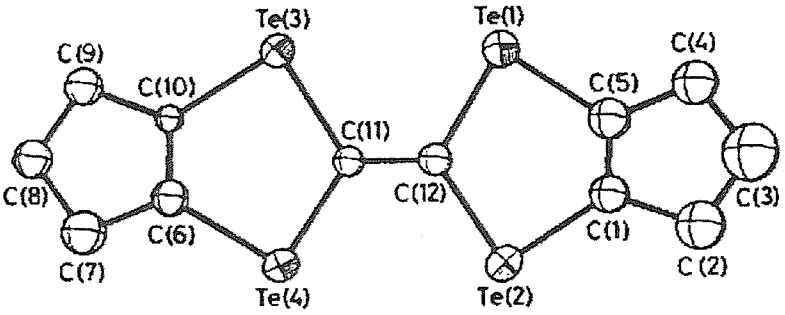

Their reaction to form telluroether species has not been investigated, and so this section reports some chemistry of dilithium 1,2-cyclopenteneditellurolate in order to establish whether these systems are suitable precursors in the formation of such ligands.

Dilithium 1,2-cyclopenteneditellurolate was prepared *via* Scheme 7.1 shown below. The control of the temperature is important due to the reactive nature of these species and thus all reagents were added at -78 ° C. Although slow warming was found to be necessary to ensure complete reaction of tellurium with the lithiated species, this was controlled so that the reaction temperature did not exceed -20 °C. The quality of the 1,2-dibromopentene was also found to be an important factor for this reaction, and thus was freshly distilled immediately before the preparation was undertaken.

Scheme 7.1. Preparation of the tellurium dianion $C_5H_6Te_2Li_2$.[12]

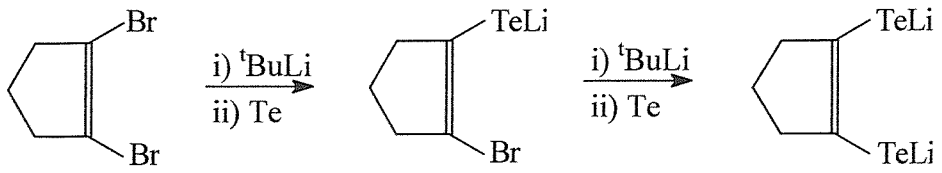

In order to establish whether this dianion would react in a similar manner to the methyltelluro-lithium and phenyltelluro-lithium analogues, i. e. straightforward nucleophilic attack, MeI was added to $[C_5H_6Te_2]^{2-}$ at -78 °C, with the aim of isolating the ligand 1,2-$C_5H_6(TeMe)_2$ (Figure 7.3).

Figure 7.3. Predicted product from the reaction of $[C_5H_6Te_2]^{2-}$ with MeI.

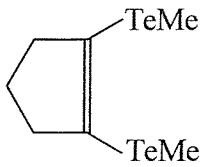

After work up to give a red oil and subsequent recrystallisation from light petroleum ether, a brown solid was obtained. The FAB mass spectrum gave a cluster of peaks at *m/z* = 388, with an isotope pattern consistent with the presence of two tellurium atoms in the

molecule. However, the mass was too high for the expected product (*m/z* for $C_7H_{12}{}^{130}Te_2$ = 356), and was found to correspond to $[C_{10}H_{12}{}^{130}Te_2]^+$ (*m/z* = 392). Therefore, on this basis the compound shown in Figure 7.4 was proposed as the product. The $^{125}Te\{^1H\}$ NMR spectrum gave one peak at δ 422 ppm, consistent with this structure, although there are few similar compounds reported. The ^1H and $^{13}C\{^1H\}$ NMR spectroscopic data are shown in Table 7.2 and Figure 7.5, which, with elemental analysis, confirmed the postulated structure. Repeating the reaction without the addition of MeI was found to give the same product.

Figure 7.4. Structure of 2,3,6,7-tetrahydro-1*H*,5*H*-dicyclopenta[1,4][1'4']ditellurin.

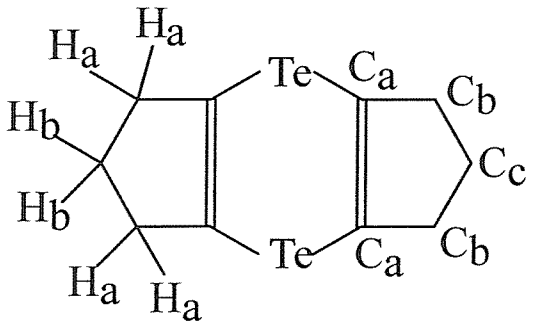

Table 7.2. ^1H and $^{13}C\{^1H\}$ NMR ($CDCl_3$, 300 K) data for 2,3,6,7-tetrahydro-1*H*,5*H*-dicyclopenta[1,4][1'4']ditellurin.

^1H NMR Data		$^{13}C\{^1H\}$ NMR Data	
2.13, q, 1H	H_b	27.7	C_c
2.62, t, 2H	H_a	42.0	C_b
		125.1	C_a

An interesting feature of this compound is the apparent stability of the $[Te(C)_2Te]$ backbone, which is obviously prone to elimination, as observed in the attempted preparation of the bidentate ligands $RTe(CH_2)_2TeR$ and $RTe(CH)_2TeR$.[15] The cyclopentene ring structure must thermodynamically disfavour this process due to the predicted formation of a strained 5-membered ring containing a triple bond.

Figure 7.5. ^{1}H NMR spectrum (300 MHz, $CDCl_3$, 300 K) of 2,3,6,7-tetrahydro-1*H*,5*H*-dicyclopenta[1,4][1'4']ditellurin.

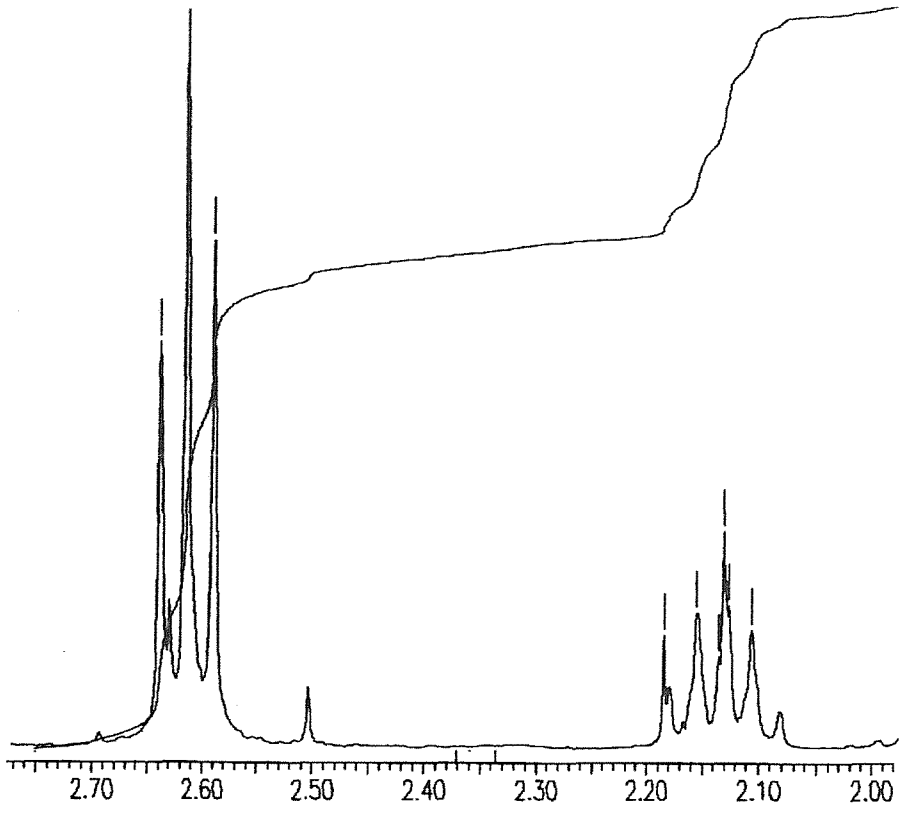

This molecule would be expected to act as a bidentate ligand, with enhanced stability due to the formation of a 5-membered chelate ring. However, analysis of this system shows that due to the rigidity of the central 6-membered ring, the lone pairs on the tellurium atoms can not coordinate in such a fashion to a metal centre, although it can act as a bridging bidentate ligand.

Initial inspection of this reaction scheme suggests that the dianion had not been formed, resulting in cyclisation of two monoanions upon warming. Therefore, addition of one equivalent of tellurium to C_5H_6BrLi to give the monoanion, should lead to this cyclised product in higher yield. In order to investigate this proposition, the monoanion was prepared as before, but rather than cooled again to -78 °C, the reaction was allowed to warm to room temperature. Subsequent work up gave a red oil which was recrystallised from light petroleum ether to give a dark orange crystalline product. The ^{125}Te{^{1}H} NMR spectrum showed one peak at δ 213 ppm, indicating that 2,3,6,7-tetrahydro-1*H*,5*H*-dicyclopenta[1,4][1'4']ditellurin had not been obtained, with the FAB mass spectrum showing

a cluster of peaks centred at *m/z* = 548 corresponding to $[C_{10}H_{12}{}^{79}Br_2{}^{130}Te_2]^+$ (*m/z* = 550). Thus, the ditelluride compound, 1,2-di(2-bromo-1-cyclopentenyl)ditellurane, shown in Figure 7.6, had been synthesised with ^1H and $^{13}C\{^1H\}$ NMR spectroscopic data (Table 7.3) confirming this assignment. The elemental analysis result was also in agreement with the calculated values.

Figure 7.6. Structure of 1,2-di(2-bromo-1-cyclopentenyl)ditellurane.

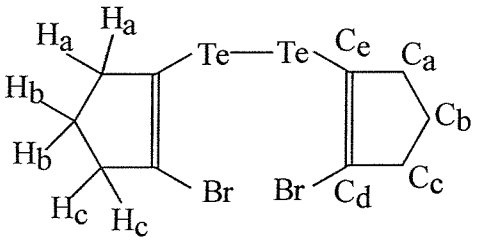

Table 7.3. ^1H and $^{13}C\{^1H\}$ NMR ($CDCl_3$, 300 K) data for 1,2-di(2-bromo-1-cyclopentenyl)ditellurane.

^1H NMR Data		$^{13}C\{^1H\}$ NMR Data	
2.04, q, 1H	H_b	23.6	C_b
2.64, t, 1H	H_c	41.4, 43.2	C_a, C_c
2.91, t, 1H	H_a	110.6	C_d
		127.3	C_e

Hence, the monoanion has been formed at low temperature, which is decomposing to the ditelluride product upon warming to room temperature. This is a common reaction pathway in tellurium chemistry where the formation of ditelluride species is favoured. Addition of dihaloalkanes to RTeLi to form the ditelluroether ligands, at room temperature, results in a similar formation of RTeTeR.

This reaction suggests that 2,3,6,7-tetrahydro-1*H*,5*H*-dicyclopenta[1,4][1'4']ditellurin must be obtained *via* a different mechanism to that first proposed. However, it is likely that the addition of a further quantity of ^{t}BuLi disfavours the formation of the ditelluride compound, thus enabling cyclisation to occur preferentially.

We were interested to establish whether this decomposition route could be hindered *via* the addition of a species that could react with the monoanion. In order to investigate this a solution of $[C_5H_6BrTe]^-$ was prepared at –78°C, and 1,2-dibromobenzene added as shown in Scheme 7.2.

Scheme 7.2. Proposed reaction scheme for the reaction of 1,2-dibromobenzene with $[C_5H_6BrTe]^-$.

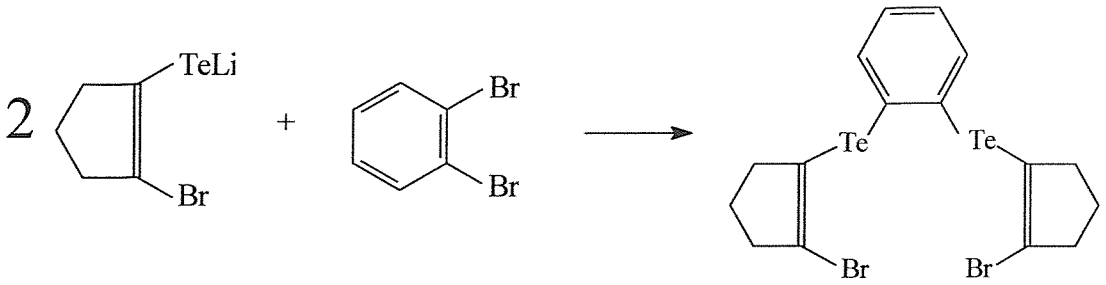

The reaction procedure was followed as before but cooled to –78°C as soon as the tellurium had dissolved, whereupon *o*-$C_6H_4Br_2$ was added dropwise. Stirring the reaction overnight gave an orange solution, which was worked up to give an oily brown solid. Addition of light petroleum ether to dissolve the oil, and subsequent cooling led to the isolation of a light yellow solid. The FAB MS showed a cluster of peaks at *m/z* = 408 corresponding to $[C_{12}H_8{}^{130}Te_2]^+$ (*m/z* = 412), with the $^{125}Te\{^1H\}$ NMR spectrum giving one peak at δ 898 ppm. The ^1H and $^{13}C\{^1H\}$ NMR spectra showed only aromatic signals, with no resonances assigned to the cyclopentene fragment. All the data are consistent with the product being telluranthrene, which has been prepared previously *via* the reaction of *o*-phenylenemercury and tellurium metal at 250 °C.[20] Therefore, transmetalation has occurred with subsequent cyclisation leading to the obtained product (Scheme 7.3).

Scheme 7.3. Proposed reaction scheme leading to the formation of telluranthrene.

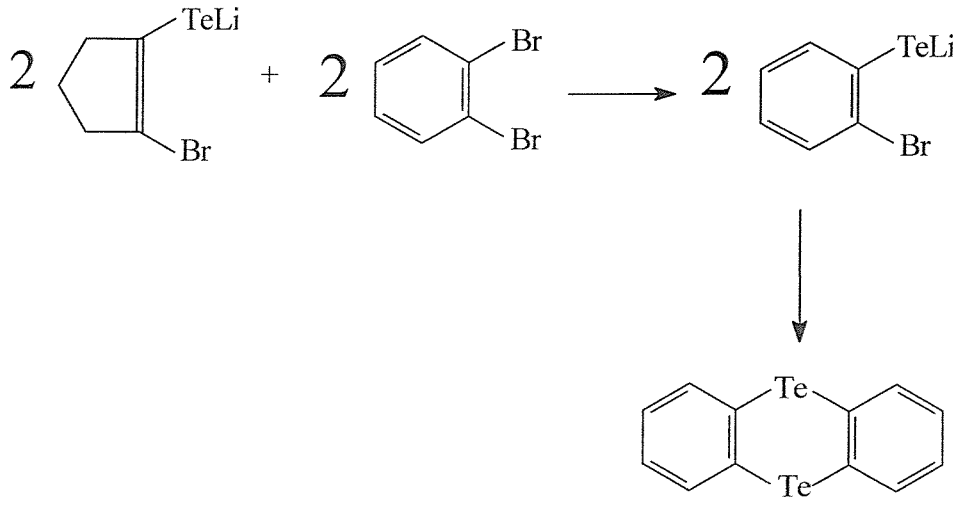

These results suggest that the preparation of both the mono- and dianions is difficult to control and although this system has led to some interesting chemistry, it seems unsuitable for the synthesis of macrocyclic ligands due to its unpredictability.

7.23 Preparation of New Tellurium Containing Cyclic and Acyclic Ligands

Due to the difficulties associated with the synthesis of tellurium ligands, mono- and bidentate ligands form the major categories of such species. There are few tridentate ligands, and just one homoleptic tritelluroether macrocycle [12]aneTe$_3$, although little work has been published on its associated coordination chemistry.[10] There is also one example of a tellurium containing macrocyclic Schiff base with Te_2N_4 donor set in a 22-membered ring.[21]

We were interested in preparing new mixed donor acyclic and cyclic ligands containing telluroether functions. Such species would allow tellurium to be studied in new coordination environments such as high oxidation state complexes, if the additional donor atoms of the ligand supported such. The preparation of macrocyclic ligands would also allow for tellurium to be studied in a macrocyclic environment and should lead to complexes with novel properties due to the thermodynamic and kinetic stability associated with such systems.

In contrast to telluroether chemistry, the preparation of thioether macrocycles is well established with the ligands [9]aneS$_3$, [14]aneS$_4$, [16]aneS$_4$ (1,5,9,13-tetrathiacyclohexadecane) and [18]aneS$_6$ (1,4,7,10,13,16-hexathiacyclooctadecane) being readily available from commercial suppliers, reflecting the interest shown in their chemical and coordinative properties. Arguably, the most interesting of these macrocycles is [9]aneS$_3$ which has been shown to be an excellent ligand due to the combined properties of the preorganisation of its lone pairs for facial coordination, and the C_2 linkages between the sulfur atoms resulting in the formation of five membered chelate rings upon coordination. Certainly some very interesting complexes have been reported with this ligand including the homoleptic species $[Rh([9]aneS_3)_2]^{2+}$,[22] $[Pd([9]aneS_3)_2]^{3+}$ (Figure 7.7) and $[Pt([9]aneS_3)_2]^{3+}$ where monomeric Rh(II), Pd(III) and Pt(III) are stabilised by this ligand.[23, 24]

Figure 7.7. Single crystal X-ray structure of $[Pd([9]aneS_3)_2]^{3+}$.[23]

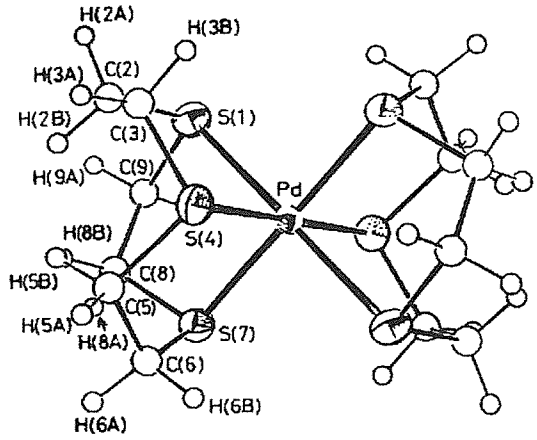

We were interested in ascertaining how the replacement of a thioether function with tellurium would change the properties of homoleptic thioether macrocycles in light of our observations of the changing donor properties down group 16 that we had previously established (Chapter 2). Therefore, it was decided to concentrate on the preparation of mixed donor thio-, telluroether ligands. The thioether functions should allow for the stabilisation of higher oxidation state complexes, with telluroether functions favouring lower oxidation states. Few similar compounds have been synthesised, although 1-thia-4-telluracyclohexane has been previously reported *via* the low yielding reaction of bis(2-chloroethyl)sulfide with Na_2Te in water using high dilution techniques.[25]

7.231 Synthesis of $MeS(CH_2)_3Te(CH_2)_3SMe$

The synthesis of $Te(CH_2CH_2CH_2OH)_2$ has been previously reported *via* the reaction of Na_2Te (generated in H_2O) and $BrCH_2CH_2CH_2OH$.[26] The preparation of the dithiol analogue, $Te(CH_2CH_2CH_2SH)_2$, would be advantageous since this would allow for ring closure with dibromoethane to give a mixed donor S/Te macrocycle. However, it was anticipated that the thiol function may complicate the reaction due its potential to polymerise *via* S-S bond formation, and therefore the reaction was first performed utilising $Br(CH_2)_3SMe$. A solution of Na_2Te was prepared in H_2O, $Br(CH_2)_3SMe$ (2 mol. equiv.) added in ethanol and the mixture refluxed for 1 hour. Subsequent work up gave the required ligand $Te(CH_2CH_2CH_2SMe)_2$ in good yield as a red oil. The FAB MS showed the expected cluster

of peaks at *m/z* = 308 corresponding to $[C_8H_{18}S_2{}^{130}Te]^+$ (*m/z* = 308) and the $^{125}Te\{^1H\}$ NMR spectrum one peak at δ 238. The rules for predicting $^{125}Te\{^1H\}$ NMR chemical shifts, discussed by O'Brien and co-workers, states that substitutions more remote than the γ-carbon (with respect to Te) have negligible effects.[16] Therefore the shift for this ligand may be directly compared with that obtained for $Te(CH_2CH_2CH_2OH)_2$ (δ 229).[26] The ^1H and $^{13}C\{^1H\}$ NMR spectroscopic data are shown in Table 7.4 and confirmed the identity of the ligand.

Table 7.4. ^1H and $^{13}C\{^1H\}$ NMR ($CDCl_3$, 300 K) data for $Te(CH_2CH_2CH_2SMe)_2$.

^1H NMR Data		$^{13}C\{^1H\}$ NMR Data	
1.98, q, 2H	$CH_2CH_2CH_2$	1.5 ($^1J_{Te-C}$ = 155 Hz)	CH_2Te
2.06, s, 3H	SCH_3	15.7	CH_3S
2.53, t, 2H	SCH_2	31.6	CH_2S
2.69, t, 2H	$TeCH_2$	36.2	$CH_2CH_2CH_2$

Unfortunately the corresponding reaction with $Br(CH_2)_3SH$[27] led to a mixture of products. The FAB MS was encouraging showing a cluster of peaks at *m/z* = 278 (*m/z* for $[^{130}Te(CH_2CH_2CH_2SH)_2]^+$ = 280), however both the ^1H and $^{13}C\{^1H\}$ spectra were complex indicating a mixture of species. The $^{125}Te\{^1H\}$ NMR spectrum gave three peaks at δ 234, 233 and 229, reasonable shifts for the required ligand, but again indicating a mixture of species present, probably polymeric in nature. The crude product was therefore columned but unfortunately, this led to decomposition, despite being performed under N_2. Therefore, it would seem likely that reaction had also occurred at the thiol function. Although the protection of the thiol groups was considered for this reaction, the methods required for deprotection would also lead to reaction at tellurium, in preference to sulfur, and thus an alternative synthetic strategy was adopted.

7.232 Synthesis of [11]aneS$_2$Te (1,4-dithia-8-telluracycloundecane)

Due to the difficulties associated with converting functional groups in tellurium containing molecules, a synthesis was devised where the addition of the telluroether functional group was the final step. The method adopted is shown in Scheme 7.4.

Scheme 7.4. Preparation of [11]aneS$_2$Te.

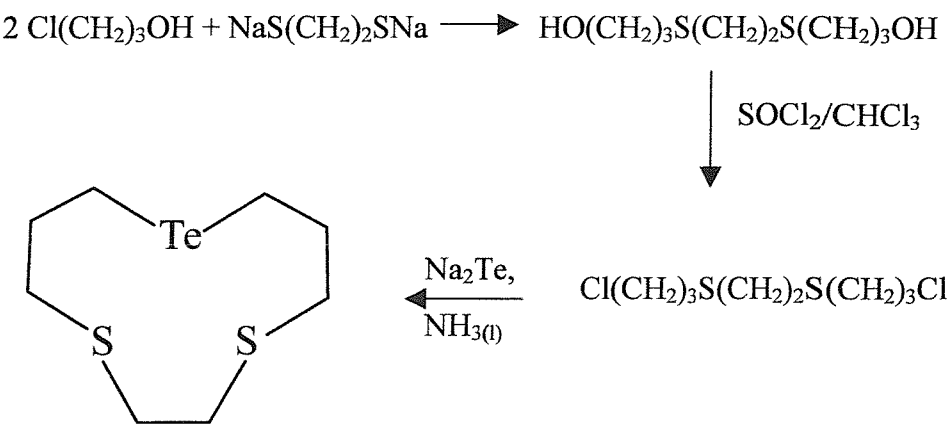

The dichloro-compound Cl(CH$_2$)$_3$S(CH$_2$)$_2$S(CH$_2$)$_3$Cl was prepared according to the literature procedure.[28] Addition of HS(CH$_2$)$_2$SH dropwise to a solution of sodium in ethanol followed by dropwise addition of Cl(CH$_2$)$_3$OH gave the compound HO(CH$_2$)$_3$S(CH$_2$)$_2$S(CH$_2$)$_3$OH, after work up, as a white waxy solid. Addition of SOCl$_2$ to a solution of this species in CHCl$_3$ subsequently gave Cl(CH$_2$)$_3$S(CH$_2$)$_2$S(CH$_2$)$_3$Cl as a brown oil. The required macrocyclic ligand was prepared *via* the addition of this dichloro- species in THF to a solution of Na$_2$Te prepared in NH$_{3(l)}$ at -78 °C. The ammonia was allowed to boil off overnight and the resulting mixture hydrolysed and extracted with CH$_2$Cl$_2$ to give a red oil. Purification by silica flash chromatography using ethyl acetate:hexane 1:3 gave the ligand as a light yellow solid.

The ^{125}Te{^{1}H} NMR spectrum showed one peak at δ 234, a similar shift to that obtained for the acyclic S$_2$Te ligand MeS(CH$_2$)$_3$Te(CH$_2$)$_3$SMe. The FAB MS showed a cluster of peaks at *m/z* = 306, with the correct isotope pattern, corresponding to [C$_8$H$_{16}$S$_2$^{130}Te]$^+$ (*m/z* = 306), the molecular ion of the required ligand, along with fragmentation peaks associated with [Te(CH$_2$)$_3$S]$^+$ due to the loss of (CH$_2$)$_3$S(CH$_2$)$_2$ through cleavage of the Te-C and S-C bonds. It should also be noted that the FAB mass spectrum was obtained of the crude product in order to establish the potential presence of larger ring systems. However, the highest mass

peak corresponded to [11]aneS$_2$Te. Elemental analysis was consistent with the expected values. The ^{1}H and ^{13}C{^{1}H} NMR spectroscopic data are detailed in Table 7.5, and the ^{13}C{^{1}H} NMR spectrum is shown in Figure 7.8. The expected coupling is observed in the ^{1}H NMR spectrum, and although the two signals from the SCH_2 groups overlap, the overall singlet and triplet pattern may be discerned. The ^{13}C{^{1}H} NMR spectrum shows four resonances corresponding to the four carbon environments, with the shift for δ(Te*C*H$_2$) markedly to low frequency than the other three resonances, consistent with other telluroether ligands and its acyclic analogue discussed above.

Table 7.5. ^{1}H and ^{13}C{^{1}H} NMR ($CDCl_3$, 300 K) data for [11]aneS$_2$Te.

^{1}H NMR Data		^{13}C{^{1}H} NMR Data	
2.05, q, 1H	$CH_2CH_2CH_2$	2.2	CH_2Te
2.67, t, 1H	$TeCH_2$	32.6	CH_2S
2.73, t, 1H	$SCH_2CH_2CH_2Te$	32.9	CH_2S
2.74, s, 1H	SCH_2CH_2S	34.7	$CH_2CH_2CH_2$

The ligand was very poorly soluble and therefore $^1J_{Te\text{-}C}$ were not observed, even after extended data accumulation.

Figure 7.8. ^{13}C{^{1}H} NMR spectrum (90.1 MHz, $CDCl_3$, 300 K) of [11]aneS$_2$Te.

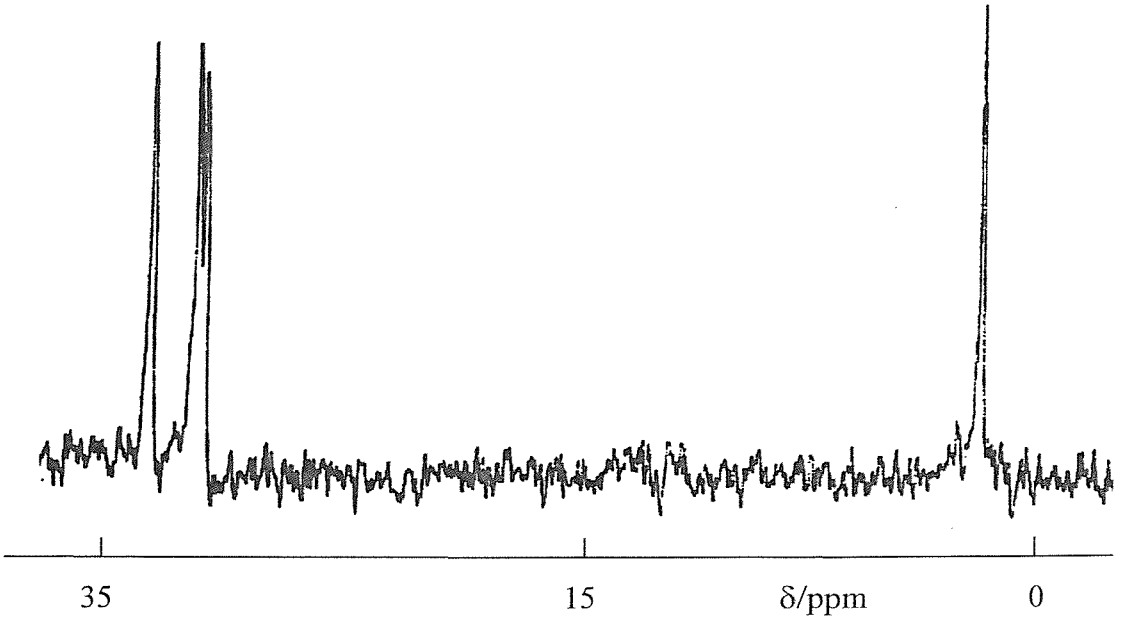

7.233 Synthesis of [12]aneS$_2$Te (1,5-dithia-9-telluracyclododecane)

This chemistry has been successfully adapted to prepare the ligand [12]aneS$_2$Te (Figure 7.9). The reaction procedure was followed as for [11]aneS$_2$Te, with the addition of a solution of Cl(CH$_2$)$_3$S(CH$_2$)$_3$S(CH$_2$)$_3$Cl in THF to Na$_2$Te in NH$_{3(l)}$ at -78 °C. Upon work up and purification *via* flash column chromatography using ethyl acetate:hexane 1:3, a light yellow oily solid was obtained.

Figure 7.9. Structure of [12]aneS$_2$Te.

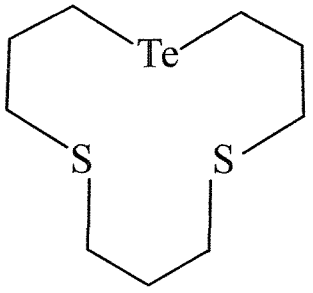

The ^{125}Te{^{1}H} NMR spectrum showed one peak at δ 217, a shift entirely consistent with a Te{(CH$_2$)$_3$}$_2$ unit. The FAB mass spectrum showed a cluster of peaks at *m/z* = 320, corresponding to the molecular ion (*m/z* for C$_9$H$_{18}$S$_2$^{130}Te = 320) along with peaks associated with the loss of [S(CH$_2$)$_3$] and [(CH$_2$)$_3$S(CH$_2$)$_3$]. The ^{1}H (Figure 7.10) and ^{13}C{^{1}H} NMR assignments are shown in Table 7.6, which with elemental analysis confirmed the purity of the ligand, showing a good match with the calculated values.

Table 7.6. ^{1}H and ^{13}C{^{1}H} NMR (CDCl$_3$, 300 K) data for [12]aneS$_2$Te.

^{1}H NMR Data		^{13}C{^{1}H} NMR Data	
1.86, q, 1H	SCH$_2$C*H*$_2$CH$_2$S	1.0	*C*H$_2$Te
2.06, q, 2H	SCH$_2$C*H*$_2$CH$_2$Te	27.7	SCH$_2$*C*H$_2$CH$_2$S
2.66, t, 2H	TeC*H*$_2$	29.0	*C*H$_2$S
2.73, t, 2H	SC*H*$_2$	30.1	*C*H$_2$S
2.78, t, 2H	SC*H*$_2$	33.5	SCH$_2$CH$_2$*C*H$_2$Te

Figure 7.10. ^{1}H NMR spectrum (300 MHz, $CDCl_3$, 300 K) of [12]aneS_2Te.

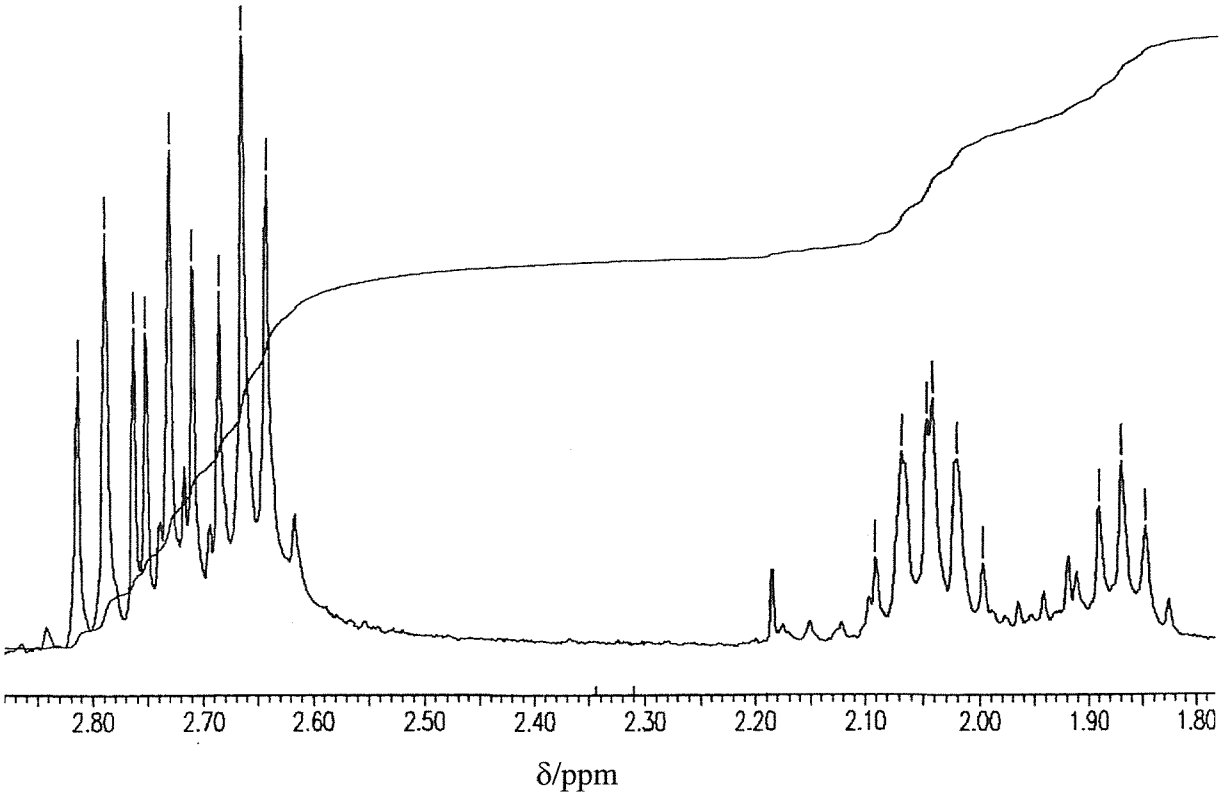

7.234 Synthesis of [14]aneS_3Te (1,4,7-trithia-11-telluracyclododecane)

This chemistry has also been successfully adapted to prepare the tetradentate macrocycle [14]aneS_3Te (Figure 7.11) *via* the reaction of Na_2Te with $Cl(CH_2)_3S(CH_2)_2S(CH_2)_2S(CH_2)_3Cl$.

Figure 7.11. Structure of [14]aneS_3Te.

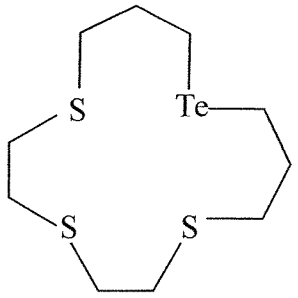

Purification of the crude product by silica gel flash chromatography using ethyl acetate:hexane 1:3 and ethyl acetate:hexane 1:20 gave a light yellow solid.

The $^{125}Te\{^1H\}$ NMR spectrum gave one peak at δ 254, again consistent with the previous ligands. The FAB mass spectrum (Figure 7.12) showed a cluster of peaks at *m/z* = 366 corresponding to the molecular ion (*m/z* for $C_{10}H_{20}S_3{}^{130}Te$ = 366), along with peaks showing the fragmentation of the ligand through cleavage of Te-C and S-C bonds. The ^1H and $^{13}C\{^1H\}$ NMR spectroscopic data are shown in Table 7.7. Elemental analysis showed a good agreement with the expected values.

Table 7.7. ^1H and $^{13}C\{^1H\}$ NMR ($CDCl_3$, 300 K) data for [14]aneS$_3$Te.

^1H NMR Data		$^{13}C\{^1H\}$ NMR Data	
2.09, q, 1H	$CH_2CH_2CH_2$	4.7	CH_2Te
2.62, t, 1H	$TeCH_2$	34.5, 34.9, 35.7	3 x CH_2S
2.73, t, 1H	SCH_2	36.1	$CH_2CH_2CH_2$
2.78, m, 2H	2 x SCH_2		

Figure 7.12. FAB mass spectrum of [14]aneS$_3$Te.

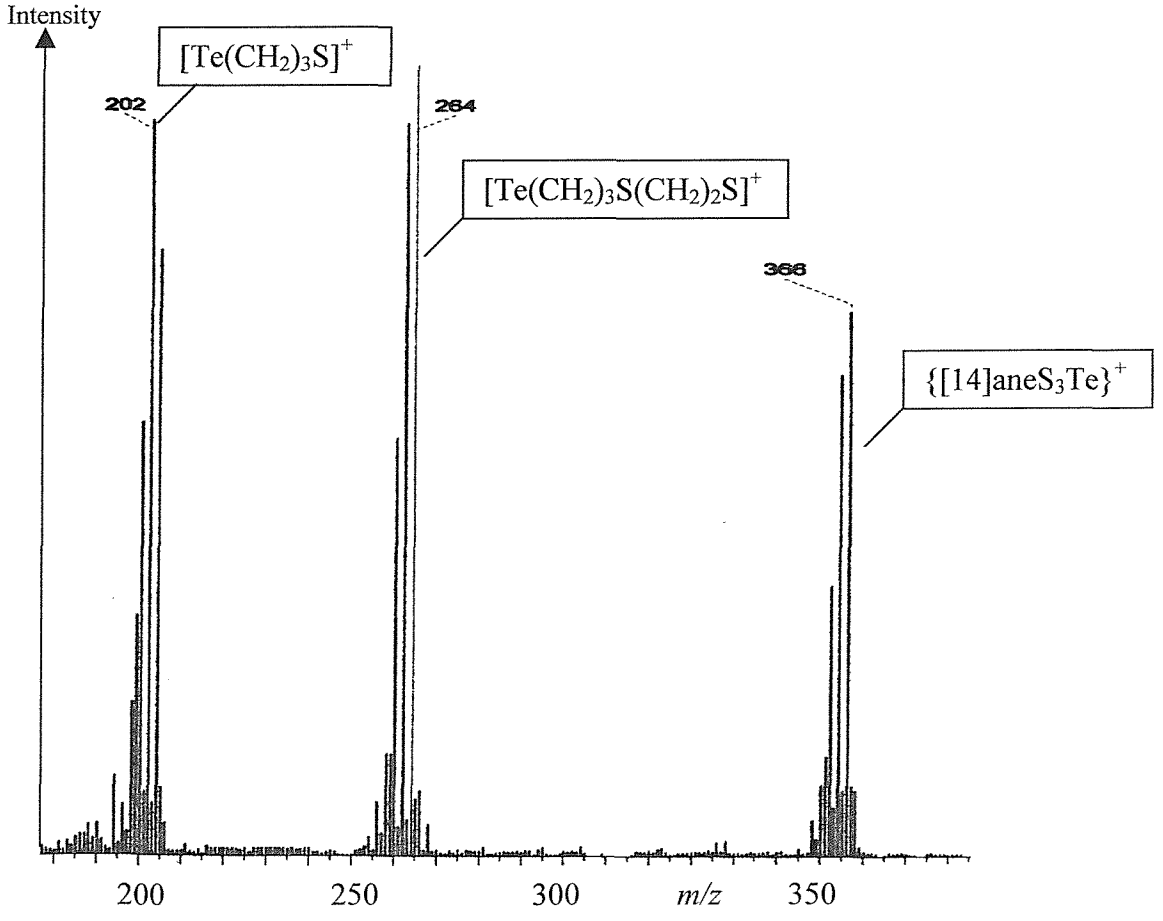

7.235 Synthesis of $Te(CH_2CH_2CH_2NH_2)_2$

The extension of this chemistry to mixed N/Te donor acyclic ligands has also been investigated, with the aim to provide convenient synthetic precursors for the preparation of new macrocyclic ligands. With this in mind, a similar route to that first undertaken to prepare the S/Te ligands was adopted, with the replacement of thiol functions with primary amines. Thus the ligand $H_2N(CH_2)_3Te(CH_2)_3NH_2$ was prepared *via* the dropwise addition of 3-chloropropylammonium chloride to a solution of sodium telluride in water. The mixture was subsequently refluxed for three hours and extracted with diethyl ether to give an orange oil. The $^{125}Te\{^1H\}$ NMR spectrum showed a shift of δ 240, again consistent with the previous ligands reported in this Chapter, and confirms the minimal effect that changing groups further than the γ-carbons have on $\delta(^{125}Te)$. The FAB mass spectrum confirmed the identity of the ligand showing a cluster of peaks corresponding to the molecular ion at *m/z* = 246, (*m/z* for $C_6H_{16}N_2{}^{130}Te$ = 246) with elemental analysis showing a good match with the calculated values. The ^1H and $^{13}C\{^1H\}$ NMR spectroscopic data are shown in Table 7.8. In contrast to the thiol chemistry, the amine protons are more basic and polymerisation does not occur.

Table 7.8. ^1H and $^{13}C\{^1H\}$ NMR ($CDCl_3$, 300 K) data for $Te(CH_2CH_2CH_2NH_2)_2$.

^1H NMR Data		$^{13}C\{^1H\}$ NMR Data	
0.98, s, br, 1H	NH_2	2.4 ($^1J_{Te\text{-}C}$ = 156 Hz)	CH_2Te
1.64, q, 1H	$NCH_2CH_2CH_2Te$	38.8	$NCH_2CH_2CH_2Te$
2.42, t, 1H	$TeCH_2$	46.8	NCH_2
2.50, t, 1H	NCH_2		

7.24 Preparation of Ag(I) Complexes with the Mixed Donor S/Te Macrocycles

The coordination chemistry of the new mixed donor S/Te macrocycles has been investigated with $Ag[CF_3SO_3]$. In a typical preparation, the macrocyclic ligand, $L_{S/Te}$, (1 mol. equiv.) was dissolved in 25 cm^3 of CH_2Cl_2 and $Ag[CF_3SO_3]$ (1 mol. equiv.) added. The reaction mixture was stirred for approximately 1 hour, during which time the $Ag[CF_3SO_3]$ dissolved and a light yellow solid was precipitated, which was filtered off and washed with diethyl ether. These species were found to be extremely insoluble even in coordinating

solvents, probably as a combination of the insolubility of the ligands with the formation of an extended structure, common in Ag(I) chemistry. Due to this and the fact that NMR spectroscopy has been shown to provide little information on the structure of such complexes (Chapter 4), just ^{1}H NMR spectra were obtained which showed resonances associated with the coordinated ligands. However, the ES$^+$ mass spectra gave clusters of peaks corresponding to $[Ag(L_{S/Te})]^+$ for all three complexes, and $[Ag(L_{S/Te})_2]^+$ for both $L_{S/Te}$ = [11]aneS$_2$Te and [12]aneS$_2$Te with IR spectroscopy displaying peaks identified with the $CF_3SO_3^-$ anion and the macrocyclic ligand. Elemental analysis showed a good match for both the [11]aneS$_2$Te and [14]aneS$_3$Te complexes illustrating a 1:1 complex. However, the [12]aneS$_2$Te species was observed to be extremely unstable and decomposed before microanalyses were obtained.

7.241 X-ray Crystal Structure of [Ag([11]aneS$_2$Te)][CF$_3$SO$_3$]

To order to confirm that the macrocyclic ligand had been synthesised, crystals suitable for single crystal X-ray diffraction were grown of [Ag([11]aneS$_2$Te)][CF$_3$SO$_3$] *via* the vapour diffusion of diethyl ether in a solution of the complex in MeNO$_2$/MeOH. Unfortunately, the crystal was poorly diffracting and analysis of the structure obtained showed it to be highly disordered as well as containing various solvent molecules. Therefore, refinement to a reasonable R factor was unsuccessful (Table 7.9). However, the expected macrocyclic ligand was revealed as well as the overall structure which shows two different Ag(I) environments, trigonal planar and tetrahedral (Figure 7.13). The trigonal planar geometry is obtained *via* bidentate coordination of one macrocycle through the thioether functions to give a five-membered chelate ring, with the remaining coordination site occupied by a telluroether function from a neighbouring macrocycle. The tetrahedral Ag(I) has a similar coordination environment, except that the extra coordination is occupied by a bridging thioether function, which binds the $\{[Ag([11]aneS_2Te)]^+\}_2$ dimers together to give a linear chain polymer (Figure 7.14). The heavy atom bond lengths *d*(Ag-Te) = 2.67(1) - 2.717(6) Å and *d*(Ag-S) = 2.60(1) - 2.80(1) Å are comparable to those found in $[\{Ag(MeTeCH_2CH_2CH_2TeMe)_2\}_n][BF_4]_n$ (*d*(Ag-Te) = 2.785(2) - 2.837(2) Å)[29] and $[Ag_n(PhSCH_2CH_2CH_2SPh)_{2n}][BF_4]_n$ (*d*(Ag-S) = 2.573(3) - 2.623(3) Å)[30] although due to the high R factor for this structure, caution must be employed when comparing these data.

Table 7.9. Crystallographic Data Collection and Refinement Parameters for [Ag([11]aneS$_2$Te)][CF$_3$SO$_3$].

	[Ag([11]aneS$_2$Te)][CF$_3$SO$_3$]
Formula	$C_9H_{16}AgF_3O_3S_3Te$
Formula weight	525.37
Crystal System	Triclinic
Space group	$P\bar{1}$
a, Å	12.49(1)
b, Å	14.328(4)
c, Å	11.648(7)
α/°	108.01(4)
β/°	109.56(7)
γ/°	94.27(4)
V, Å^3	1830(2)
Z	4
D_{calc}, g/cm^3	2.086
μ(Mo-K_α), cm^{-1}	30.35
Unique obs. reflections	6449
Obs. reflections with $[I_o > 2\sigma(I_o)]$	4172
R	0.187
R_w	0.231

$R = \Sigma (|F_{obs}|_i - |F_{calc}|_i) / \Sigma |F_{obs}|_i$, $R_w = \sqrt{[\Sigma w_i (|F_{obs}|_i - |F_{calc}|_i)^2 / \Sigma w_i |F_{obs}|_i^2]}$

Figure 7.13. X-ray crystal structure of [Ag([11]aneS$_2$Te)][CF$_3$SO$_3$] showing local geometry around Ag(I) centres. Ellipsoids are drawn at 40 % probability and H-atoms omitted for clarity.

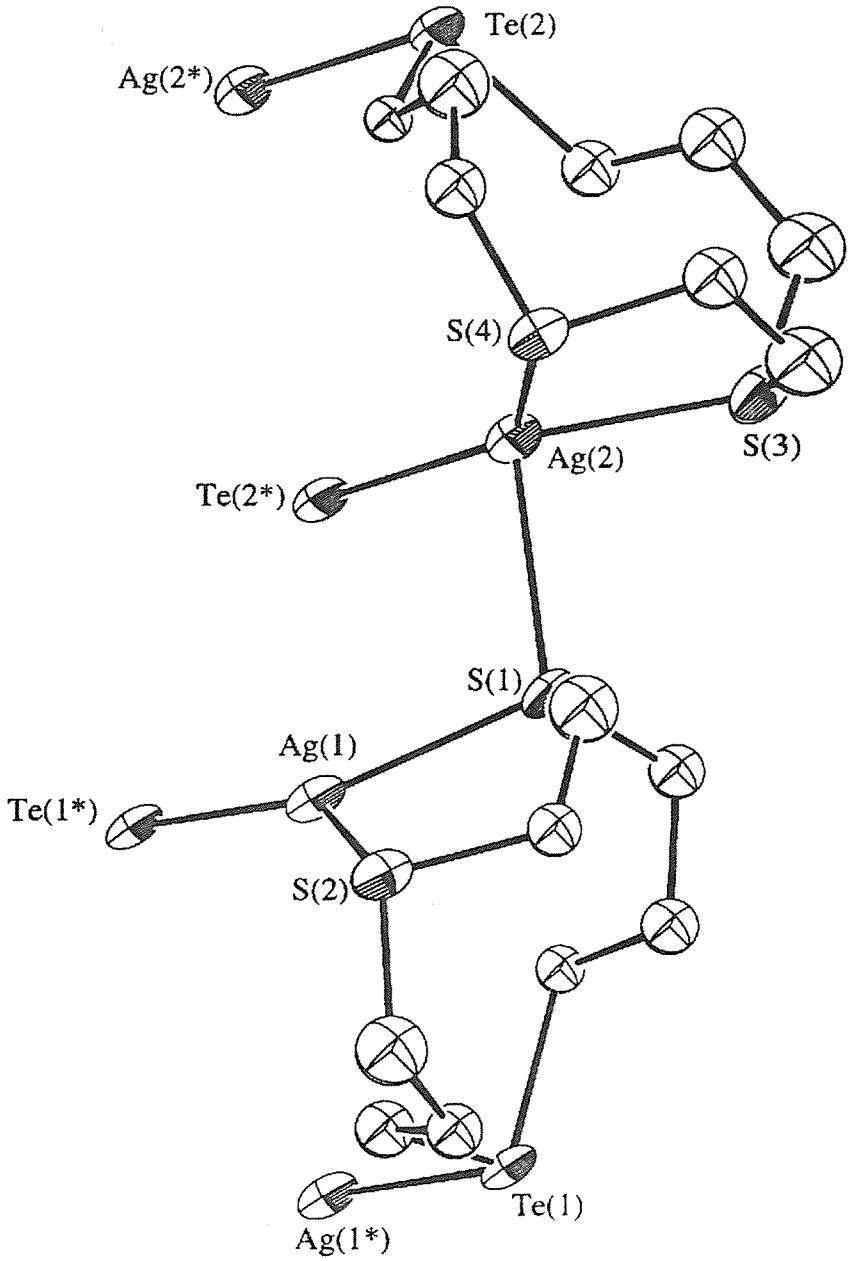

Figure 7.14. X-ray crystal structure of [Ag([11]aneS$_2$Te)][CF$_3$SO$_3$] showing extended structure. Ellipsoids are drawn at 40 % probability and H-atoms omitted for clarity.

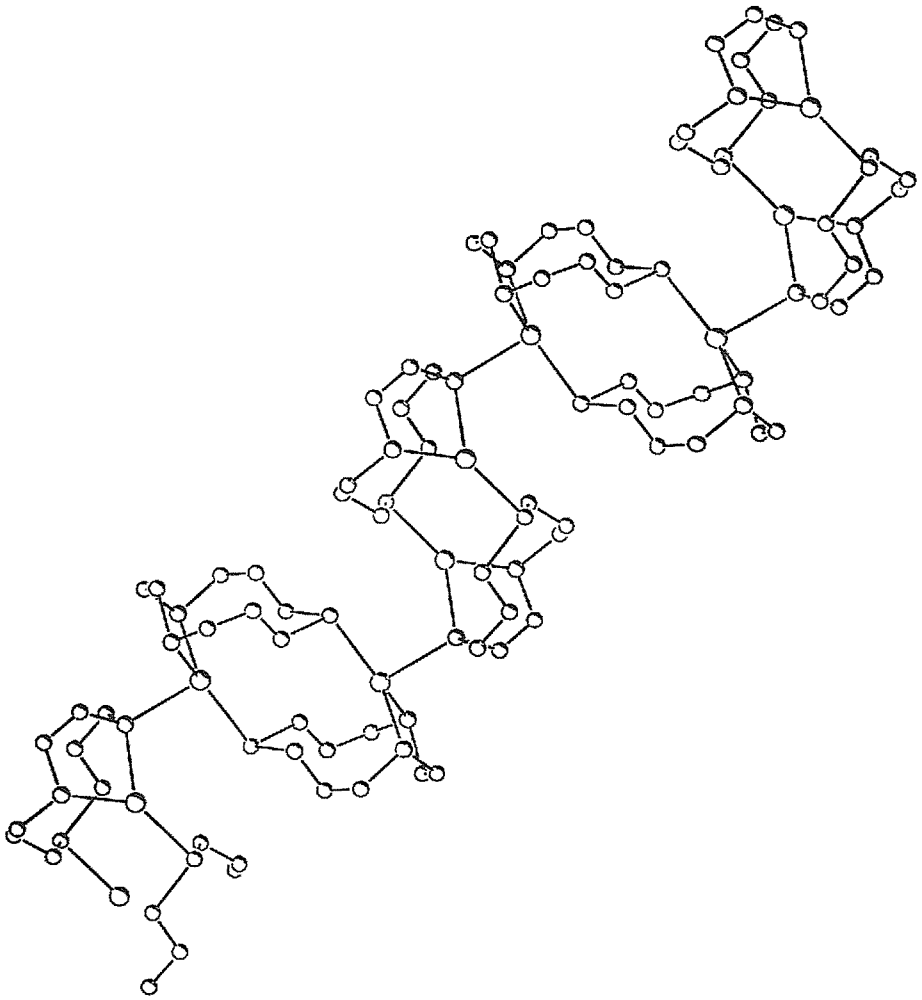

7.3 Conclusions

The first section of this Chapter has detailed improved syntheses for the ligands $MeC(CH_2SMe)_3$ and $MeC(CH_2SeMe)_3$ reporting the isolation of just the trisubstituted ligand, which contrasts with previous syntheses where mixtures of mono-, bi, and tri-substituted products were obtained. More importantly the tritelluroether, $MeC(CH_2TePh)_3$, has also been prepared in moderate yield which has allowed for comparisons to be made between methyl and phenyl substituted tripodal telluroether ligand complexes.

The chemistry of cyclopentene-1,2-ditellurolate has been investigated and has led to the isolation of some unexpected products and illustrated some aspects and unpredictability of tellurium chemistry. The preparation of the cyclised product 2,3,6,7-tetrahydro-1*H*,5*H*-dicyclopenta[1,4][1'4']ditellurin has shown that C_2 linkages between Te atoms may be obtained, providing the elimination of the backbone is disfavoured, and that these systems are prone to cyclisation. However, the isolation of the compound 1,2-di(2-bromo-1-cyclopentenyl)ditellurane has also depicted the preference for the formation of ditelluride systems over cyclisation, common in organo-tellurium chemistry. The reaction of $[C_5H_6BrTe]^-$ with 1,2-dibromobenzene has led to the isolation of telluranthrene, which had only previously been prepared by utilising rather extreme reaction conditions, representing the transmetallation of tellurium.

The mixed donor ligands $MeS(CH_2)_3Te(CH_2)_3SMe$ and $H_2N(CH_2)_3Te(CH_2)_3NH_2$ have been prepared as part of a study into the synthesis of new ligands containing telluroether functions. This chemistry has been successfully adapted to prepare the macrocyclic ligands [11]aneS_2Te, [12]aneS_2Te and [14]aneS_3Te. These species will allow tellurium to be studied in a macrocyclic environment as well as providing complexes with novel properties by the combination of thio- and telluroether functions and should lead to some interesting comparisons with the homoleptic thioether macrocyclic chemistry already established. The Ag(I) complexes of these ligands have been prepared with the crystal structure of the complex $[Ag([11]aneS_2Te)][CF_3SO_3]$ showing two Ag(I) environments. For the trigonal planar Ag(I) ions, coordination occurs to one macrocyclic ligand *via* bidentate coordination of the thioether functions and another macrocycle through the telluroether function. For the tetrahedral Ag(I) ions, the extra coordination site is occupied by a bridging sulfur atom from a neighbouring macrocyclic ligand.

7.4 Experimental

The intermediates $MeC(CH_2Br)_3$,[31] $Br(CH_2)_3SMe$,[32] $Cl(CH_2)_3S(CH_2)_2S(CH_2)_3Cl$, $Cl(CH_2)_3S(CH_2)_3S(CH_2)_3Cl$ and $Cl(CH_2)_3S(CH_2)_2S(CH_2)_2S(CH_2)_3Cl$ were prepared *via* the literature procedures.[28]

$MeC(CH_2SMe)_3$. Prepared by adapting the literature method.[13] 1,1,1-tris(bromomethyl)ethane (7.5 g, 0.024 mol) was added dropwise to a solution of NaSMe (7.5 g, 0.11 mol) in dry ethanol (150 cm^3). After the addition was complete, the reaction mixture was refluxed for 18 hours, after which time the majority of the ethanol was distilled off. The resulting mixture was hydrolysed with water (100 cm^3) and the organic phase separated. The aqueous layer was then extracted with diethyl ether (4 x 25 cm^3) and the combined organic phases dried ($MgSO_4$) for 18 hours. The mixture was filtered and the solvents removed *in vacuo* to give the required ligand as a yellow oil. Yield 4.2 g, 83 %. ^1H NMR ($CDCl_3$, 300 K): δ 1.10 (s, 1H, CCH_3), 2.15 (s, 3H, SCH_3), 2.65 (s, 2H, SCH_2). $^{13}C\{^1H\}$ NMR ($CDCl_3$, 300 K): δ 17.9 (SCH_3), 24.0 (CCH_3), 41.4 (C), 44.4 (SCH_2).

$MeC(CH_2SeMe)_3$. Prepared by adapting the literature method.[14] Selenium powder (11.04 g, 0.14 mol) and dry THF (200 ml) were frozen using a liquid nitrogen bath and methyl lithium in diethyl ether (100 cm^3, 0.14 mol) added. On warming to room temperature with stirring, the selenium dissolved to give a pale yellow solution. 1,1,1-tris(bromomethyl)ethane (7.0 g, 0.022 mol) was added dropwise and the mixture refluxed for 18 hours. After cooling to room temperature, the mixture was hydrolysed with water (100 cm^3) and the organic phase separated. The aqueous layer was then extracted with diethyl ether (4 x 25 cm^3) and the combined organic phases dried ($MgSO_4$) for 18 hours. The mixture was filtered and the solvents removed *in vacuo* to give the required product as a yellow oil. Yield 6.2 g, 80 %. ^1H NMR ($CDCl_3$, 300 K): δ 1.05 (s, 1H, CCH_3), 1.94 (s, 3H, $SeCH_3$), 2.67 (s, 2H, $SeCH_2$). $^{13}C\{^1H\}$ NMR ($CDCl_3$, 300 K): δ 6.58 ($SeCH_3$), 25.33 (CCH_3), 37.96 ($SeCH_2$), 40.66 (C). $^{77}Se\{^1H\}$ NMR (neat sample, 300 K): δ 24.4.

$MeC(CH_2TePh)_3$. A suspension of tellurium powder (23.0 g, 0.18 mol) in dry THF (150 cm^3) was frozen using a liquid nitrogen bath and phenyl lithium in diethyl ether (100 cm^3, 0.18 mol) added. The mixture was allowed to thaw and stirred at room temperature for 1

hour, to give an orange solution. The mixture was refrozen in the liquid nitrogen bath and 1,1,1-tris(bromomethyl)ethane (9.3 g, 0.03 mol) injected into the flask. The mixture was allowed to thaw, stirred at room temperature for 18 hours and refluxed for 1 hour. After cooling to room temperature, the mixture was hydrolysed with water (100 cm^3) and the organic phase separated. The aqueous layer was extracted with diethyl ether (4 x 25 cm^3) and the combined organic phases dried ($MgSO_4$) for 18 hours. The mixture was then filtered and the solvents removed *in vacuo* to give a deep red oil, which was recrystallised twice from light petroleum ether to yield the product as an orange powder. Yield 2.5 g, 12 %. Analysis: Calculated for $C_{23}H_{24}Te_3$: %C, 40.4; %H, 3.5. Found: %C, 40.1; %H, 3.2. $^{125}Te\{^1H\}$ NMR (neat sample, 300 K): δ 387. FAB MS (3-NOBA), *m/z* = 684; calc. for $[MeC(CH_2{}^{130}TePh)_3]^+$ 690.

2,3,6,7-tetrahydro-1*H*,5*H*-dicyclopenta[1,4][1'4']ditellurin. Freshly distilled 1,2-dibromocyclopentene (1.42 g, 6.3 x 10^{-3} mol) was added to dry THF (100 cm^3) and the mixture cooled to -78 °C. ^{t}BuLi (7.4 cm^3, 0.013 mol) was added dropwise to give a yellow solution which was stirred for 5 minutes, after which time freshly ground tellurium powder (0.811 g, 6.3 x 10^{-3} mol) was added and the grey slurry allowed to slowly warm. After approximately 30 minutes, all the tellurium had dissolved and the mixture was re-cooled to -78 °C, whereupon the addition of ^{t}BuLi and tellurium was repeated to give a light yellow solution. The mixture was allowed to warm to room temperature and stirred for 1 hour. Addition of H_2O (50 cm^3) and subsequent extraction of the aqueous layer with diethyl ether (4 x 25 cm^3) gave an orange solution which was dried overnight with $MgSO_4$. Filtration and removal of the solvent *in vacuo* gave a red oil, which was recrystallised using light petroleum ether to give a brown solid. Yield 80 mg, 66 %. Analysis: Calculated for $C_{10}H_{12}Te_2$: %C, 31.0; %H, 3.1. Found: %C, 30.9; %H, 3.4. $^{125}Te\{^1H\}$ NMR ($CDCl_3$, 300 K): δ 422. FAB MS (3-NOBA), *m/z* = 388; calc. for $[C_{10}H_{12}{}^{130}Te_2]^+$ 392.

1,2-di(2-bromo-1-cyclopentenyl)ditellurane. To a solution of freshly distilled 1,2-dibromocyclopentene (1.89 g, 8.4 x 10^{-3} mol) in THF (100 cm^3) at -78 °C was added ^{t}BuLi (9.9 cm^3, 0.017 mol) dropwise to give a yellow solution after stirring for 5 minutes. Freshly ground tellurium powder (1.07 g, 8.4 x 10^{-3} mol) was then added, the mixture stirred for a further 5 minutes at -78 °C and allowed to warm to room temperature. After 30 minutes the resulting red solution was hydrolysed (20 cm^3), the aqueous layer extracted with diethyl ether

(4 x 25 cm^3), dried overnight ($MgSO_4$), filtered and the solvent removed to give a red oily solid. Addition of light petroleum ether and subsequent cooling led to the precipitation of a brown crystalline solid. Yield 1.1 g, 48 %. Analysis: Calculated for $C_{10}H_{12}Br_2Te_2$: %C, 21.9; %H, 2.2. Found: %C, 21.7; %H, 2.1. $^{125}Te\{^1H\}$ NMR ($CDCl_3$, 300 K): δ 213. FAB MS (3-NOBA), *m/z* = 548, 275; calc. for $[C_{10}H_{12}{}^{79}Br_2{}^{130}Te_2]^+$ 550, $[C_5H_6{}^{79}Br^{130}Te]^+$ 275.

Telluranthrene. ^{t}BuLi (5 cm^3, 8.5 x 10^{-3} mol) was added dropwise to a solution of freshly distilled 1,2-dibromocyclopentene (0.95 g, 4.2 x 10^{-3} mol) in THF (100 cm^3) at -78 °C and the mixture stirred for 5 minutes. Freshly ground tellurium powder (0.54 g 4.2 x 10^{-3} mol) was then added, the grey slurry stirred for a further 5 minutes and then allowed to warm to room temperature until all the tellurium had dissolved. The resulting yellow solution was re-cooled to -78 °C and 1,2-dibromobenzene (0.5 g, 2 x 10^{-3} mol) added dropwise, the mixture stirred for 1 hour at - 78 °C and then allowed to warm slowly to room temperature overnight. The resulting orange solution was hydrolysed (20 cm^3), the aqueous layer extracted with diethyl ether (4 x 25 cm^3) and dried overnight ($MgSO_4$). After removal of the solvent *in vacuo* a brown oily solid was obtained, which was recrystallised from light petroleum ether to give a light yellow solid. Yield 250 mg, 61 %. Analysis: Calculated for $C_{12}H_8Te_2$: %C, 35.4; %H, 2.0. Found: %C, 35.1; %H, 1.8. $^{125}Te\{^1H\}$ NMR ($CDCl_3$, 300 K): δ 898. FAB MS (3-NOBA), *m/z* = 408; calc. for $[C_{12}H_8{}^{130}Te_2]^+$ 412.

$Te(CH_2CH_2CH_2SMe)_2$. Freshly ground tellurium powder (3.19 g, 0.025 mol) was added to a mixture of sodium hydroxide (13 g) and sodium formaldehyde sulfoxylate (10 g) in water (50 cm^3). The mixture was then refluxed until the solution became colourless and a white precipitate was observed. 1-bromo-3-methylthio-propane (8.45 g, 0.05 mol) in ethanol (30 cm^3) was then added and the mixture refluxed for 1 hour. After cooling, diethyl ether (25 cm^3) was added and the organic layer separated. The aqueous layer was then extracted with diethyl ether (4 x 25 cm^3) and the combined organic extracts dried overnight ($MgSO_4$). After filtration and removal of the solvent *in vacuo* a red oil was obtained. Yield 6.2 g, 81 %. Analysis: Calculated for $C_8H_{18}S_2Te$: %C, 31.4; %H, 5.9. Found: %C, 31.2; %H, 5.6. $^{125}Te\{^1H\}$ NMR ($CDCl_3$, 300 K): δ 238. FAB MS (3-NOBA), *m/z* = 308, 219; calc. for $[C_8H_{18}S_2{}^{130}Te]^+$ 308, $[C_4H_9S^{130}Te]^+$ 219.

$Te(CH_2CH_2CH_2NH_2)_2$. To a solution of Na_2Te (0.025 mol) in H_2O prepared *via* the procedure described above was added 3-chloropropaneamine hydrogen chloride (6.5 g, 0.05 mol) in ethanol (40 cm^3) dropwise. The mixture was refluxed for 3 hours, cooled and extracted with diethyl ether (4 x 25 cm^3). The organic layer was dried overnight ($MgSO_4$), filtered and the solvent removed *in vacuo* to give an orange oil. Yield 5.4 g, 89 %. Analysis: Calculated for $C_6H_{16}N_2Te$: %C, 29.6; %H, 6.6; %N, 11.5. Found: %C, 30.2; %H, 6.9; %N, 11.0. $^{125}Te\{^1H\}$ NMR ($CDCl_3$, 300 K): δ 240. FAB MS (3-NOBA), *m/z* = 246, 188; calc. for $[C_6H_{16}N_2{}^{130}Te]^+$ 246, $[C_3H_8N{}^{130}Te]^+$ 188.

[11]aneS_2Te. To a solution of sodium (0.93 g, 0.04 mol) in $NH_{3(l)}$ (400 cm^3) at -78 °C was added tellurium powder (2.58 g, 0.02 mol) and the mixture allowed to warm slowly. When a white precipitate of Na_2Te was observed, the mixture was re-cooled to -78 °C and $Cl(CH_2)_3S(CH_2)_2S(CH_2)_3Cl$ (5 g, 0.02 mol) in THF (100 cm^3) added dropwise over 30 minutes. The mixture was warmed to room temperature and the NH_3 allowed to boil off overnight to give a red solution which was hydrolysed (200 cm^3), the organic layer separated and the aqueous layer extracted with dichloromethane (4 x 40 cm^3). The combined organic extracts were dried overnight ($MgSO_4$), filtered and the solvent removed *in vacuo* to leave a red oil. This crude material was purified by silica gel chromatography [hexane-ethyl acetate (3:1)] to afford the ligand as a pale yellow solid. Yield 1.7 g, 28 %. Analysis: Calculated for $C_8H_{16}S_2Te$: %C, 31.6; %H, 5.3. Found: %C, 31.9; %H, 5.5. $^{125}Te\{^1H\}$ NMR ($CDCl_3$, 300 K): δ 234. FAB MS (3-NOBA), *m/z* = 306, 204; calc. for $[C_8H_{16}S_2{}^{130}Te]^+$ 306, $[C_3H_6S{}^{130}Te]^+$ 204.

[12]aneS_2Te. To a solution of Na_2Te (0.025 mol) in $NH_{3(l)}$ (400 cm^3), prepared by following the procedure detailed above, was added at -78 °C a solution of $Cl(CH_3)_3S(CH_2)_3S(CH_2)_3Cl$ (6.5 g, 0.025 mol) in THF (100 cm^3) over 30 minutes. After the addition was complete the mixture was allowed to warm up to room temperature and the NH_3 boiled off overnight. The mixture was worked up as above to give a red oil. Purification by silica gel chromatography [hexane-ethyl acetate (3:1)] afforded the ligand as a light yellow oily solid. Yield 1.4 g, 18 %. Analysis: Calculated for $C_9H_{18}S_2Te$: %C, 34.0; %H, 5.7. Found: %C, 33.5; %H, 5.3. $^{125}Te\{^1H\}$ NMR ($CDCl_3$, 300 K): δ 217. FAB MS (3-NOBA), *m/z* = 320, 246, 204; calc. for $[C_9H_{18}S_2{}^{130}Te]^+$ 320, $[C_6H_{12}S{}^{130}Te]^+$ 246, $[C_3H_6S{}^{130}Te]^+$ 204.

[14]aneS_3Te was prepared in a similar manner using Na_2Te (0.015 mol) and $Cl(CH_2)_3S(CH_2)_2S(CH_2)_2S(CH_2)_3Cl$ (4.7 g, 0.015 mol) to give a red oil. Purification was achieved using silica gel chromatography eluting with hexane-ethyl acetate (3:1) and hexane-ethyl acetate (20:1) to give a light yellow solid. Yield 1.6 g, 29 %. Analysis: Calculated for $C_{10}H_{20}S_3Te$: %C, 33.0; %H, 5.5. Found: %C, 33.1; %H, 5.4. $^{125}Te\{^1H\}$ NMR ($CDCl_3$, 300 K): δ 254. FAB MS (3-NOBA), *m/z* = 366, 264; calc. for $[C_{10}H_{20}S_3{}^{130}Te]^+$ 366, $[C_5H_{10}S_2{}^{130}Te]^+$ 264.

[Ag([11]aneS_2Te)][CF_3SO_3]. Ag[CF_3SO_3] (25 mg, 9.7 x 10^{-5} mol) was added to a solution of [11]aneS_2Te (29 mg, 9.7 x 10^{-5} mol) in dry CH_2Cl_2 (30 cm^3) and the reaction stirred for 1 hour, during which time a light yellow precipitate was observed that was filtered off and washed with diethyl ether. Yield 30 mg, 63 %. Analysis: Calculated for $C_9H_{16}AgF_3O_3S_3Te$: %C, 19.3; %H, 2.9. Found: %C, 19.5; %H, 3.0. ^1H NMR ($CDCl_3$, 300 K): δ 2.2 (br, 1H, $TeCH_2CH_2CH_2S$), 2.7 (br, 1H, $TeCH_2$), 2.8 - 3.2 (m, 2H, 2 x SCH_2). ES^+ (MeCN), *m/z* = 717, 454, 413; calc. for $[^{107}Ag([11]aneS_2{}^{130}Te)_2]^+$ 719, $[^{107}Ag([11]aneS_2{}^{130}Te)(NCMe)]^+$ 454, $[^{107}Ag([11]aneS_2{}^{130}Te)]^+$ 413. IR/cm^{-1} 2959(w), 1364(m), 1263(s), 1155(m), 1098(m), 1030(m), 834(w), 636(m), 572(w), 517(w).

[Ag([12]aneS_2Te)][CF_3SO_3] was prepared in similar manner to give a light yellow solid that decomposed rapidly to give a black solid (38 %). Analysis: see text. ^1H NMR ($CDCl_3$, 300 K): δ 1.8 (br, 1H, $SCH_2CH_2CH_2S$), 2.1 (br, 2H, $TeCH_2CH_2CH_2S$), 2.4 - 3.0 (m, 6H, 2 x SCH_2, $TeCH_2$). ES^+ (MeCN), *m/z* = 745, 427; calc. for $[^{107}Ag([11]aneS_2{}^{130}Te)_2]^+$ 747, $[^{107}Ag([12]aneS_2{}^{130}Te)]^+$ 427. IR/cm^{-1} 2945(w), 1359(s), 1275(s), 1154(m), 1080(m), 1032(m), 636(m).

[Ag([14]aneS_3Te)][CF_3SO_3] was prepared in similar manner to give a light yellow solid (55 %). Analysis: Calculated for $C_{11}H_{20}AgF_3O_3S_4Te$: %C, 21.3; %H, 3.2. Found: %C, 21.0; %H, 3.6. ^1H NMR ($CDCl_3$, 300 K): δ 2.1 (m, 1H, $TeCH_2CH_2CH_2S$), 2.60 (m, 1H, $TeCH_2$), 2.8 - 3.1 (m, 3H, SCH_2). ES^+ (MeCN), *m/z* = 473; calc. for $[^{107}Ag([14]aneS_2{}^{130}Te)]^+$ 473. IR/cm^{-1} 2967(w), 1364(s), 1263(s), 1098(m), 1030(m), 803(w), 636(m).

X-ray Crystallographic Studies

[Ag([11]aneS_2Te)][CF_3SO_3]. Details of the crystallographic data collection and refinement parameters are given in Table 7.9. The crystals were grown *via* the vapour diffusion of diethyl ether into a solution of the complex in $MeNO_2$/MeOH. Data collection used a Rigaku AFC7S four circle diffractometer operating at 150 K, using graphite-monochromated Mo-K_α X-radiation (λ = 0.71073 Å). No significant crystal decay or movement was observed, although the crystals were poorly diffracting. The structure was solved by heavy atom methods[33] and developed by iterative cycles of full-matrix least-squares refinement[34] and difference Fourier syntheses. Although the overall structure of the complex was revealed, satisfactory refinement was not obtained.

7.5 References

[1] A. Toshimitsu and S. Uemura, in *The Chemistry of Organic Selenium and Tellurium Compounds,* S. Patai and Z. Rappoport (eds.), Wiley, New York, 1986, vol. 2, Chap. 14, pp. 581.

[2] D. K. Cabbines and D. W. Margerum, *J. Am. Chem. Soc.,* 1969, **91**, 6540.

[3] A. J. Blake, A. J. Holder, T. I. Hyde and M. Schröder, *J. Chem. Soc., Chem. Commun.,* 1989, 1433.

[4] A. F. Hill and J. D. E. T. Wilton-Ely, *Organometallics*, 1997, **16**, 4517.

[5] J. R. Lancaster, *The Bioinorganic Chemistry of Nickel*, VCH Publishers, New York, 1988.

[6] P. M. Collman, H. C. Freeman, J. M. Guss, M. Murata, V. A. Norro, J. A. M. Ramshaw and M. P. Venkatappa, *Nature*, 1978, **272**, 319.

[7] L. F. Lindoy, *The Chemistry of Macrocyclic Ligand Complexes*, Cambridge University Press, Cambridge, 1989.

[8] R. B. Lauffer, *Chem. Rev.,* 1987, **87**, 901.

[9] D. Sellmann and L. Zapf, *Angew. Chem. Int. Ed. Engl.,* 1984, **23**, 807.

[10] Y. Takaguchi, E. Horn and N. Furukawa, *Organometallics*, 1996, **15**, 5112.

[11] K. Lerstrup, D. Talham, A. Bloch, T. Poehler and D. Cowan, *J. Chem. Soc., Chem. Commun.,* 1982, 336.

[12] F. Wudl and E. Aharon-Shalom, *J. Am. Chem. Soc.,* 1982, **104**, 1154.

[13] R. Ali, S. J. Higgins and W. Levason, *Inorg. Chim. Acta,* 1984, **84**, 65.

[14] D. J. Gulliver, E. G. Hope, W. Levason, G. L. Marshall, S. G. Murray and D. M. Potter, *J. Chem. Soc., Perkin Trans. II,* 1984, 429.

[15] E. G. Hope, T. Kemmitt and W. Levason, *Organometallics,* 1988, **7**, 78.

[16] D. H. O'Brien, N. Deren, C. K. Huang, K. J. Irgolic and F. F. Knapp Jr., *Organometallics,* 1983, **2**, 305.

[17] D. M. Giolando, T. B. Rauchfuss and A. L. Rheingold, *Inorg. Chem.,* 1987, **26**, 1636.

[18] P. J. Carroll, M. V. Lakshmikantham, M. P. Cava, F. Wudl, E. Aharon-Shalom and S. D. Cox, *J. Chem. Soc., Chem. Commun.,* 1982, 1316.

[19] K. Lerstrup, D. Talham, A. Bloch, T. Poehler and D. Cowan, *J. Chem. Soc., Chem. Commun.,* 1982, 336.

[20] N. L. M. Dereu, and R. A. Zingaro, *J. Organomet. Chem.,* 1981, **212**, 141.

[21] S. C. Menon, H. B. Singh, R. P. Patel and S. K. Kulshreshtha, *J. Chem. Soc., Dalton Trans.,* 1996, 1203.

[22] S. C. Rawle, R. Yagbasan, K. Prout and S. R. Cooper, *J. Am. Chem. Soc.*, 1987, **109**, 6181.

[23] A. J. Blake, A. J. Holder, T. I. Hyde and M. Schröder, *J. Chem. Soc., Chem. Commun.*, 1987, 987.

[24] A. J. Blake, R. O. Gould, A. J. Holder, T. I. Hyde, A. J. Lavery, M. O. Odulate and M. Schröder, *J. Chem. Soc., Chem. Commun.*, 1987, 118.

[25] J. D. McCullough, *Inorg. Chem.*, 1965, **4**, 862.

[26] T. Kemmit, Ph. D. Thesis, University of Southampton, 1989.

[27] S. A. Karjala and S. M. McElvain, *J. Am. Chem. Soc.*, 1933, **55**, 2966.

[28] W. E. Hill, W. Levason and B. Sheikh, *J. Organomet. Chem.*, 1981, **219**, 163.

[29] W. -F. Liaw, C. -H. Lai, S. -J. Chiou, Y. -C. Horng, C. -C. Chou, M. -C. Liaw, G. -S. Lee and S. -M. Peng, *Inorg. Chem.*, 1995, **34**, 3755.

[30] J. R. Black, N. R. Champness, W. Levason and G. Reid, *J. Chem. Soc., Chem. Commun.*, 1995, 1277.

[31] H. B. Schurink, *Org. Synth.*, 1937, **17**, 73.

[32] W. Levason, C. A. McAuliffe and S. G. Murray, *Inorg. Chim. Acta.*, 1976, **17**, 247.

[33] PATTY, The DIRDIF Program System, P. T. Beurskens, G. Admiraal, G. Beurskens, W. P. Bosman, S. Garcia-Granda, R. O. Gould, J. M. M. Smits, C. Smykalla. Technical Report of the Crystallography Laboratory, University of Nijmegen, The Netherlands, 1992.

[34] TeXsan: Crystal Structure Analysis Package, Molecular Structure Corporation, Texas, 1995.

Appendix

Infrared spectra were measured as CsI discs using a Perkin-Elmer 983 spectrometer over the range 180 - 4000 cm^{-1}, or in solution using NaCl plates on a Perkin-Elmer 1600 FTIR spectrometer.

Mass spectra were run either by fast atom bombardment (FAB) using 3-NOBA (3-nitrobenzyl alcohol) as a matrix on a VG Analytical 70-250-SE Normal Geometry Double Focusing Mass Spectrometer or by positive electrospray (ES) in MeCN solution (0.1 μM) using a VG Biotech Platform.

^{1}H NMR spectra were recorded using a Bruker AM300 spectrometer operating at 300.13 MHz and are referenced to Me_4Si ($\delta = 0$). $^{13}C\{^{1}H\}$, ^{31}P, ^{55}Mn, $^{77}Se\{^{1}H\}$, $^{125}Te\{^{1}H\}$ and ^{195}Pt NMR spectra all were recorded in 10 mm diameter tubes using a Bruker AM360 spectrometer operating at 90.1, 145.8, 89.3, 68.7, 113.6 or 77.2 MHz respectively and are referenced to Me_4Si, 85 % H_3PO_4, external saturated, aqueous $K[MnO_4]$, external neat Me_2Se, external neat Me_2Te and $[PtCl_6]^{2-}$ in D_2O respectively ($\delta = 0$). For the carbonyl complexes $[Cr(acac)_3]$ was added to the NMR solutions prior to recording $^{13}C\{^{1}H\}$ NMR spectra and a pulse delay of 2 seconds was employed to take account of the long relaxation times. Microanalyses were carried out by the University of Strathclyde microanalytical service.

Electrochemical studies used an Eco Chemi PGstat20 with 0.1 mol dm^{-3} $^{n}BuNBF_4$ supporting electrolyte in MeCN or CH_2Cl_2, Pt working and auxiliary electrodes and are referenced to a standard calomel reference electrode. All potentials were referenced *verses* ferrocene-ferrocenium.

All preparations were conducted in degassed solvents under a dinitrogen atmosphere with standard Schlenk techniques being employed.